Advanced analytical and microbial methods for biopharmaceutical and pharmaceutical products and processes

A thesis submitted by

Charlotte Bell

For the award of Engineering Doctorate

in Biopharmaceutical Process Development

Biopharmaceutical and Bioprocessing Technology Centre

School of Chemical Engineering and Advanced Materials

Newcastle University

November 2014

Preface

This thesis describes research that was undertaken as part of an Engineering Doctorate in Biopharmaceutical Process Development which was carried out in collaboration with GlaxoSmithKline (GSK) and sponsored by the Engineering and Physical Sciences Research Council (EPSRC).

The thesis takes the format of a 'thesis by portfolio' which details a number of projects that are linked by the theme of analytical methods used/or with the potential to be used in the pharmaceutical industry.

Being an industrially focussed Engineering Doctorate, the projects reflect the research requirements of industry, and changed over the period of study to meet new research challenges within the company.

The concluding chapter (Chapter 8) sets out recommendations to industry that have been made based on the outcomes of the research.

Abstract

In recent years, pharmaceutical research has begun to shift from the development of small molecule chemical entities, to complex high value, low volume biologics. The cost of batch losses or product recall due to the presence of microbial, chemical or physical contaminants can have serious implications for a business. It is therefore important that as the complexity of pharmaceutical products increases, the techniques utilised in the analysis and characterisation of these products and their excipients also moves forward, thereby ensuring product quality and patient safety. This research explores three areas of analysis and characterisation relating to pharmaceutical products: microbial testing; oxidative stability testing and container integrity testing.

The detection and identification of microbiological contamination using traditional microbial methods (TMMs) have a number of limitations such as long testing times and reliance on subjective assessment leading to operator error. More recently developed rapid microbial methods (RMMs) have been designed to overcome these limitations and their uptake would enable microbial testing to align with the process analytical technology (PAT) approach to process monitoring and control. A review of available techniques and those implemented by a large pharmaceutical company, GlaxoSmithKline has highlighted that a number of RMMs are being utilised, but their widespread adoption in the pharmaceutical industry faces several barriers including: economic and financial; institutional; legislative and regulatory; and technical.

Another important area of pharmaceutical product analysis is that of oxidative stability testing. A comparison was undertaken of two machines for measuring oxidative stability (the Rancimat (Metrohm) and the ACL Instrument (ACL Instruments, Switzerland) to investigate their performance and assess their applicability for the testing of pharmaceutical excipients. The testing of corn oil, selected as a model substance, revealed a strong correlation between the results from the two machines. An aspect of oxidative stability testing is concerned with residual levels of peroxides therefore the ACL Instrument was compared to iodometric titration, a highly empirical traditional approach, for the quantification of peroxides in corn and Menhaden oil. Good correlation was found between peroxide levels measured by the two methods, but the results from the ACL Instrument showed a dependence on oil type, meaning that a standard would be required each oil type. Additional testing was carried out on

polysorbates, pharmaceutical excipients that are known to pose stability issues in final formulations, due to containing residual amounts of peroxides. Using the ACL Instrument it was possible to detect differences in oxidative stability between grades and types of polysorbate. It was not possible to discriminate between batches of the same grade.

The final testing that is carried out on pharmaceutical products stored in glass vials, is container integrity testing. High voltage leak detection (HVLD) is one method utilised and concerns exist as to whether the high voltages present can cause ozone formation in the container headspace, leading to degradation of the drug product. A method involving potassium indigo trisulphonate was developed for the detection of ozone and a test protocol implemented. This approach showed that ozone was produced in containers with a low fill volume, but at a very low concentration and hence it should not affect the stability of the final product.

The research carried out in this thesis has drawn together evidence on RMMs; furthered understanding of the applicability of oxidative stability testing for pharmaceutical excipients; and has highlighted the importance of investigating the effect of container integrity testing methods on the final pharmaceutical product.

Contents

Figures

Tables

Abbreviations

ACL	advanced chemiluminescence
amu	atomic mass unit
AOCS	American Oil Chemists' Society
APHA	American Public Health Association
API	active pharmaceutical ingredient
ATP	adenosine triphosphate
AUC	area under the curve
AV	anisidine value
BP	British Pharmacopoeia
CD	conjugated diene
CDV	conjugated diene value
CFU	colony forming unit
CL	chemiluminescence
CLI	chemiluminescence intensity (cts/mg/s)
DoE	design of experiments
Da	daltons
DNPO	bis-(2,4-dinitrophenyl)oxalate
DSC	differential scanning calorimetry
EngD	Engineering Doctorate
EP	European Pharmacopoeia
FDA	Food and Drug Administration
FOX2	ferrous oxidation-xylenol orange
FTIR	Fourier transform infrared spectroscopy
GSK	GlaxoSmithKline
HP-PS80	high purity polysorbate 80
HPO	hydroperoxides

HTPB	hydroxy-terminated polybutadiene
HVLD	high voltage leak detection
ICH	International Conference on Harmonisation of Technical Requirements for Registration of Pharmaceuticals for Human Use
IMD	instantaneous microbial detection
IP	induction period
IPEC	International Pharmaceutical Excipients Council
IR	indigo reagent
IR1	indigo reagent 1
IR2	indigo reagent 2
kV	kilovolt
mA	milliampere
MALDI	matrix assisted laser desorption/ionisation
meq	milliequivalent
MLT	microbial limits test
MUFA	monounsaturated fatty acid
MS	mass spectrometry
NaDS	sodium diphenylaminesulfonate
NF	national formulary
nm	nanometer
NPV	net present value
OIT	oxidation induction time
PAT	process analytical technology
PCR	polymerase chain reaction
PDA	Parenteral Drug Association
PEG	polyethylene glycol

Ph Eur	European Pharmacopeia
PIT	potassium indigo trisulfonate
PLS	partial least squares
PN	peroxide number
PO-CL	peroxyoxalate chemiluminescence
PP	payback period
PTFE	polytetrafluoroethylene
PUFA	polyunsaturated fatty acid
PV	peroxide value (millequivalents peroxide per 1000g test sample)
Py-MS	pyrolysis mass spectrometry
QbD	quality by design
QC	quality control
RMM	rapid microbial methods
ROI	return on investment
RSD	relative standard deviation
RTR	real-time release
SOP	standard operating procedure
TBA	thiobarbituric acid
TBARS	thiobarbituric acid reactive substances
TCPO	Bis-(2,4,6,-trichlorophenyl)oxalate
TGA	thermogravimetic analysis
TFA	trifluoroacetic acid
TLI	total luminescence intensity (cts/g)
TOF	time-of-flight
Trp	tryptophan
UHMWPE	ultra-high molecular weight polyethylene
USP	United States Pharmacopoeia

UV   ultraviolet

V   volts

WFI   water for injection

XO   xylenol orange

Publications

Bell, C., F. Käser, E. Martin, and G. Scott, *Comparison of the Rancimat and the ACL Instrument for Measuring the Oxidative Stability of Corn Oil.* **Journal of the American Oil Chemists' Society, 2014. 91(5): p. 733-746.**

Chapter 1. Scope and aims of the research

In pharmaceutical research and development and production, there has been a shift of focus from small molecules to a dual focus on small and large molecules. This is was highlighted by Evens and Kaitin [1] in an analysis of the biotechnology industry which detailed the increase in commercially available biotechnology products from only 16 in the 1980s, to over 200 in 2014. In addition to those products on the market, there are currently over 900 in clinical trials. These biotechnology products are categorised in Figure 1.1 which shows the steady increase in the number of products in clinical trials since 2001 highlighting the growth of biotechnology.
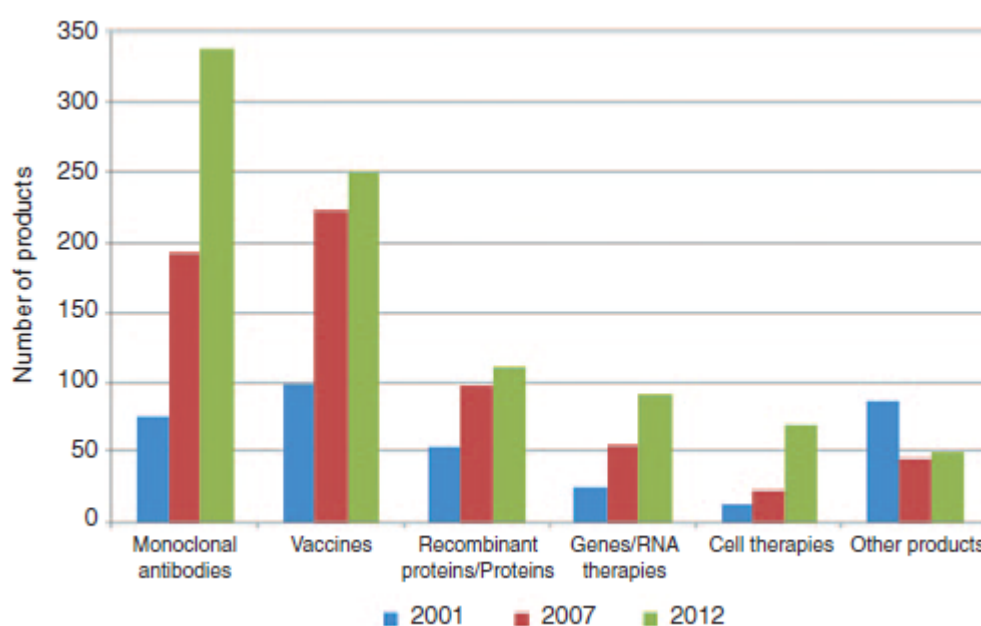
Figure 1.1 - Types of biotechnology products in clinical trials during 2001, 2007, and 2012 [1]

Challenges associated with biotechnology products arise with maintaining the integrity of protein structures during manufacture, in formulation and once packaged, which is essential for achieving the desired therapeutic effect. Proteins are highly complex large structures and are prone to structural changes induced by high temperatures, shear, oxidative species and pH changes [2]. Due to their instability in the gastrointestinal tract they are often administered parenterally. To enhance the bioavailability of the protein and to improve its stability, various excipients are contained within the formulation for example, surfactants and antioxidants. What is paramount is that these excipients do not cause detriment to the active pharmaceutical ingredient (API).

Upon storage of the final product, aggregation and surface adsorption can be problematic.

The costs associated with the development and production of protein-based high value, low volume products means that losses of finished product due to contamination with chemical, physical or microbial contaminants can have severe implications. It is therefore important that as technology moves forward and more complex and costly pharmaceuticals are manufactured, that analytical techniques utilised in the characterisation of pharmaceuticals and excipients also move forward in order to aid in the adequate analysis of these products and excipients. In addition to this, reduction in process times is a key factor for biologics, as timely market penetration is crucial for success [3].

There is high demand for analytical techniques that are able to provide answers to a number of different questions along the pharmaceutical development line. These analytical techniques are becoming increasingly complex to be able to keep pace with the increasing complexity in pharmaceutical product design. This thesis explores some of the challenges arising with analytical techniques for microbiology (Chapter 2), oxidative stability testing (Chapter 3, Chapter 4 and Chapter 5) and container integrity testing (Chapter 6 and Chapter 7) that are utilised, or have potential to be utilised, in the pharmaceutical industry.

Some analytical methods, such as those used in microbiology, have been used without modification for several decades, but are now being improved to enable faster more efficient testing. The move towards lean manufacturing means that it is no longer acceptable or economical to hold product at several stages of the production process, whilst waiting for microbiology results. Rapid microbiology methods (RMMs) have been developed to reduce testing times and improve reliability however there has not been wide uptake of these due to several barriers, which are discussed in Chapter 2.

Stability testing of final pharmaceutical products is required before they can be released and a number of different types of stability studies are undertaken which involve subjecting the formulation to different combinations of heat, light and humidity over a range of time periods. These stability studies also contribute to the determination of appropriate packaging material and shelf lives of final formulations.

As protein products are susceptible to oxidation, it is increasingly important to ensure that those excipients that are included to enable the effective delivery of the protein formulations do not pose a detriment to the protein itself, in terms of compromising its stability. Proteins are made up of amino acids and some of these are prone to oxidation. Should amino acids on the protein chain be oxidised then a change in tertiary structure of the protein could occur which may lead to a loss of activity, or a change in function which could be harmful for the patient. Antioxidants are often added to formulations to 'mop up' any potentially oxidising species, however, some common excipients are known to be potentially oxidising, such as polysorbates. In the past when formulations were less complex chemical entities rather than large protein structures, the effect of polysorbates were not as potentially damaging. However, polysorbates have been found to contain residual levels of peroxides and in addition to this, their structure lends itself to autoxidation and the formation of more peroxides, which can accumulate in a formulation over time and cause stability issues for the formulation [4].

As analytical technologies advance there are sometimes concerns that have previously not been considered or have been overlooked. In the case of container integrity testing, methods have evolved over decades to become extremely sophisticated and automated, with machines able to check several thousand vials per hour. Where possible, detrimental effects to vials and formulations are minimised, however some issues that manufacturers do not fully consider could have implications on formulations. Manufacturers may only carry out basic assessments on instruments because they cannot consider all of the options available such as possible filling materials.

As previously mentioned in the preface, this 'thesis by portfolio' explores analytical testing in the pharmaceutical industry, and in particular three areas which over the course of the Engineering Doctorate had importance for the industrial collaborator GlaxoSmithKline: Rapid microbial methods (RMMs), methods for measuring oxidative stability and container integrity testing methods. The recommendations for industry that came from this study can be found in Chapter 8. The chapters presented in this thesis had the following specific aims:

- Chapter 2 - This research was initially going to focus on the potential of matrix assisted laser desorption ionisation time of flight (MALDI-TOF) mass spectroscopy and its application in microbial testing of pharmaceutical products, however it was not possible to take this forward into experimental research as there were several research groups and companies, such as Bruker, who were already making significant progress in this area. Additionally, the costs associated with carrying out research on this method were high and so this research project was not taken forward. The chapter therefore reviews the use and benefits of RMMs and the barriers to their acceptance in the pharmaceutical industry. The review has been included as an informative guide, which presents several sources of evidence around the potential of RMMs, for industrialists who may be considering implementing RMMs.

- Chapter 3 investigates the performance of a chemiluminescence instrument, the ACL Instrument, against a standard instrument used for measuring oxidative stability, the Rancimat and the chapter also details research on the operational aspects of these two instruments. This work was built on further in Chapter 4 where the ACL Instrument is compared to a standard method for measuring peroxide values, the American Oil Chemists' Society Peroxide Value titration [5]. In both Chapter 3 and Chapter 4, corn oil and Menhaden oil (fish oil) were used as model oils for testing, as their oxidative stability is well documented. The conclusions from the work in Chapter 3 and Chapter 4 showed that the ACL Instrument had potential to be applied to testing of pharmaceutical excipients so this work was taken further in Chapter 5.

- Chapter 5 investigated the applicability of the ACL Instrument for measuring the stability of polysorbates, common pharmaceutical excipients whose stability has become an issue as the sensitivity to oxidation of complex pharmaceuticals has increased.

- Chapter 6 and Chapter 7 details research carried out with the aim of identifying, developing and implementing an analytical method to investigate whether a container integrity testing procedure (high voltage leak detection (HVLD)) produces

ozone within containers, which could potentially be detrimental to the pharmaceutical product.

Chapter 2. The move towards the adoption of Rapid Microbial Methods in the pharmaceutical industry.

2.1 Introduction

Microbial contamination poses a potential risk to drug quality and safety. It is crucial that pharmaceuticals and biopharmaceuticals do not contain microorganisms as these can be detrimental to human health when ingested, applied to the body or injected into the bloodstream. As well as being problematic if present in the final product, microorganisms can also cause problems during manufacture, with their toxins affecting growth in the production phase during bioprocessing and microbial enzymes and biofilms reducing downstream processing efficiency [6].

There are a number of possible sources of contamination within the drug manufacturing process, hence microbial testing is employed at many stages of the process, more specifically: incoming raw materials, the manufacturing environment and personnel are all subjected to routine monitoring. Types of testing undertaken include: the microbial limits test (MLT), bioburden testing, water testing, bacterial endotoxin testing and final product release testing [7]. It is essential that any contamination is detected as early as possible, so that manufacture can be halted, product release suspended and the root cause of contamination investigated.

In contrast to other technologies associated with pharmaceutical manufacture, which have become more sophisticated over the past decades, such as process automation for production and packaging, microbial testing lags behind. Techniques that were used in the 19th century are still being widely used today. There have been improvements in microbial technologies which have become more sophisticated and are now used in the clinical setting to provide more rapid diagnosis of infection and in the food and beverage industry, however, in pharmaceutical manufacturing, the acceptance and implementation of these technological advances has been slower and more challenging.

2.2 Traditional microbial testing

Traditional methods for the detection of microbial contaminants are generally straightforward and inexpensive [8]. They often include a capture step such as the filtration of liquids or the swabbing of a surface. Samples are then cultured to allow the growth of any microorganisms that may be present. Their identification is reliant on visual observation and hence expert interpretation and biochemical tests are required, making the testing labour and time intensive. The process from sampling to identification can be in the order of hours up to days and even weeks for slow growing microorganisms.

An example of the time and labour intensive nature of traditional microbial methods (TMMs) is seen in the final pharmaceutical product sterility testing set out in the Food and Drug Administration (FDA) Code of Federal Regulations Title 21 – Food and Drugs [9]. For this type of testing the bulk or final container material is inoculated into fluid thioglycollate medium and incubated at 30-35°C for a period of no less than 14 days. The requirements are that this medium is then visually examined on the third, fourth, or fifth day, again on the seventh or eighth day and then on the fourteenth day thereby necessitating substantial operator time requirement as well as storage provision. The testing can be prolonged if the original inoculum causes difficulties in visual examination or if there is an absence of growth, with additional steps having to be taken and hence lengthening the testing time beyond 14 days [10]. The product is warehoused during this period, which contributes to increased costs. In this case, microbial testing acts a bottleneck during the product release process.

As well as the time delays and labour intensity associated with TMMs, they are also prone to operator error and subjectivity, often resulting in false results. Many conventional microbiological methods are subject to sampling error, dilution error, plating error, incubation error and operator error. Some methods of testing are only designed to detect specific species, which means that several tests are required. It is therefore desirable to utilise more automated rapid microbial methods (RMMs), providing consistent and reliable results in minutes, as opposed to hours or days. Economics, throughput, and convenience are stated as reasons to use alternatives to TMMs. However, despite the limitations presented for TMMs, they are still widely

used in the pharmaceutical industry as they do satisfy requirements and changing of methods requires a high amount of re-validation.

There are three key questions when dealing with microbial detection and identification [12] and these are:

1) Is there any microbial contamination present? (Detection)
2) How many microbes are there? (Enumeration)
3) What are they? (Identification)

TMMs have traditionally been designed to answer one of these questions at a time, but some more recently developed methods are capable of answering more than one of these questions. An ideal method would be able to answer all three of these questions in real-time, however a technology that can do this has not yet been developed, although advances have been made and these are discussed in section 2.4.

2.3 Process Analytical Technology (PAT)

With a wealth of technology at the disposal of pharmaceutical companies and new technologies being developed, it is now possible to take a more innovative approach to optimising drug manufacture to improve the overall efficiency of processes and obtain quality products in less time, at reduced costs. In 2004, the Food and Drug Administration (FDA) launched a new initiative, 'Pharmaceutical cGMPs for the 21st Century - A Risk-Based Approach' [13]. This was a step towards modernising the regulation of pharmaceutical manufacturing and product quality. As part of this report, the FDA issued a further document, 'Guidance for Industry: PAT — A Framework for Innovative Pharmaceutical Development, Manufacturing, and Quality Assurance' [14], designed to help with the introduction of new technologies to improve the efficiency and effectiveness of manufacturing process design, control and quality assurance.

The FDA regards process analytical technology (PAT) to be "*a system for designing, analyzing, and controlling manufacturing through timely measurements (i.e., during processing) of critical quality and performance attributes of raw and in-process materials and processes, with the goal of ensuring final product quality*" [13]. In short, the FDA's PAT initiative aims to push forward the optimisation of pharmaceutical manufacturing and quality control by encouraging companies to adopt state-of-the-art

methods for process control and analysis. Some of these methods make it possible to consider more data from the process and relate this to effects on final product quality, therefore making it possible to build quality in to products – quality-by-design (QbD). To build quality into products, it is necessary to have a wealth of process understanding and understand the complex relationships between multiple variables.
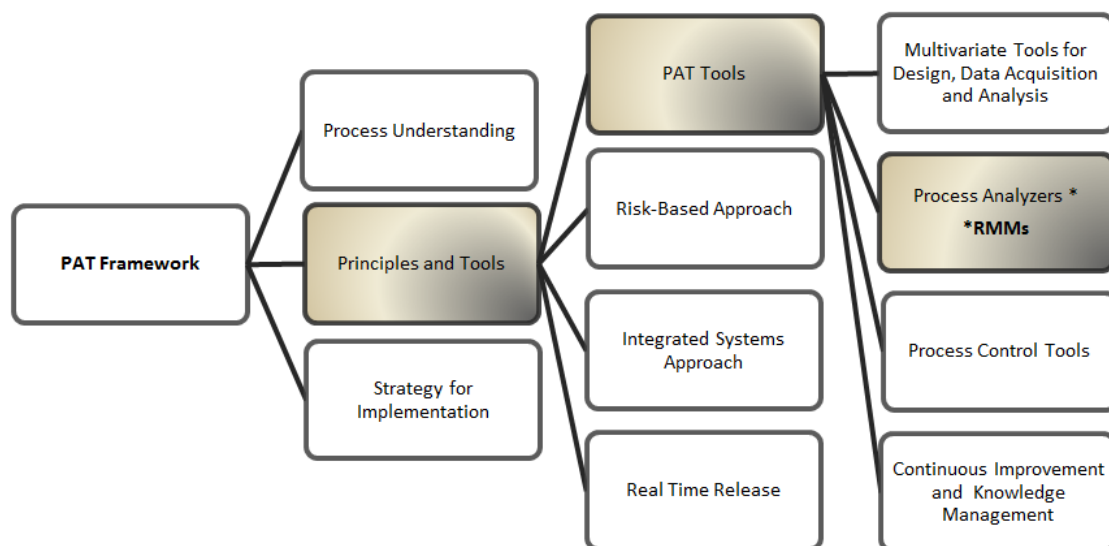
Figure 2.1 - Summary of FDA's PAT Framework [14]

Figure 2.1 is a diagrammatic summary of the FDA's PAT framework with the areas where RMMs fit into the landscape shaded in grey. Within the PAT framework there is a section addressing principles and tools, within this there is a section on PAT tools which incorporates four topic areas; multivariate tools for design, data acquisition and analysis; process analysers; process control tools; and continuous improvement and knowledge management. Process analysers are the area in which RMMs fit within this framework. As technologies advance, the development and implementation of RMMs as PAT tools alongside the use of other online measuring devices, providing real-time data throughout the drug manufacturing process and through its analysis, could help to drive efficiency and improve process understanding. An example of a RMM under validation that can provide real-time results, the Azbil BioVigilant Instantaneous Microbial Detection (IMD) air monitoring system, is discussed in the following section 2.4, but currently the majority of tests available for microbial detection utilise offline techniques therefore cannot give real-time results. Ideally, microbiological testing will

progress towards real-time to enhance the efficiency of pharmaceutical manufacture whilst not compromising patient safety.

2.4 Benefits of RMMs and their implication for the pharmaceutical industry

The emergence of new pharmaceuticals such as cell based products has challenged the applicability of TMM approaches [15]. These new products are produced in lower volumes, at higher costs, using shorter manufacturing life cycles and generally have much shorter shelf lives than small molecule more traditional pharmaceuticals. This is problematic and to some extent incompatible with TMMs that require growth based detection with visual examination, large sample volumes and manual examination of cultures which are labour and time intensive [16]. Products such as these highlight the need for the implementation of RMMs, to increase the sophistication of methods and ensure they are fit for purpose. Sterility testing for cellular and gene therapy products guidance [16] states that RMMs can be: growth-based, viability-based, or surrogate-based markers of microorganisms. Growth based methods are those where a period of subculture is required in order to achieve a detectable signal. Viability based tests detect a particular substance or indicator of cell viability and surrogate based markers detect components of a cell [17].

The advantage of a move towards the utilisation of RMMs would be that the manufacturing process would be shortened due to less holding steps caused as a result of waiting for results of microbial testing. The final pharmaceutical product could be released to the market earlier, ensuring the security of supply to customers and making the plant free for the manufacture of another product/batch. It would also reduce costs associated with warehousing of packaged final products waiting to be released. By utilising more real-time methods in microbial testing, processes could be stopped and contamination investigated as soon as it occurs therefore, RMMs could reduce the likelihood of batch loss and the associated impact on profits.

Although RMMs can offer advantages over TMMs in several testing situations, RMMs are not suitable for all cases. For example, TMMs are implemented in the production of penicillin seed and production batches as the potential of RMMs has been investigated but these were not found to offer any advantage over existing TMMs. This is because in this particular scenario, the time taken for TMMs is not as much of an

issue as in release testing of other low volume, high value pharmaceutical products. This is an example of where RMMs would not be appropriate and companies must be aware that RMMs cannot be used in every situation in order to increase return on investment (ROI).

The adoption of RMMs in the pharmaceutical industry has gradually increased over the period 2001–2011 with the number of companies using RMMs increasing [18]. RMMs have the potential, as the European pharmacopoeia states, to '*lead to cost-effective microbiological control and improved assurance for the quality of pharmaceutical products*' [19]. There are a number of RMMs on the market and those which have been considered or are in use in the pharmaceutical industry are summarised in this chapter along with the application for which they are used, the sample type that can be tested and sample preparation time, time to result, the microorganisms it can detect and whether or not the RMM can distinguish between live and dead cells. There is a large amount of work ongoing in the pharmaceutical industry associated with the validation of RMMs as their importance in manufacturing has been recognised. Observations during visits to a number of pharmaceutical manufacturing sites highlighted that, despite these methods providing results in a shorter timescale than TMMs, they may not be straightforward to perform, involving multiple steps and requiring skilled operators. Nevertheless, there was a significant time saving from using these RMMs, for example the Milliflex® Rapid Microbiology Detection System, which has been validated by pharmaceutical companies for the system suitability and air and surface bioburden determination.

Novartis validated and now use a RMM, the Milliflex® Rapid Microbiology Detection System, for some in-process testing and for the final test before a product can be released [20]. The Milliflex® Rapid Microbiology Detection System is used for detection and identification of bacteria, yeast and moulds in filterable samples and can be utilised to test pharmaceutical water, bioburden, in-process products and final products and beverages. After an overnight incubation step, viable organisms down to one colony forming unit (CFU) can be detected, 16-24 hours after sampling. The method can detect between live and dead cells. As well as validating this method, Novartis also helped others learn from this experience through the development of a

roadmap for regulatory acceptance for the validation of the method for other products.

The Pallcheck™ Luminometer is an adenosine triphosphate (ATP) bioluminescence instrument which can be used in the release testing of sterile products and quality monitoring of pharmaceutical water for injection. Samples can be filterable or swabs and following an enrichment step, results are available in 1 minute for the quantification of a known contamination, or 24 hours for products that are expected to be contamination free [21]. The method can distinguish viable cells through ATP bioluminescence. The Pallcheck™ Luminometer has been approved for use in the testing of nasal spray and other non-sterile finished products within the pharmaceutical industry and an advantage of using the Pallcheck™ Luminometer is that product release times have been shortened by 4 days, resulting in cost savings associated with the warehousing of final product. Where these RMMs may not be useful is in testing of production batches where the final product has not been purified, as background ATP bioluminescence from cell culture medium could interfere with the results. In these cases, TMMs would be utilised, so do still serve an important purpose.

Another RMM which has been routinely used is the ChemScanRDI® (AES Chemunex) [22] which, since the acquisition of AES Chemunex by bioMérieux has been rebranded, ScanRDI®. The ScanRDI® system uses solid phase cytometry to detect viable cells and can detect down to one living cell per sample, with time to result being 3-4 hours. The sample is initially mixed with a fluorescent substance which is taken up by viable cells and then filtered prior to scanning the membrane. This method is used for the testing of Imitrex nasal spray bulk solution and surface monitoring during Imitrex filling [23]. The ScanRDI® is 21 CFR part 11 compliant [22] regarding the storage of data from the system.

One method currently under validation in this industry is the Azbil BioVigilant Instantaneous Microbial Detection (IMD) air monitoring system. This real-time monitoring system measures the air quality in a clean room and can differentiate between biological and inert particles. The system uses a laser light source and measures the mie scattering of particles with a fluorescence detector, to indicate the

nature of the particles and their viability [24]. When particles pass through the interrogation zone of the detection unit, they pass through the laser light beam and scatter the light. The extent of scattering indicates the particle size. If the particle exhibits intrinsic fluorescence this indicates that it is a biological particle whilst a lack of fluorescence indicates that the particle is inert [25]. Advantages of this method are that: no reagents are required; there is minimal operator input and the device offers real-time data through its ability to simultaneously measure particle size and biological status. It is possible to use the device for continuous or discrete sampling and it has functions for video and data collection, allowing review should there be a need to reinvestigate historic data. It is also compliant with USP <1223>, EP 5.1.6 and 21 CFR part 11, regulation regarding electronic storage of data [19, 26, 27].

The BioVigilant IMD system can be used for the monitoring of classified areas such as clean rooms, fill lines, isolator systems and safety cabinets and can also be used for process support such as media fills and risk assessment [28]. There are a number of features and benefits of the Biovigilant IMD, summarised in Table 2-1 and these include: reduced time after shutdown i.e. by providing real-time data on the effectiveness of cleaning post-contamination; testing of operator performance in aseptic technique i.e. by monitoring in real-time the presence of microorganisms arising during operator movement; and it can increase efficiency overall due to real-time data giving time savings in a number of scenarios. Real-time data acquisition allows for the root cause of contamination to be more easily determined due to being able to link the data to occurrences within the clean room i.e. transfer of materials in or out, therefore corrective action can be taken much sooner should contamination be detected. This is extremely useful compared to TMMs where results may be attained hours or days after the occurrence of the contamination making it difficult to determine the root cause and significantly reducing the opportunity for corrective action. Also, in the case of low level contamination some TMMs are less sensitive than the BioVigilant IMD system as it can detect down to a single cell.

BioVigilant IMD-A Features	Benefits
Instantaneous detection	Can facilitate determination of the root cause of contamination
No sample handling, reduced labour	Several tests available using the device and freedom of location
Continuous monitoring/ real-time data	Allows effect of time of day to be measured
Video camera alongside data collection and playback function	Allows monitoring and correlation with activities, personnel, unusual activity
Sensitive down to single cell level	Pinpoint source by detecting low level contamination

Table 2-1 - Features and benefits of BioVigilant IMD-A

As well as facilitating root cause analysis of contamination, the BioVigilant IMD system can also monitor in real-time how effective the corrective action has been, without a delay that would be incurred using TMMs. Overall the system can increase quality assurance and reduce the cost and time associated with investigation of contamination.

The VITEK® 2 system from bioMérieux is used widely in the clinical setting for bacterial identification and is routinely used for the identification of microorganisms. The system requires a solution containing the microorganism to be placed on a card, which is then placed into the machine, which can hold up to 60 cards. Advanced colourimetry provides discrimination between species, with a low rate of misidentified species and time to result of 5.2-6.7 hours [29-31]. This system can be used for environmental samples and final products and is 21 CRF part 11 [27] compliant. A disadvantage of this method over other methods introduced in this chapter is that it cannot distinguish between live and dead cells.

One particular method that has been developed over the last 20 years for the identification of microbes and is now making its way into the pharmaceutical sector is matrix assisted laser desorption ionisation (MALDI time-of-flight (TOF) mass spectrometry (MS) [32]. In MALDI-TOF MS gaseous breakdown products released by heating microbial isolates in a vacuum are analysed by mass spectrometry, providing characteristic spectra. Intact microbial cells, when subject to intense ionisation under MALDI-TOF MS, release a distinctive pattern of charged species, giving rise to a mass spectrum. The peaks on the spectrum correspond to different bacterial proteins and these peaks are used to identify the bacteria. Using complex algorithms spectra can be compared to known peaks in a database as an aid to rapid identification. One critical

aspect of this technique is that isolates require culture prior to analysis, which makes the technique more time consuming.

Many groups [33-35] have investigated MALDI-TOF MS as a method for bacterial identification and it is already used as a RMM in some settings, for example for the rapid identification of clinically relevant isolates [36]. MALDI-TOF MS can offer speed, sensitivity and tolerance to contaminants which, when coupled with the automated system, makes this a powerful tool [34]. Bruker Daltonics produce the MALDI Biotyper platform and its SmartSpectra™ Acquisition system has capacity to analyse 96 samples in 30 minutes [37].

Using MALDI-TOF MS, Hartmeyer *et al* [38] successfully identified *Streptococcus pneumoniae* within half an hour of receiving a patient's sputum sample. Minimal sample preparation was required and the result was confirmed by culturing techniques. In terms of the economic benefit of using MALDI-TOF MS as a RMM, significant cost savings can be made over time. Although initial capital expenditure is high, this can be recovered through time savings of the method. Expenditure on consumables is low and the machine does not need to be run by a skilled mass spectrometrist, as with clear standard operating procedures (SOP), it can be run by a laboratory technician.

In August 2013, bioMérieux received FDA approval to market its VITEK® MS automated identification system for the rapid identification of microorganisms, which utilises MALDI-TOF MS [39]. This system is aimed at clinical microbiology laboratories and provides a fast, accurate and robust testing platform compliant with 21 CRF part 11 [27] and employs sophisticated barcoding systems for tracing samples. It is being marketed for the clinical setting for the identification of disease-causing bacteria and yeast to enable fast treatment. It does however, have potential application in pharmaceutical microbiology laboratories, should it be possible to augment the spectral databases within the system to include relevant commonly encountered organisms from the pharmaceutical manufacturing environment.

2.5 Sources of information and guidance on RMMs

A number of official guidelines exist relating to the validation of rapid microbial methods and their implementation in the pharmaceutical industry including:

- Parenteral Drug Association (PDA) Technical Report Number 33: Evaluation, Validation and Implementation of New Microbiological Testing Methods [40]

- United States Pharmacopeia (USP) <1223> Validation of Alternative Microbial Methods [26]

- European Pharmacopeia (EP) 5.1.6 Alternative Methods for Control of Microbiological Quality [19].

Within the pharmaceutical sector, criticism exists that these different sets of guidance redefined terms that were previously used for chemical analysis but which have been transferred across to microbiology although some of the terms are not easily adapted and have resulted in confusion for microbiologists. The harmonization of these guidelines would make information clearer, however, the differences between some traditional methods and RMMs mean that their comparison for equivalence required for regulatory purposes, is often quite complicated as the two different measures are very hard to compare due to the nature of the results, so the process may always be inherently complex.

As well as the existence of official guidelines, there are other resources to help companies understand the benefits of RMMs and make informed choices. The website rapidmicromethods.com [41] provides a product matrix which gives information to allow users to compare RMMs currently on the market or undergoing development. The website also provides useful resources to help with understanding the return on investment (ROI), payback period (PP) and net present value (NPV) of RMMs. This is critical information when building an economic case for the adoption of a RMM. It is crucial for companies to understand whether the implementation of a RMM can give them a competitive advantage, otherwise implementation may not be financially justifiable. Despite the existence of useful resources such as the rapidmicromethods.com website and the industry guidance, barriers remain to the widespread adoption of RMMs.

2.6 Common barriers to the adoption and implementation of RMMs

There are many barriers that must be overcome to realise the implementation of RMMs and these can be categorised into: economic and financial; institutional; regulatory and legislative; and technical.

Some of the economic and financial reasons that act as barriers to the adoption of RMMs are the capital cost of purchasing equipment, the cost of validation and the cost of retraining personnel. The capital cost of a rapid system may appear high and mechanisms to calculate the benefits of implementing the method are complicated. When RMMs are compared to TMMs, appropriate consideration must be given to all factors contributing to the cost of performing the TMMs including: laboratory space, consumables, labour and time. If such factors are omitted from the financial justifications then it is not possible to make a fair comparison between RMMs and TMMs, and the view that TMMs are inexpensive and RMMs are expensive may be wrongly assumed. It is also necessary for businesses to explore their drivers for change for example, new product lines may come on stream that could benefit from RMMs or there could be a need for the expansion of capacity due to improved efficiency through utilisation of PAT tools across the manufacturing process. Although resources exist to enable companies to calculate the benefits of capital outlay on RMMs, there may be other barriers preventing companies from adopting RMMs including institutional barriers.

Institutional barriers such as the lack of understanding and time to investigate new methods compared with the detailed knowledge base around TMMs means that the adoption of change and new RMMs will be challenging. Furthermore, a fear of the unknown exists in that more advanced methodologies with lower limits of detection may uncover results that were not previously possible to achieve and this may have implications on existing acceptable limits [42].

Another institutional barrier is a potential lack of availability of technically competent personnel to validate or operate the technology. Although some RMMs do not require a skilled operator once installed and validated, the process of validation requires a specialist approach specifically in terms of planning and this expertise may not exist within the company, as TMMs will not have required expertise of this kind. When a

RMM is being adopted, it is crucial that the right personnel are involved during the process so that a thorough understanding of the RMM capability is gained and expertise is transferred from the manufacturer to the operators [43].

A lack of awareness of new technologies amongst managers may result in no investigation into the applicability of RMMs, leaving the company potentially disadvantaged. Similarly, where innovation and cost saving are being made in other areas of the pharmaceutical production process that managers are conversant with, the perceived benefits of RMM adoption may be overlooked.

A further barrier is the validation required to satisfy regulation and legislation. If a company has a validated process for a pharmaceutical and this involves TMMs, then the cost and risk of validating the process with RMMs could be high and if unsuccessful may be viewed as a waste of resources. Companies can therefore be risk averse when it comes to the adoption of new methods that will require subsequent validation, due to the high cost and time involved. As previously mentioned, there are a number of pieces of official guidance on validation of alternative methods [44]. Not all of these guidance sources contain the same information, but rather, must be considered together to give the most information. This was highlighted by Sandle [45] when comparing the USP and EP chapters when it was noted that although the required information was present across all of the documents, it was not contained in one document. The most notable difference in these documents is the terminology for example, the USP refers to 'verification' whereas the EP refers to 'validation'. Differences in terminology and a lack of harmonized guidance can act as a barrier to the adoption of RMMs as these make the process of understanding regulation less straightforward and more time consuming. As chapters of these guidance documents undergo revisions, it is hoped that harmonisation can occur to make the documents more accessible and effective.

Technical barriers in the validation of RMMs include the number of parameters to be tested with a large number of test micro-organisms in order to validate the system, however, the use of these technologies in a process allows an increased knowledge of the microbiology associated with a pharmaceutical process and better management of deviations with rapid investigation of root cause and root entry.

Moving from one type of measurement to another is a technical barrier that can complicate validation, as TMMs were mainly concerned with CFUs whereas RMMs may use one of a number of different indicators including cell viability, cell count and spectral fingerprint. Moving from the indicators used in TMMs to those in RMMs would require a change in acceptance criteria within the pharmaceutical company and would also have to be considered by regulatory bodies.

As well as changes in the nature of the results and complex validation there are also barriers to the integration of the technology with existing technologies and workflows, and in some cases, extra requirement for lab space, such as MALDI-TOF MS due to the large instrument. Changes in operator routines may also be disruptive and require re-organisation and the wider applicability of the methods for other microbial testing secondary to the RMMs main application may need to be investigated. It is important however, that RMMs are not utilised for testing where they are not necessary i.e. where they provide no benefit over a TMM, as their implementation is resource intensive, as highlighted in this section.

2.7 Conclusions and future outlook for RMMs

This chapter has highlighted the potential advantages that RMMs can offer to pharmaceutical manufacturers and the barriers that exist to their implementation. The adoption of RMMs must be considered on a case-by-case basis and all factors given thorough consideration to ensure that the most appropriate approaches are adopted and that barriers to implementation can be overcome. The availability of RMMs is on the increase as instrument manufacturers develop new technologies. Despite recognition from regulators as to the importance of RMMs, a key barrier identified to the adoption of RMMs was the need for more harmonised regulation and guidance from the key regulatory authorities. There has been a slow adoption of RMMs in the EU and this has been attributed to a more complex regulatory approval process which has hindered approval compared to the system in the US [46]. In addition to this, TMMs continue to be utilised in the pharmaceutical industry as they are validated, suitable for many uses. With more harmonised regulation for RMMs and more companies now adopting RMMs it is anticipated that the sharing of best practice and information will increase the awareness and understanding surrounding these

methods and in turn may increase their adoption thereby improving the efficiency of microbial testing in the pharmaceutical industry. Recommendations for industry regarding RMMs are summarised in Chapter 8, section 8.1, Table 8-1.

Chapter 3. Comparison of the Rancimat and ACL Instrument for measuring the oxidative stability of corn and Menhaden oil

3.1 Introduction

This chapter investigates the performance of a chemiluminescence instrument, the ACL Instrument, against a standard instrument used for measuring oxidative stability, the Rancimat and also investigates operational aspects of the two instruments.

3.1.1 *The importance of oxidative stability testing in the pharmaceutical industry*

Oxidative stability is a key quality parameter and its measurement is utilised in many areas including: food shelf-life prediction [47, 48]; biodiesel analysis [49-51]; polymer degradation and durability studies [52-54] and pharmaceutical stability testing [56]. The occurrence of oxidation in raw materials and finished pharmaceutical formulations is highly undesirable and can result in a reduction in shelf life and in some cases lead to subpotent and/or dangerous products, thereby impacting on patient safety. Depending on the substance in question, other issues caused by oxidation can affect the quality of the product including colour changes and bad odours.

Stability testing of final pharmaceutical products is required before they can be released. A number of different types of stability studies are undertaken which involve subjecting the formulation to different combinations of heat, light and humidity over a range of time periods. These stability studies also contribute to the determination of appropriate packaging material and shelf lives of final formulations.

For substances that are known to be prone to oxidation, the problem of oxidation can be addressed to a certain extent through the use of antioxidants. However, problems can arise when substances thought to be stable to oxidation are contaminated with a pro-oxidant such as peroxides (residual levels of which are found in found in some excipients) and in this case may fall below the prescribed quality standards. Peroxides occurring due to autoxidation can be present in excipients at any ageing stage and may be a consequence of manufacturing conditions e.g. the use of hydrogen peroxide in cleaning processes. Peroxide levels in pharmaceutical formulations are critical as, elevated levels can lead to the early onset of oxidation before the end of the shelf life, which may affect the quality and safety of a final product. As well as the obvious

concerns for patient safety, elevated peroxide levels resulting in a drug recall can be extremely costly for a pharmaceutical company. There are several examples of recent alerts by the FDA on elevated peroxide levels in raw materials and oxidation in final formulations, for example in October 2010 high levels of peroxide were found in Crospovidone (cross linked polyvinyl N-pyrrolidone), which was manufactured by a Chinese company and imported into the USA. This contamination arose during a polymerization step of the manufacturing process and the peroxide level was 4 times the limit stated in global compendial monographs [57].

In 2008, Abbot recalled batches of Calcilo XD® Low-Calcium/Vitamin D-Free Infant Formula with Iron powder due to oxidation of the product inside the 400g cans. Warnings were issued about the possibility of gastrointestinal upset, nausea and sickness that might be associated with ingesting the oxidised product [58].

For these reasons it is important that peroxide levels and the oxidative stability of pharmaceutical excipients and final products continue to be tested. With the advent of biotechnology, drug formulations are becoming more complex and an increasing number of protein therapeutics are gaining market approval. Oxidation in these formulations in particular, can cause risks to patient safety and this must be fully investigated to ensure the safety of formulations and their resistance to oxidation. The oxidation of proteins can lead to modification of the protein structure which in turn can alter the action of the protein when it enters the body. The structural changes that can occur in proteins undergoing oxidation may also be difficult to characterise due to the complexity and size of the protein structure compared to the scale of the modification. The effect of oxidation of proteins is discussed further in Chapter 5 section 5.1.3. Oxidative stability testing is therefore crucial in this industry and must continue to develop and adapt to the advances occurring in new product development, to ensure it is fit for purpose.

Stability of excipients, those materials present in the formulation that do not exert the pharmaceutical effect, must satisfy the specifications set out in pharmacopoeias. Examples of specifications that must be within pharmacopoeial limits include peroxide value. These values do not however give the whole picture of the stability of an

excipient or what effect it might have on the final formulation over time, hence why the final formulation undergoes further testing over time.

In Chapter 5 the stability testing of polysorbates is investigated using alternative methods to those currently used in the pharmaceutical industry. By exploring the use of methods utilised for stability measurement in other industries, for example the Rancimat in the biodiesel industry and the ACL Instrument in the food industry, it may be possible to learn more about the stability of pharmaceutical excipients and exploit these alternative methods. New methods such as the ACL Instrument, which was previously only available as an individual laboratory constructed machine, have now been commercialised which makes the method suitable for further exploration into its applicability in excipient testing. Before introducing some of the methods available for measuring oxidative stability, a review of the autoxidation process is given.

3.1.2 *The autoxidation process*

Autoxidation is a process which is typically detrimental to the performance of the substance in question as it causes a change in chemical composition thereby affecting the behaviour of the substance and hence its function. The chemistry involved in the autoxidation reaction is complex with reaction pathways being dependent on the initial breakdown of the substance and how subsequent reactions propagate and terminate. For this reason, a universal test for oxidative stability is not available and hence measurement methods focus on sets of compounds produced at different stages in the autoxidation process.

In Edwin N Frankel's book titled '*Lipid Oxidation*' [59], a detailed discussion of autoxidation is presented, however for the purposes of this study the basic mechanisms by which autoxidation occurs are discussed, enabling an understanding of how the different oxidative stability testing methods work. The basis of these discussions is a simplified version of Frankel's explanations and reaction schemes.

Autoxidation is described as '*the reaction of molecular oxygen with organic compounds under mild conditions*' [59] and the pathway by which this process happens is extremely complex. Free radical autoxidation proceeds via a chain reaction process with initiation, propagation and termination stages. Free radicals are chemical species

possessing one unpaired electron which gives the radical high reactivity towards other chemicals.

There are a number of mechanisms and initiators (I) that can start off the autoxidation reaction including: heat, catalysts and light. The reaction of oxygen with an easily abstracted hydrogen atom has also been proposed as an initiation mechanism. At normal room temperature, hydrogen atoms that are 'activated' by neighbouring olefinic bonds or aromatic systems undergo autoxidation, in contrast to saturated hydrocarbons which are more stable under these conditions [60]. In reaction scheme 1, an initiator (I) abstracts a hydrogen from an unsaturated lipid (LH) to form a lipid free radical (L$^\bullet$):

$$\text{Reaction scheme 1} \qquad \text{LH} \xrightarrow{\quad I \quad} \text{IH} + \text{L}^\bullet$$
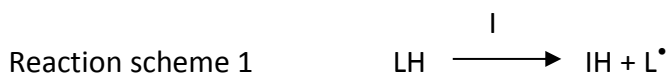
Hydroperoxides (LOOH) are present in lipid formulations and contribute to the initiation step of lipid autoxidation, shown in reaction schemes 1, 2, 3 and 4. The hydroperoxides can form radicals (LO$^\bullet$, $^\bullet$OH) through thermal decomposition (reaction scheme 2), catalysis by transition metals (TM) (reaction scheme 3) and via photodegradation when a sensitiser, in this case a ketone (RCOR), is exposed to light (*hv*) (reaction scheme 4).

$$\text{Reaction scheme 2} \qquad \text{LOOH} \longrightarrow \text{LO}^\bullet + {}^\bullet\text{OH}$$

$$\text{Reaction scheme 3} \qquad \text{LOOH} + \text{TM}^{2+} \longrightarrow \text{LO}^\bullet + \text{OH}^- + \text{TM}^{3+}$$

$$\text{Reaction scheme 4} \qquad \text{RCOR} + hv \longrightarrow \text{RCO}^\bullet + {}^\bullet\text{R}$$
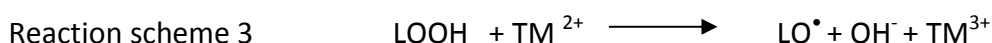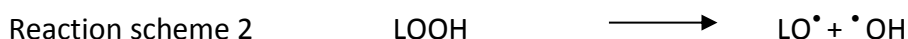
There are several propagation steps that can occur and some are faster than others depending on the structure of the molecule being attacked. Two of these steps are shown in reaction schemes 5 and 6. Formation of peroxyl radicals occurs when the lipid radical reacts with molecular oxygen (k_o) in a rapid reaction (reaction scheme 5). This occurs much more quickly than hydrogen transfer (k_p) between the peroxyl radical and an unsaturated lipid (reaction scheme 6).

$$\text{Reaction scheme 5} \qquad \text{L}^\bullet + \text{O}_2 \xrightarrow{\quad k_o \quad} \text{LOO}^\bullet$$

$$k_p$$

Reaction scheme 6 $LOO^\bullet + LH \xrightarrow{\quad} LOOH + L^\bullet$

The step in reaction scheme 6 occurs at the weakest hydrogen bond and happens much more slowly than reaction scheme 5, so is the rate-determining step of the reaction. It is for this reason, that the structure of the carbon backbone of a lipid and the position of hydrogens on the chain affect the stability of the lipid to autoxidation and how susceptible the molecule is to reactions with peroxyl radicals. Mixtures of isomeric hydroperoxides can be formed during the propagation stages, depending on exactly where the radicals attack in the chain.

For the reactions of autoxidation to terminate, radicals combine to give non-radical final products (reaction scheme 7) and as with the earlier steps of initiation and propagation, there are several ways this can occur.

$$k_t$$

Reaction scheme 7 $LOO^\bullet + LOO^\bullet \xrightarrow{\quad}$ non-radical product

$$k_t$$

Reaction scheme 8 $LOO^\bullet + LOO^\bullet \xrightarrow{\quad} [LOOOOL] \xrightarrow{\quad}$ non-radical products + O_2
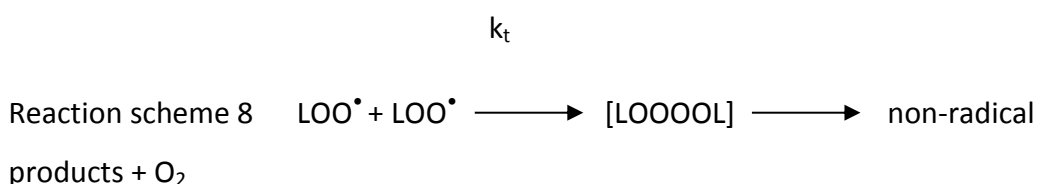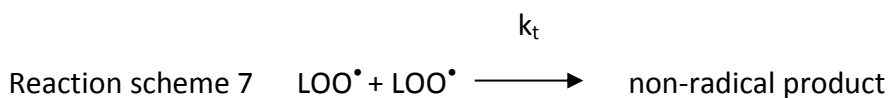
Some of the reactions that occur in the termination (k_t) stages, although generating a non-radical product, can also generate another radical which then goes onto propagate the reaction further. Reaction scheme 8 shows the termination stage at atmospheric pressure between two peroxyl radicals. The termination reaction proceeds via an unstable tetraoxide intermediate which upon decomposition via the Russell mechanism, gives non-radical products, O_2 and the emission of light. It is this 'chemiluminescence' (CL) emission that is measured by the ACL Instrument (section 3.1.5).

Alcohols can be generated by alkoxyl radicals reacting with unsaturated lipids (reaction scheme 9) and aldehydes and other unstable products can also be formed (reaction scheme 10). Although these are termination steps, a radical can still be generated which can go onto initiate further reactions. It is these final products of autoxidation,

alcohols and aldehydes, which are measured by the Rancimat method (section 3.1.4), as they dissolve in the water of the measuring vessel and cause a rise in conductivity.

Reaction scheme 9 $\qquad$ $LO^\bullet + LH \longrightarrow LOH + L^\bullet$

Reaction scheme 10 $\qquad$ $LO^\bullet \longrightarrow RCHO + L^\bullet$

Reaction scheme 11 $\qquad$ $2\ LOO^\bullet \longrightarrow LOOL + O_2$

Reaction scheme 12 $\qquad$ $LO^\bullet + L^\bullet \longrightarrow LOL$

Reaction scheme 13 $\qquad$ $2\ L^\bullet \longrightarrow L-L$

Reaction scheme 14 $\qquad$ $LOO^\bullet + AH \rightleftharpoons LOOH + A^\bullet$

Additional termination reactions can be caused by condensation between peroxyl, alkoxyl and alkyl radicals and at lower temperatures, peroxyl radicals can combine to form peroxyl-linked dimers and oxygen (reaction scheme 11). Ether-containing and carbon-carbons dimers can form at low oxygen pressures and high temperatures (reaction scheme 12), through the combination of alkyl and alkoxyl radicals. A further termination reaction which is extremely important and subject to much interest is the combination of a radical with an antioxidant (AH) (reaction scheme 14) [59]. The use of antioxidants is not widely discussed in this thesis, but is referred to in the future work section.

3.1.3 *Summary of methods for measuring oxidative stability*

The autoxidation process, as discussed, is a complex pathway with many stages, which differ depending on the starting chemical concerned. There is no universal test for oxidation, but a series of methods are available that focus on specific products along the pathway. A number of methods, including wet chemistry techniques, commercially available instrumentation and test kits are considered in this section and are summarised in Table 3-1. Several of the methods in Table 3-1 are performed on samples at room temperature, to determine their oxidation state at that particular point in time. This can give an indication of how a substance might behave after storage, but only limited information can be gained from a single measure under one set of conditions. The quote from Kanner *et al* [61], captures the essence of the complexity of oxidative stability testing. 'The complexity of the chemistry involved

defies the possibility of one, universal, analytical test for unconditional evaluation of the oxidation deterioration' [61].

As oxidation can be a slow process, measuring oxidation under normal storage conditions would take a significant period of time which could be unfeasible. In some substances, the onset of oxidation is not seen for years at room temperature. For this reason accelerated tests are undertaken which use high temperatures and gas flows to induce oxidation reactions more rapidly than would otherwise occur at room temperature.

With so many branches to the oxidation pathway, as evidenced from the reaction schemes discussed in section 3.1.2, it is often necessary to use several methods in combination, to obtain a clearer picture of the oxidative stability of a substance. Primary oxidation products, such as hydroperoxides, can be measured using iodometric titration to obtain a peroxide value (PV). Method Cd 8b-90 for the measurement of PV was published by the American Oil Chemists' Society [5]. An additional method for the measurement of the total hydroperoxides is the ferrous oxidation-xylenol orange assay (FOX2). This involves the spectrophotometric determination of Fe(II) under acidic conditions at 560nm, after complexing with xylenol orange. One test for the measurement of secondary oxidation products formed during the termination stages of autoxidation is the thiobarbituric acid reactive substances (TBARS) test, where levels of aldehydic substances including malondialdehyde are quantified. Other termination products, α and β alkenals are measured using the anisidine value (AV). UV absorbance at 233nm can be used to measure the conjugated dienes formed through the shifting of double bonds in polyunsaturated fatty acids (PUFAs) as the oxidation process progresses.

Assay	Principle	What does it measure?	Reference
Differential scanning calorimetry (DSC)	Measurement of weight loss and heat evolution respectively. They do not directly measure oxidation but are useful as a measure of stability and to understand the physical properties of a material.	Heat evolution.	[52]
Thermogravimetric analysis (TGA)		Mass change (mg) & ΔT ($^{\circ}$C).	
Ferrous oxidation-xylenol orange assay (FOX2)	Reduction of hydroperoxides by Fe(II) under acidic conditions, which forms a complex with xylenol orange and this is then measured using a spectrophotometer at 560nm.	Quantification of total hydroperoxides present.	[62]
UV Absorbance	Useful, convenient, rapid method for measuring oxidation of liposomal preparations. An oxidation index of the ratio of absorbance at 233nm to the absorbance at 215nm (A_{233nm}/A_{215nm}) would need to be defined for each instrument to account for variations between effects of stray light in different instruments.	Conjugated dienes and trienes caused by oxidation.	[63]
Iodometric assay	Refluxing in 10:1 isopropanol/acetic acid with excess sodium iodide, then determine I_3^- at 350nm.	Hydrogen peroxide and other hydroperoxides.	[64]
Peroxide value	Standard method – iodometric titration.	Total peroxides in oil (meq. Peroxide/1kg test sample).	[5]
Thiobarbituric acid reactive substances (TBARS)	Proposed over 40 years ago and commonly applied for measuring lipid peroxidation. Thiobarbituric acid reacts with malondialdehyde and the levels of the resulting compound can be measured using the spectrophotometer. Lacks specificity, as reaction conditions have large effect on colour, also other compounds could interfere with spectrophotometer reading.	Malonaldehyde levels.	[65-67]
Anisidine/ p-Anisidine Value	'100 times the optical density measured at 350nm, in a 1.0cm cell of a solution containing 1.0g oil in 100ml of a mixture of solvent and reagent'. Reported to be an unreliable method in some cases.	Short chain aldehydes e.g. hexanal, butanal.	[68, 69]
Peroxide test sticks - Quantofix®	Test stick is dipped into sample and after 5 seconds, is compared with a colour scale. Hydrogen peroxide turns the paper blue.	Hydrogen peroxide, other organic and inorganic hydroperoxides.	[70]
Rancimat	Accelerated method based on heating aerated sample and monitoring associated rise in conductivity of water in measuring vessel. Oxidation induction time (OIT) is used as the indicator of stability.	Conductivity change over time, OIT.	[72, 73]
ACL Instrument	Accelerated method based on heating and exposure of sample to air whilst measuring chemiluminescence (CL) emission.	CL of sample.	[75]
PetroOXY	Accelerated method based on pressure drop when sample is heated in a hermetically sealed chamber.	Induction time.	[76]

Table 3-1- Summary of methods for measuring oxidative stability

Real-time measurements such as PV and AV represent the stability of the substance at a particular point in time. Repeated measurements can be taken over time to track the level of oxidation however, in some substances the onset of oxidation is not observed for years at room temperature. Consequently these measurements are more suited to carrying out routine testing on incoming raw materials to determine their stability and state of degradation and whether they satisfy a pre-determined criteria. They are not appropriate for the determination of shelf-life of an intermediate or final pharmaceutical product. For this reason, accelerated stability methods that use elevated temperatures and increased gas flows to induce the oxidation process are used. Data from tests under accelerated conditions can then be extrapolated to predict stability at room temperature and to determine shelf-life.

The two accelerated methods used in this research are the Rancimat and the ACL Instrument (section 3.1.4 and 3.1.5). These instruments measure changes associated with the termination stages of autoxidation. More specifically the ACL Instrument measures chemiluminescence associated with the recombination of radical species and the Rancimat measures a change in conductivity of a measuring solution associated with the formation of volatile secondary oxidation products. Issues relating to accelerated stability testing include the extrapolation of data from exaggerated to normal conditions to predict shelf-life and this is explored in section 3.5.7.

3.1.4 *Measuring oxidation using the Rancimat*

The basis of the Rancimat method centres on the measurement of volatile secondary products formed during autoxidation: alcohols, aldehydes and carboxylic acids. The formation of these is associated with the termination stage of the autoxidation process as described in section 3.1.2.

A schematic of the Rancimat setup is shown in Figure 3.1 with the red arrows indicating the direction of the air flow. The sample (liquid or solid) to be analysed is housed in a sample tube which is positioned in a heating block. A stream of air is passed through the sample as it is heated. The secondary oxidation products are carried in the airflow from the reaction vessel to the measuring vessel where they dissolve in the deionised water and subsequently the air leaves the measuring vessel via the exhaust. A conductivity probe is positioned in the measuring vessel. When the

volatile secondary oxidation products dissolve in the water the conductivity change is recorded and this indicates the progress of the oxidation reaction. Two evaluation modes are available with the Rancimat: the induction period and the stability time.
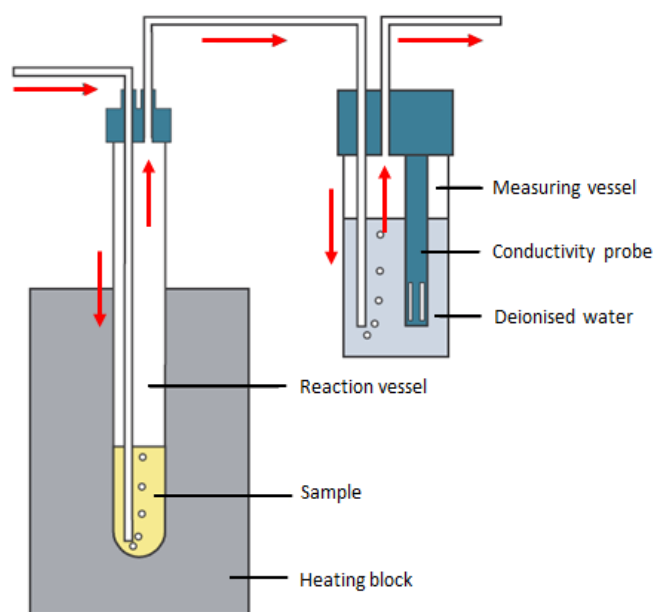
Figure 3.1 - Schematic representation of the Rancimat experimental set-up

The time-point associated with the rise in conductivity, caused by an increase in secondary products, is referred to as the induction period (IP). The IP is the time to the break point of the conductivity versus time curve, Figure 3.2, and determination is based on criteria regarding the height and width of the second derivative of this curve (section 3.4.6) and indicates the oxidative stability of a substance. IP is determined automatically but can be determined manually with tangents. IP can be compared across substances as long as the same Rancimat method (e.g. heating temperature and gas flow rate) is utilised. Within this thesis the IP will be referred to as the oxidation induction time (OIT) (with the exception of when discussing results from other authors), as the two terms are used interchangeably. The stability time (tΔK) is the time taken for a specific rise in conductivity to occur. In this case it was set to 50μs cm^{-1}, the value used by Mendez [72] when comparing Rancimat evaluation modes.

Due to the ease of sample preparation, the Rancimat is a simple and effective tool for measuring the oxidative stability of biodiesel, fats and oils, and its compact form means it is ideal for bench-top analysis. The machine is pictured in Figure 3.3. It has

been widely reported that the Rancimat method of measuring oxidative stability in fats and oils is both reproducible and easy to use [77, 78].

A typical graph produced by the Rancimat can be observed in Figure 3.2. In this case, 8 samples were tested simultaneously and their OITs are marked on the curves. Also measured in this case is the stability time. The OIT can be clearly identified in this case, as the period between the start of the measurement and the rapid rise in conductivity at 18 hours.
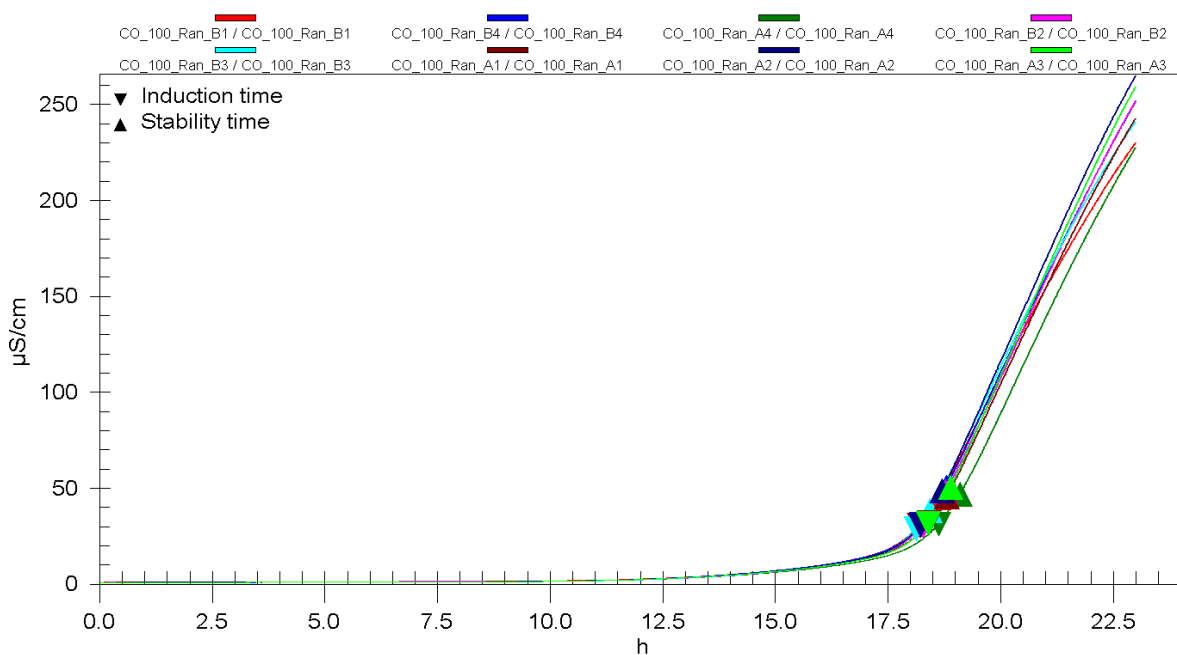
Figure 3.2 -Typical graph generated by Rancimat apparatus showing OITs and stability times

The Rancimat can be utilised as part of a European standard DIN EN 14112 [79] to perform determination of oxidative stability of fatty acid methyl esters (FAME). It can also be used as part of BS EN ISO 6886:2008 [80] in the determination of oxidative stability of animal and vegetable fats and oils.

Figure 3.3 – Rancimat [71]

3.1.5 *Measuring oxidation using chemiluminescence*

The ACL Instrument measures the chemiluminescence associated with the emission of photons during autoxidation. Chemiluminescence (CL) is defined as: '*the production of electromagnetic radiation (ultraviolet, visible, infrared) observed when a chemical reaction yields an electronically excited intermediate or product, which either luminesces or donates its energy to another molecule, which then luminesces*' [81].

The photons counted by the ACL Instrument arise during the termination stages of autoxidation when the recombination of the radical peroxide species causes the formation of an excited triplet carbonyl which upon relaxation to the ground state emits a photon via the Russell mechanism [82]. It is this label-free photon emission that is detected and recorded by the ACL Instrument. A schematic of the autoxidation reaction can be seen in Figure 3.4.
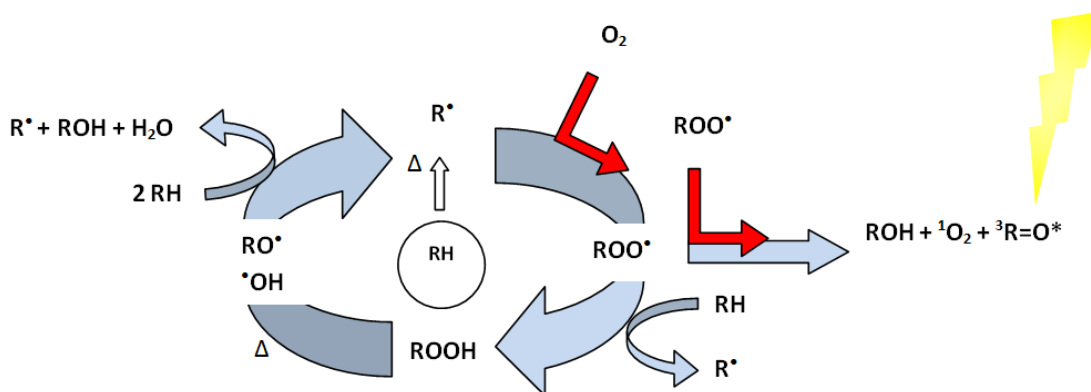
Figure 3.4 - Autoxidation of hydrocarbon based materials showing the emission of CL [83]

Initiation starts from the initial substance (RH) in the centre of the diagram and propagation is represented by the arrows circling the centre. The termination stage is shown on the right hand side of the diagram along with the generation of chemiluminescence, via the Russell mechanism, highlighted by the lightning strike.

Upon reaching a critical peroxide concentration, the oxidation begins to accelerate auto-catalytically and this is observed as a rapid increase in the CL intensity (CLI). The time that passes before this auto-catalytic event, is known as the OIT and is calculated with tangents placed on the CL curve. The oxidative stability and state of degradation can be analysed quantitatively with the ACL Instrument (Figure 3.5) and these measures can act as indicators of the quality of a material.

Figure 3.5 - ACL Instrument [84]

The ACL Instrument used in this study consists of a passivated silver furnace cell which facilitates precise temperature control (± 0.02K) and a cooled photomultiplier tube with photon counting capability. The shutter system (aperture) enables different photon counting modes such as: continuously open; continuously closed; or dark count

subtraction. A schematic of the ACL Instrument's furnace cell, aperture and detector is displayed in Figure 3.6.
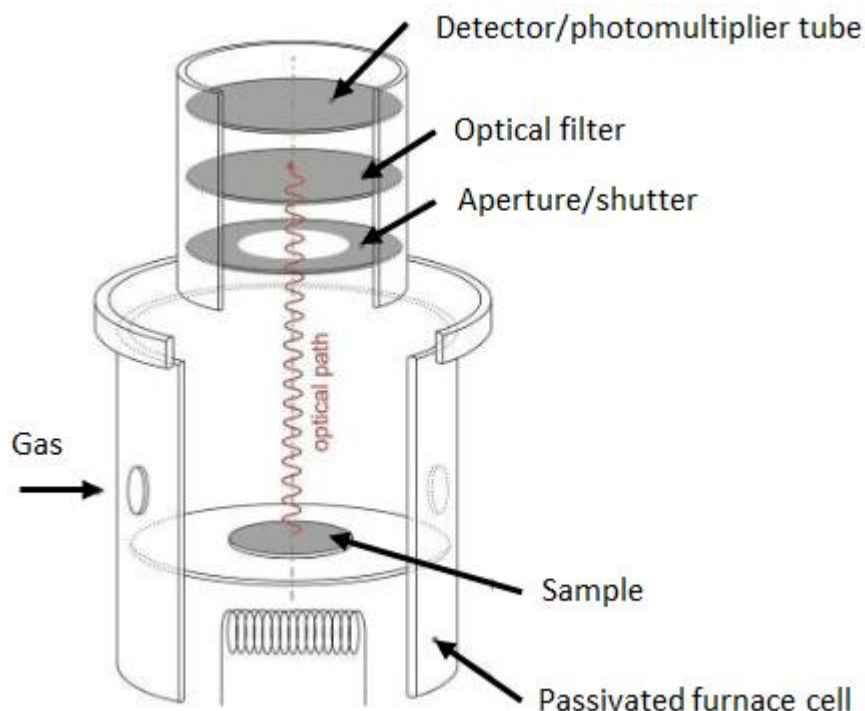
Figure 3.6 - Schematic of ACL Instrument furnace cell and detector [74]

Samples ranging from 1-50mg are weighed onto a sample holder, either an aluminium pan with a borosilicate glass cover or a borosilicate glass slide, which is then placed into the furnace cell. Nitrogen gas is used to purge the furnace cell in the initial stages of testing and synthetic air is used as a reaction gas for the testing of oxidative stability, with nitrogen used for testing of accumulated hydroperoxides. The use of the ACL Instrument for measurement of hydroperoxides through the testing of samples in a nitrogen atmosphere is discussed further in section 4.1. The furnace cell is heated (with a temperature profile determined by the operator, which can be isothermal or dynamic depending on the nature of the information that is required) and the photon counter is used to track the oxidation reaction via CL. Data can be acquired using several shutter modes, but in this research, the dark count subtraction mode was used. In this mode, the photo counter performs a photon count whilst the shutter is open and then whilst the shutter is closed. The instrument software then subtracts the closed count from the open count to account for noise arising in the detector. A CL curve is generated and the OIT is calculated using a tangent method. An example CL

curve is shown in Figure 3.7 and this shows the oxidation of a substance under isothermal conditions at 90°C.
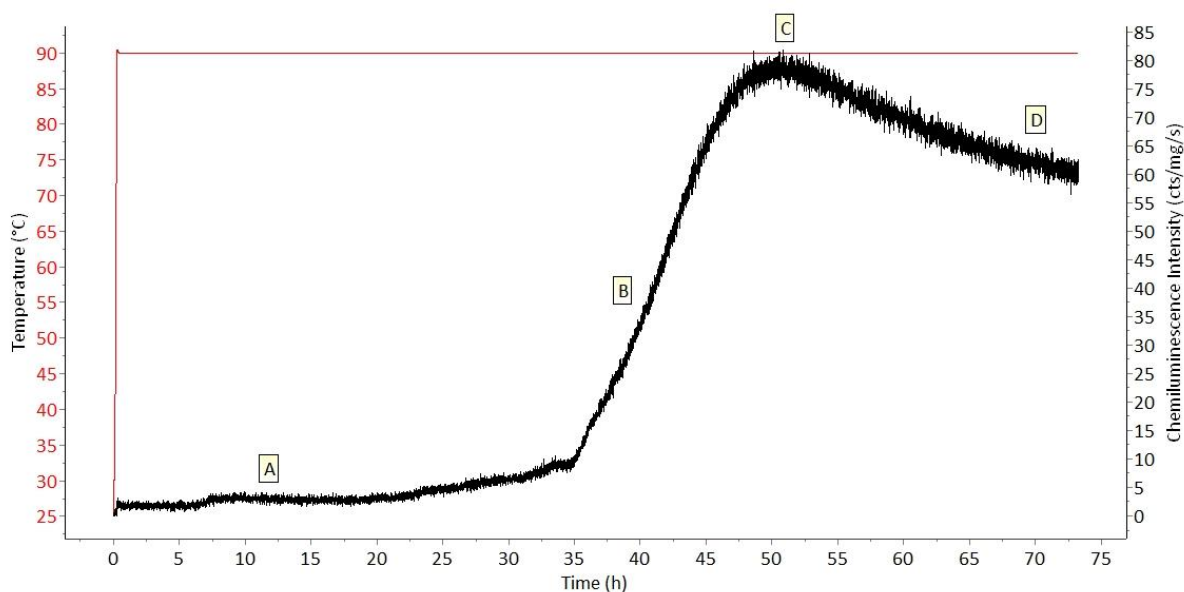
Figure 3.7 - Chemiluminescence curve showing the oxidation reaction progress.

A – induction period, no oxidation taking place
B – autoxidation begins, sharp rise in CLI
C – autoxidation reaction reaches its peak
D – extent of autoxidation reaction reduces, material is now different to starting material

Section A on the CL curve in Figure 3.7 shows the induction period, where very little oxidation is taking place between 0 and 20 hours. After 20 hours initiation begins which is evident through the gradual rise in CL. Section B shows a sharp rise in CLI which corresponds to the propagation of the oxidation reactions. Section C indicates the point at which the maximum CLI is reached and termination reactions begin to prevail, as the CLI drops. Section D, shows the progress of the termination stages and by this point the material has undergone oxidation and is different to the starting material. CL profiles can be more complex than the example in Figure 3.7 and these will be seen in later sections of this thesis.

In contrast to the widespread reporting on the use of the Rancimat for the measurement of oxidative stability, there are fewer papers on the application of CL, [73, 85, 86] with only two papers focussing on the use of the ACL Instrument for measuring stability [87, 88]. The operation of the instrument is addressed in two standards, DIN 51835-1 [89] and DIN 51835-2 [90], which concern the use of the ACL

Instrument for the determination of the oxidative stability of oils and lubricating greases (petroleum products) by CL. The ACL Instrument has not previously been compared to the Rancimat as a method for measuring oxidative stability of oils.

3.1.6 *Application of the Rancimat and chemiluminescence methods for measurement of oxidative stability of oils*

CL methods that have previously been utilised [86, 91-93] to measure oxidative stability have involved a number of reagents and steps. The advantage of the ACL Instrument is that no reagents are required and there is minimal operator input. The ACL Instrument measures the label-free CL arising directly from the test substance without the need for CL reagents. A previous study by Matthäus [73] compared the performance of the Rancimat and CL for assessing the oxidative stability of different vegetable oils. In this study, samples were removed from the Rancimat at a number of time points and tested in quadruplicate by a CL method involving luminol, a hemin catalyst and sodium carbonate. A correlation of 0.9865 was found between the IP determined by the Rancimat and the CL method for five different oils (walnut, safflower, sunflower and two rapeseed oils) at 120°C, with no significant difference between the mean IP for the two methods (P<0.005). The effect of temperature on the IP was also considered and analysis was performed at 110, 120, 130°C and it was shown that both methods were comparable (r=0.9978), with no statistical difference evident between the means (P<0.005) [73].

A study carried out by Burkow *et al* [86] looked at the effect of antioxidants on cod liver oil and compared the relative change in hypochlorite activated CL at 35°C with the IP determined at 80°C with the Rancimat. A correlation of 0.3390 was observed. It was hypothesised that the temperature difference of 45°C affected the mechanisms and degradation rates of the polyunsaturated fatty acids (PUFA). Additionally, it was conjected that the low correlation was a result of different ways of measuring the different products of oxidation. This is in contrast to Matthäus's [73] findings which showed a good correlation (r=0.9978) between results obtained using the Rancimat and CL methods, however as stated, different CL methods were used by Matthäus and Burkow.

3.1.7 *Specifications of corn oil and fish oil from Menhaden*

The stability of oil is greatly affected by the content and degree of unsaturation of the fatty acids contained within the oil. Edible oils that have a high degree of unsaturation are more susceptible to lipid oxidation [94]. Fish oil from Menhaden (referred to as Menhaden oil) and corn oil were considered in this research due to the different compositions of fatty acids contained within the two oils. Menhaden oil is of interest to the pharmaceutical industry as a number of fish oil products are present in companies' portfolios for nutraceutical use e.g. supplements.

Fatty Acid	Specification	
	Corn oil	Menhaden oil
<C14	≤ 0.1%	-
Myristic acid C14:0	≤ 0.1%	6-9%
Palmitic acid C16:0	8.6 - 16.5%	15-20%
Palmitoleic acid C16:1	≤ 0.5%	9-14%
Stearic acid C18	1.0 - 3.3%	3-4%
Oleic acid C18:1	20.0 - 42.2%	5-12%
Linoleic acid C18:2	39.4 - 62.0%	<3%
Linolenic acid C18:3	0.5 - 1.5%	<3%
Octadecatetraenoic acid C18:4	-	2-4%
Arachidic acid C20	≤ 0.8%	-
cis-11-Eicosenoic Acid C20:1	≤ 0.5%	-
Arachidonic acid C20:4	-	<3%
Eiscosapentaenoic acid C20:5	-	10-15%
Docosanoic acid C22	≤ 0.3%	-
13-Docosenoic (Erucic) C22:1	≤ 0.1%	-
Docosahexaenoic acid C22:6	-	8-15%
Tetracosanoic acid C24	≤ 0.4%	-
Unidentified fatty acids	-	20%
Peroxide	≤ 10.0	Not reported

Table 3-2 - Fatty acid composition of corn oil and Menhaden oil (from supplier's material specification)

Table 3-2 shows the fatty acid compositions of corn and Menhaden oil. The major differences between the two oils is seen in the content of Palmitoleic acid (C16:1), a monounsaturated fatty acid, with corn oil containing less than ≤ 0.5% and Menhaden oil containing between 9-14%. There is also a large difference between the content of

linoleic acid (C18:2), an unsaturated fatty acid, with corn oil containing 39.4-62% and Menhaden oil containing <3%. Menhaden oil also contains a higher percentage of polyunsaturated fatty acids (PUFA), 10-15% eiscosapentaenoic acid (C20:5) and 8-15% docosahexaenoic acid (C22:6), which are not reported to be present in corn oil and for this reason, it could be expected that Menhaden oil would have poorer oxidative stability compared to corn oil. Menhaden oil also contains 20% unidentified fatty acids, a category which is not reported in the corn oil specification. A graphical representation of the fatty acid composition of the two oils, Figure 3.8, allows comparison of the major differences.
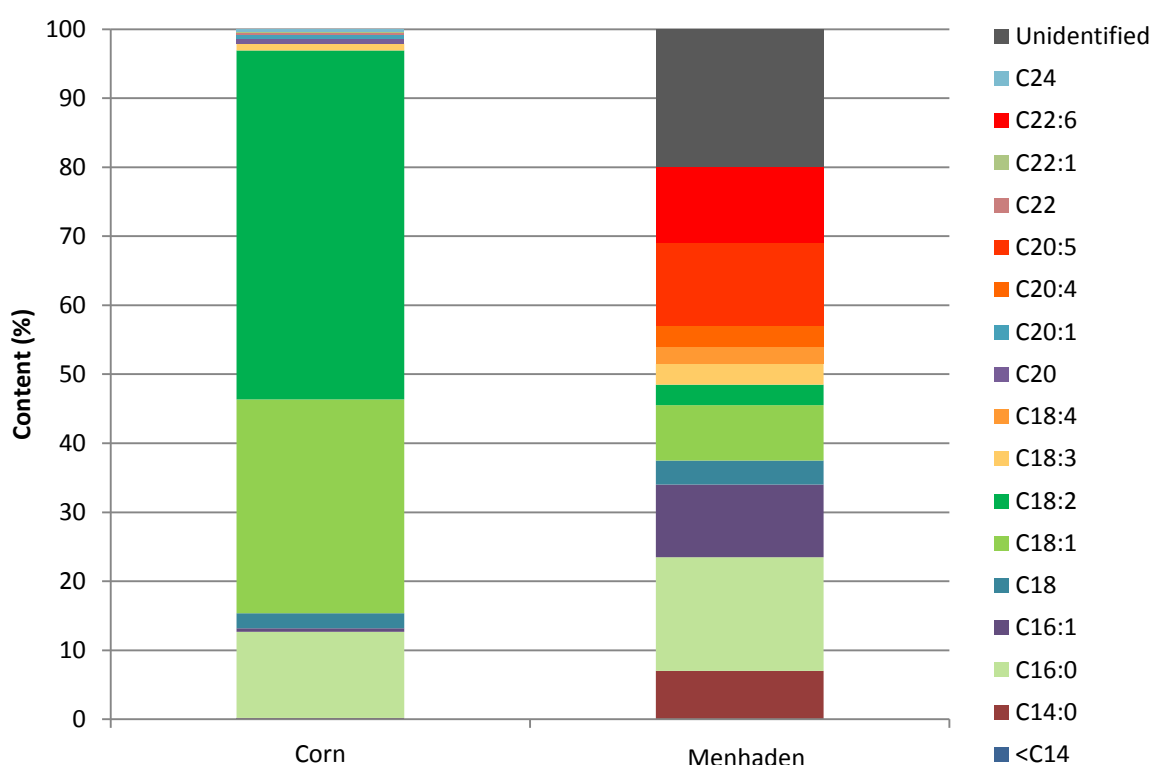
Figure 3.8 - Fatty acid composition of corn oil and Menhaden oil

The major differences in the fatty acid compositions of these oils, makes them ideal to compare using the two accelerated oxidative stability methods. If there is no dependence on oil type for CL measurements, then it could be expected that the ACL Instrument should give values that always corresponds to Rancimat OITs, however, it could be expected that the ACL values are dependent on oil type, as reports in the literature about measurement of peroxide value stated that there is an oil dependence effect [92]. Dependency on oil type would mean that a standard of known quality

would first need to be characterised using the ACL Instrument in order to compare each subsequent sample to.

As previously mentioned the structure of the carbon backbone of a lipid including the number and position of double bonds within the structure has a major effect on the susceptibility of the product to autoxidation. Unsaturated fatty acids are more prone to oxidation than saturated fatty acids due to the increased number of carbon-carbon double bonds (C=C) contained within the molecule. These provide a site at which radicals can attack. An example of the susceptibilities of fatty acids to oxidation is given for a number of different fatty acids: oleic; linoleic; linolenic acid and eiscosapentaenoic acid, that are present in the two oils considered in this thesis. Oleic acid (C18:1) (Figure 3.9) has one carbon-carbon double bond, linoleic (C18:2) (Figure 3.10) has two carbon-carbon double bonds and linolenic (C18:3) (Figure 3.11) has three carbon-carbon double bonds. Eiscosapentaenoic contains five carbon-carbon double bonds (Figure 3.12).
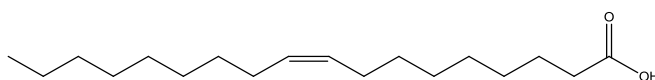
Figure 3.9 - Oleic acid
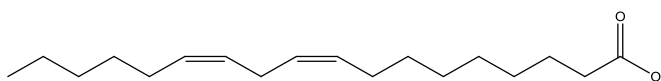
Figure 3.10 - Linoleic acid
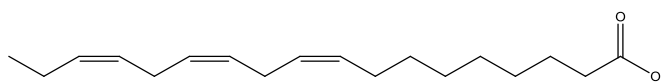
Figure 3.11 - Linolenic acid
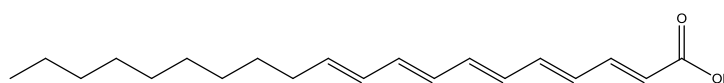
Figure 3.12- Eicosapentaenoic acid

The sites that are susceptible to radical attack in these fatty acids are the methylene groups allylic to the double bonds. These allylic C-H bonds, rather than other C-H bonds within the molecule, will react preferentially with radicals [95]. The higher the degree of unsaturation within the molecule, the more susceptible it is to oxidation, so in this case, the susceptibility of these fatty acids is linolenic>linoleic>oleic, with

linolenic being 2.4 times more susceptible than linoleic and linoleic being 40 times more susceptible than oleic [59].

By knowing the fatty acid composition of the oil, it is possible to draw conclusions about the oxidative stability of the oil. The percentage composition of fatty acids in fats and oils varies greatly between different types of oil. Due to the number of sites on fatty acid molecules that can be attacked by radicals, many radicals of different structures are formed during the initiation and propagation steps of autoxidation depending on the site of attack, contributing to the complexity of the autoxidation pathway.

3.2   Aim

Experimental work was undertaken to investigate the different operating modes of the ACL Instrument and to compare these with results obtained using the Rancimat. The investigation into the potential of new analytical methods and comparison to standards from other industries is important to the pharmaceutical industry, as it can facilitate the uptake of new analytical methods that may be more efficient, provide more information or for example cost savings. The particular focus of the experimental study was to:

1) determine whether a correlation exists between the oxidative stability values obtained from two accelerated stability methods: the Rancimat and the ACL Instrument.

2) investigate the effect of sample holder material used with the ACL Instrument and to make recommendations as to which material provides the most repeatable results.

3) investigate the effect of storage temperature on oxidative stability of corn oil to determine whether the ACL offers any advantages over the Rancimat for long term stability studies (up to 6 months in this case) where subtle changes in the oxidation state of a substance may occur

4) investigate whether the measures reported from the ACL Instrument are absolute, in that they will always correlate to the measurement given by the Rancimat, using a comparison between corn oil and Menhaden oil

5) review the operational considerations for the ACL Instrument and the Rancimat

3.3   Experimental

3.3.1   *Materials*

Corn oil and Menhaden oil were purchased from Sigma-Aldrich. Bottled synthetic air and nitrogen were obtained from BOC gases. 22mm borosilicate glass slides and aluminium pans (99.99% purity – Cr 0.144, Cu 1.62, Fe 1.67, Mn 0.05 ppm) with borosilicate glass covers were supplied by ACL Instruments. 150mm clear glass reaction vessels were purchased from Metrohm. Silicone oil for temperature determination on the Rancimat was purchased from Sigma-Aldrich. A Rancimat conductivity validation kit was purchased from Metrohm. Between runs, Menhaden oil was stored in an amber bottle, under nitrogen in a fridge at ~4°C. Corn oil was stored in an amber bottle, in the dark, under nitrogen at ambient temperature, conditions that have been used in a previous study with the Rancimat [96].

3.4   Methods

3.4.1   *Validation of the Rancimat*

Validation of the Rancimat heating block temperature and conductivity measurement was carried out in accordance with instructions from the manufacturer, Metrohm [71].

3.4.2   *Measurement of oxidative stability using the Rancimat*

Measurements of the oxidation induction times (OIT) of oils were made using an 873 Biodiesel Rancimat (Metrohm). Samples of corn oil were tested at 70, 80, 90, 100, 110, 120 and 130°C and samples of Menhaden oil were tested at 60, 70, 80, 90, 100, and 110°C. The low temperature of 60°C was not used for testing of corn oil, as run length at this temperature would have been over 400 hours which was unfeasible. Menhaden oil was not tested at 120 and 130°C due to its instability at high temperature which meant that at these temperatures oxidation would have happened at the point that the run was started, making data analysis difficult.

The Rancimat was operated using ambient air filtered through a molecular sieve (0.3nm pore size), at 10L/hr. 8 repeats (8 samples of the same batch of corn oil) were analysed simultaneously at each temperature and 3 repeats (3 samples of the same batch of Menhaden oil). 3 repeats of Menhaden oil were used as opposed to 8 repeats,

as the repeatability of the method was found to be satisfactory after the initial testing of corn oil (shown in Table 3-3). The number of repeats could therefore be reduced for efficiency and cost savings. Block A and B were used separately, with 3 samples in each block, meaning that two temperatures could be investigated simultaneously when investigating Menhaden oil. Samples (3.00g ± 0.01g) were housed in disposable 150mm clear glass reaction vessels. Isothermal heating mode was used for these experiments with the sample being introduced into the heating block once the desired temperature was reached.

Rancimat measuring vessels, conductivity probes and connecting tubing were cleaned rigorously between runs, using alkaline laboratory glass cleaning solution followed by rinsing with propan-2-ol and deionised water. They were then dried in an oven at 80°C for 2 hours, according to recommendations from Metrohm. Reaction vessels and glass air tubes were disposed of and replaced after each run.

Reference temperature correction values (ΔT) provided in the Rancimat user manual were applied across the temperature range 80-130°C. ΔT is the deviation between the current sample temperature and the temperature of the heating block. No reference ΔT value existed for 70°C so this was determined manually according to the method specified in the Metrohm Rancimat manual [71], using an external temperature probe and silicone oil. This determination was carried out in duplicate and the values were averaged to obtain a ΔT of +0.66°C for 70°C, which compared with the ΔT values published by Metrohm, +0.7°C for 80°C and +0.8°C for 90°C [71].

Automatic determination of OIT was used to avoid introducing error associated with the manual placement of tangents on the conductivity curve and the stability time was calculated as the time taken to reach a conductivity of 50μs cm^{-1}.

3.4.3 *Measurement of oxidative stability using the ACL Instrument with isothermal chemiluminescence*

Corn oil was used as a model substance as its oxidative stability is well documented [96, 97]. Corn oil samples were run with isothermal temperature profiles at 70, 80, 90, 100, 110, 120 and 130°C. Menhaden oil samples were run with isothermal temperature profiles at 60, 70, 80, 90, 100, 110°C, to provide a comparison to corn oil. The ACL Instrument was operated using bottled synthetic air at a flow rate of 1.8L/hr.

Runs were carried out in triplicate, except for corn oil samples at the lower temperatures of 70°C and 80°C where duplicates were performed due to the significantly long run times of between 5-10 days. Samples weighing from 9.00 – 13.8 mg were placed onto 22mm borosilicate glass slides and positioned in the centre of the furnace cell. Sample drops were carefully placed onto the centre of the glass slide to keep the geometry as similar as possible between samples.

Menhaden oil samples were subjected to a conditioning stage of 10 minutes at ambient temperature in nitrogen, in order to evacuate the sample compartment of oxygen and allow the sample to reach room temperature. Corn oil samples were conditioned for 6 minutes, as these were not subject to cold storage. Following this, the temperature was ramped up to the required isothermal temperature and the gas supply was switched to synthetic air. The machine's chiller unit was set to 20°C. If condensation was observed on the glass covering the detector between runs this, along with the furnace cell, were cleaned using propan-2-ol and pure cotton.

3.4.4 *Effect of sample holder material on oxidative stability of corn oil*

For the comparison of sample holder material, corn oil was used as a test substance. Aluminium pans and borosilicate glass slides were investigated. Isothermal runs were carried out in triplicate at 100, 110, 120 and 130°C, a common temperature range used in lipid oxidation studies of vegetable oils [78, 97]. Samples weighing from 18.40 - 23.40 mg were placed on aluminium pans with borosilicate glass covers and samples weighing from 18.60 – 24.60 mg were placed on glass 22 mm borosilicate glass slides. All samples were tested as described in the previous section 3.4.3.

3.4.5 *Effect of storage temperature on the oxidative stability of corn oil*

Corn oil samples stored in the dark for 6 months at ~4, ~27 and ~40°C were tested for oxidative stability at 0, 3 and 6 months using both the Rancimat and ACL Instrument. One sample (~4°C) was stored in the fridge (minimum 0°C, maximum 8°C, average 3.67°C), one sample (~27°C) in the laboratory (minimum 25°C, maximum 31°C, average 27.34°C) and one sample (~40°C) in an oven (minimum 39°C, maximum 42°C, average 40.15°C). Samples were tested in duplicate on the Rancimat at 100°C, 110°C, 120°C, with a gas flow rate of 10L/hr and on the ACL Instrument at 100°C, 110°C, 120°C.

3.4.6 *Data processing*

The OIT is a measure commonly used for a number of different techniques including differential scanning calorimetry, CL and the Rancimat, to indicate the oxidative stability of a substance [52, 73, 86]. The OIT is automatically calculated by the Rancimat software and is based on the maximum of the second derivative of the conductivity curve represented by a dotted line in Figure 3.13. The second derivative corresponds to the point where the maximum rate of change in conductivity of the distilled water in the measuring vessel is measured. The evaluation delay and evaluation suppression are two features of the method which can be used to delay the evaluation of the OIT or prevent the OIT being calculated if several oxidation events occur in one substance.
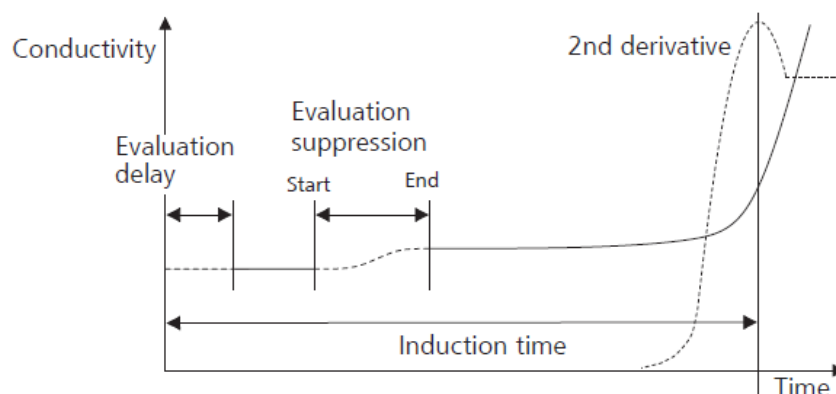
Figure 3.13 - Typical conductivity curve obtained from the Rancimat showing the relationship between second derivative and induction time [71]

The calculation of the OITs from the CL curves was carried out manually using Calisto, Thermal Analysis Software (AKTS/SETARAM Instrumentation). The CL curves were first smoothed using the Savitzky Golay filter function on Calisto. A low point filter (5 or 10 point) was applied as there was minimal noise in the signal. The OIT was then taken as the intersection of two manually-drawn tangents and it was corrected by subtracting the time that the sample was exposed to nitrogen from the OIT, to reflect the time that the sample was exposed to only synthetic air, as the initial ramp was carried out in nitrogen until isothermal temperature was reached.

The sections of the CL curve that were considered to be indicators of oxidative stability and that are discussed in this chapter are shown in Figure 3.14. These are: (a) the initial

rate or CL intensity (CLI_{ini}), defined as '*the emission rate that corresponds to the minimum intensity during an induction period prior to the main degradation CL peak*' [53] (b) the intensity of the maximum chemiluminescence signal (CLI_{max}); (c) the standard OIT measurement (OIT), (d) an OIT (OIT_{minor}) that occurs prior to the main OIT and (e) Peak-2, the peak associated with the OIT_{minor} in the early part of the CL curve. A slight inflection associated with OIT_{minor} was observed for corn oil and was investigated as an additional measure however, this may not be evident for every oil studied and may represent the occurrence of a different oxidation event to that associated with the main peak in the CL curve.
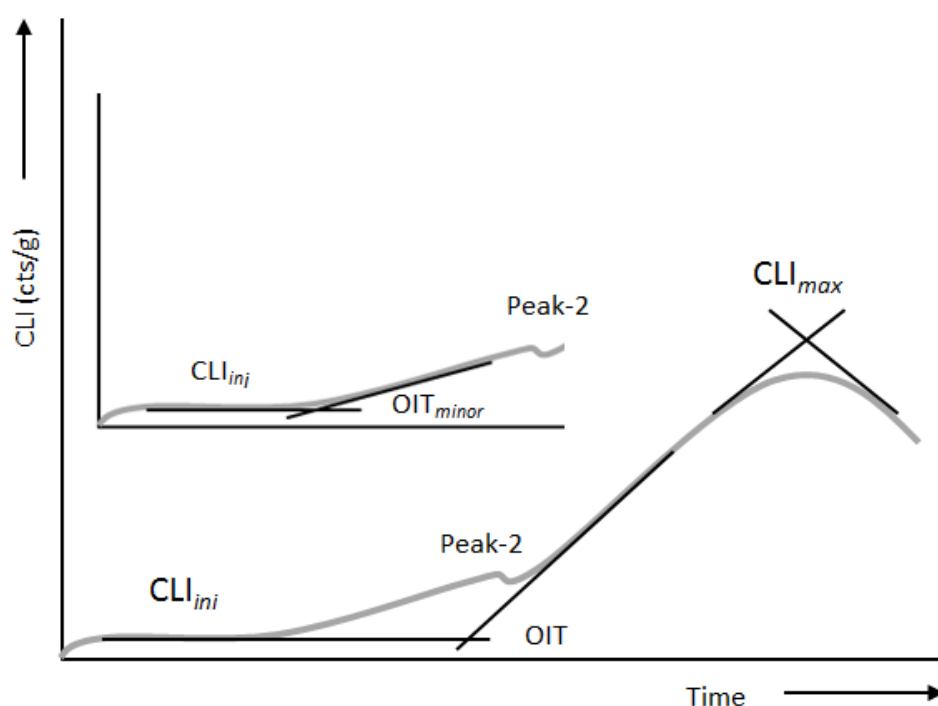
Figure 3.14 - Measures taken from the CL curve

3.5 Results and Discussion

3.5.1 *Initial testing of the ACL Instrument*

Initial testing of the ACL Instrument was carried out using the laboratory compressed air supply. It was found that the results were not repeatable in terms of curve shape, and hence it was decided to switch the air supply to bottled synthetic air to reduce the risk of contamination by lubricants in the compressor. In addition to this, CLI depends on the geometry of the sample and detector system and on the thickness and transparency of the sample. It has been claimed that comparison of CL intensities of

samples is not reliable [98]. The geometry of the sample is not easy to control. The volumetric pipette that was initially used for dispensing the oil samples was changed to a positive displacement pipette in an attempt to obtain more repeatable sample masses and geometries. It did however prove difficult to achieve repeatable sample masses, since due to the viscosity of the oil, a small amount of oil was also present on the outside of the pipette tip, which contributed towards the sample mass. Geometries were kept as similar as possible, with samples discarded if masses were so high that the shape of the drop of oil on the slide was much larger than previous samples. The photon count was normalised to mass and hence a range of sample masses was not detrimental to the results. Good repeatability was seen in results from this study, where geometry was controlled only by visual observation of oil spot size and shape.

3.5.2 *Initial testing of the Rancimat*

For the Rancimat the influence of sample size was not considered, as the sample size is specified in the standard method and hence the results can be compared to those values reported in the literature. The effect of temperature on oxidation was considered in the analysis. Physical form was not considered as this was not a parameter that was required to be investigated in this instance, as all samples of interest were liquids. Light was not considered in the analysis as it was not possible to eliminate light with the experimental set up and in addition to this, any effect of light can be mitigated through storage in the dark. Sample position (block A vs block B) was investigated and no significant differences were found between the sample mean OITs as shown in Table 3-3. Each block contained 4 samples. The column to the far right of Table 3-3 shows the p-value for the t-test carried out between the mean OIT of block A and block B at each different temperature. All p-values are above 0.05 indicating that there are no significant differences between the means measured in each block.

Temperature (°C)	Block A Mean (h)	Block A SD (h)	Block A SE (h)	Block B Mean (h)	Block B SD (h)	Block B SE (h)	2 sample t-test p value
130	2.18	0.13	0.07	2.27	0.06	0.03	0.29
120	4.41	0.05	0.03	4.38	0.12	0.06	0.66
110	8.95	0.08	0.04	8.88	0.08	0.04	0.30
100	18.42	0.17	0.08	18.22	0.07	0.03	0.07
90	38.44	0.26	0.13	38.63	0.19	0.10	0.30
80	84.96	0.40	0.20	84.97	0.60	0.30	0.99
70	174.10	27.10	14.00	194.20	6.94	3.50	0.25

Table 3-3 - Statistical testing of Rancimat means from block A and block B

3.5.3 *Measurement of the oxidative stability of corn oil*

In this study, the ability of the ACL Instrument to measure the oxidative stability of corn oil using CL was evaluated against a standard method, the Rancimat, which uses conductivity to quantify oxidative stability. Figure 3.15 shows the CL curves of corn oil for the temperature range 70-130°C. A clear trend is observed in terms of the shape and position of the CL curves over the temperature range studied. With every 10°C increase in temperature, the time to CLI_{max} approximately halves. This is in accordance with the literature [73]. The three measures from the CL curve (OIT, OIT_{minor} and time to CLI_{max}) were compared to the OIT and tΔK determined automatically by the Rancimat. These are compared graphically in Figure 3.19 and the results are summarised in Table 3-4 along with the standard errors of the mean (SEM) observed in the measurements taken by each instrument. The SEMs are similar when comparing the Rancimat and ACL OIT as the indicator, with the exception that at 70°C the SEM associated with the ACL OIT (1.20) was lower than for the Rancimat (2.30) indicating that in general the two instruments have similar precision. The OIT_{minor} and CLI_{max} measures were associated with higher error values across the temperature range 70–130°C and it can be concluded that the OIT is a more reliable indicator of oxidative stability. The standard error of regression (S) for each instrument was calculated from OIT measurements obtained across the temperature range 70–130°C. The ACL Instrument was more accurate with a smaller error (S = 0.0198675) compared to the Rancimat (S = 0.0326136).

The mean Rancimat OIT and the mean ACL OIT appear to be more similar for higher temperatures. However after performing a 2 sample t-test (Minitab 16 statistical software), it was found that they were significantly different (p=0.000) for all temperatures investigated. For two temperatures, 80 and 110°C, it was not possible to

perform a 2 sample t-test, as all results from the ACL Instrument were the same, giving rise to a standard deviation of zero.
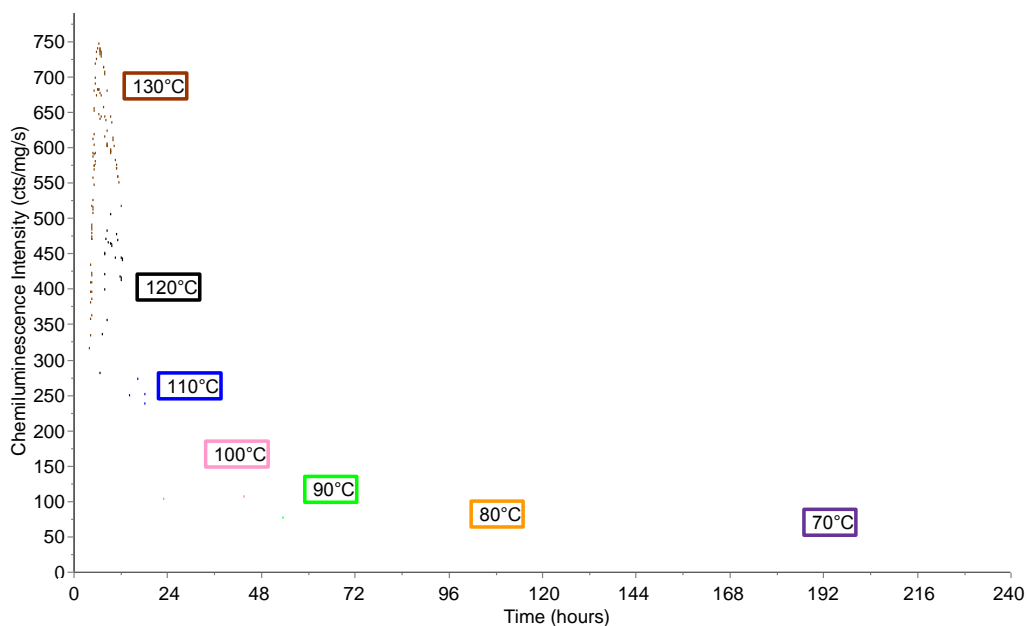
Figure 3.15 - CL curves of corn oil over the temperature range 70-130°C

	Rancimat		ACL Instrument		
Temp (°C)	OIT (h)		OIT (h)	OIT$_{minor}$ (h)	Time to CLI$_{max}$ (h)
130	**2.23^a*(0.04)**		**2.63^b*(0.00)**	**0.93^b** (0.00)	**5.83^b** (0.10)
120	**4.40^a* (0.03)**		**4.93^b*(0.08)**	**1.76^b** (0.03)	**9.06^b** (0.23)
110	**8.92^a(0.03)**		**9.23^b(0.00)**	**3.46^b** (0.03)	**15.50^b** (0.32)
100	**18.32^a* (0.06)**		**17.63^b*(0.08)**	**7.80^b** (0.19)	**27.50^b** (0.09)
90	**38.54^a* (0.08)**		**34.28^b*(0.12)**	**16.93^b** (0.00)	**49.40^b** (0.41)
80	**84.97^a(0.17)**		**71.73^b(0.00)**	**35.73^b** (1.39)	**97.33^b** (1.60)
70	**191.41^c*(2.30)**		**161.73^d*(1.20)**	-	**196.53^d** (0.00)

Table 3-4 - Mean values for the oxidation induction time (OIT), OIT$_{minor}$ and time to CLI$_{max}$ of corn oil measured by the Rancimat and ACL Instrument.
Values in parenthesis represent standard error of the mean (SEM)
[a] Average of 8 runs, [b] Average of 3 runs, [c] Average of 7 runs, as one outlier removed from Rancimat data set, [d] Average of 2 runs, * data with an asterisk are significant at P>0.000

Differences between the means of the indicators used to quantify stability using the Rancimat and ACL Instrument are expected as the machines measure oxidation in two different ways. Of more interest is to identify whether results from the Rancimat and the three measures quantified from the CL curve are correlated, indicating that the changes measured by each method although chemically different (secondary product formation by the Rancimat, and peroxide recombination by the ACL) are in agreement in terms of the progress of oxidation. Plotting the mean OIT results for the Rancimat

and the three measures quantified from the CL curve against each other, a strong correlation was observed, in

Figure 3.16, Figure 3.17 and Figure 3.18. The strong correlation (R^2=0.9995) between the Rancimat OIT and the ACL OIT (

Figure 3.16) and the similarity between induction times indicate that these two methods are potentially interchangeable for quantifying oxidative stability. Although the OITs differ in magnitude, as expected, the Rancimat OIT and ACL OIT$_{minor}$ correlation (Figure 3.17) was strong (R^2=0.9994). Using OIT$_{minor}$ as an indicator would mean that run times at temperatures at or above 100°C could be shortened however, below this temperature it was not possible to calculate OIT$_{minor}$. Although the slight inflection in the early part of the CL curve (OIT$_{minor}$) (position of which is shown in Figure 3.14) could possibly be used as an indicator of stability, further investigation as to whether this characteristic is evident in other oils is warranted and it was shown in this research that this early peak in the CL curve of corn oil was not a characteristic that was evident in the CL curves of Menhaden oil, Figure 3.20. A strong correlation (R^2=0.9988) was also observed between the Rancimat OIT and the ACL CLI$_{max}$ (Figure 3.18).
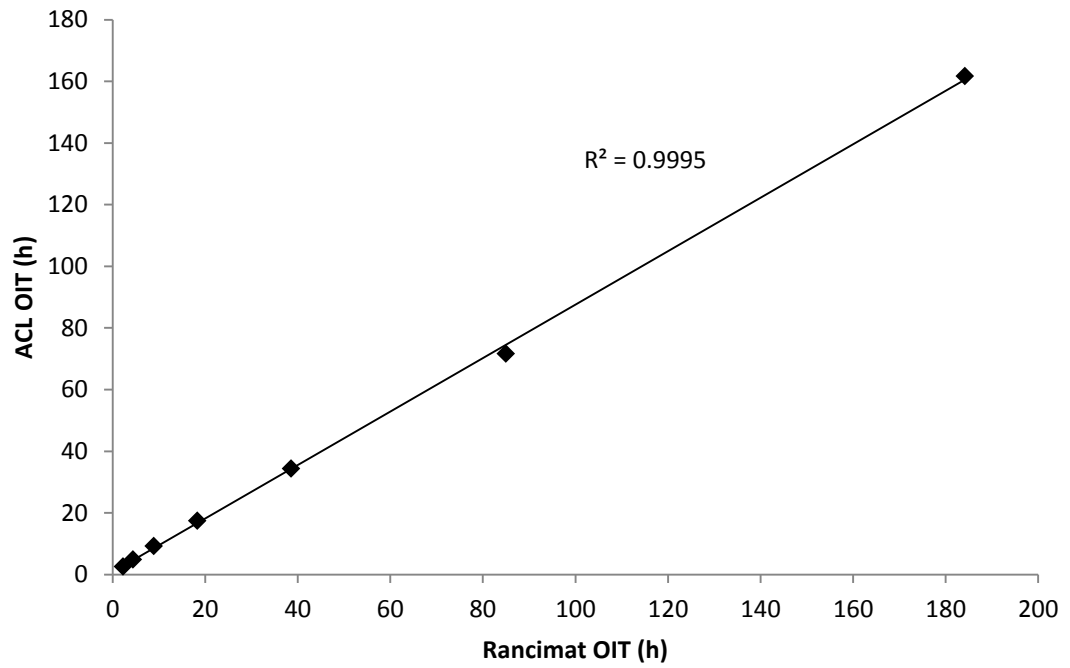
Figure 3.16 - Correlation plot for corn oil ACL OIT and Rancimat OIT
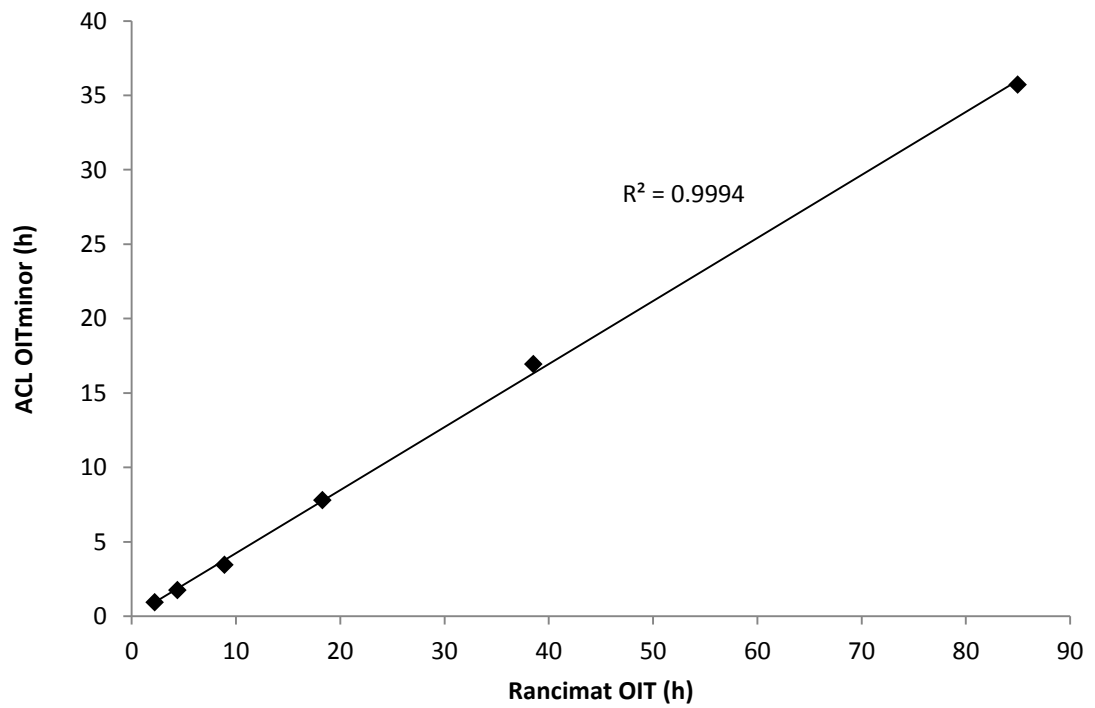
Figure 3.17 - Correlation plot for corn oil ACL OIT$_{minor}$ and Rancimat OIT
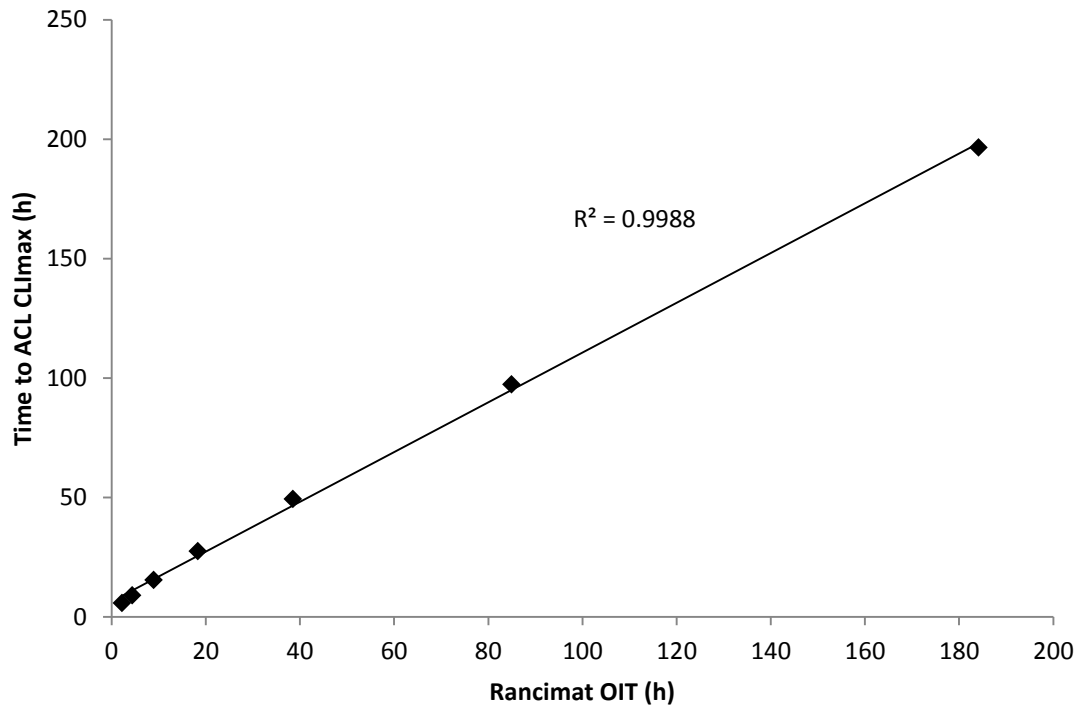
Figure 3.18 - Correlation plot for corn oil ACL CLI$_{max}$ and Rancimat OIT

A further measure calculated was the Q10 number which describes the increase in oxidation rate for a 10°C increase in temperature, calculated according to Equation 3.1 [77]:

$$Q10 = \frac{\text{OIT at T}}{\text{OIT at T} + 10°C}$$

Equation 3.1

The Q10 number describes the magnitude of the temperature effect on the oxidation rate of the oil, with a higher Q10 number indicating that a smaller temperature change is required to induce a certain change in the rate of lipid oxidation [97]. The Q10 numbers were calculated as: 2.09 (Rancimat OIT), 1.80 (ACL CLI$_{max}$), 1.99 (ACL OIT), 2.08 (ACL OIT$_{minor}$) and 2.04 (Rancimat tΔK), showing that the aforementioned trend holds, that with a 10°C increase in temperature the OIT approximately halves (indicated by a Q10 number of 2.00). The Q10 numbers were compared statistically using a two sample t-test and there was no significant difference between the Q10 numbers calculated using the Rancimat OIT and ACL OIT$_{minor}$ (p = 0.628) again indicating that these two measures compare favourably for the measurement of oxidative stability of corn oil. A statistically significant difference was found between

the ACL OIT and Rancimat OIT (p = 0.006) and the ACL CLI$_{max}$ and Rancimat OIT (p = 0.000).

The next step was to investigate the kinetics of corn oil oxidation as measured by the two methods. Natural logarithms of the OITs were calculated and plotted against the inverse temperature in an Arrhenius plot, shown in Figure 3.19.
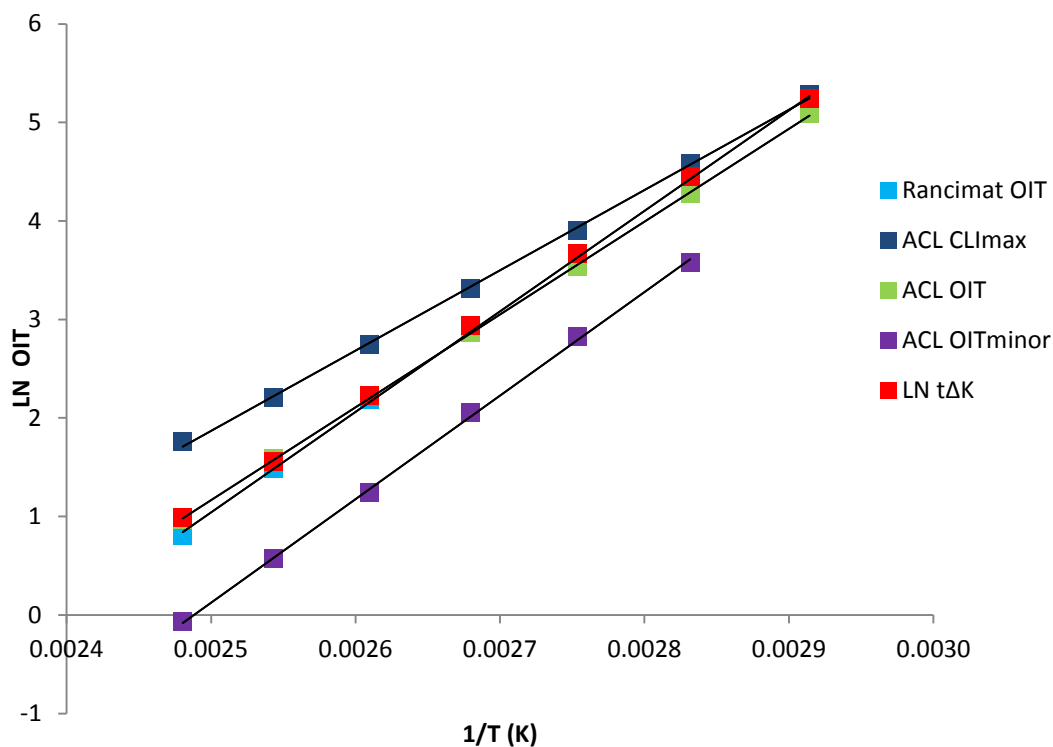
Figure 3.19 – Arrhenius plot of mean OITs and time to CLI$_{max}$ of corn oil as measured by the Rancimat and ACL Instrument over the temperature range 70-130°C.

An Arrhenius plot allows for the understanding of reaction kinetics with the gradient of the line corresponding to the activation energy of the reaction. Equation 3.2 is the linear form of the Arrhenius equation:

$$\ln(k) = \ln(A) - (Ea/RT)$$
<div align="right">**Equation 3.2**</div>

where k is the degradation rate at the event of the OIT, A is the frequency factor (intercept), Ea is the activation energy (kJ/mol) (gradient), R is the molar gas constant (8.3143 J/mol K) and T is the absolute temperature (K). The activation energies (*Ea*, kJ/mol) were calculated and compared for the various measures of stability taken from the CL and Rancimat curves and these are presented in Table 3-5.

Measure	Activation Energy (kJ/mol)	Frequency factor (A) (h^{-1})
ACL CLI$_{max}$	67.79	9.08×10^{-9}
ACL OIT$_{minor}$	87.44	4.31×10^{-12}
ACL OIT	78.33	1.90×10^{-10}
Rancimat OIT	84.81	2.39×10^{-11}

Table 3-5 - Activation energy and frequency factor for corn oil calculated from Rancimat and ACL Instrument measurements

The most similar *Ea* values were observed for the measurements from the Rancimat OIT, ACL OIT$_{minor}$ and ACL OIT. This suggests that the reactions occurring at the onset of oxidation associated with a rise in CL leading to the OIT$_{minor}$ and OIT event are also leading to the increase in conductivity associated with the OIT measurement for the Rancimat. The *Ea* is specific for each oil system [98], so it can be concluded that the similarity in the *Ea* values calculated for the Rancimat and ACL Instrument (in particular the OIT$_{minor}$) means that there is potential to use these methods interchangeably. Despite the ACL Instrument and Rancimat measuring different indicators of the oxidation reaction progress, CL and conductivity respectively, they provide similar kinetic information about the reaction.

3.5.4 *Measurement of the oxidative stability Menhaden oil*

The CL curves of Menhaden oil tested at temperatures 60-110°C are shown in Figure 3.20. From observing the curves at each temperature there appears to be a lack of repeatability in terms of peak height however the peak position is similar for triplicate measurements and when considering the calculated OITs and time to CLI$_{max}$, in Table 3-6, the low standard errors of the means show that the results were repeatable.
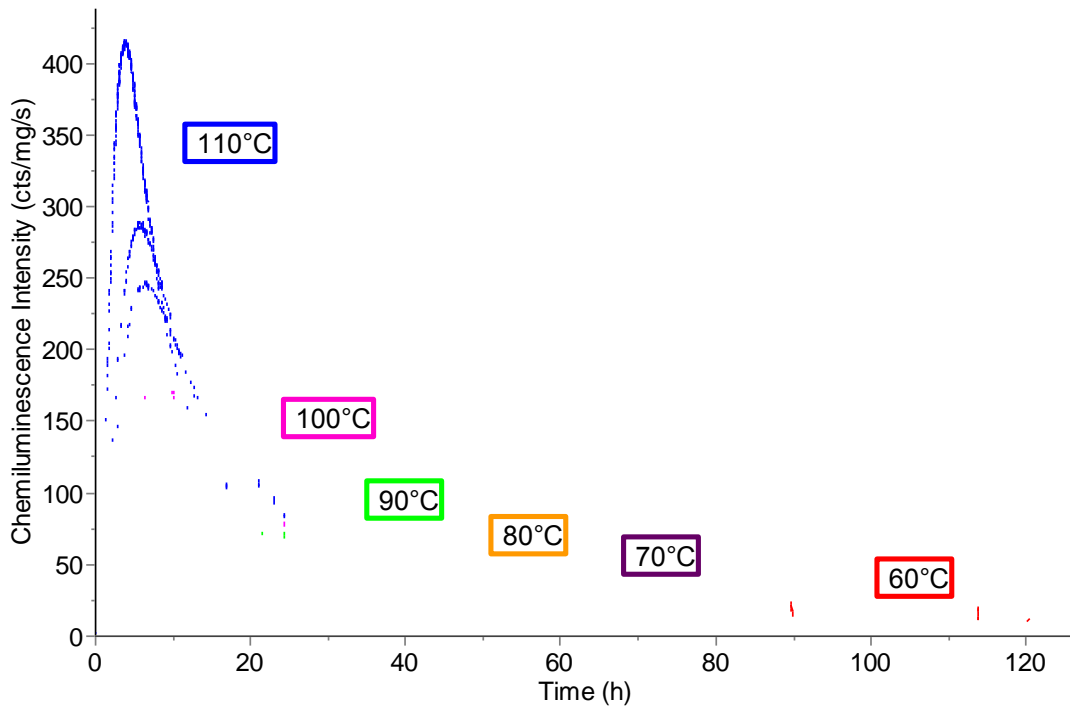
Figure 3.20 - CL curves of Menhaden oil oxidation over the temperature range 60-110°C

Samples were first tested across the set of temperatures and then this was repeated three times, rather than carrying out three repeats at each temperature. The rational for carrying out the runs in this order was because it was important to capture stability information across the range of temperatures before there was aging of the oil and this was a potential issue due to the runs at lower temperatures being in the order of 120 hours (5 days).

Figure 3.21 shows the OITs determined from the Rancimat and ACL Instrument and the tΔK (stability time) from the Rancimat and these approximately halve with every 10°C temperature increase, as would be expected. These values are summarised in Table 3-6.

Rancimat				ACL Instrument		
Temp (°C)	OIT (h)	tΔK (h)		OIT 1 (h)	Time to CLI_{max} (h)	Peak TLI (cts/g)
110	0.15 (0.03)	0.82 (0.02)		0.40 (0.06)	4.97 (0.75)	3.28×10^9 (9.33×10^7)
100	0.44 (0.00)	1.28 (0.04)		0.52 (0.10)	8.45 (0.55)	3.01×10^9 (1.30×10^8)
90	1.40 (0.11)	2.11 (0.05)		1.77 (0.20)	10.44 (0.66)	2.31×10^9 (7.62×10^7)
80	2.73 (0.02)	3.97 (0.05)		3.52 (0.38)	18.38 (0.38)	1.98×10^9 (8.08×10^7)
70	5.98 (0.02)	7.64 (0.13)		7.93 (1.28)	31.07 (2.87)	1.64×10^9 (1.15×10^8)
60	13.52 (0.07)	16.09 (0.31)		13.75 (1.33)	47.28 (1.02)	1.28×10^9 (7.23×10^7)

Table 3-6 - Mean values and standard error of the mean (in parentheses) for the measures for Menhaden oil taken from the Rancimat and ACL Instrument
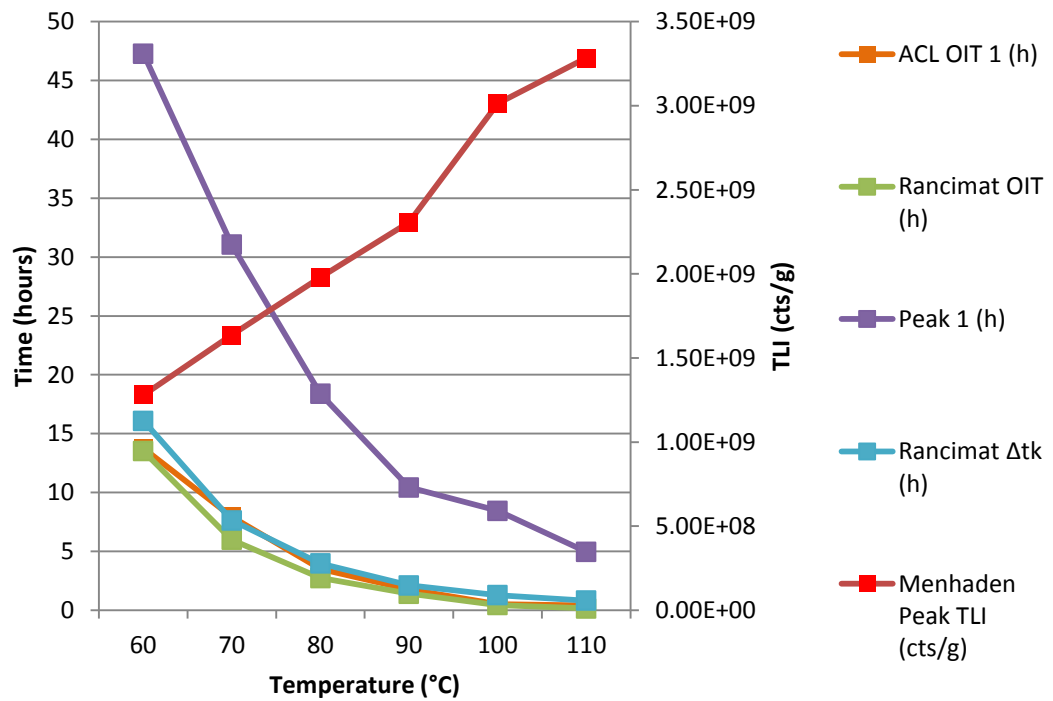
Figure 3.21 - Effect of temperature on stability of Menhaden oil, shown by different stability indicators from the ACL Instrument and Rancimat

Figure 3.21 shows that as the testing temperature increased the ACL OIT, Rancimat OIT and Rancimat tΔk followed a similar trend. The TLI to CLI_{max} increased linearly as the temperature increased, due to peroxide formation during oxidation, which gives rise to CL. Between the temperatures of 90 and 100°C there was a change in the slope of this linear relationship, possibly indicating a change in kinetics. In addition to this there was also a change in slope of the time to CLI_{max} data between 80 and 90°C. These possible changes in kinetics shown by the change in slope were not as clear with the ACL OIT 1 and Rancimat OIT data, however when this data is plotted as a natural logarithm of OIT in an Arrhenius plot, Figure 3.28, it became more evident and this is discussed later in this section.

For lower temperature oxidation between 60-90°C the linear trend holds and values for the Rancimat and ACL Instrument measurements are similar, however after the slope changes at higher temperatures of 100-110°C the natural logarithms of ACL OIT and Rancimat OIT are different to each other. This suggests that during higher temperature oxidation in Menhaden oil, chemical reactions giving rise to the ACL signal and Rancimat may be related in a different way to at lower temperatures. The

Rancimat tΔK follows a similar trend to ACL OIT values after the break in line slope, as well as before, following the trend of the ACL OIT 1.
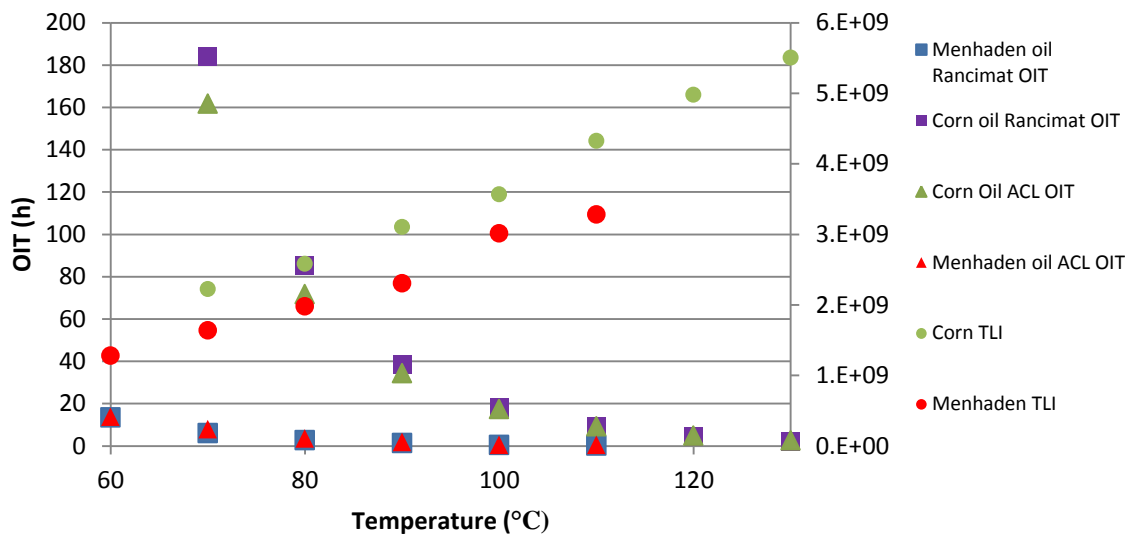
Figure 3.22 - OITs for corn oil and Menhaden oil measured using the Rancimat and ACL Instrument and TLI

Figure 3.22 highlights the differences in oxidative stability of corn and Menhaden oil shown in the Rancimat and ACL Instrument results. Measurements from both machines show that Menhaden oil has much lower OITs than corn oil, indicating that its oxidative stability is lower than that of corn oil. With Menhaden oil being less stable, it may be expected that the intensity of CL would be greater as a higher degree of oxidation takes place at the same temperature compared to corn oil, however this is not the case. What is in fact seen is that Menhaden oil has lower peak TLI than corn oil over the temperature range studied. This could be due to the nature of the hydroperoxides giving rise to the CL signal and this will be discussed further in Chapter 4 which investigates the measurement of hydroperoxides by CL and iodometric titration.

As for corn oil, a correlation analysis was performed to compare the results from the two machines for Menhaden oil oxidation. In this case there was no presence of OIT$_{minor}$ on the CL curve so this measure was not considered. From Figure 3.23 a good correlation between the ACL OIT and Rancimat OIT ($R^2 = 0.9827$) is observed.

The correlation between the Rancimat OIT and the time to CLI_{max}, Figure 3.24 is slightly lower (R^2 = 0.9646). Figure 3.24 reflects the results in Figure 3.20 and Table 3-6 which show that the time to CLI_{max} has poorer repeatability than the ACL OIT.
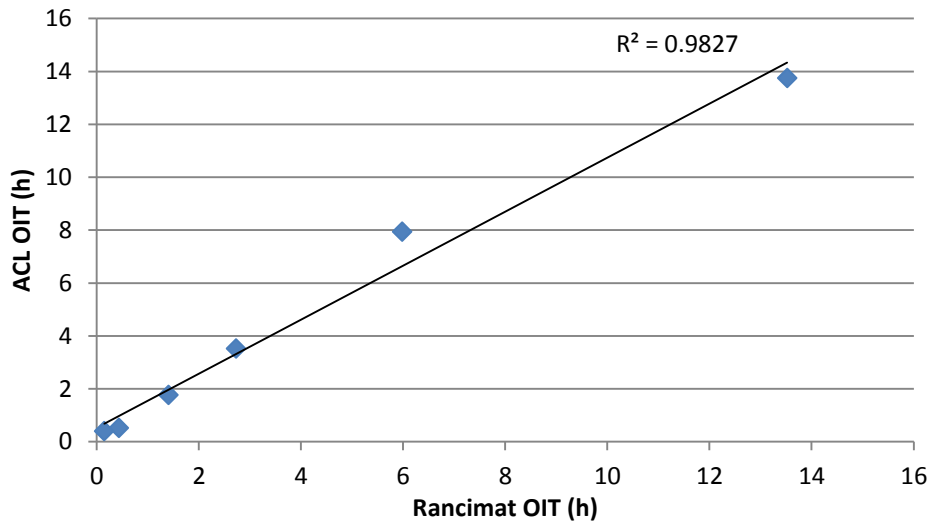
Figure 3.23 - Correlation plot of Menhaden oil ACL OIT and Rancimat OIT
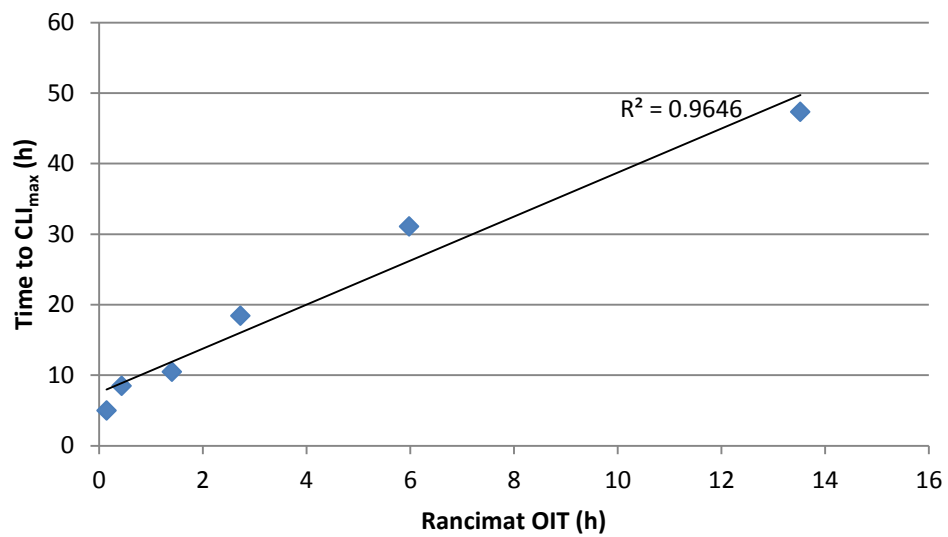
Figure 3.24 - Correlation plot of Menhaden oil Rancimat OIT and time to CLI_{max}
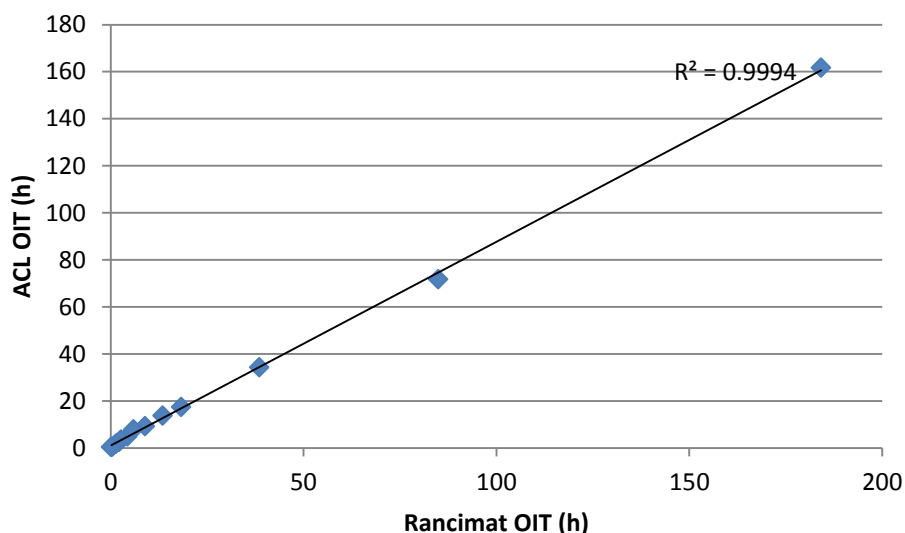
Figure 3.25 - Correlation plot of ACL OIT 1 and Rancimat OIT (corn oil and Menhaden oil)

Figure 3.25 shows the correlation between ACL OIT 1 and Rancimat OIT for all of the mean values of OIT for corn oil and Menhaden oil. The strong correlation (R^2 = 0.9994) indicates that there is a strong relationship between the OIT measures from the two instruments, indicating that the ACL OIT and Rancimat OIT measurements are capturing the same information, despite being based on different measurement principles. This is indicates that the relationship between ACL OIT and Rancimat OIT is not dependent on oil type and hence the ACL Instrument and Rancimat have the potential to be used interchangeably as methods for measuring oxidative stability of oils, as long as OIT is used as the indicator. It would be interesting to test an oil with a distinctly different fatty acid profile to investigate this further. Coconut oil or palm kernel oil, both contain much higher percentages of dodecanoic acid (C12) than corn oil and Menhaden oil, so would provide a good comparison.

When considering the relationship between the Rancimat OIT and the ACL TLI measurement, shown in Figure 3.26, there is a poor linear correlation between the results from the two oils. Billingham states that *'the TLI value is proportional to the amount of hydroperoxides in a sample and thus gives a measure of the degree of oxidation' [99].* These results show that the TLI does give a measure of the degree of oxidation, however it is oil dependant when considering the relationship with the Rancimat OIT, Figure 3.26 and the ACL OIT, Figure 3.27. There is a clear separation between correlation of Rancimat OIT and TLI for the two oils and between ACL OIT and TLI, which distinguishes between the two oils. The TLI data shown previously in Figure

3.22 showed a linear trend with increasing temperature for TLI, in contrast to the trend observed for Rancimat and ACL OIT which decreases by approximately half with each temperature increase of 10°C. Therefore for each oil, an increase in TLI corresponds to a greater degree of oxidation, however the TLI cannot be linked to the Rancimat or ACL OIT in terms of interchangeable measures.
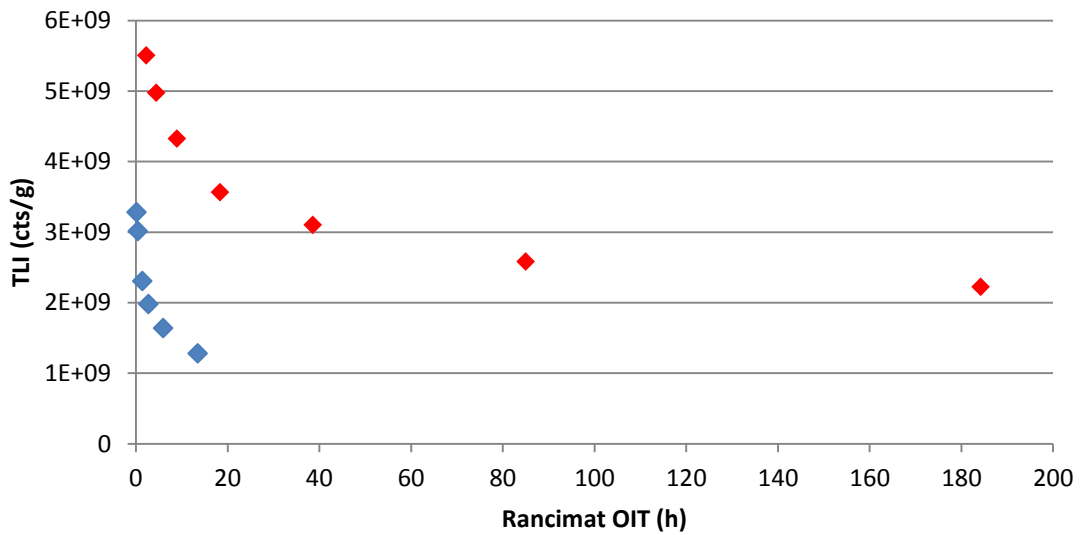
Figure 3.26 - Correlation plot of corn and Menhaden oil Rancimat OIT and ACL TLI Corn oil (♦), Menhaden oil (♦).
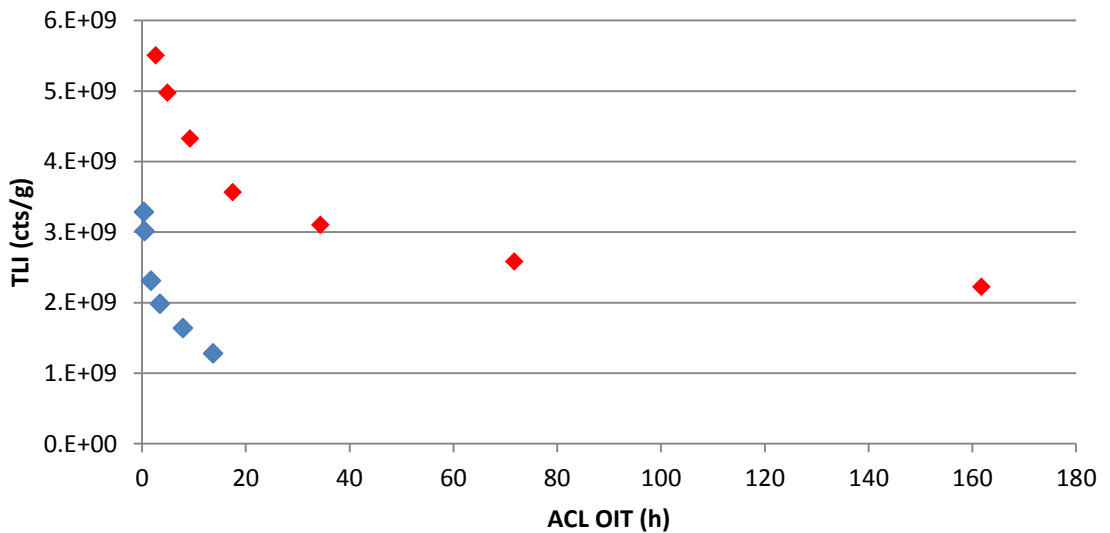
Figure 3.27 - Correlation plot of corn and Menhaden oil ACL OIT and ACL TLI Corn oil (♦), Menhaden oil (♦).

Temperature change (°C)	Q10 (Rancimat OIT)		Q10 (ACL OIT)	
	Menhaden oil	Corn oil	Menhaden oil	Corn oil
60→70	2.26	-	1.73	-
70→80	2.19	2.17	2.26	2.25
80→90	1.95	2.20	1.99	2.09
90→100	3.21	2.10	3.42	1.97
100→110	2.98	2.05	1.29	1.89
110→120	-	2.03	-	1.89
120→130	-	1.98	-	1.86

Table 3-7 - Q10 numbers for Menhaden oil and corn oil

Q10 numbers were calculated for Menhaden oil from the Rancimat and ACL OIT measures and compared to corn oil, Table 3-7. The Q10 number in the case of corn oil was approximately 2.00 with each temperature increase of 10°C, whereas the Q10 number for Menhaden oil was approximately 2.00 for the temperature range 60-90°C however between 90 - 100°C and 100 - 110°C, it increased to 3.21 and 2.98 respectively (Rancimat). This trend was also apparent in the results from the ACL OIT with a Q10 of 3.42 between 90 - 100°C which then dropped to 1.29 between 100 - 110°C. The increase in Q10 number to above 3, coincided with the change in kinetics at this temperature in Menhaden oil which was identified from the Arrhenius plot in Figure 3.28.
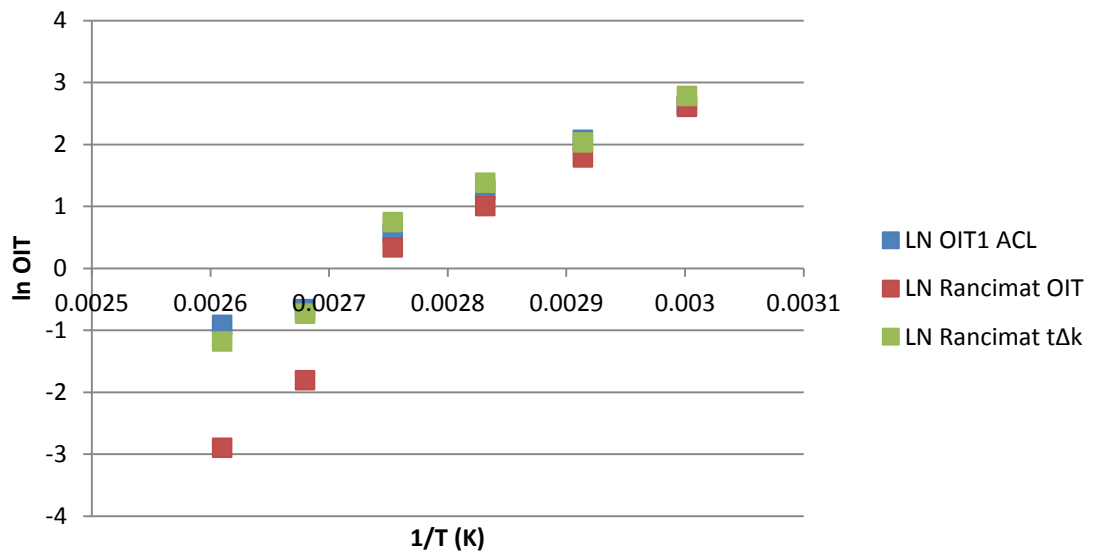
Figure 3.28- Arrhenius plot of Menhaden oil oxidation

The Arrhenius plot in Figure 3.28 shows the change in kinetics for temperatures 100°C and 110°C, as the straight line on the Arrhenius plot is interrupted and this

interruption is more pronounced in the Rancimat results than those of the ACL OIT. The linear relationship between temperature and induction period of fish oil oxidation has been reported in the literature by several authors, with fish oil being investigated at lower temperatures than vegetable oils as it is more sensitive to oxidation. The relationship between temperature and OIT of corn oil is linear across the range of temperatures 70-120°C (shown in Figure 3.19) whereas Menhaden oil only displayed a linear relationship between 60-90°C, beyond which the kinetics changed. Both the methods were able to distinguish this change in kinetics.

Measure	Activation Energy (kJ/mol)	
	Menhaden oil	Corn oil
ACL CLI$_{max}$	50.76	67.79
ACL OIT$_{minor}$	-	87.44
ACL OIT	69.94	78.33
Rancimat OIT	76.30	84.81
Rancimat tΔK	67.97	-

Table 3-8 - Activation energies of Menhaden oil and corn oil calculated from Rancimat and ACL Instrument measures

When comparing the *Ea* for the two oils, as shown in Table 3-8 it is clear that Menhaden oil has the lower oxidative stability of the two oils indicated by its lower activation energy when calculated using each measure. The lower stability of Menhaden oil compared to corn oil can be attributed to the higher percentage of PUFA in the oil that contain 3 or more double bonds, in contrast to corn oil which contains higher levels of monounsaturated fatty acids and PUFA with only 1 or 2 double bonds, as discussed in section 3.1.7.

3.5.5 *Effect of sample holder material on oxidative stability of corn oil*

Two sample holders are available to use with the ACL Instrument and these were both considered: borosilicate glass slides and aluminium pans with borosilicate glass covers. CL data obtained for each temperature were plotted against time, to observe how the oxidation reaction proceeded. Figure 3.29 and Figure 3.30 show the CL curves for corn oil tested using borosilicate glass slide samples holders and aluminium pan sample holders respectively. From these CL curves, OIT, time to CLI$_{max}$ and time to peak 2 were calculated along with the relative standard deviations (%RSD) and these are summarised in Table 3-9. When considering the results from the runs carried out using aluminium pans, the determination of OIT and OIT$_{minor}$ was difficult as the oxidation

reaction began quickly hence there was a lack of baseline from which to draw the tangent, so the time to Peak-2 rather than OIT$_{minor}$ was considered.
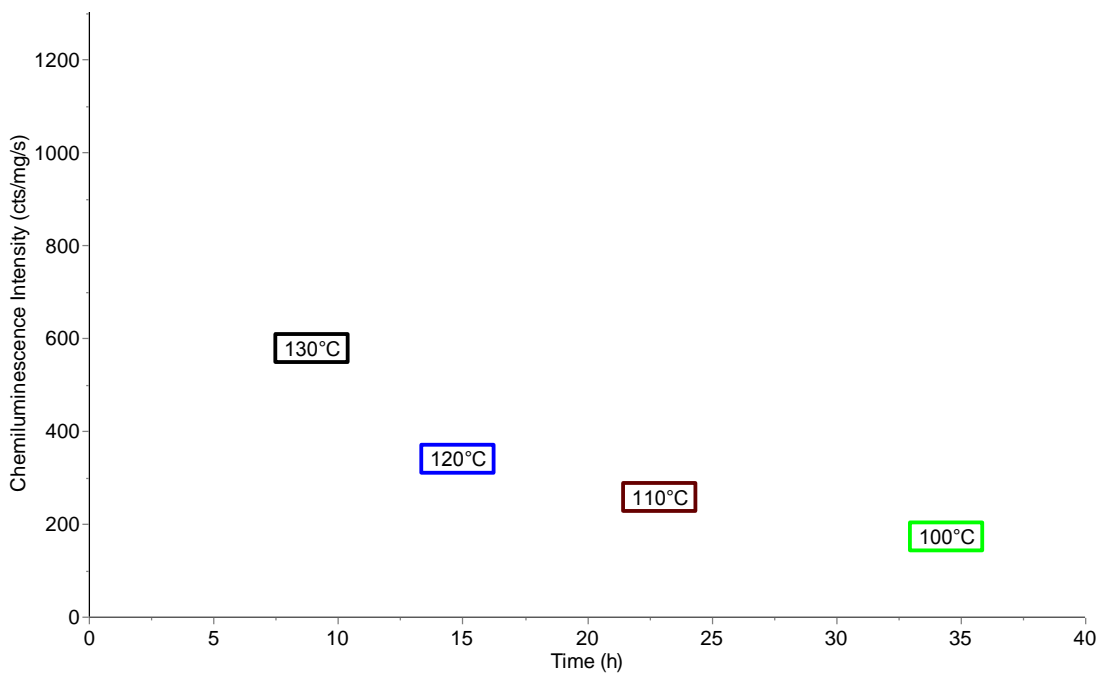
Figure 3.29 - CL curves of corn oil obtained using borosilicate glass slide sample holders
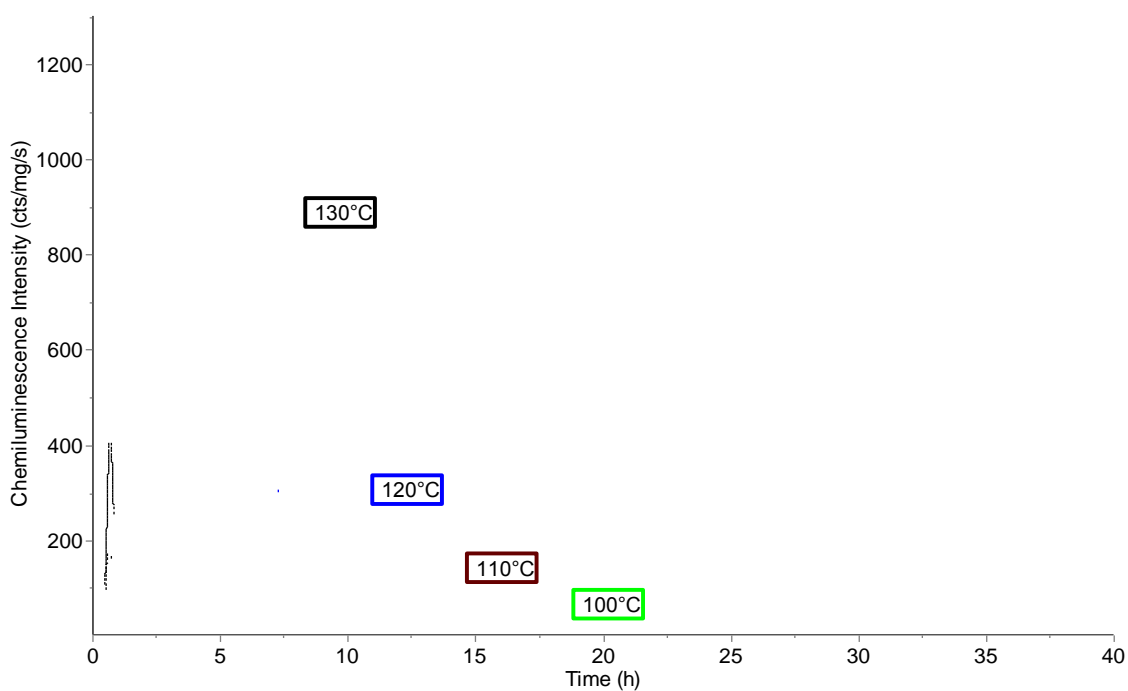
Figure 3.30 - CL curves of corn oil obtained using aluminium pan sample holders

Measure	%RSD at 130°C		%RSD at 120°C		%RSD at 110°C		%RSD at 100°C	
	Aluminium	Glass	Aluminium	Glass	Aluminium	Glass	Aluminium	Glass
CLI_{max}	11.89	2.43	87.30	1.51	35.46	2.08	86.70	2.04
Peak 2	29.85	3.62	23.60	1.79	46.28	1.55	23.23	1.13
OIT	52.22	2.63	53.85	1.32	51.04	1.92	69.00	0.45
TLI to CLI_{max}	58.99	8.95	81.26	3.15	75.90	2.19	75.49	4.72
TLI to peak-2	54.07	4.47	19.47	4.68	34.78	22.68	37.41	10.74

Table 3-9 - % Relative standard deviations for measurements carried out on aluminium pans and glass slides

When comparing Figure 3.29 and Figure 3.30 an initial peak observed to be present in the CL curve using borosilicate glass slides was much more pronounced for the aluminium pans and the CLI_{ini} increased when the aluminium pans were used, indicating that a higher level of oxidation was occurring. The oxidative stability of corn oil was found to be much lower for the aluminium pans, with OIT being much shorter. Higher CLI values were observed during the runs carried out on aluminium pans and also the time to CLI_{max} was much shorter, for example CLI_{max} was 10h at 120°C with borosilicate glass slides whereas CLI_{max} was 5h at 120°C with an aluminium pan.

Although the aluminium pans have a purity of 99.99%, the metals that are present in trace quantities, Cr 0.144, Cu 1.62, Fe 1.67, Mn 0.05ppm, appear to be exerting a catalytic effect on the oxidative stability of corn oil. Thus it is hypothesised that the lower apparent oxidative stability of corn oil when measured using aluminium pans, compared to borosilicate glass slides, is due to traces of metals which react with the fatty acids contained in the corn oil. This conclusion is endorsed from the results of a previous study [87]. It is well known that transition metals may catalyse lipid oxidation and these results further confirm these findings [100, 101]. Furthermore, some of the oxidation reactions appear to be quenched when aluminium pans were used, in contrast to when glass slides were used and the reactions continued. This could be attributed to the ppm amounts of metals present in the aluminium pan catalysing the decomposition of hydroperoxides [59, 102]. Overall the repeatability of the experiments was much better when using borosilicate glass slides compared to aluminium pans, as observed in Figure 3.29 and Figure 3.30 and quantitated through the analysis of the relative standard deviations (%RSD) of the OITs, Table 3-9. As well as looking at the OIT data and the shape of the CL curves, it is also possible to consider the *Ea* of the corn oil oxidation reaction. It has been reported that metal catalysts

lower the *Ea* of the oxidation reaction by increasing the rate of lipid oxidation by around 42-59kJ/mol [59]. Figure 3.31 shows the Arrhenius plot for corn oil oxidation measured using the two different sample holders.
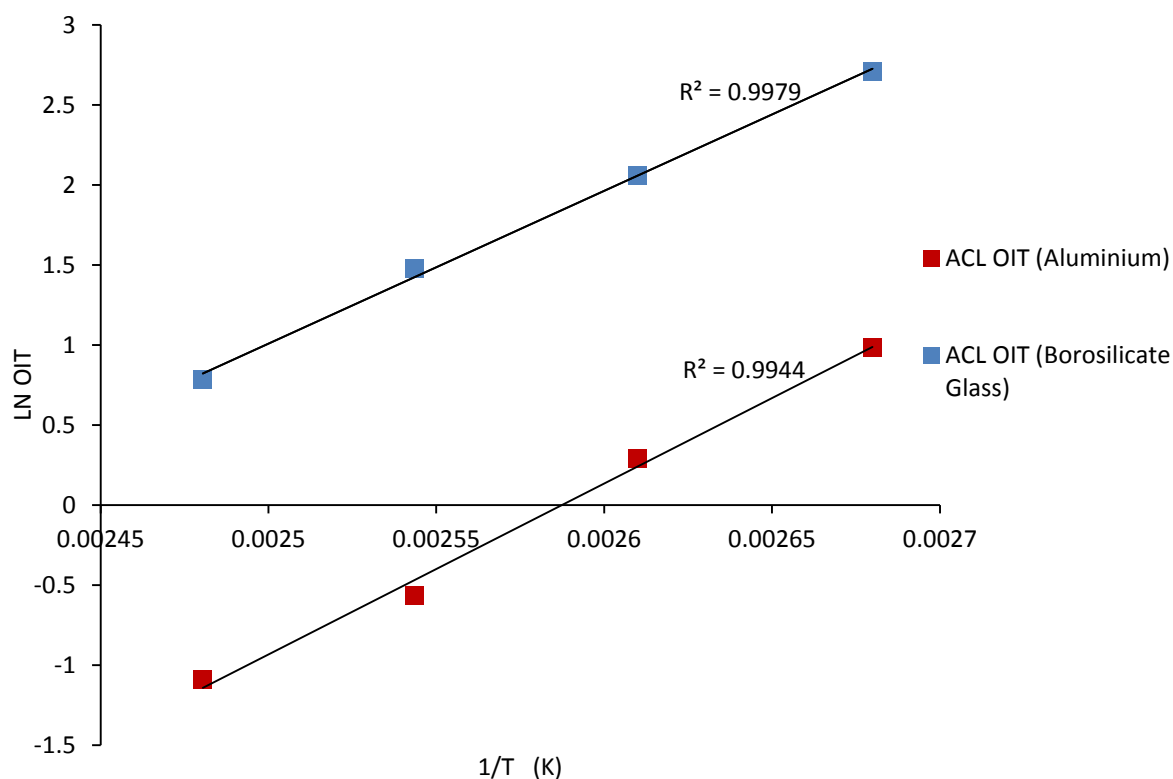
Figure 3.31 - Arrhenius plot for corn oil oxidation with aluminium pan and borosilicate glass slide sample holders

Measure	Aluminium		Glass	
	Activation Energy (*Ea*) (kJ/mol)	Frequency factor (*A*) (h^{-1})	Activation Energy (*Ea*) (kJ/mol)	Frequency factor (*A*) (h^{-1})
OIT	88.85	5.45 x 10^{-11}	79.39	7.05 x 10^{-9}
CLI$_{max}$	34.96	6.41 x 10^{-3}	60.01	6.34 x 10^{-7}
Peak 2	81.36	7.63 x 10^{-10}	88.95	4.81 x 10^{-12}

Table 3-10 – Activation energy and frequency factors of corn oil with different sample holders

Ea values calculated using measures from the CL curve for aluminium pans and glass slides are presented in Table 3-10. It was found that the aluminium pan reduced the *Ea* by 25.06kJ/mol, compared to using borosilicate glass slides, when using the CLI$_{max}$ data to calculate the *Ea*. When using the peak 2 data to calculate the *Ea*, the *Ea* observed when using borosilicate glass slides (88.96kJ/mol) was reduced by 7.62kJ/mol by using aluminium pans (81.36kJ/mol). Both of these observations suggest that the aluminium pans are having the effect of lowering the *Ea* of corn oil oxidation, however, when considering the *Ea* calculated from the OIT measurements, it was found that the *Ea*

when using borosilicate glass slides was increased by 9.46kJ/mol compared to when using the aluminium pan, which is in contrast to the results from the CLI$_{max}$ and peak 2 data. This apparent increase in corn oil Ea could be attributable to the larger variation in the data from the results with aluminium pans, which is represented by the large relative standard deviations, Table 3-9, causing the mean to not be representative of the data. This was compounded by the difficulty in calculating the OIT as placement of tangents on curves that lacked a baseline was problematic.

The results obtained indicate that there is a clear effect of sample holder material on the oxidative stability of corn oil and this is implied by the differences in shapes and repeatability of curves obtained for the two types of sample holder. Significant differences ($p < 0.05$) were observed between the results from the aluminium pans and borosilicate glass slides for all parts of the curve measured. Consideration of Ea calculated using CLI$_{max}$ and Peak-2 data shows that aluminium pans reduce the Ea of corn oil oxidation however the calculations of Ea using OIT contradict this, showing glass slides to reduce the Ea. This was attributed to difficulties in tangent placement and the resulting misrepresentation of the means due to the large relative standard deviations in the results from aluminium pans.

3.5.6 *Six month storage study*

The next stage in the comparative study of the ACL Instrument and the Rancimat was to investigate the ability of the machines to measure changes in stability associated with storage, as changes occurring during the storage period may be subtle, but very important in terms of product quality and safety. The sensitivity of the two machines differs due to the nature of their measurement, i.e. the Rancimat measures the increase in the conductivity of a solution over time, hence its integrated signal does not have the sensitivity to show a reduction in conductivity, so if the production of a species which gave rise to an increase in conductivity was ceased, then the conductivity would plateau. It is not possible for the conductivity in the measuring cell to reduce. In contrast, the ACL Instrument uses direct measurement with a single photon counting mechanism, so each count is a separate count and is not dependant on the previous count. It is therefore possible to see peaks appearing at intervals across the main oxidation curve that may relate to specific oxidation events. Although this can be observed to a degree with the Rancimat, when conductivity rises, the

resolution when using CL is much greater as the non-integrating signal shows the rise and fall in CL as oxidation proceeds.

A number of studies [53, 87] have looked into the shapes of CL curves arising from polymer oxidation. Celina *et al* [53] stated that more sensitive techniques, such as CL, were required to explore the degradation behaviour during the induction period, since for materials that age in an induction time like fashion (with very little oxidation followed by a sharp onset), changes that occur in this period are small but can result in the failure of the material.

Jacobson *et al* [103] investigated the shape of CL curves generated from ultra-high molecular weight polyethylene (UHMWPE) and related these with the measurement of hydroperoxide and carbonyl levels using Fourier Transform Infrared (FTIR) spectroscopy. It was found that when heating UHMWPE at 120°C, the CL curve was a double sigmoidal shape and it was shown that the initial peak corresponded to hydroperoxides while the second peak followed the build-up of carbonyls. At a lower temperature of 70°C, the double sigmoidal curve shape was not observed, with only a single peak being registered, which was found to coincide with an increase in hydroperoxides and carbonyls. In this research, a double sigmoidal curve shape was seen with corn oil, thus it may be possible to assume the same reasoning behind the curve shape as described by Jacobson [103].

The build-up of hydroperoxides in a substance can cause a reduction in oxidative stability. When oils are put into storage, it is known for hydroperoxides to build up [104]. This research investigated the effect of storage temperature on oxidative stability. For the temperatures investigated, it was hypothesised that storage at the lowest temperature of ~4°C would inhibit any decrease in oxidative stability, whereas the temperatures ~27°C and ~40°C would cause a decrease in oxidative stability, resulting in a faster degradation rate. These three temperatures were chosen to represent refrigerated storage (~4°C), laboratory storage (~27°C) and the higher temperature of ~40°C was chosen as an accelerated storage condition. Although it is unlikely that oils would be subjected to this temperature over a 6 month period, this was chosen in an attempt to induce changes in the oils that could subsequently be measured by the methods under investigation. The aim of these experiments was to

see how the two instruments compared in terms of detecting subtle changes in oxidative stability that occurred during storage and to observe how the CL curve of corn oil changed over time.

In previous work by Celina *et al* [53] on hydroxy-terminated polybutadiene (HTPB) elastomer, the I_{ini} (CLI_{ini} in this study) was found to increase with aging and the time to CLI_{max} was found to reduce with aging. These two measures, CLI_{ini} and time to CLI_{max} are discussed in relation to the CL curves obtained, in addition to OIT and $OIT_{minor.}$

When comparing the CL curves generated at 0 months with the CL curves generated after 3 months, Figure 3.32, the CLI_{ini} increases slightly for samples stored at ~27 and ~40°C, however, the sample stored at ~4°C showed no increase in CLI_{ini}. However these results must be considered in the context of the repeatability of the CLI_{ini} and CLI_{max} measures from the initial runs prior to the samples being stored (0 months).

Repeatability of the CLI_{ini} is good as evidenced by superimposing the curves. In contrast, CLI_{max} shows poorer repeatability at 120°C and 110°C than at 100°C where the repeatability is good. The issue of repeatability must be considered when analysing the results, as the changes in the stability of the oils from one storage time point to the next may be so slight that they are masked by the experimental error highlighted by the results shown in Figure 3.32 for the corn oil oxidation at 0 months and 120°C.
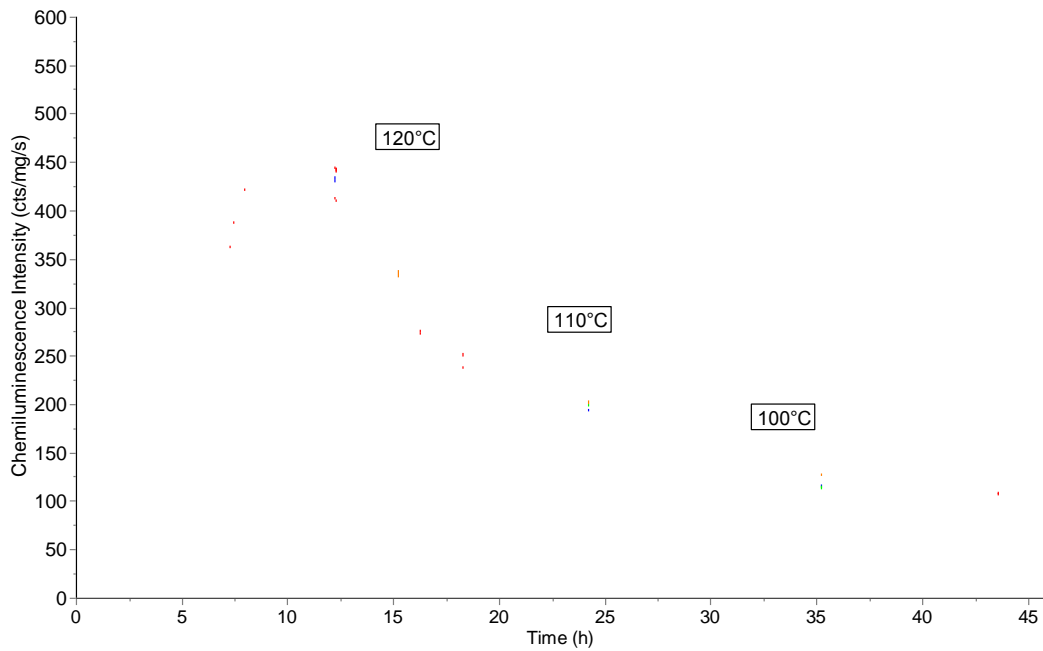
Figure 3.32- CL curves for corn oil stored for 0 and 3 months, tested at 100, 110 and 120°C (— 0 months, — 3 months ~4°C, — 3 months ~27°C, — 3 months 40°C)

From Figure 3.32, for the CL curves obtained at 100°C, the CLI_{max} for samples stored at all temperatures were very similar with no reduction in CLI_{max}. The time to CLI_{max} (shift of the curve to the left) however was slightly shorter at 3 months, than at 0 months for ~4°C and was further reduced for samples aged at ~27 and ~40°C. The reduction of time to CLI_{max} and the increase in CLI_{ini} in the samples stored at ~27 and ~40°C suggest that storage at these temperatures promoted aging compared to storage at ~4°C. For the CL curves at 110°C, the CLI_{max} across all storage temperatures is similar to that at 0 months when the repeatability of the initial runs is considered. The time to CLI_{max} is again slightly reduced for ~4°C and a further reduction is observed for ~27 and ~40°C. Finally for the CL curves at 120°C the CLI_{max} is again similar to that at 0 months when taking into account the repeatability at 0 months, but in this case, the time to CLI_{max} is only slightly reduced for the samples stored at ~27 and ~40°C, with the sample stored at ~4°C being very similar to that at 0 months. It could be expected that samples stored for 6 months would display a further reduction in time to CLI_{max} and a further increase in CLI_{ini} as ageing progresses. However this does not appear to be the case for corn oil in the tests carried out. Figure 3.33 shows the results from testing at 6 months where only a slight increase in time to CLI_{max} and no change in CLI_{ini} are observed. The most noticeable change in the CL curves of aged corn oil when measured at 110°C and 120°C

is the reduction in CLI_{max} whilst at 100°C, the CLI_{max} after 3 and 6 months remain similar. These observations consider the shape and position of the CL curves, but it is also possible to examine the OITs calculated from these curves, shown in Table 3-11.
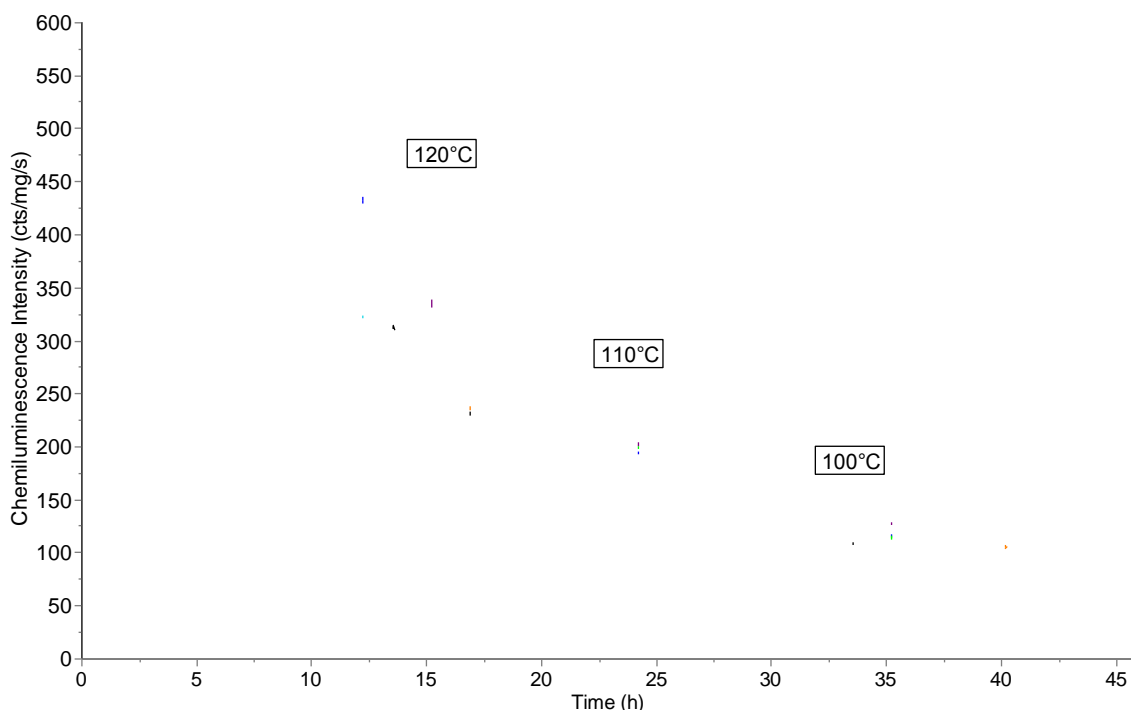
Figure 3.33 - CL curves for corn oil stored for 3 and 6 months

(— **3 months ~4°C,** — **3 months ~27°C,** — **3 months 40°C,** — **6 months ~4°C,** — **6 months ~27°C,** — **6 months 40°C)**

Storage time (months)	Storage temperature (°C)	Rancimat		ACL Instrument			
		OIT (h)	Ea (kJ/mol)	OIT (h)	OIT_{minor} (h)	Time to CLI_{max} (h)	Ea (kJ/mol)
0	-	8.92 [a] (0.08)	86.99	9.23 [b] (0.002)	3.53 [b] (0.10)	15.50 [b] (0.55)	77.53
3	40	6.87	87.70	7.47	2.57	13.27	83.48
3	27	6.96	88.72	6.67	2.67	13.47	80.05
3	5	8.52	85.25	8.07	3.17	15.27	76.50
6	40	6.13	75.72	7.08	1.88	13.38	91.92
6	27	3.58*	67.43	4.78	0.68	10.88	82.70
6	5	8.00	73.72	8.68	3.28	14.68	89.07

[a] = average of 8 runs, [b] = average of 3 runs, standard deviation in parenthesis

Table 3-11 - Effect of storage time and temperature on oxidation measured at 110°C using the Rancimat and ACL Instrument

The OIT values from the Rancimat measurements after 3 months had all reduced compared to those at 0 months, with the smallest reduction observed for the lowest temperature storage. After 6 months, a further reduction was observed in the OIT of the samples stored at 40 and 4°C. When considering the ACL Instrument results, the OIT dropped in all samples after 3 months storage, again with the smallest reduction

being observed for the lowest temperature storage condition. The OIT_{minor} and time to CLI_{max} all dropped to below the starting values for these measurements. After 6 months, it appears that the time to CLI_{max} had increased for the sample stored at 40°C, however when considering the standard deviation of the CLI_{max} measurements from 0 months, this measurement lies within the error.

Arrhenius plots were drawn and the *Ea* of each sample was calculated from the OIT measurements determined by CL and the Rancimat. The *Ea* of each sample at the storage time points, 0, 3 and 6 months are shown in Table 3-11.

It is interesting to note that after 3 months of storage at ~27 and ~40°C there is a slight increase in E_a from 77.53 to 80.48kJ/mol respectively indicating an improvement in stability, whereas for the sample stored at ~4°C, the E_a has dropped slightly. The difference in E_a across the three samples follows the opposite pattern to what is expected, in this case the lower temperature storage gives the lowest E_a with the increasing temperatures giving increasing E_a. The contrast is expected, as lower temperature storage should keep the E_a high, relative to higher temperature storage which will reduce stability and cause a reduction in E_a.

After 6 months, E_a calculated from the CL data from samples had dropped below the initial E_a at 0 months, which is what would be expected to happen, as stability is reduced. However the sample stored at ~40°C had a higher E_a than the samples stored at ~4 and ~27°C which is not what is expected, this pattern was also observed in the Rancimat results.

The E_a calculated from the Rancimat data, Table 3-11, showed that there were minimal differences in the values over the timescale studied. This was in contrast to the E_a calculated from the CL data, where the E_a had reduced for samples stored at all three temperatures, after 6 months, the E_a calculated from the Rancimat data for samples stored at ~4 and ~40°C (89.07 and 91.92 kJ/mol) were higher than at 0 months (86.99 kJ/mol), with a reduction in E_a only being seen for the sample stored at ~27°C.

The sample that was tested at ~27°C after 6 months was from the same batch as the original sample, however it was not the sample that was tested at 3 months as a fault with the lid was detected between 3 and 6 months, which meant this sample was not

suitable for testing. A sample that had also been stored at ~27°C for 6 months, but unopened at 3 months was tested instead.

It is difficult to draw clear conclusions from these data, as the expected trends were not observed and also the issue with the lid fault on the sample stored at ~27°C made the results for this temperature at 6 months difficult to compare with the other results. When taking into account the experimental error (presented as standard deviations in Table 3-11) between the OITs (from which the E_a is calculated), it could be concluded that the differences in E_a may be explained by experimental error, rather than actual changes in oxidative stability. No repeats were carried out on the samples tested at 3 and 6 months, however the sample at 0 months was tested three times to see how the difference in OIT affects the E_a. The E_a calculated for each of the three repeats at 0 months and found to be 76.84, 78.60 and 77.18 kJ/mol, which demonstrates the repeatability of this measurement for this particular sample, with the standard deviation being 0.93kJ/mol.

In summary it can be concluded that there was little change in terms of E_a over the 6 month storage period, for the three storage temperatures investigated, ~4, ~27 and ~40°C. The pattern that was expected to be observed, a decrease in E_a over time, with a larger decrease for the higher storage temperatures, was not observed and this could be attributed to experimental error. In addition, the changes in CLI$_{max}$ and CLI$_{ini}$ were also not always consistent with what would be expected, as indicated by previous reports in the literature [53]. Taking these factors into consideration, it is concluded that in the timeframe and under the storage conditions investigated, corn oil only undergoes minor, if any, changes in stability, which in this case are masked by experimental error. Storage for a longer time period of 12 months may induce further changes in the degradation state of the oils which could then be investigated by CL. A higher storage temperature could also be used to achieve a greater aging of the samples. It is anticipated that CL can give more detailed information about stability than the Rancimat due to the sensitivity and resolution of the method. If it is possible to detect subtle changes in the CL curve of aged samples, then with further development, CL methods could be used as a fingerprinting technique by which samples with unknown levels of degradation could be compared to a library of CL curves of samples with known degradation.

3.5.7 *Operational considerations of the ACL Instrument and Rancimat*

Although both the Rancimat and ACL Instrument have merits as accelerated oxidative stability methods, in that they speed up the investigation of oxidative stability and can give a clear picture of stability, they are not without limitations, which must be taken into consideration in order to place the results in context.

The results for the ACL Instrument in terms of the OIT are strongly correlated with the Rancimat, but in contrast to the Rancimat it does not present an issue at low temperatures when run times are long. More specifically at 70°C with corn oil, evaporation occurred in the measuring cell of the Rancimat, leading to a loss of conductivity signal due to the conductivity probe no longer being immersed in the measuring liquid. 50ml of distilled water is placed into the Rancimat measuring vessel at the beginning of the run, and air from the reaction vessel bubbles though this water for the duration of the run. When carrying out runs at $70^{\circ}C$ with corn oil, the machine was running for approximately 15 days and the water in the measuring vessel evaporated. At this particular temperature with corn oil, the evaporation coincided with the inflection of the conductivity curve and so the measurement was interrupted prematurely as there was insufficient measuring solution to cover the conductivity probe. It is clear to see from Figure 3.34, a graph of conductivity versus time from the Rancimat, that at around 200 hours the lines on the graph are interrupted and the conductivity signals drop to zero at around 210 hours, representing the point at which there was no longer any water in contact with the conductivity probe. When evaporation does not occur, the conductivity should continue to rise at this point. Evaporation therefore leads to misleading OITs, as the full reaction progress is not captured due to the interruption of the measurement hence it is not possible to use the OIT data.
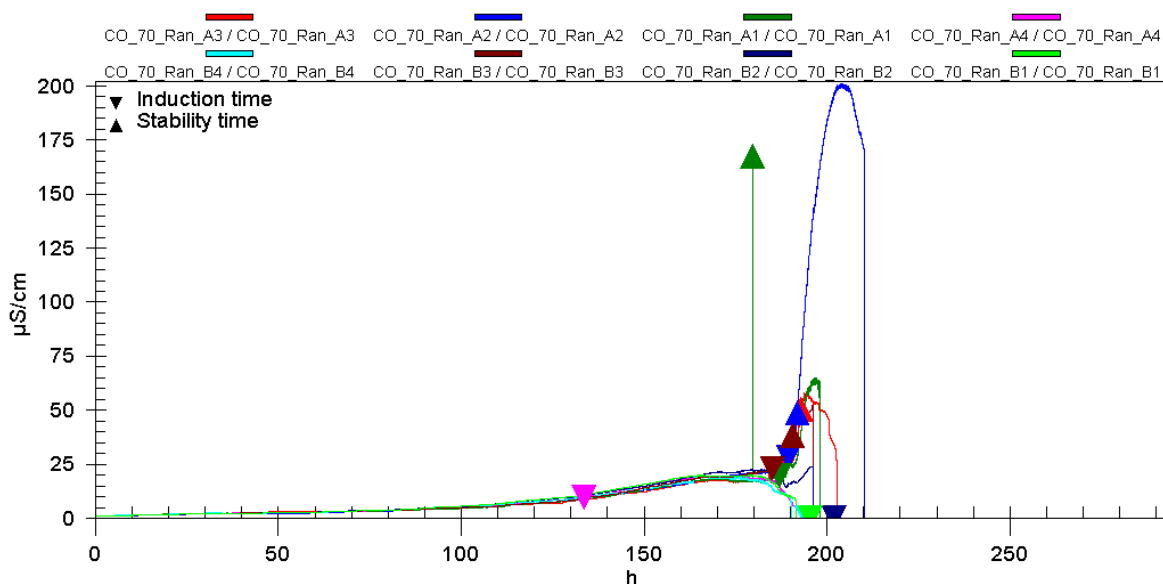
Figure 3.34 - The effect of evaporation in the Rancimat measuring vessel on OIT

In this research, evaporation occurred between 180-210 hours at 70°C, however, there have been reports in the literature of evaporation from the measuring cell interfering with measurement after only 70 hours [105]. It is not possible to overcome this problem due to the constraints of the machine. Adding more distilled water into the measuring vessel would make results difficult to interpret and they would not be comparable to runs at other temperatures with 50ml water in the measuring vessel and this approach is not recommended by the manufacturers. For other oils, such as Menhaden oil, it is possible to test at 70°C or lower as the stability is lower than corn oil with the OITs being lower than for corn oil, hence before evaporation occurs. For oils with similar stability to corn oil, 70°C appears to be the lower limit of temperature that can be reliably tested. Placing the Rancimat in a temperature controlled environment may help to extend the time period before evaporation occurs. The problem of evaporation is not encountered with the ACL Instrument as a measuring vessel is not required.

Both the Rancimat and ACL Instrument are straightforward to operate and set-up. The ACL Instrument set-up involves placing a sample on a glass slide and placing this into the furnace cell, programming the measurement set up and then starting the run. The Rancimat takes slightly longer to set up than the ACL Instrument, as it requires the assembly of a number of plastic parts and requires time for the heating block to reach temperature before starting the run.

The slide and pans used to house samples with the ACL Instrument are disposable and minimal cleaning of the furnace cell and glass cover of the detector is required if condensation is seen (section 3.4.3). In contrast, the Rancimat must be cleaned between each run. An advantage of the Rancimat is that 8 samples can be tested simultaneously whereas with the ACL Instrument only single samples can be tested.

An advantage of the ACL Instrument over the Rancimat is the option to connect different bottled gas supplies to the gas inlets, making the study of substances under particular gases possible. This allows for the study of stability in an oxidative environment and additionally the study of peroxide accumulation in an inert environment (e.g. nitrogen or argon), an aspect that is not possible using the Rancimat. The ability to carry out runs with dynamic temperature profiles (discussed in section 4.4.2) is a further benefit of the ACL Instrument, for more complex kinetic studies.

In this research, the Rancimat was not being used to predict shelf-life, however, potential drawbacks with the Rancimat method include the prediction of shelf-life via extrapolation of results obtained at high temperatures e.g. 110°C, to lower temperatures e.g. 20°C. The concern that exists here is that this extrapolation may be a poor indicator of behaviour at room temperature as different oxidation mechanisms may be occurring at the experimental high temperatures compared to those at lower 'normal' temperatures. High temperatures may provoke reactions that would not occur at room temperature. Oxidation can become limited by the availability of oxygen at high temperatures as it is less soluble, therefore the Rancimat may not provide a true to life recreation of the oxidation process at normal temperatures making it necessary to test at different temperatures in order to gain reliable results [106]. Although in this research, shelf-life prediction is not a direct aim, these limitations must be borne in mind, as ultimately these methods are being investigated to decide if they have applicability in pharmaceutical raw material stability testing.

When comparing the way in which samples are treated by these two machines, it is interesting to consider the exposure of the samples to oxygen. The machines have very different sample sizes, with the ACL Instrument requiring a sample size of <50mg and the Rancimat requiring a sample size of 3.00g ± 0.01g, hence the surface area to

volume ratio of the two samples will be different. The way that the air comes into contact with the sample also differs for each machine. With the Rancimat, the air is bubbled through the sample via an air tube which protrudes into the sample and the ACL Instrument has a furnace cell through which air is passed over the sample as it sits on the glass slide. The differences in aeration of samples could affect the time at which the OIT occurs. For example, when using aluminium pans, these are covered with a glass slide, and hence air supply will be limited compared to samples being housed on glass slides. A lower saturation of oxygen within a sample will inevitably slow down the autoxidation process however it is difficult to measure how the results from each machine differ on this basis, so this difference was accepted for the purpose of this research.

A limitation that has been mentioned in section 3.5.5 concerns the experimental setup when using aluminium pans. The effect of the aluminium on the oxidative stability must be considered for each different oil as it appears that it has the potential to affect the results. The use of glass slides is therefore a more reliable method to adopt from the start of any experiments, to avoid having to carry out initial tests on the effect of aluminium pans on the behaviour of a sample.

One benefit of the ACL Instrument over the Rancimat is that the sample size required is <50mg which is significantly less than the 3.00g required for the Rancimat. This could be useful when low volume high value products require testing, however for the majority of bulk pharmaceutical raw materials that need to be tested, removing 3.00g for testing would not pose a problem.

Regarding the software that accompanies each machine, both have a clear user interface for inputting experimental parameters and for visualising and downloading results. An advantage of the Rancimat software is the automatic calculation of OIT which is not a feature of the ACL software, where data must be downloaded and a manual calculation of OIT using tangents is required, which can introduce operator error. There is scope for automation of this step, which would reduce this error.

3.5.8 *Suggestions for improvements to the ACL Instrument*

From an industrial perspective, an important consideration is the notion of throughput as with numerous incoming raw materials to sample, it is desirable to have a high

throughput method for measuring oxidative stability, so that data acquisition is timely and does not delay results and the manufacture of product. It became apparent during this research, that the major issue with the ACL Instrument was the single sample housing, hence the low throughput of samples, due to the nature of oxidative stability testing and the tendency towards long run times. This coupled with the nature of the samples that require testing, e.g. samples that may be unstable meaning that obtaining repeats of measurements is difficult. By the time a set of testing had been carried out, the sample could have undergone aging, which limits the number of repeats that could be carried out for some testing scenarios. In contrast, the multi-sample set-up with the Rancimat provided the ability to test 8 samples simultaneously.

It may be unfeasible for a laboratory to purchase multiple ACL Instruments, due to capital costs and laboratory bench space, however if the supplier could consider a re-design, to incorporate more furnace cells per instrument, as shown in Figure 3.35, then this would increase the throughput of the machine and make it more attractive both from a technical and commercial point of view. A multi-cell computerised CL instrument has been used in research by Zlatkevich and Martella [98] however reports of its use since are scarce.
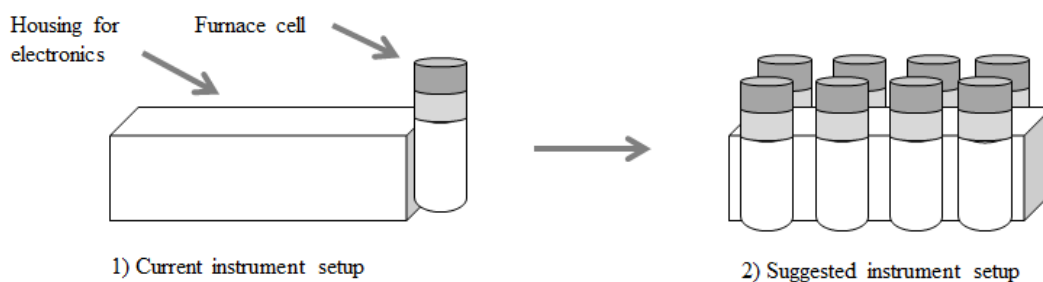
Figure 3.35 - Possible adaptation of the ACL Instrument to improve throughput

As well as modifications to the number of furnace cells on each instrument, addition of hardware modules is possible, to investigate samples under different humidity conditions, and filters to allow measurement of photons at particular wavelengths, which would allow more complex research studies. Through ACL Instruments working closely with pharmaceutical companies, it may be possible to create augmented furnace cells that could be used to facilitate long term stability studies of final products, with the added concept of CL monitoring of stability for the duration of the

testing. This would allow for more complex stability information to be collected during the study that could then be interrogated and linked to the performance of products.

3.6   Conclusions

The research reported in this chapter has highlighted the strong correlation between the OITs determined by the ACL Instrument and Rancimat for determining the oxidative stability of corn oil and Menhaden oil, showing the potential for the two machines to be used interchangeably. It shows the potential of the ACL Instrument as a method for measuring oxidative stability and one which compares favourably to the Rancimat when considering OIT measurements. As well as giving a measurement of OIT, the ACL Instrument may be able to provide the user with more information about the oxidative behaviour of a substance than the Rancimat, due to possible observations of multiple oxidation events on the CL curve, as shown in Figure 3.7, providing better resolution than the integrated signal that is generated by the Rancimat.

Testing of Menhaden oil and comparison to the results from corn oil showed that another indicator of oxidative stability from the CL curve, the TLI, showed an oil dependence in terms of its correlation with ACL and Rancimat OIT. Menhaden oil was found to be less stable that corn oil at the same testing temperatures, highlighted by the lower OITs displayed and the lower E_a, which was expected due to the higher concentration of PUFA which made the Menhaden oil more susceptible to oxidation.

The results obtained from running experiments with two different sample holders highlighted that aluminium pans can cause a catalytic effect on the oxidation of corn oil and that borosilicate glass slides give more repeatable results. Significant differences (p <0.05) were observed between the results from the aluminium pans and borosilicate glass slides for all parts of the curve measured. Consideration of *Ea* calculated using CLI$_{max}$ and peak-2 data showed that aluminium pans reduced the activation energy of corn oil oxidation however calculations of *Ea* using OIT contradict this, showing glass slides to reduce the *Ea*. This was attributed to difficulties in tangent placement and the issue that the % relative standard deviations were large for the results from the aluminium pans, hence there was significant variability associated with the analysis. The research highlighted that aluminium pans cause a catalytic effect

on the oxidation of corn oil and that borosilicate glass slides give more repeatable results. For the purpose of measuring the oxidative stability of oils such as corn oil, it is therefore recommended that glass slides are used as they are inert and devoid of the catalytic activity associated with aluminium pans.

Finally, the six month storage study showed that subtle changes in oxidative stability may be detectable with the ACL Instrument, however it was inconclusive as to whether over a period of 6 months, the oxidation state of the corn oil changed significantly. A longer time period of storage would be required to investigate this further.

3.7   Future work

As mentioned in section 3.5.4, by testing an oil that has a different fatty acid profile such as coconut oil or palm kernel oil, containing higher percentages of dodecanoic acid (C12) than corn oil and Menhaden oil, it would be possible to compare the oxidation measures from the methods further. This would further augment the TLI data and develop an understanding of the relationship between TLI and OIT and the nature of the species being captured by the CL measurement compared to those giving rise to the Rancimat and ACL OITs.

Further studies into the ability of the ACL Instrument to detect changes in aged samples of oil, are necessary to test samples under different stress conditions such as higher temperature and also to extend the testing period to 12 months. It would also be desirable to perform repeat measurements at each time point, but this may require an additional ACL Instrument, or for the throughput of the instrument to be increased.

In addition to this it would be valuable to investigate the applicability of the additional hardware modules that are available with the ACL Instrument. The humidifier module may be useful as it could be used for testing final pharmaceutical formulations under stability conditions specified in the regulatory guidelines (specific temperature and humidity combinations) and tracking the progress of stability with CL. For photosensitive excipients or final products, the photo-oxidation module could be investigated. More information would be gained about the nature of the oxidative reactions taking place during testing by using the spectrometer module which allows for the identification of individual emissions between 280-780nm.

In order to understand those chemical reactions in the substance that give rise to the CL signal, the ACL Instrument could be used in parallel with other methods such as electron paramagnetic resonance spectroscopy, to help elucidate the mechanisms behind the occurrence of peaks in the CL curve and link these to the chemistry of the substance. This was not possible to explore in this research as it was outside of the experimental aim. For the pharmaceutical industry the primary use of the instrument should be to compliment other methods used in research and development. To build on the research carried out in this chapter, in the future, the ACL Instrument will be evaluated as a means of understanding lipid rancidity and stability in lipid emulsion products.

Recommendations for industry regarding the use of the ACL Instrument are summarised in Chapter 8, section 8.4, Table 8-2. The following chapter, Chapter 4 investigates the ACL instrument for the quantification of peroxides when testing oils in an inert atmosphere, which further tests the capability of the ACL Instrument and its different operating modes.

Chapter 4. Comparison of the ACL Instrument and iodometric titration for measurement of peroxides

4.1 Introduction

The research in this chapter moves on from the previous chapter where the ACL Instrument was investigated for measuring oxidative stability and focusses on the capability of the ACL Instrument to quantify peroxides, a specific chemical indicator of oxidative degradation. In this chapter the ACL Instrument is compared to a standard method for measuring peroxide value, the American Oil Chemists' Society Peroxide Value titration [5].

4.1.1 *Hydroperoxides and their role in the oxidation of oils*

The importance of ensuring that products are stable to oxidation was highlighted in Chapter 3, section 3.1.1. As well as measuring the oxidative stability of a substance as a whole, using the methods investigated in Chapter 3, it is also possible to measure the levels of oxidation products that are formed during the oxidation of fats and oils.

When oils undergo oxidation, several reaction products are formed, and the progress of their formation is shown in Figure 4.1. Peroxides, primary oxidation products, are formed during the initiation and propagation stages of autoxidation and they decompose during the termination stages as the production of non-volatiles and volatiles continue to rise and the unsaturated fatty acids and antioxidants continue to fall. The use of PV to indicate oxidative stability must be approached with caution as when oils oxidise, as shown in Figure 4.1, the hydroperoxide content peaks and then falls. Consequently it is possible that an oil with an extensive level of oxidation has a low PV, as the peroxides formed in the initial stages of oxidation have decomposed.
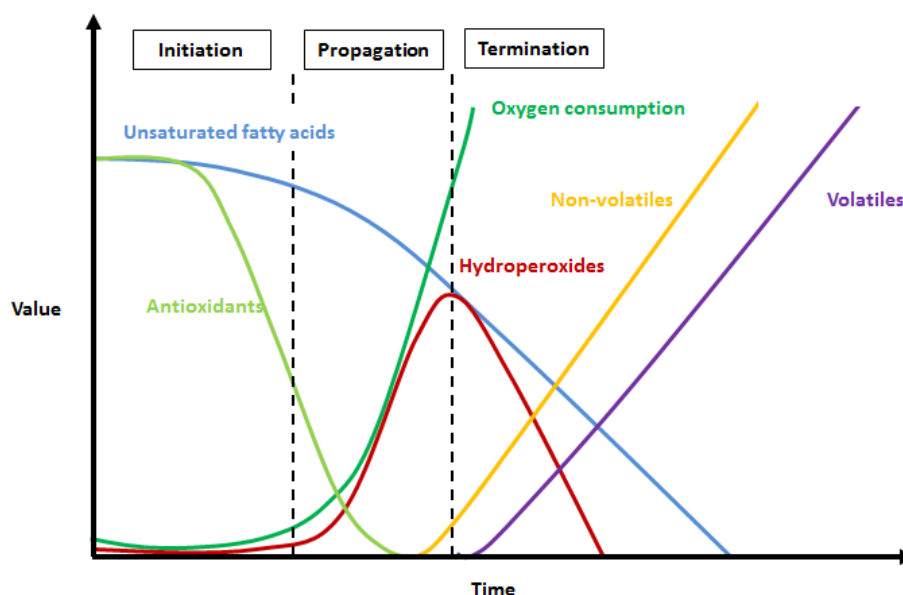
Figure 4.1 – Time dependant formation of autoxidation products in vegetable oils [107]

Hydroperoxides can accumulate during storage and once at a critical level, can cause stability issues and affect the quality of the oil. The total accumulated hydroperoxides in a substance provides a measure of oxidation progress, [93, 108] which can indicate the stability, quality and aging history of an oil.   It is therefore necessary to measure the levels of hydroperoxides in order to be able to ensure that oils are suitable and safe for use, and so that suitable storage conditions and shelf lives can be determined. The measurement of hydroperoxides is the focus of this chapter.

4.1.2 *Methods for measuring peroxides*

A number of methods exist for the quantification of the level of peroxides in a product, including wet chemistry methods, spectrophotometric and potentiometric methods and also techniques such as FTIR spectroscopy [109-111] and chemiluminescence (CL) [91-93, 112]. Wet chemistry methods include iodometric titration and ferrous oxidation in xylenol orange. A standard iodometric titration based method that is widely used for determining PV in fats and oils is the American Oil Chemists' Society (AOCS) Cd 8b-90 Peroxide Value Acetic Acid-Isooctane Method [5]. Iodometric titration based methods are highly empirical and therefore consequently variations in the procedure can impact on the results, furthermore for PVs ≥ 70 meq peroxide/kg results are not reliable and this needs to be considered when analysing results [5]. In addition, iodometric titrations contain a number of steps to be implemented and produce chemical waste, including glacial acetic acid and isooctane which require disposal. An

additional issue with iodometric titration is the determination of the endpoint which relies on the observation of a colour change. In some cases oils are strong in colour before the addition of potassium iodide so the endpoint is not colourless which makes endpoint determination more problematic. Furthermore, interference from oxygen in the air can give rise to higher than actual PVs, so shaking should be gentle to minimise this. As well as the reaction occurring during the titration being affected by the presence of oxygen, iodine can also be absorbed by unsaturated fatty acids in the oils. The titrations, should be performed in diffuse daylight or artificial light shielded from a direct light source [5] or they can be performed in the dark under nitrogen, however this approach is impractical and therefore rarely used.

Some wet chemistry methods are combined with spectrophotometry including the ferric thiocyanate method which is based on the reaction of peroxides with ferrous iron (iron (II)) ions to form ferric iron (iron (III)) ions which go onto react with thiocyanate ions giving a red colour. The red colour can be measured at 500-510nm.

The ferrous oxidation-xylenol orange (FOX2) assay [113] works on a similar principle to the ferric thiocyanate method and is based on the conversion of ferrous to ferric ion via hydroperoxides, which then complex with xylenol orange (XO) ((3,3-Bis(N, N-bis(carboxymethyl)aminomethyl)-o-cresosulfonepthalein) tetrasodium salt), which is determined spectrophotometrically by absorbance between 540-600nm [114]. The FOX2 method unlike the iodometric titration method is not sensitive to oxygen, which is an advantage, although it has been reported that the XO reagent itself can change colour on storage and an absorbance difference was noted between suppliers and batches [114]. Both iron based methods require low amounts of sample and solvent and are sensitive, however they have the disadvantages of interference by pigments contained in the oils [114]. The response of the FOX assay is also dependent on the type of hydroperoxides present in the sample, but one study reported that a strong correlation (r = 0.975) was found between results from the FOX method and AOCS iodometric titration for oxidised soybean oil [115].

FTIR spectroscopy has also been used for the determination of hydroperoxides, although this may not be a practicable option in all cases due to the cost of the instrumentation. Van de Voort *et* al [109] used FTIR to predict PV after the

construction of a partial least squares (PLS) model, and the set-up was investigated as a possible automated alternative to wet chemistry methods. The development of a PV calibration in this manner is fairly complex however Van de Voort *et al* produced a calibration that could directly predict the PV of an oil from its FTIR spectrum. Further work was aimed at pre-programming the instrument to remove the need for operator expertise in FTIR and achieve transferability of the method to other machines [109].

An alternative method for quantifying hydroperoxides is chemiluminescence (CL). Samples are heated with a dynamic temperature profile, in a non-oxidising inert atmosphere such as nitrogen, and any accumulated hydroperoxides are thermally decomposed. During decomposition, the hydroperoxides emit CL and the total CL emission (total luminescence intensity (TLI)) is directly proportional to the hydroperoxide concentration which is calculated as the integral of the CL curve, with a baseline equal to zero, as shown in Figure 4.2. The baseline equal to zero is used to capture all of data from the run. The TLI gives a measure of oxidation progress [116] which gives an indication of quality and aging history of the sample.

Integration : 2.86E+7 (cts/g)
T : 25.07 and 198.25 (°C)
t : 0.1 and 66.7 (min)
Peak Maximum : 147.47 (°C) / 49.628 (min)
Peak Height : 14.646 (cts/mg/s)
Onset : 82.918 (°C) / 28.124 (min)
Offset : ! / !
Baseline Type : Horizontal
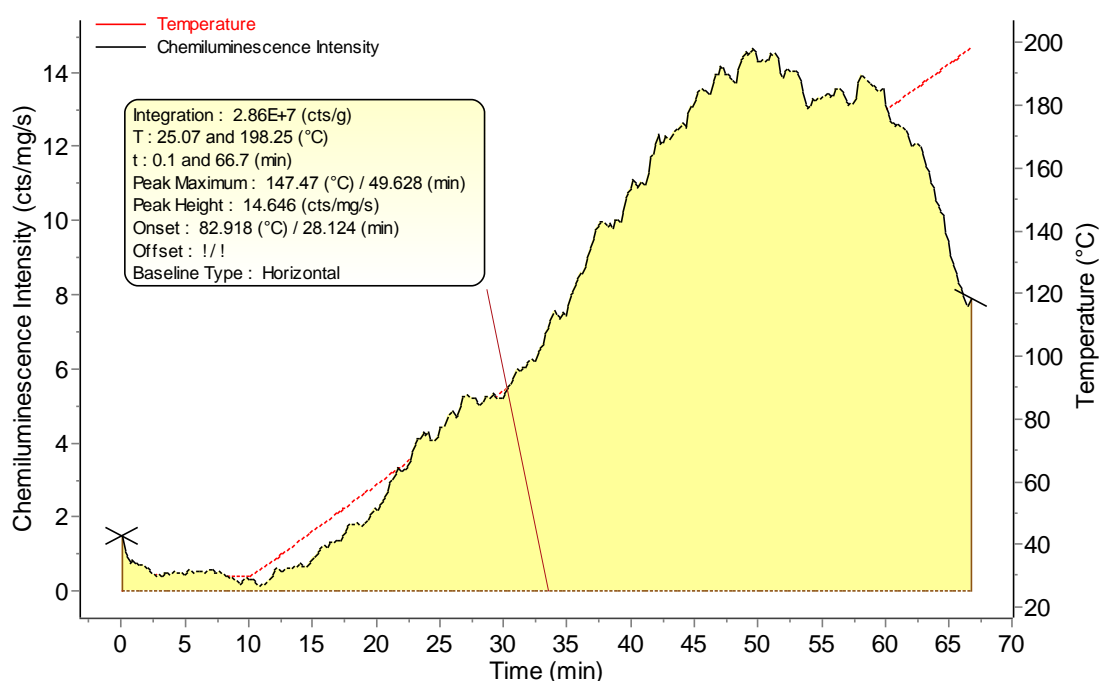
Figure 4.2 – Integration of CL curve with baseline equal to zero (horizontal), for a sample heated with a dynamic temperature profile under nitrogen.

CL has a number of advantages including its simplicity of detection, as only a detector and recorder are needed. No external light source is required and the absence of

background light greatly improves the limit of detection [81, 117]. The use of CL to measure peroxide levels has previously been reported in the literature [91, 93, 116] however, unlike in this research, the CL methods utilised were not label-free so required additional reagents. In contrast to wet chemistry methods such as iodometric titration, where results may be acquired in around 5 minutes per sample (excluding set up time to make up reagent solutions), the time taken to acquire results using CL is around 65 minutes.

Rolewski *et al* [93] used a luminol-enhanced CL (LCL) method to directly measure the amount of formed hydroperoxides in lipid emulsions during oxidation. It was found to be a reliable and rapid method, but although appropriate for fats and oils, it was not as applicable for more complex substances due to interference from other components including transition metals and enzymes that competed with the hydroperoxides as oxidising agents. Rolewski reported sensitivity and simplicity as two advantages of LCL over the existing methods of iodometric titration, the FOX assay, FTIR and conjugated diene values [93]. In Rolewski's research, the additives used in the CL method were luminol, which acted as a light amplifier to enhance the otherwise weak quantum yield signal and hemin which served as a catalyst and co-oxidant in the decomposition of hydroperoxides.

Fearon *et al* [52] compared CL to differential scanning calorimetry (DSC) and found that by using CL it was possible to determine the decomposition of hydroperoxides in rubber, which had not been possible with DSC. CL revealed peaks that were not observed with DSC and these peaks disappeared if the sample was tested again, suggesting decomposition of hydroperoxides. Upon cooling and reheating of the rubber, these CL peaks were no longer present, indicating that residual peroxides had been decomposed upon heating. This study showed that CL can provide more detailed information about the oxidative behaviour of a substance compared to DSC.

Another CL method for PV determination is peroxyoxalate chemiluminescence (PO-CL). PO-CL reactions involve hydrogen peroxide oxidation of aryl oxalate esters in the presence of a fluorophore. The excited state compound, e.g. hydrogen peroxide, does not emit light itself unless the fluorophore is present. The oxalates used in these reactions: Bis-(2,4,6,-trichlorophenyl)oxalate (TCPO) and bis-(2,4-dinitrophenyl)oxalate

(DNPO) are insoluble in water and susceptible to hydrolysis and so organic solvents were required [81]. PO-CL has been investigated to identify whether it can be used as a simple procedure to detect and quantify hydrogen peroxide or total peroxides in oil samples. Stepanyan *et al* [91] set out to develop a method that would enable measurements on olive oil to be untaken away from the laboratory. TCPO was used as a reagent and the method that was developed was described as straightforward, despite the use of several reagents in the measurement protocol. The method involved combining oil samples with several reagents, vortexing for 10 seconds and then combining this with TCPO reagent in a cuvette. The cuvette was then placed in a CL analyser and a reading taken, with the maximum CL intensity being reached after 1-3 minutes and staying steady for 10 seconds. The procedure that was developed successfully allowed the evaluation of PV within the range 0.6–100 meq O_2 per kg and the measurements had standard deviations of 1-5%, which is relatively low and not dissimilar to the official EU method that it was benchmarked against.

Hypochlorite-activated CL was reported by Yamamoto *et al* [112] for the detection of low levels of hydroperoxides. In hypochlorite-activated CL, oil samples are mixed with *tert*-butanol and sodium hypochlorite is added to increase the sensitivity of the technique, resulting in a strong CL emission. Yamamoto *et al* [112] stated that the method was sufficiently sensitive to detect low levels of lipid hydroperoxides with PVs of less than 1 and it was also claimed that this method proved convenient. Burkow *et al* [85] studied the correlation between sodium hypochlorite-activated CL and traditional methods for measuring oxidative stability. Using hypochlorite-activated CL it was possible to detect small changes in oxidative rancidity with high sensitivity when compared to other more traditional methods of PV, thiobarbituric acid value (TBAV) and fatty acid composition. Good reproducibility was seen using this method, compared with some of the chemical methods studied alongside it including PV and fatty acid composition. Strong correlations (r=0.920-0.999) were reported between hypochlorite-activated CL and PV, TBAV, anisidine value (AV), Kreis rancidity index, UV measurement at 233nm and sensoric score [85]. Although the sensitivity of this method was claimed to be higher than that of traditional PV measurements, many experimental factors were found to affect the results, including solvent, mixing, and amount of hypochlorite, thereby introducing error. Despite this, the reproducibility of

the method was found to be high, with a standard deviation of 3% (sample-to-sample, day-to-day) which was claimed to be lower than other chemical methods and the speed of result acquisition was relatively fast compared to more laborious methods, at 5 minutes per sample [85].

In contrast to the CL techniques previously mentioned, the ACL Instrument under investigation in this research (described in section 3.1.5) is simple to operate and samples require no reagents, hence it is label-free. The only waste it produces is from the disposable sample holders. The operator time required to set up the machine is minimal and the machine can run unattended which significantly reduces operator time and operator related error. An issue with the ACL Instrument is that only one sample can be analysed at a time and run times can be over 60 minutes. Additionally, the machines furnace cell must be allowed to cool down to around 30°C before the sample can be removed and another introduced. This can take up to an hour, depending on the temperature that the run is carried out at. Also, there is a capital cost associated with the instrument, which makes this an expensive technique compared to some of the wet chemistry methods.

This chapter draws a comparison between the American Oil Chemist's Society (AOCS) Official Method Cd 8b-90 (iodometric titration) [5], the ACL Instrument (introduced in Chapter 3) and Conjugated Diene (CD) Value.

4.1.3 *Methods for inducing a range of peroxide values*

There have been a number of reports that have utilised elevated temperatures in the aging of oils. Nielsen *et al* [118] heated tuna oil at 40°C, and rapeseed and fish oil at 50°C with stirring in the presence of air and the absence of light over a period of 5 days [118]. Kim *et al* prepared oxidised soybean oil samples by purging 200mL purified soybean oil with air at a rate of 10 mL air per minute for 48h whilst heating at 50°C [104]. Moh *et al* [119] aged crude palm oil by purging air though 1kg of oil at 90°C and removing 50g samples at 15 minute intervals, generating a range of peroxide values from 2.17-10.28 meq peroxide/kg test substance. A fluorescent light source at 4200 lux was used by Yildiz *et al* [115]. For the purpose of this investigation, elevated temperatures were selected as the preferred method of aging, due to previous reports

of its effectiveness and due to the availability of appropriate equipment to facilitate this.

4.2 Aim

The AOCS Cd 8b-90 Peroxide Value Acetic Acid-Isooctane Method [5] is used for the measurement of PV for all normal fats and oils including margarine. In contrast, no reports exist concerning the use of the ACL Instrument for the measurement of PV in oils and whether the method can be used to compare the stability of oils with different compositions. It may be the case that the method is dependent on oil type and that a standard is required for each oil type as a benchmark. As the stability of oil is affected by the content and degree of unsaturation of the fatty acids contained within the oil, in order to test the dependence of the CL and AOCS PV measurement methods on oil composition, corn oil and Menhaden oil were considered due to their differences in fatty acid content, as described in Chapter 3, section 3.1.7.

The focus of this was to compare the two methods for measuring the peroxide levels in corn oil and Menhaden oil samples that have been artificially aged using a combination of temperature and aeration. More specifically the aims were to:

1) compare the results from the ACL Instrument and AOCS PV method for the measurement of peroxide levels in artificially aged corn oil and Menhaden oil

2) consider the results from the CL and PV measurements and investigate their relationship with conjugated diene values (CDV)

3) investigate the dependence of the PVs on oil type and heating temperature

4) investigate which measure from the CL curve provides the strongest correlation with the results obtained using the AOCS PV method

5) review system performance and method-to-method differences taking into account potential sources of error with each method

6) contrast the operational considerations of the ACL Instrument and AOCS PV method

4.3 Experimental

4.3.1 *Materials*

Corn oil and Menhaden oil (Sigma Aldrich) were used as test substances and all details of materials associated with the Rancimat apparatus and the ACL Instrument are found in Chapter 3, section 3.3.1. The Rancimat apparatus (Metrohm, Switzerland) was used in this investigation not as an analytical device, but as a method of heating and aerating samples to cause artificial ageing and induce a range of PVs. 22mm borosilicate glass slides were used with the ACL Instrument for this testing to eliminate the catalytic effect of aluminium pans highlighted in Chapter 3.

For AOCS PV titrations the following chemicals were used: glacial acetic acid 99+% and 2, 2, 4-trimethylpentane 99.5+% (GLC) for HPLC (Fisher Scientific) and potassium iodide, sodium thiosulfate, starch, potassium dichromate, sodium lauryl sulphate, 5% sodium hypochlorite, concentrated hydrochloric acid 35-37% (Sigma Aldrich). For measurement of CDV, HPLC grade hexane was used (Fisher Scientific).

4.4 Methods

4.4.1 *Ageing of oils to induce a range of peroxide values*

In this research oil samples were heated to induce the formation of peroxides thereby artificially aging the oils. The Rancimat was used to heat and aerate the oil samples due to its capacity to heat 8 samples simultaneously. 9g of oil was placed into each glass reaction tube to provide sufficient aged sample for the study and the oil was heated and aerated with ambient air at an airflow rate of 10L/hr. Samples of corn oil and Menhaden oil were heated at 70, 90, 100 and 120°C (corn only). A sample tube was removed every 30 minutes over a period of 4 hours and was purged with nitrogen then sealed. Between the removal of oil and the measurement of PV, samples were stored under nitrogen in the dark, in a fridge at 4°C, to prevent further degradation.

4.4.2 *CL determination of accumulated hydroperoxides*

Determination of the content of accumulated hydroperoxides in the oils using CL was achieved through the application of a dynamic temperature profile. This involved heating the sample from 30-200°C at a rate of 2.98°C/min. The ACL Instrument was

operated using bottled nitrogen at a flow rate of 60ml/min and runs were carried out in triplicate for corn oil and Menhaden oil. Samples ranging from 6.3 – 14.1mg were placed onto 22mm borosilicate glass slides and positioned into the furnace cell where they were subject to conditioning for 10 minutes at 30°C prior to the commencement of the temperature ramp. Data was acquired using the dark count subtraction mode. In this mode, the detector performs a photon count whilst the shutter is open and whilst the shutter is closed and the two measurements are subtracted. This approach takes into account the noise occurring in the detector.

4.4.3 *Determination of Peroxide Value using AOCS Cd 8b-90 Acetic Acid-Isooctane Method*

The PV was measured in triplicate according to the AOCS Cd 8b-90 Peroxide Value Acetic Acid-Isooctane Method [5]. It is determined by quantifying the amount of peroxides (milliequivalents (meq) of peroxide per 1000g test sample):

$$\text{PV (milliequivalents peroxide per 1000g test sample)} = \frac{(S - B) \times M \times 1000}{\text{mass of test portion, g}} \qquad \text{Equation 4.1}$$

where *S* is the volume of titrant (mL of test sample), *B* is the volume of titrant (mL blank), and M is the molarity of sodium thiosulfate solution. The sodium thiosulfate solutions were standardised against a potassium dichromate primary standard.

4.4.4 *Determination of conjugated diene value (CDV)*

Corn oil samples were diluted with HPLC grade hexane (1:600 or 1:6000 depending on the absorbance reading) and this was used as a blank. The UV absorbance of corn oil samples was measured, using a UV/Vis spectrophotometer (Jenway 6705 UV/Vis) over the range 200-400nm.

CDVs were calculated using UV absorbance at λ = 233nm according to Equation 4.2 and Equation 4.3 [120]:

$$C_{CD} = A_{233}/(\varepsilon \times l) \qquad\qquad \textbf{Equation 4.2}$$

$$\text{CD value} = [C_{CD} \times (0.9 \times 10^4)]/W \qquad\qquad \textbf{Equation 4.3}$$

where C_{CD} is the concentration in mmol/ml (molar concentration), A_{233} is the absorbance of the lipid solution at 233nm, ε is the molar absorptivity (extinction coefficient - 29000mol/L), l is the path length of the cuvette in cm (1 cm), 0.9×10^4 is the factor that encompasses the volume of hexane used to dissolve the oil sample (0.9mL) as well as a unit conversion (1000µmol/mmol) and W is the weight of the sample in g (0.00009g).

4.5 Results and Discussion

The ACL Instrument's literature states that hydroperoxides can be *'quantitatively measured'* through testing in a non-oxidative environment using the total luminescence intensity (TLI) measurement, which is directly proportional to the hydroperoxide concentration [121]. The TLI is therefore used as an indirect marker for age and quality of the test substance. A limitation of this approach is that the TLI is not directly linked back to hydroperoxide concentration for instance, there is no calculation by which the TLI can be converted to give units that are associated with PV and hence the TLI measure provided by the ACL Instrument cannot stand alone as a method for quantifying the specific level of hydroperoxides. It is therefore necessary for the TLI results to be compared to another approach to determine the relationship to the comparator measure thereby obtain the concentration of peroxides.

As stated by Kim *et al* [104], *'Peroxide value determined by an iodometric titration method measures only the hydroperoxides (ROOH) and does not measure the peroxides between fatty acids in dimers (ROOR), trimers, polymers and endoperoxides of fatty acids.'* In contrast, the ACL Instrument measures all CL emitted from the recombination of peroxides, whatever their chemical make-up, therefore it could be expected that the values arising from PV titration and CL testing will exhibit some level of correlation, but not necessarily across oil types. In the work by Szterk and Lewicki [92], it was found that PVs determined spectrophotometrically and by CL were strongly correlated, for certain oils [92].

The hypothesis being investigated in this case study was that: the ACL Instrument does not allow the direct quantification of hydroperoxides and hence the data must be benchmarked against samples with known hydroperoxide concentration. In addition to this, it was hypothesised, based on existing evidence from CL studies, that the correlation between PV and TLI will be oil dependent.

Corn oil was aged over a period of 4 hours at 120°C and the aged samples were then tested on the ACL Instrument using a dynamic temperature profile (30-200°C at a rate of 2.98°C/min). Menhaden oil was aged over a period of 4 hours at 70°C, as 120°C would have caused oxidation too quickly as fish oil is less stable than corn oil, due to its higher percentage composition of PUFA. CL curves for the aged corn oil samples can be seen in Figure 4.3 and for Menhaden oil in Figure 4.4.
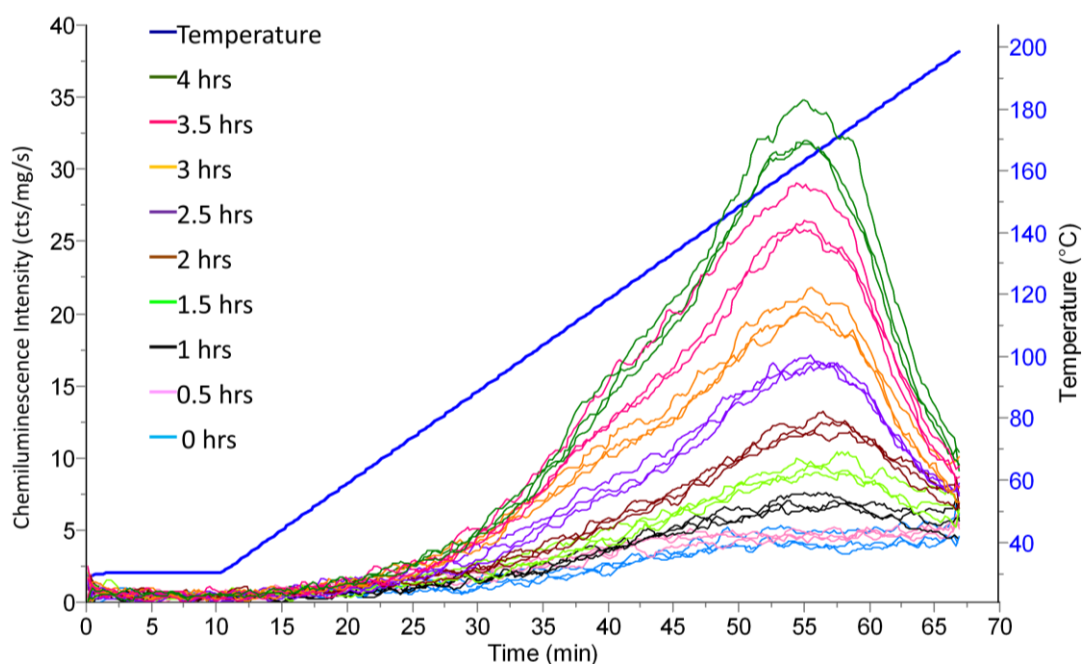
Figure 4.3 - CL curves of corn oil samples heated over 4 hours at 120°C
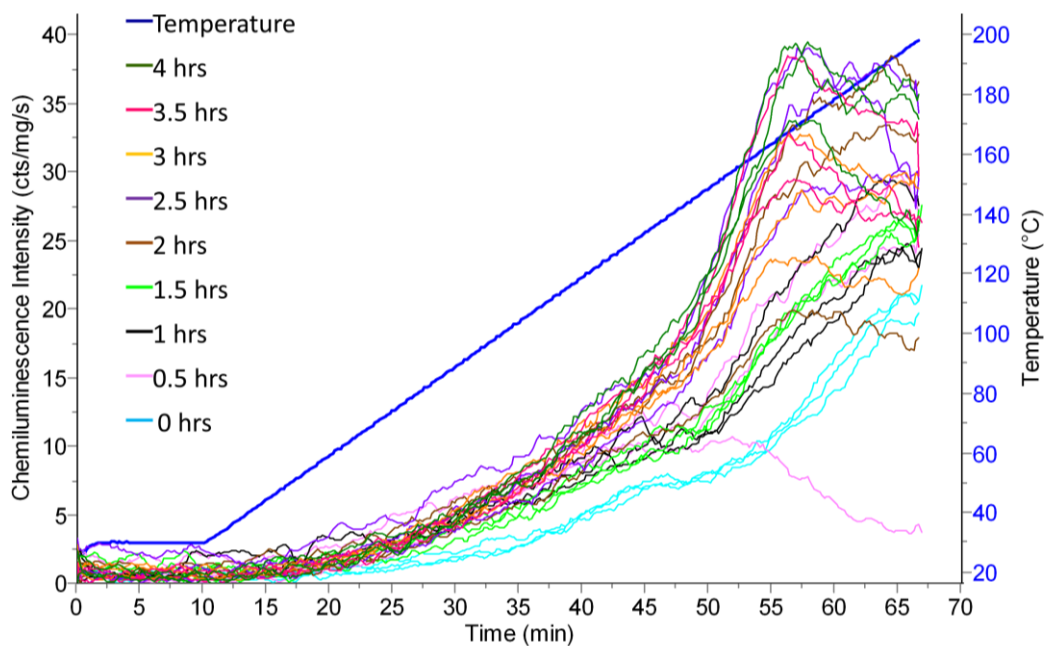
Figure 4.4 - CL curves of Menhaden oil samples heated for 4 hours at 70°C

With both samples, corn oil and Menhaden oil, as sample ageing time increases, there is an increase in the CLI. This increase in CLI over aging time indicates that the samples contain an increasing amount of accumulated hydroperoxides as they are artificially aged for longer periods. There is clearer separation between the CL curves of aged samples of corn oil from each aging time point compared to those in Menhaden oil.

When contrasting the CL curves obtained for corn oil and Menhaden oil in Figure 4.3 and Figure 4.4 it is apparent that the curves have slightly different profiles. With corn oil samples, the CLI reaches a peak and then reduces as the run temperature increases giving a pronounced bell shaped CL curve, whereas with Menhaden oil the bell shaped curve is not pronounced. The bell shaped CL curves for corn oil samples indicated that those peroxides that were formed during the artificial aging process prior to CL testing began to decompose, indicated by the rise in CLI to the CLI_{max} (at ~160°C for all samples) after which CLI began to fall until the end of the run where the CLI had dropped close to the intensity at the start of the run, indicating that peroxide decomposition had slowed. In contrast to corn oil, the peroxides formed during the aging process with Menhaden oil did not appear to fully decompose over the temperature range 30-200°C, indicated by the lack of a bell shaped CL curve. At the

end point of the CL testing when the samples had reached 200°C, in all samples apart from one, the CLI was still rising. This may indicate that those peroxides formed in Menhaden oil during the artificial aging are more thermally stable than those formed in corn oil. What is interesting to note is that the CLI_{max} for the sample of corn oil and Menhaden oil heated for 4 hours (observed in Figure 4.3 and Figure 4.4), is of a very similar intensity of 35-40 cts/mg/s.

The TLI is proportional to the amount of accumulated hydroperoxides present in the sample. To calculate the TLI, integrals (with a horizontal baseline equal to zero) were calculated across the whole CL curve with values expressed in counts per gram (cts/g).
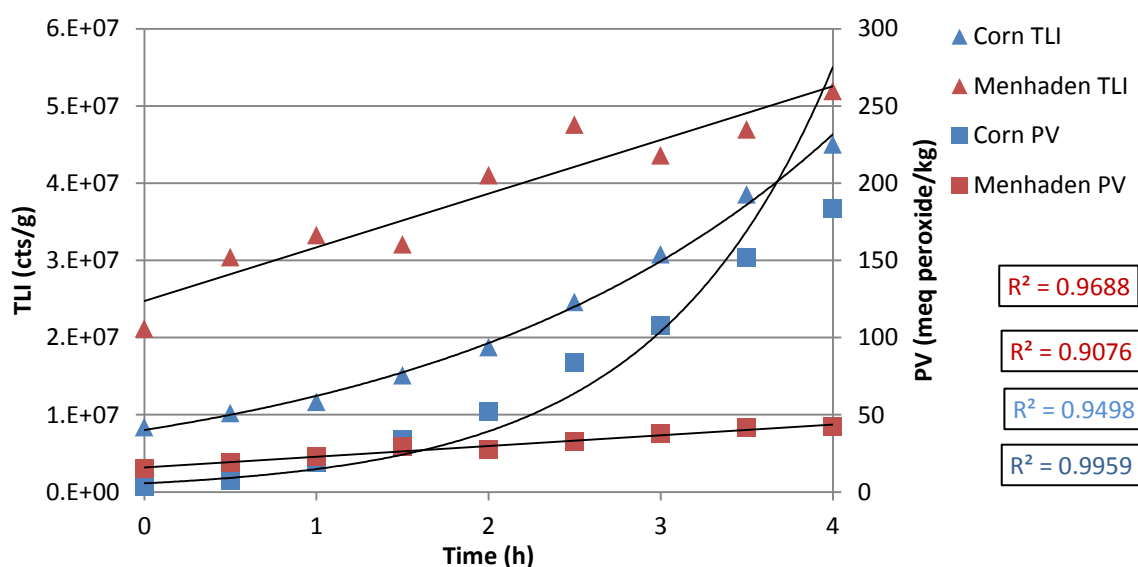
Figure 4.5 - TLI and PVs for corn oil (120°C) and Menhaden oil (70°C) artificially aged over 4 hours

The TLI and PVs for corn oil and Menhaden oil were plotted against time, Figure 4.5. For Menhaden oil, there is a good fit of the linear trend line for each measurement method, with the PV having a better fit (R^2 = 0.9688) than the TLI (R^2 = 0.9076). This steady increase in PV and TLI and the linear trend indicates that over the 4 hour period of aging of the Menhaden oil at 70°C, the oxidation progress did not get beyond the initiation stage where peroxides are being formed, which was shown schematically in Figure 4.1. In contrast, over the 4 hour period of aging of the corn oil at 120°C, the corn oil displayed an exponential relationship for both PV (R^2 = 0.9498) and TLI (R^2 = 0.9959) indicating that the oxidation in this case had progressed to the propagation stage, where the formation of peroxides sees an exponential increase. It is interesting to note that high TLI values in this comparison, Figure 4.5, were not always found to

correspond to high PVs. and after the 4 hours aging time, both the Menhaden oil and corn oil had reached a similar TLI, but the PV values were significantly different. This difference could have arisen for two reasons: 1) from the difference in the composition of the oils, with Menhaden oil containing a higher level of PUFA than corn oil, leading to formation of peroxides which are captured differently by the two methods 2) formation of different peroxides in the initiation and propagation stages of oxidation. One example of a type of peroxide that could lead to poor correlation between the PV and CL methods is cyclic peroxides, as these are not measured via the iodometic titration method, but are measured via CL [122].
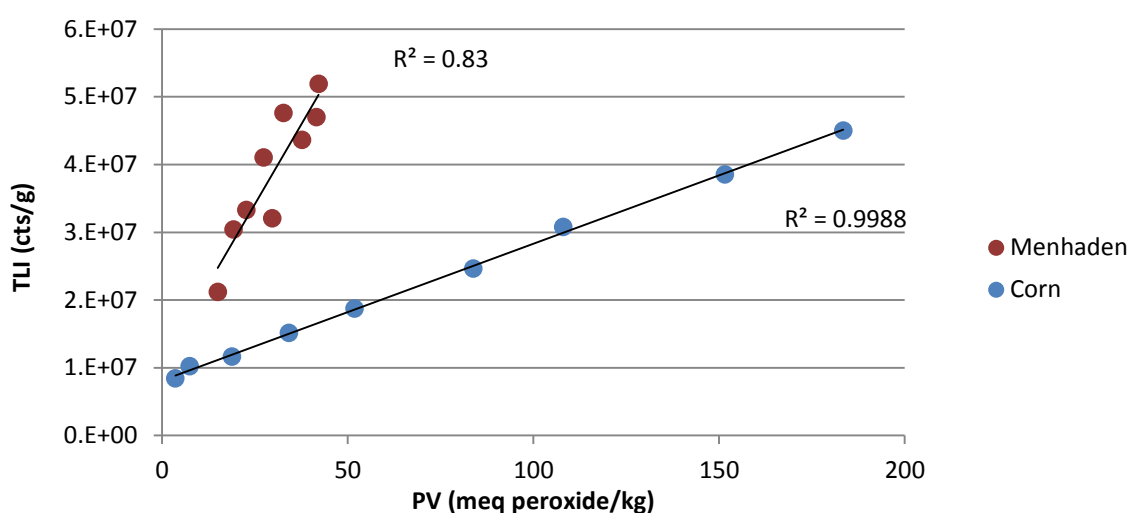
Figure 4.6 - Correlation between PV and TLI for corn oil (120°C) and Menhaden oil (70°C)

A strong correlation was observed between the PV and TLI values for corn oil (R^2=0.9988) and Menhaden oil (R^2=0.83), Figure 4.6. From Figure 4.6 it can be concluded that the TLI value is not absolute, as the trend lines do not overlay because the TLI values for Menhaden oil are higher than those for corn oil in the low PV range. It was not possible to draw firm conclusions after the initial testing at 120°C for corn oil and 70°C for Menhaden oil, due to the temperature difference in the aging of the oils leading to the two oils being at a different stage of oxidation progress so testing was then extended to allow the comparison of both oils at the same temperatures. Corn oil was aged for 4 hours at 70°C and the results are shown in Figure 4.7.
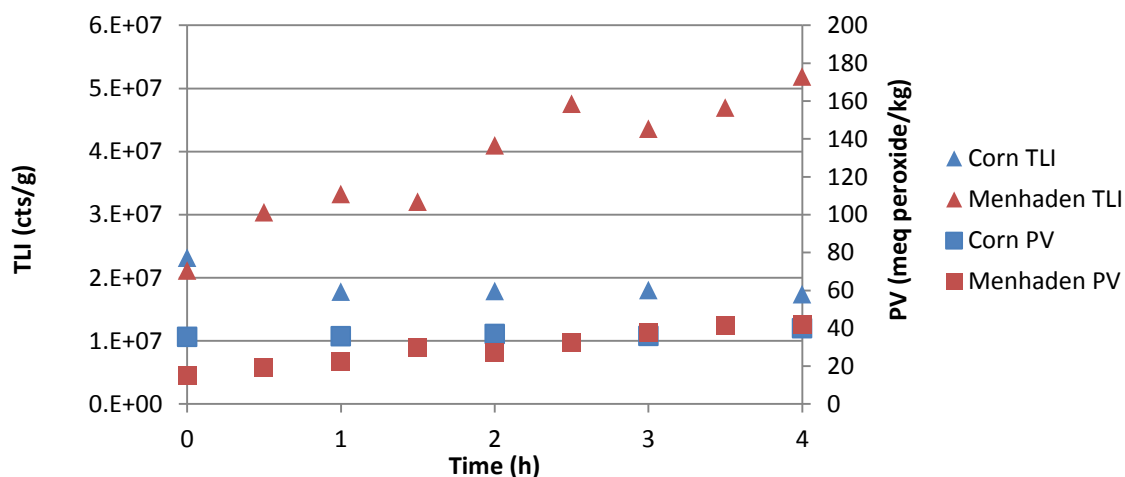
Figure 4.7 - TLI and PVs of corn oil and Menhaden oil artificially aged over 4 hours at 70°C

Figure 4.7, shows the PV and TLI of corn and Menhaden oil aged at 70°C for 4 hours, the PV of corn oil rose from 35.44 to 40.06 over the 4 hours aging period, which is only a slight rise and the Menhaden oil rose from 15.02 to 41.58 meq peroxide/kg which was a more prominent rise than corn oil at this temperature. This indicated that the oxidation progress of both oils was still in the initiation phase during this time period. Despite the PVs of both oils being in the range 15.02 - 41.08 meq/peroxide/kg, the TLI values were at different levels, with corn oil TLIs between 1.74 - 2.32 x 10^7 cts/g and Menhaden oil TLIs being 2.12 x 10^7 - 5.19 x 10^7 cts/g. When considering the correlation between PV and TLI at this temperature, shown in Figure 4.8, for Menhaden oil the correlation between the two values is quite strong (R^2 = 0.83), however for corn oil the correlation appears to be weak and negative (R^2 = 0.2549). If the sample from the first time point is removed the negative correlation becomes stronger (R^2 = 0.8027). The separation between the correlation data for the two oils in Figure 4.8 indicates that there is an oil dependence factor, arising in the CL method even when in this case both oils are in the initiation stages of oxidation.
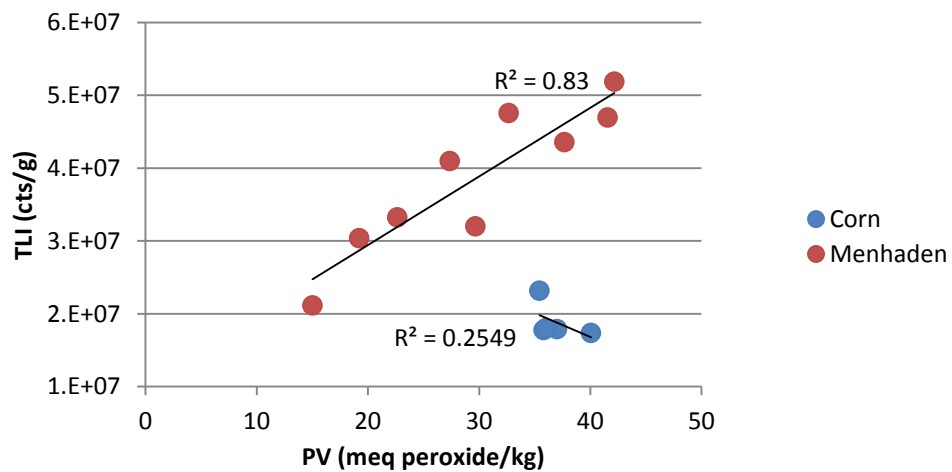
Figure 4.8 - Correlation plot of PV and TLI for corn oil and Menhaden oil artificially aged over 4 hours at 70°C

Both oils were aged at 90°C to investigate this further. When considering the results from the testing, shown in Figure 4.9, the corn PV increased linearly (R^2=0.9836) over the aging time at this temperature, from 10.36 – 40.71 meq peroxide/kg, which was a more pronounced increase than at the lower heating temperature of 70°C.
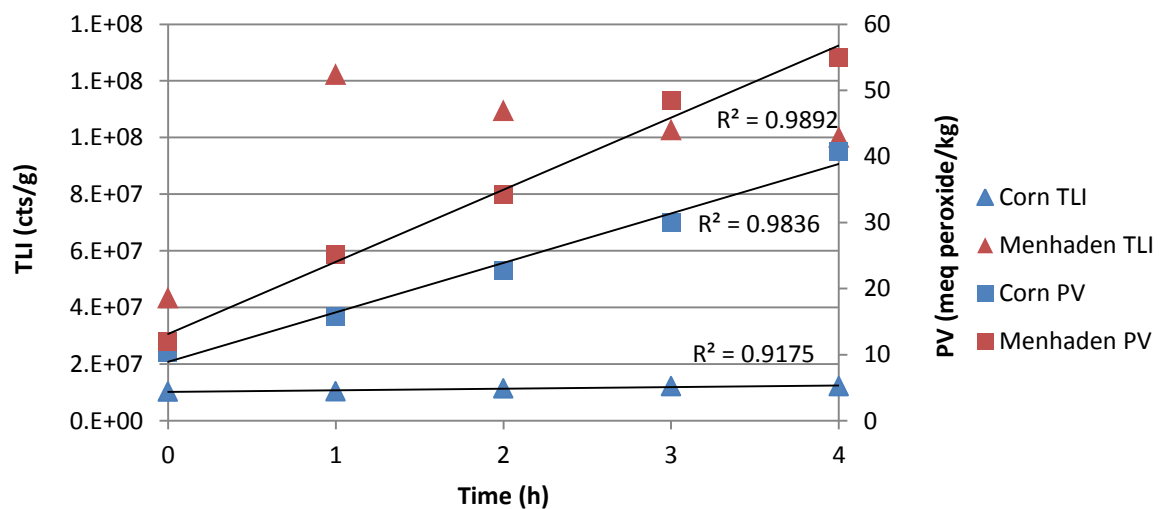
Figure 4.9 - TLI and PVs for corn oil and Menhaden oil artificially aged over 4 hours at 90°C

In contrast to this, the corn oil TLI remained stable, with no significant change. The Menhaden oil PV results also showed a steady linear increase (R^2=0.982) over the time period however the TLI sharply rose sharply after 1 hour and then steadily decreased with heating time, displaying a negative logarithmic correlation (R^2=0.9973) with aging time at 90°C. This steady decrease in TLI over the aging time suggests that at 90°C peroxides are decomposing with prolonged exposure to this temperature, the oxidation progress had reached the termination stages, whereas the corn oil oxidation

was still in the initiation stages. The correlation plot in Figure 4.10 showed a strong negative correlation (R^2=0.9226) between PV and TLI for Menhaden oil, for oil aged at 90°C (first time point removed). This negative correlation may have arisen because after one hour of aging at 90°C the peroxides that were formed then began decomposing as heating continued. This meant that when the aged samples were tested on the ACL Instrument, a proportion of the peroxides detected by the CL measurement were already decomposed and so the TLI dropped after each hour of aging time. This suggests that those peroxides giving rise to the AOCS PV measurement are different to those giving rise to the TLI measurement in this case.
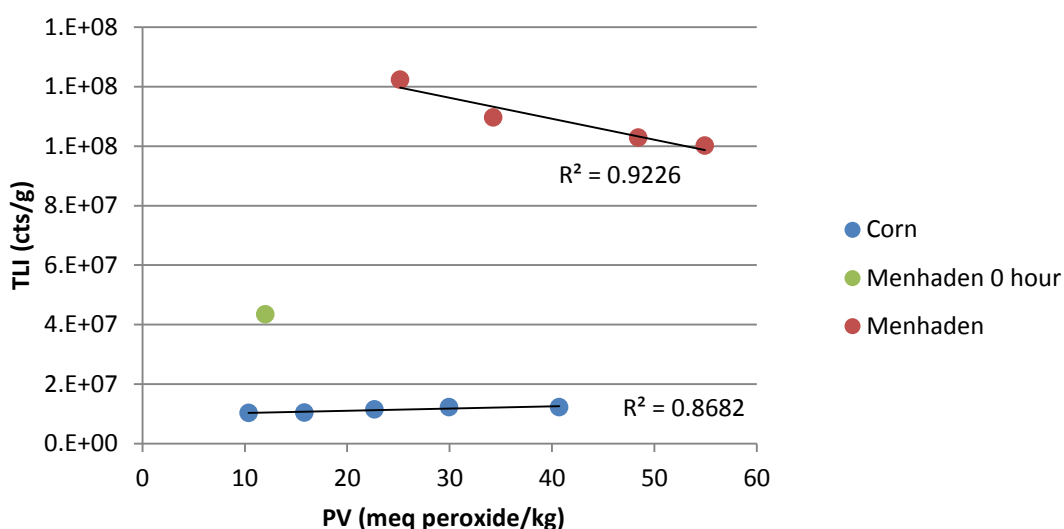
Figure 4.10 - Correlation plot of PV and TLI for corn oil and Menhaden oil artificially aged over 4 hours at 90°C

The results from testing corn oil at 100°C, Figure 4.11, show a steady rise in PV from 13.66 – 54.94 meq peroxide/kg and a slight rise in TLI from $9.57 \times 10^6 – 1.27 \times 10^7$ cts/g. For Menhaden oil at this temperature, the PV rose to much higher values from 12.00 – 197.27 meq peroxide/kg. Those PVs above 70 are outside the range of the AOCS PV method, as above this value the results can be unreliable. The TLI for Menhaden oil rose sharply after 1 hour and then fell from 2 hours, which is in contrast to the PV which rose over the duration of the heating, however, did appear to have less pronounced increase between 3 and 4 hours. It is difficult to conclude which stage of oxidation the Menhaden oil was at when aged over 4 hours at 100°C, as the trend in PV data indicated that the oxidation may at the propagation stage, whereas the TLI indicated that the oil was in the propagation stages until 2 hours after which point

termination began. Corn oil appeared to be in the initiation stages as the linear increase in PV and TLI was similar to at 90°C.
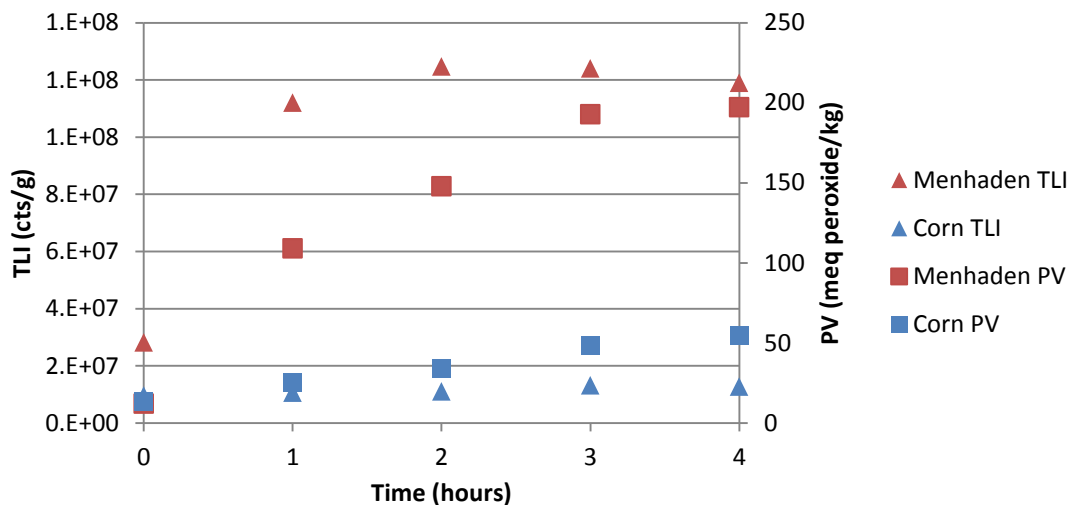
Figure 4.11 - TLI and PVs for corn oil and Menhaden oil artificially aged over 4 hours at 100°C

The correlation between PV and TLI for corn oil at this temperature was strong (R^2=0.9385), Figure 4.12. For Menhaden oil the correlation was calculated after removing the results from 0 hours, due to the sharp initial rise in TLI and the linear correlation was poor (R^2=0.3721) indicating that there was no linear relationship. This could be a result of the aging capturing peroxides during the propagation and termination stages over the 4 hour sampling window. As with the results at 70°C and 90°C, there was a clear separation between the results for the two oils suggesting a dependence on oil type or type of peroxides formed in different stages of oxidation progress.
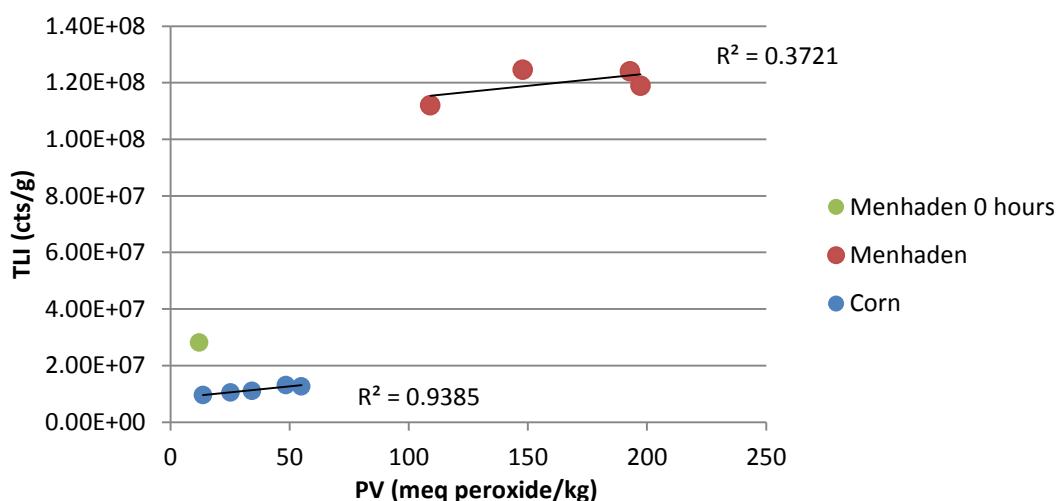
Figure 4.12 - Correlation plot of PV and TLI for corn oil and Menhaden oil artificially aged over 4 hours at 100°C

After considering the results observed in Figure 4.9 and Figure 4.11, where it was shown that Menhaden oil reached PVs above the limit of the AOCS PV method, Menhaden oil was not tested at 120°C to provide comparison to corn oil. It was concluded that this temperature would be too high and would result in PVs that were either beyond the range of the AOCS PV method, or would result in peroxides being decomposed and PVs therefore would be low despite the samples being highly oxidised. In addition to this, the CL oxidation profile of Menhaden oil, observed in Figure 3.20, section 3.5.4, Chapter 3 showed that at 100°C Menhaden oil reached CLI_{max} after ~10 hours and at 110°C it reached CLI_{max} after ~5 hours. It could therefore be expected that at 120°C after ~2.5 hours ageing, the CLI_{max} would be reached and therefore aging samples at this temperature for 4 hours, would decompose any peroxides formed before CLI_{max} was reached.

The results from testing of corn and Menhaden oil were then combined, Figure 4.13, and as expected, due to the different aging temperatures, different oil compositions and different stages of oxidation progress, a weak (R^2 = 0.3137) correlation between PV and TLI over the different heating temperatures and two different oils is evident.
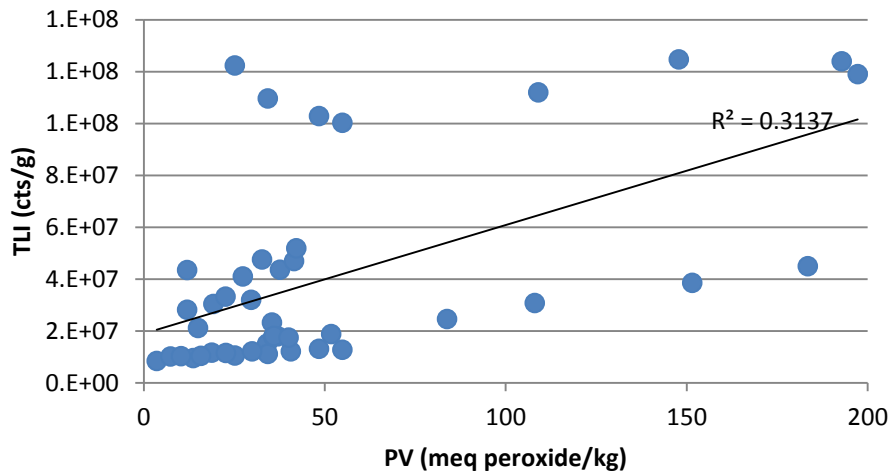
Figure 4.13 – Correlation plot of corn oil and Menhaden oil PV and TLI across all temperatures

These results were then assessed separately for corn and Menhaden oil, Figure 4.14. The correlation for corn oil PV and TLI was $R^2 = 0.905$ whereas for Menhaden oil, $R^2 = 0.5032$. As previously mentioned, the AOCS PV method used in this study to measure PV has limitations above 70 meq peroxide/kg test substance. Considering all samples with a PV less than 70, two distinct groupings can be observed in Figure 4.14. One grouping has TLI values in the order of 4.00E+07 cts/g for PVs of up to 70 and another grouping in the range of 1.20E+08 cts/g across all PVs.
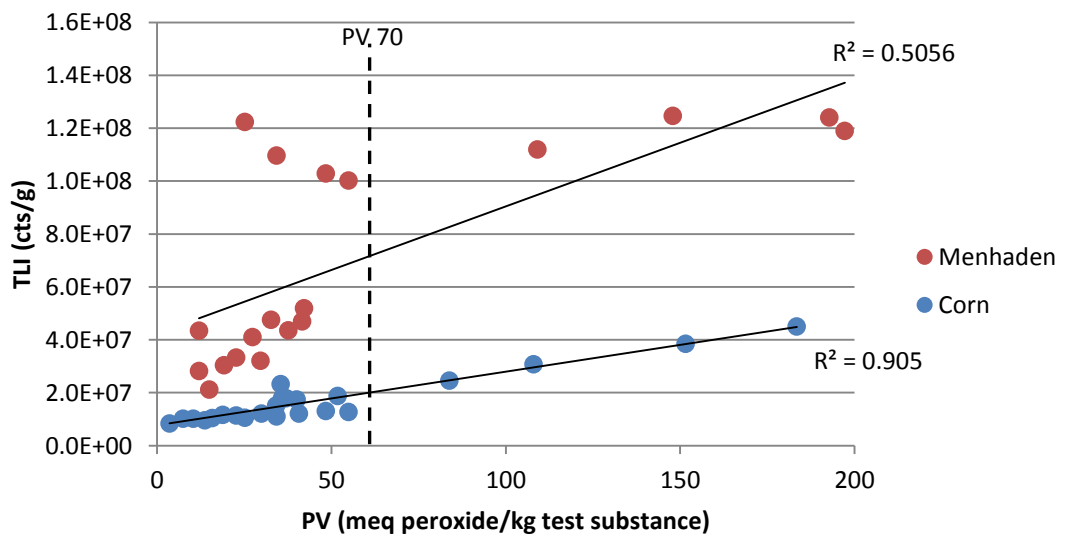
Figure 4.14 – Correlation plot of corn oil and Menhaden oil PV and TLI across at all temperatures

The two distinct groupings of data points within the Menhaden oil data highlight the effect of temperature on Menhaden oil oxidation. The grouping around 4.00E+07 cts/g is the data from the runs at 70°C and the groupings with the higher TLI are results from

runs carried out at 90 and 100°C where the oxidation progress of samples being tested was observed to be in the termination stages and propagation/termination stages respectively.

The analysis was repeated removing those samples with a PV over 70, Figure 4.15. The correlation for PV and TLI for Menhaden oil with the exclusion of PVs over 70 meq peroxide/kg test substance was lower (R^2 = 0.2927) than with PV> 70 included (R^2 =0.5056). However this included data from heating Menhaden oil at 90°C which showed the oxidation progress to be in the initiation stages in terms of PV but in the termination stages in terms of TLI, Figure 4.9. The correlation for PV and TLI for corn oil was also lower (R^2 = 0.378) than with PV> 70 included (R^2 = 0.905). This could indicate that the relationship between TLI and PV was stronger at higher temperatures for corn oil, whereas for Menhaden oil the relationship was stronger at lower temperatures.
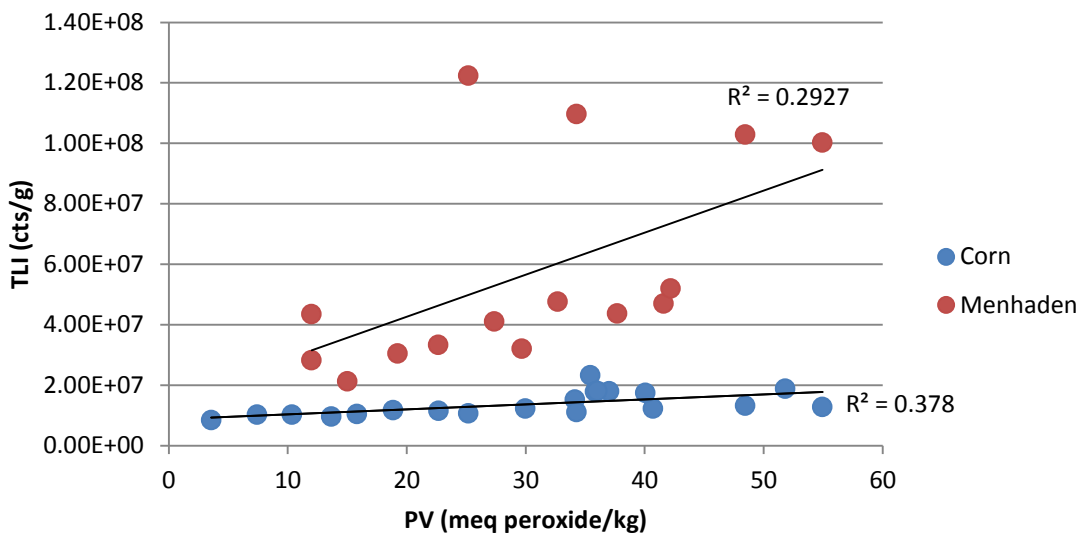
Figure 4.15 – Correlation plot of TLI and PVs <70

One final comparison between the oils was made, which considered only data from those temperatures at which the oils were in the initiation stages during 4 hour aging period. This encompassed results from Menhaden oil at 70°C, corn oil at 70, 90 and 100°C and the correlation between PV and TLI is shown in Figure 4.16. This was carried out to eliminate the effect of oxidation progress from the analysis.
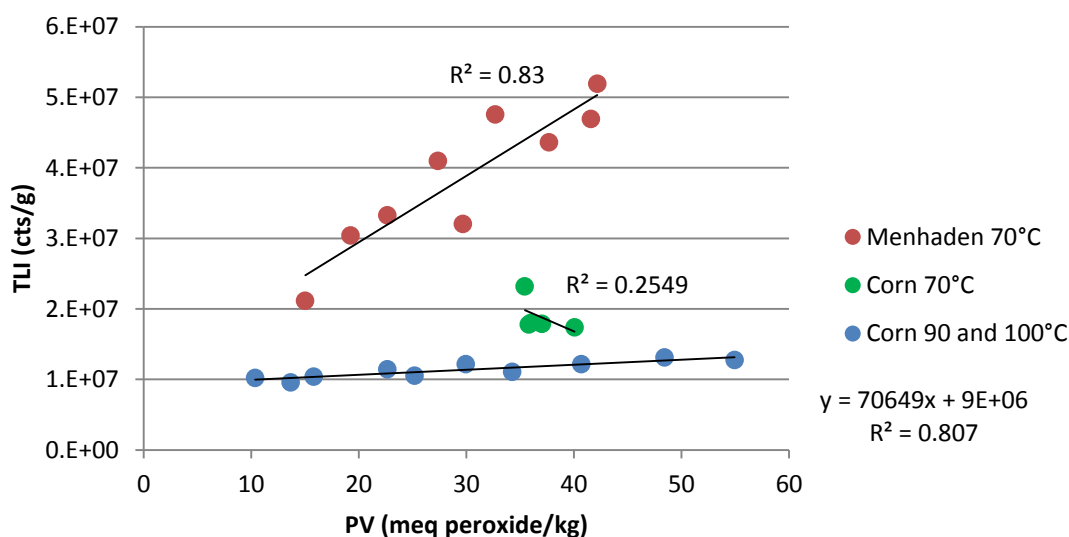
Figure 4.16 - Correlation plot of TLI and PVs for Menhaden and corn oil during initiation stage of oxidation progress
(Menhaden oil aged at 70°C for 4 hours, corn aged at 70, 90, 100°C for 4 hours)

The correlations between PV and TLI in the initiation stages of oxidation for both the Menhaden (R^2 = 0.83) and corn (R^2 = 0.807) are strong, but are distinctly separated. The correlation between PV and TLI of corn oil at 70°C stands out from the other corn oil data and this may be due to the corn oil being at the very early stages of initiation at this temperature as there was very little change in the TLI results and only slight changes in the PV. The data presented in Figure 4.16 strongly supports the conclusion that there is both an oil dependency and a dependency on oxidation progress that affects the correlation between PV and TLI in oils.

The precision of each of the measures, the PV and the TLI, was investigated using the relative standard deviation (%RSD). The %RSD provides an indication of the precision of the assay and the metric allows the comparison of data sets with significantly different means as the value is dimensionless. Relative standard deviation was used by Stepanyan *et al* [91] in the analysis of CL and PV data from spiked samples of corn oil and for the CL method were in the order of 1-5%. The %RSD was calculated for each of the mean values across all CL and PV temperatures and time points for both corn and Menhaden oil and was also calculated for only the results from samples that displayed a PV of <70, Table 4-1. This enabled the analysis of precision to address results from a range of oil ageing states. The PV gave better precision than the ACL TLI in terms of a

lower %RSD for both cases, when all results were considered and when only results with PVs <70 were considered.

Oil	All results		Results with PV <70	
	PV (mean %RSD) n=24	ACL TLI (mean %RSD) n=19	PV (mean %RSD) n=20	ACL TLI (mean %RSD) n=11
Corn	6.64	9.57	6.44	10.28
Menhaden	4.96	10.55	2.77	11.78

Table 4-1 - Mean %RSD values for PV and TLI results from corn oil and Menhaden oil across the range of heating temperatures 70-120°C

The AOCS method states values for precision that were determined in inter-laboratory tests however these do not include corn oil and Menhaden oil [5]. Repeatability values were stated for a number of oils and these represent the difference between two test results on the same material, in the same laboratory and under the same conditions [5]. %RSD values were stated for the following oils: coconut oil (5.38, n=14), Linola oil (5.14, n=15), lard (6.34, n=13), tallow (5.61, n=11), beef fat (2.93, n=11), olive oil (4.08, n=16) and palm stearin (7.86, n=16). %RSD values found in this research were with this range, corn oil (6.44, n=20) and Menhaden oil (2.77, n=20) suggesting that the method was performed with comparable precision to the inter-laboratory testing.

An additional indicator, conjugated diene value (CDV), was measured using UV spectrophotometry and calculated according to Equation 4.2 and Equation 4.3. In the early stages of autoxidation almost immediately after peroxides are formed, the non-conjugated double bonds that are present in natural unsaturated lipids are converted to conjugated double bonds within unsaturated fatty acids, and increase the absorbance at 233nm [123]. In a study where CDV was compared to PV, the CDV was found to plateau, whereas PV initially increased but then decreased over time [124], however the oil was heated at 170°C which is a higher temperature than those used in this research. In this research, corn oil aged at 120°C and Menhaden oil aged at 70°C were tested. A clear trend was evident in corn oil, Figure 4.17, and Menhaden oil, Figure 4.18, with all measures in PV, CDV, TLI and TLI (to CLI_{max}), showing an increase with heating time. These results were in agreement with an increase in oxidation being associated with an increase in CD formation. The TLI (to CLI_{max}) measure in this instance was the area under the CL curve up to CLI_{max}, this was not possible to calculate for Menhaden oil as the CL curve was not bell shaped.
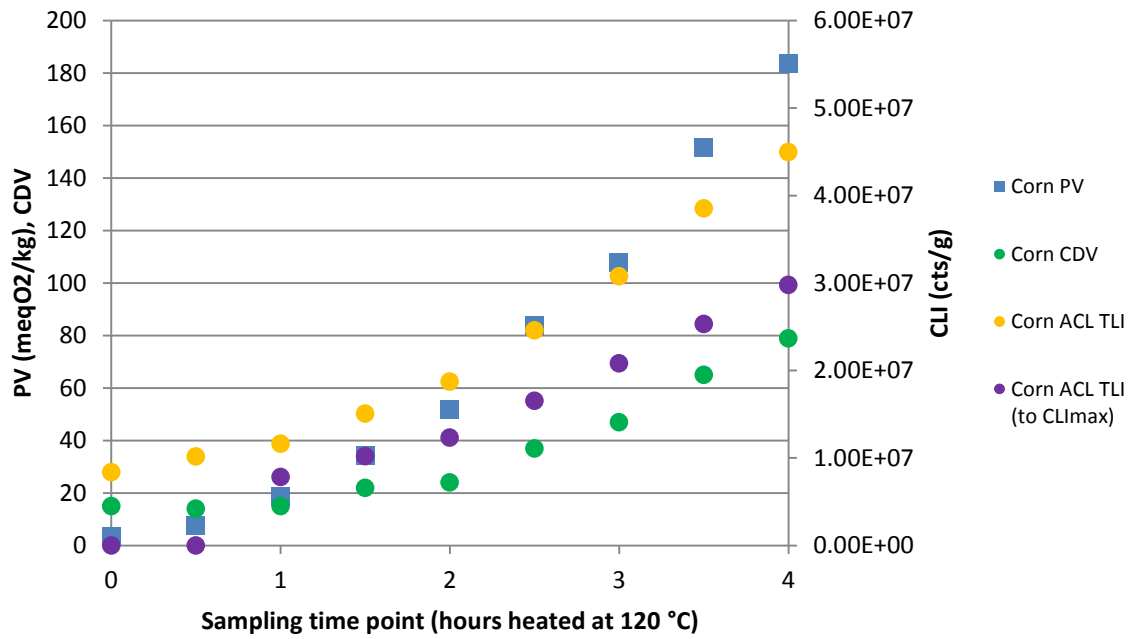
Figure 4.17 - Change in PV, CDV, TLI and TLI (to CLI_{max}) for corn oil, heated over 4 hours at 120 °C
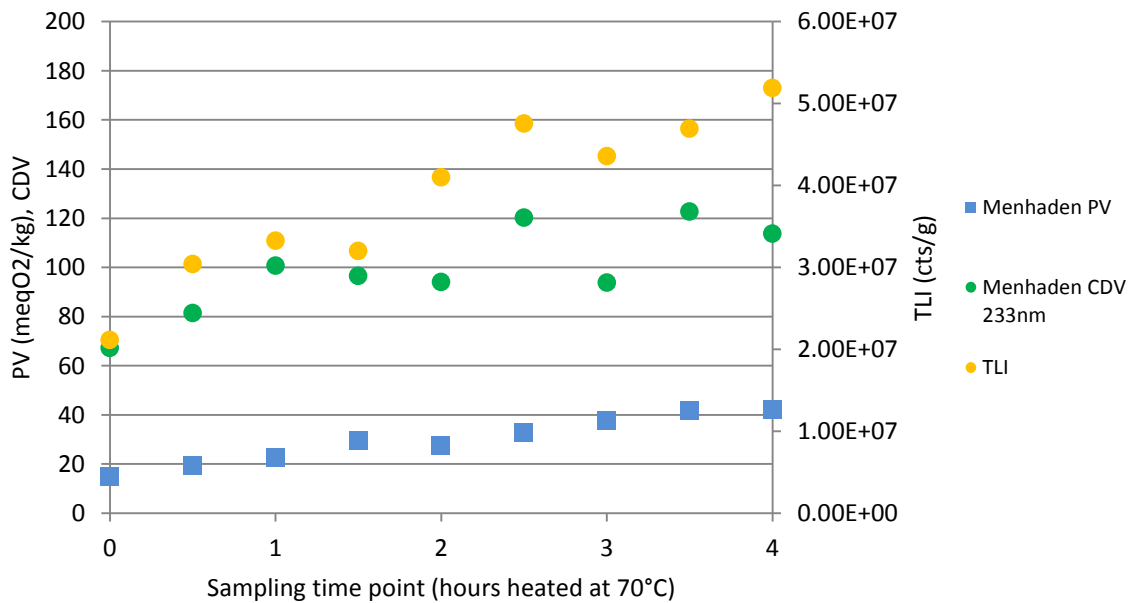
Figure 4.18 - Change in PV, CDV, TLI for Menhaden oil, heated over 4 hours at 70°C

Parameter	Correlation (R^2 values) Corn oil 120°C	Correlation (R^2 values) Menhaden oil 70°C
PV vs CDV	0.9864	0.6618
TLI vs CDV	0.9838	0.7501
TLI (to CLI_{max}) vs CDV	0.9897	Not calculated as no peak

Table 4-2 - Correlations of CDV, PV, TLI and TLI (to CLI_{max})

The correlations between CDV and the other measures in this study (PV, TLI and TLI to CLI$_{max}$) were calculated and displayed in Table 4-2. The strong correlation between CDV and PV (R^2 =0.9864), for corn oil oxidation indicates that there was a strong relationship between these two values at the temperature at which the corn oil was aged (120°C). This correlation was not as strong for Menhaden oil (R^2 = 0.6618) aged at 70°C. A strong correlation was observed in corn oil between the CDV and two measures from the CL curve, TLI (R^2=0.9838), and TLI (to CLI$_{max}$) (R^2= 0.9897). The strong correlations between the measures in corn oil indicate that the methods are capturing peroxides and the structural changes associated with the reaction of those peroxides. The weaker correlation between CDV and PV for Menhaden oil may be due to the lower amount of linoleic acid in this oil compared to corn oil. A previous study by Marmesat *et al* [125] found that hydroperoxides formed from linoleic acid contribute to the CDV but those formed from oleic acid do not. Hence in an oil with a higher amount of linoleic acid than Menhaden oil ($<$ 5% linoleic acid), such as corn oil (~50% linoleic acid), it could be expected to have a stronger correlation between PV and CDV. The percentages of oleic acid contained in the two oils were closer to each other, with Menhaden containing ~10% oleic and corn ~30% and with both fatty acids present in different amounts in both oils, it was not possible to link the difference in correlation to a particular difference in fatty acid content.

4.6   Operational considerations

When comparing the ACL Instrument and the AOCS titration method, it is necessary to consider the operational aspects and which method offers the most benefit overall in terms of inputs, time, waste disposal, operator involvement and costs. Table 4-3 summarises the operational factors for the ACL Instrument and the AOCS titration method. The factors have been chosen as these are common considerations when looking to adopt new methods. The sample size associated with the AOCS titrations, 0.3-5g, has been criticised in the literature [126, 127] as being too large, especially when experimental oils, those in short supply or expensive products need to be tested. The development of a method to reduce the sample size and waste associated with the AOCS PV has been discussed by Crowe and White [126]. This method required sample sizes of 0.5g, used only 10% of the chemicals required in the standard ACOS method and was found to correlate with the AOCS method with a strong linear

relationship (R^2=0.998). In contrast, the ACL Instrument requires 1-50mg of sample. This would warrant application of the ACL Instrument in testing of experimental oils, those in short supply or expensive products. However for pharmaceutical raw materials testing, a sample size of 0.3-5g as is required by the AOCS method, does not pose a problem for the testing of some materials such as polysorbate as large quantities are available, but for the active pharmaceutical ingredients (API) this may not be the case, as large quantities may be costly. With regards to the waste generated by the two methods, the AOCS PV method titrations produces several millilitres of waste per titration, so when performing multiples repeats, there is a significant amount of liquid waste to dispose. The method also requires the use of a fume hood and requires rigorous cleaning of glassware with detergent and rinsing with propan-2-ol to remove oily residues. The ACL Instrument in contrast produces no liquid chemical waste and requires disposal of only a sample holder into a sharps bin after each run and 1-2mL propan-2-ol on cotton wool for cleaning of the furnace cell between runs.

Factor	ACL Instrument	AOCS Titration [5]
Sample size	0.1-20mg	0.3-5g
Inputs	Sample holder, nitrogen supply, electricity	Liquid and solid chemicals, flammable and toxic
Equipment	Bench-top, PC, gas cylinders	Fume hood, glassware, stirrer
Waste	Sample holder, cotton buds	Mixed liquid chemical waste
Setup time	Setup ~5 min	3 hrs preparation per batch
Operator time	None	~5 min
Cleaning time	~ 1 min	~ 5 min per sample
Time to result	Variable: 2 hrs	~5 min
Data processing	Manual using software: 10 min per result	Instant result
Functionality	Quantification of peroxides, oxidative stability	Measurement of peroxide value
Equipment costs	High	Low
Type of test	Destructive	Destructive
Reagent volume	None	50-150mL
Sensitivity	High [84]	Low [128]
Specificity	CL directly proportional to $c[ROO^\bullet]$, $c[ROOH]$ [129]	Substances that oxidise potassium iodide
Reference material	Non-specified	Non required
Test conditions	Optimisation possible	Conditions specified in method
Precision	Corn TLI %RSD 10.28 n=11 Menhaden TLI %RSD 11.78 n=11	Corn oil %RSD 6.44 n=20 Menhaden oil %RSD 2.77, n=20
Interference	None	Oxygen, light, absorption of iodine by unsaturated fatty acids
Detection limit	None specified	0-≥70meq peroxide/kg test substance, method is erratic ≥70

Table 4-3 – Comparison of operational factors for ACL Instrument and AOCS titration

The two methods require differing operator input. To set up the PV titrations, several solutions are required with preparation taking around 4 hours and this must be carried

out for each batch of titrations. The ACL Instrument takes around 5 minutes to set-up, and can then be left to run without operator input. The PV titrations require an operator to perform all of the tests, one at a time, with each titration taking around 5 minutes. Although the PV titrations require an operator, it is possible to carry out around 24 titrations in 2 hours, whereas the ACL Instrument takes around 2 hours to run one sample, which includes testing time and cooling of the furnace cell before another run can be started. The cleaning required after the titrations takes around 3 minutes for each sample and for the ACL Instrument cleaning takes around 1 minute for each sample.

Interference from light and oxygen in the air can cause error in measurements performed by titration, but carrying these out in the dark in the absence of air is not practical. An additional source of error is the absorption of iodine at unsaturated bonds [130]. In contrast, the conditions inside the furnace cell of the ACL Instrument are tightly controlled so there is no interference from light and oxygen in the air and no reagents are added, which removes these as potential sources of error in this method. Additionally, there is minimal variation introduced by the operator during the measurement as this is automated and does not rely on visual observation and judgement of colour change.

No reference material is required for the AOCS titration and the ACL Instrument literature does not state that any reference material is required. However in this research, it has been shown that a reference material would be required of known or acceptable quality against which subsequent samples can be compared, if precise values are required as necessary in pharmaceutical analysis. In addition to testing a reference material, it is also necessary to define a method to use with the ACL Instrument, for example, deciding on the speed of the temperature ramp and the gas flow, whereas with the AOCS PV method, it is prescriptive and the operator must follow the protocol. The ACL Instrument therefore requires several decisions and possible pre-testing to determine the experimental setup before tests can begin. Ideally a set of standard methods would be designed for use in testing of pharmaceutical excipients or products.

Data acquisition from the PV titrations involves one calculation, so results are immediate. The CL data must be exported from the instrument and each spectrum plotted using a software package, taking a few minutes per spectra. If the machine was put into routine use, there is scope for this data processing step to be automated, which would increase the speed of data analysis and remove operator error. This is currently not available.

4.7 Conclusions

It was hypothesised that the ACL Instrument could not provide an absolute value for peroxide levels, which would be correlated to the PV when testing across different oils and across oils aged at different temperatures. The results from this research support this hypothesis and although some results showed that a strong correlation existed between the TLI and PV for corn oil and Menhaden at a number of temperatures, these strong correlations were not seen across all results from aged samples. It was concluded that this could have been due to the different fatty acid compositions for the two oils, giving rise to different types of peroxide, which are picked up to differing extents by both methods. This suggests that compared to CDV and PV, which are used as a comparative indicators across a number of oils, CL measurements of peroxides cannot yet be used in this way. From this research it is not possible to conclude which method gives the most reliable measure of peroxides, however, it is expected than the CL method may capture many different types of peroxide in contrast to the PV method which only captures peroxides that are reduced by the iodide ion.

Consequently for the ACL Instrument to be utilised for the quantification of peroxide levels, it would be necessary to develop a calibration model. This would involve determining the peroxide level using the AOCS PV method, or another method which has been identified as providing a suitable means to measure peroxides, and then measuring the TLI for a sample of oil with sufficient quality. This TLI and CL curve would then form the basis of a CL standard for that particular oil. It would also be necessary to allow the oil to age naturally (in a long term study) with further PV and TLI measurements recorded to understand how the CL relationship changes over time, and whether the PV and TLI measurements correlate strongly over the aging period. This would allow a more detailed understanding of CL mapping of ageing and also

provide a robust quality standard for a particular oil, against which samples of an unknown age/quality could be tested.

The methods were comparable in terms of their precision, with %RSD values in similar ranges, with those for TLI being slightly higher than PV. The advantage of using the ACL Instrument over the titration method is that it is much less labour intensive, easier and quicker to set up, produces a lot less chemical waste and does not require a fume hood. However, one major disadvantage of the method is the throughput of samples, being much lower than the titration method. What the ACL Instrument does provide however, is more information about the substance as the shape of the CL curve, for example in this instance the bell shaped curve vs. lack of bell shaped curve, can be considered as well as values calculated for quantifying peroxides.

4.8   Future work

This work could be extended to a wider range of oils with differing fatty acid compositions, to develop a better understanding of the effect of oil type on the correlation between PV and TLI. By investigating a number of oils it may be possible to deduce relationships that could provide information to understand the relationship between the two methods. However this would be time consuming, as carrying out replicates on the ACL Instrument would take a long time.

In this investigation, heating and aeration were used to age the oils and induce a range of peroxide values. In future work another approach to comparing the AOCS PV method and the ACL Instrument may be through the preparation of peroxide standards. The preparation of peroxide standards has been described by several authors and the methods of preparation vary. Some studies used artificial aging of the oils to induce the formation of peroxides [104] and some studies used spiking with hydrogen peroxide, or *tert*-butyl hydroperoxide [109]. When investigating FTIR as a method for peroxide determination, Van de Voort [109] used a 3M solution of *tert*-butyl hydroperoxide (TBHP). This was diluted in isooctane and its PV measured. Commercially available oils were then tested for their PV and then had TBHP, oleic acid and water added in random (w/w) amounts. The PVs of the standards were then measured and the base oil PV subtracted from the total PV, to understand the effect of the addition of TBHP. Stepanyan *et al* [91] used the equation of the regression line to

determine the relationship between the PV (meq peroxide kg^{-1}) and CL intensity, as part of an investigation into the suitability of CL as a method for evaluation of total peroxides in model oil samples spiked with hydrogen peroxide. Recoveries were calculated for the method to deduce whether it was possible to measure PV using the CL method. This was successful and recoveries with an average of 93% were achieved. However, to test neat samples of oil that may be used for food or nutritional supplements requires a method that can measure all peroxides present and spiking studies may not help to understand what types or levels of peroxide are present as these spiked peroxides may react with the oil altering its composition.

Another approach to creating a set of standards was discussed by Kim et al [104] who artificially aged a sample of soybean oil by purging it with 10mL/min air whilst heating the oil at 50°C for 48 hours. This soybean oil with a known PV of 51 was then added to original soybean oil, to a set of standards with PVs 0, 2, 4, 6, 8, 10 meq peroxide kg. The heating time and the temperature used by Kim *et al* to artificially age the oils is longer and lower respectively, than the time and temperature used to age the oils in this research. An approach such as that of Kim could be used to test the linearity of the two methods.

Future work in this research would consider the CL curve for an oil during oxidation and set up an experiment which sampled the oil at points across the whole CL curve, Figure 4.19, before and during initiation, propagation and termination stages. This would then allow the comparison of the two methods, on one oil, over the course of oxidation, which would make it possible to see if at a certain stage of the oxidation progress the relationship between the two measurements changed.
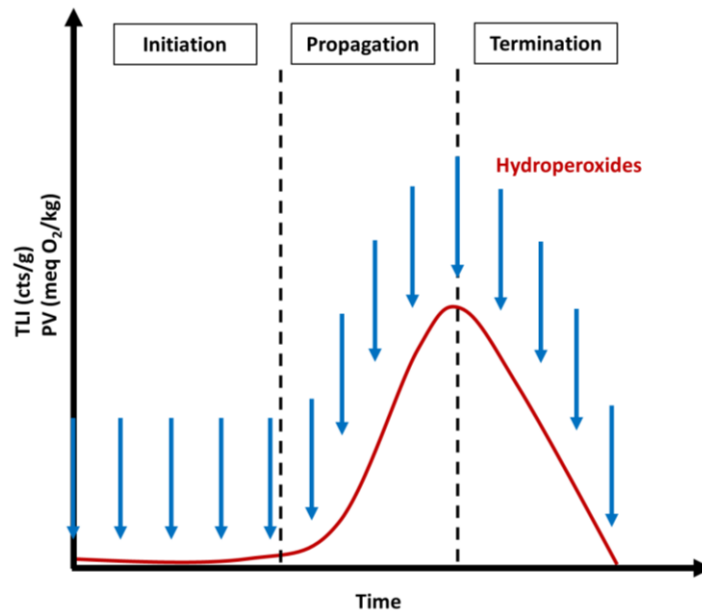
Figure 4.19 - Example of sampling points across the whole CL curve for measurement of PV and TLI

If CL were to be used as a tool for testing the peroxide levels of oils, there would need to be work carried out to standardise the method or create a library of spectra providing 'CL fingerprints' for numerous oil standards of high quality and low oxidative stability (as determined by other methods), to which oils of unknown quality could be compared. Recommendations for industry regarding the use of the ACL Instrument for quantification of peroxides are summarised in Chapter 8, section 8.4, Table 8-2.

Chapter 5. The ACL Instrument as a fingerprinting tool for determining polysorbate stability

5.1 Introduction

Chapter 5 utilises the methods investigated in Chapter 3 and Chapter 4 (ACL Instrument, Rancimat and AOCS titration) to investigate the applicability of the ACL Instrument for measuring the stability of polysorbates, common pharmaceutical excipients whose stability has become an issue as the sensitivity to oxidation of complex pharmaceuticals has increased.

5.1.1 *Stability testing of pharmaceutical formulations*

Stability testing is a critical aspect of any drug development programme and is performed at many stages during the development process: on the active pharmaceutical ingredient (API), the excipients that are formulated with the API and also on those final pharmaceutical products that are on the market. Stability testing exists to determine an appropriate shelf life and storage conditions for the final product. The shelf life is a period of time within which the active pharmaceutical ingredient (API) undergoes no degradation or changes that will affect its activity and hence it remains fit for purpose.

This research focusses on stability testing of excipients, in particular, polysorbates. These excipients are tested by manufacturers before release to ensure that they meet specifications and certain pharmacopoeia standards before they can be included in pharmaceutical formulations. Traditionally, excipients were viewed as 'inert' substances [131] and little attention was paid to the effect they could pose on drug formulations, however, now it has been recognised that they play an important role in drug formulation stability. Excipients can interact with the active pharmaceutical ingredient (API) causing physical changes to the formulation such as reduced dissolution or chemical changes such as API degradation [132]. The regulatory guidelines surrounding pharmaceutical stability testing, discussed in 5.1.2, focus on the drug substance and the drug product rather than the excipients themselves. As drugs become more complex and move away from small chemical entities to biopharmaceuticals/biologics which comprise large complex protein structures, the

impact of excipients on the stability of the final formulation may become more of a challenge. However, at this current time, no universally accepted protocol exists for the evaluation of the compatibility of drugs with excipients [132].

The stability of an API depends largely on its structure but once formulated it becomes affected by the excipients present, the packaging and the storage conditions. By furthering the understanding of the stability of excipients it may be possible to minimise the number of stability issues that occur once formulations have been filled and finished [133]. This research investigates a method that may have the potential to determine if subtle differences exist in the stability of polysorbates, which is of particular interest as polysorbates are present in a number of pharmaceutical products. On past occasions when the supply of polysorbate has changed i.e. a change in the manufacturing site, differences in the characteristics and performance of the polysorbates was recognised. Finding new methods to aid in the characterisation and stability measurement of polysorbates is therefore important to augment the understanding of the link between these excipients and product quality and safety.

5.1.2 *Stability testing regulation*

There are a number of regulatory requirements for stability testing which are covered in guidelines published by the International Conference on Harmonisation of Technical Requirements for Registration of Pharmaceuticals for Human Use (ICH). The guidelines are briefly summarised in terms of their reference to excipients and degradants, which are the focus of this research into polysorbate stability.

In these guidelines the drug product is defined in Q1A (R2) as: *'the dosage form in the final immediate packaging intended for marketing.'* The drug substance is defined as: *'the unformulated drug substance that may subsequently be formulated with excipients to produce the dosage form'* and the excipient is defined as *'anything other than the drug substance in the dosage form'* [134]. The 'degradation product' as mentioned in the guideline Q3B(R2) is defined as: *'An impurity resulting from a chemical change in the drug substance brought about during manufacture and/or storage of the new drug product by the effect of, for example, light, temperature, pH, water, or by reaction with an excipient and/or the immediate container closure system'* [135]. A problem with this definition of degradation product is that it does not include

degradation products arising from the breakdown of an excipient, which could pose an equally damaging threat to quality and safety as a degradation product of the drug substance itself.

Guideline Q3A(R2) [136] covers impurities in new drug substances and classifies impurities into three categories: organic impurities (process and drug-related), inorganic impurities and residual solvents. The organic impurities are further broken down into: starting materials, by-products, intermediates, degradation products and reagents, ligands and catalysts. Guideline Q3B(R2) [135] covers impurities in new drug products, however, it excludes impurities arising from the degradation of excipients. This is potentially an issue as, later in the chapter, examples of how the degradation of excipients can be detrimental to formulations will be discussed. The guideline Q3B(R2) focusses only on the degradation of the drug product or, interactions of the drug product with an excipient or the container closure system. This guideline does not cover the degradation products of excipients themselves and does not address the effect that these may have on the final formulation. However, a report on the qualification of excipients for use in pharmaceuticals from the International Pharmaceutical Excipient Council (IPEC) states that excipient stability can be investigated using accelerated protocols from ICH Q1A [137].

Guideline Q5C covers the stability testing of biotechnological/biological products and states that: *'The use of relevant physicochemical, biochemical and immunochemical analytical methodologies should permit a comprehensive characterisation of the drug substance and/or drug product (e.g., molecular size, charge, hydrophobicity) and the accurate detection of degradation changes that may result from deamidation, oxidation, sulfoxidation, aggregation or fragmentation during storage.'* [11] In this guidance there is a reference to of the effects of excipients and the guidance encourages monitoring of these and how these affect the shelf life and quality of the final product: *'Additives (e.g., stabilisers, preservatives) or excipients may degrade during the dating period of the drug product. If there is any indication during preliminary stability studies that reaction or degradation of such materials adversely affects the quality of the drug product, these items may need to be monitored during the stability program. The container/closure has the potential to adversely affect the product and should be carefully evaluated'.*

In the guidance Q5C, the definition of degradation product is different to the definition given in Q3B(R2). In Q5C the degradation product is defined as: *'a molecule resulting from a change in the drug substance (bulk material) brought about over time. For the purpose of stability testing of the products described in this guideline, such changes could occur as a result of processing or storage (e.g., by deamidation, oxidation, aggregation, proteolysis). For biotechnological/biological products some degradation products may be active.'* The definition of degradation product in Q5C only refers to the degradation of the drug substance and not the excipient. Additionally, the definition suggests that the degradation products in biotechnological/biological drugs may be active, however, it does not refer to the degradation of the excipients and there is evidence to suggest that these can also be active, which is discussed later in the chapter.

5.1.3 *Polysorbates and challenges arising from the inclusion of polysorbates in formulation*

Polysorbates are non-ionic surfactants that are widely used in protein formulations to reduce aggregation [138] and it is estimated that 70% of monoclonal antibodies on the market contain either polysorbate 80 or polysorbate 20 [139]. Polysorbates prevent aggregation by reducing interfacial stresses at the air/liquid, ice/liquid interfaces and also at the interface with surfaces. In the absence of polysorbates, particulates can be formed and aggregation can occur, which for parenteral pharmaceuticals, poses a threat to product quality and patient safety.
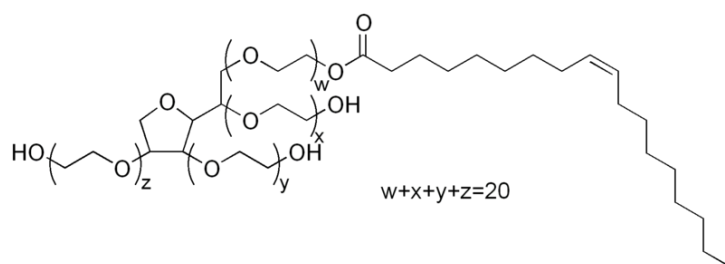
Figure 5.1 - Structure of Polysorbate 80

Polysorbates 20, 60 and 80, are composed of fatty acid esters of polyoxyethylene sorbitan and are heterogeneous substances due to the fatty acid esterification process. All polysorbates have a common backbone, the sorbitan ring, Figure 5.1, but are distinguished by differences in the structure of the fatty acid side chains. These fatty acid side chains contain sites prone to free-radical attack. In polysorbate 80 the fatty

acid side chain is based on monooleate whilst in polysorbate 60 monostearate and polysorbate 20 these are monolaurate. Unsaturated fatty acids (those with carbon-carbon double bonds) are more prone to free-radical attack than saturated fatty acids, and polyunsaturated more so that monounsaturated as they provide more sites for free-radicals to attack [50]. Polysorbate 80 is therefore more susceptible to oxidative degradation than polysorbate 60 and 20, due to a higher degree of unsaturation on the monooleate fatty acid side chain. Particular attention should be paid to the oxidative stability of formulations containing polysorbates as they are known to promote oxidation and polysorbate 80 has previously been used to oxidise drugs during stability assessment [140]. Significant lot-to-lot, and manufacturer-to-manufacturer [62] variability has been identified for polysorbates, consequently it is important to understand how this might impact on the final formulation [141] and this is addressed in this research.

The type of polysorbate which is chosen to formulate with the API is crucial for ensuring formulation robustness. Polysorbates can undergo refining and super refining which are processes are carried out to improve the stability of the polysorbate. The distinguishing feature between super refined polysorbate and standard grade polysorbate is that the former undergoes a chromatographic purification step which facilitates the removal of polar impurities such as aldehydes and peroxides, whilst retaining the integrity of the polysorbate. This refining process aims to prevent adverse interactions between the excipient and the APIs and enhance the stability of the final pharmaceutical formulation.

Recently, Singh *et al* highlighted the importance of the grade of polysorbate on formulation stability [138]. The photostability of a product was investigated in the presence of four different types of polysorbate: Polysorbate 80 Super-Refined (Mallinckrodt Baker), Polysorbate 80 National Formulary (NF) (Mallinckrodt Baker), Polysorbate 80 NF (EMD Chemicals) and Ultra-pure Polysorbate 80 (HX), (NOF Corporation). The product that was formulated with super-refined polysorbate 80, was found to retain the highest percent of monomer (indicator in this study) and displayed the lowest level of oxidation compared to product formulated with the other polysorbates, highlighting that the grade impacts on product stability.

Differences in manufacturing conditions, purification, packaging and storage conditions result in differences in peroxide levels and other impurities between the same grades manufactured by different suppliers. The degradation of polysorbate could lead to a reduction in polysorbate concentration which may increase the risk of protein aggregation and possibly compromise patient safety through giving rise to an immune response in the patient when a parenteral formulation is injected into the bloodstream [142]. Another issue surrounds the effects of the degradants of polysorbates on the protein structure.

Chemical impurity profiles have received limited attention [62] and in the case of polysorbates there is evidence that they are susceptible to autoxidation, resulting in the formation of reactive oxygen species e.g. peroxides which in turn can cause oxidation of the formulation [143], thereby impacting on their application. Peroxides have been shown to affect the stability of a number of drugs including penicillin which was inactivated and oxytetracycline which was markedly affected by peroxides arising from polyethyle glycols [144].

Examples of detrimental effects caused by polysorbates on formulations have included both liquid and solid dosage forms. In a study carried out by Cory *et al* [145] on ibuprofen tablets stored at 70°C/75% RH for 3 weeks, it was found that the presence of polysorbate 80 caused an increase in degradation of the API, compared to other excipients such as povidone [146].

Ha *et al* [4] investigated the effect of polysorbate 80 on a model protein IL-2 mutein during storage. IL-2 mutein was chosen because of the susceptibility of the methionine residue to oxidation at room temperature storage. When polysorbate 80 containing high levels of peroxide was formulated with IL-2 mutein, immediate IL-2 mutein oxidation occurred during annealing in the lyophilisation process. The example of IL-mutein highlights how important the susceptibility of excipients are when developing protein formulations, and hence processing steps such as lyophilisation in this case, must be scrutinised when proteins susceptible to oxidation are formulated with polysorbate.

Oxidation of proteins can occur at susceptible side chains, through the addition of oxygen to methionine, cysteine, histidine, tryptophan or tyrosine residues. When

studying the effects of polysorbate 20 quality on the stability of a recombinant humanized monoclonal antibody fragment, Lam *et al* [147] saw that an increased peroxide level in polysorbate 20 during the formulation step of the manufacturing process resulted in the oxidation of the tryptophan (Trp) residue in the protein. They also concluded that the Trp oxidation mechanism involved free radical formation [147]. As well as containing residual levels of peroxide, polysorbates can also undergo photodissociation leading to the production of a singlet oxygen which then can react with methionine residues.

5.1.4 *Measurement of stability in polysorbates*

The peroxide levels of polysorbates have traditionally been measured using the peroxide value. This is a static indicator that quantifies the peroxide level at a particular time point. The European Pharmacopeia (Ph Eur) specifies a limit for the peroxide number (PN) ≤10 and it is assumed that a higher level of peroxides will have a greater detrimental effect than a lower level. This relationship may be not directly applicable as the mechanisms of degradation caused by peroxides are extremely complex. Kishore *et al* [141], identified over 50 types of product arising from the degradation of polysorbate. Consequently polysorbate is a difficult substance to predict the behaviour of once it has been formulated. Bearing in mind these complex degradation pathways and resulting products the following quote from Narang *et al* [148] highlights how the applicability of standard methods can be limited, *'the compendial limits on peroxide level may or may not be sufficient to assure satisfactory product stability'*. A peroxide level provides an indication of the peroxide content at a particular time point, but the performance of the substance over time whilst on the shelf may be different. Peroxide levels have also been shown to increase on storage [148]. Narang *et al* [149] investigated the effects of storage on peroxide levels in povidone, an excipient used as a suspending agent in solutions and a disintegrant and binder in tablets. Results formed a complex picture of peroxide formation, the initial concentration of peroxide in povidone was 74.7 ± 3.1 ppm. After 2.5 months at 40°C/11% relative humidity (RH) the peroxide level increased to 124.7 ± 12.2ppm and after 28 months this increased further to 261.3 ± 40.3ppm. After 2.5 months at 25°C/11% RH the peroxide level had increase to 99.3 ± 11.0ppm and after 28 months had increased further to 206.7 ± 18.0ppm. At high humidity the peroxide levels

dropped, after 2.5 months at 25°C/60% RH to 44.0 ± 6.0ppm and after 28 months no peroxides were detected. This effect was even more pronounced at high temperature and humidity 40°C/60% RH where peroxide level dropped to 8.7 ± 4.2ppm after 2.5 months and no peroxides were detected after 28 months. Reduction in peroxide levels under high humidity conditions may have been due to increased mobility of the excipient which has increased its ability to react hence quenching of the peroxide formation reaction, water-peroxide exchange and quenching of singlet oxygen [149]. What was important in this study was that recommended storage conditions of low humidity for povidone power were challenged, as these gave rise to the highest level of peroxide accumulation.

Wasylaschuk *et al* [62] identified the need for a simple, rapid, and sensitive methodology for measuring total hydroperoxide content (ROOH and H_2O_2) for common pharmaceutical excipients, both soluble and insoluble. Whereas peroxide levels using the traditional peroxide value measure may have provided a simple and rapid test, the sensitivity may not be satisfactory. Some methods that exist for the testing of other excipients are not suitable for polysorbates e.g. UV spectrophotometry, as polysorbate 80 does not possess a chromophore. A test for peroxides should be able to quantify the initial levels of peroxide in the polysorbate and ideally also be applicable to testing of the final formulation. Using testing to monitor manufacturing and refining processes may also be beneficial to help understand how manufacturing parameters can affect the levels of residual peroxides.

The ACL Instrument, described in Chapter 3 and Chapter 4, has not previously been investigated for measurement of the stability of polysorbates and it shows potential for being a useful method for this purpose, based on results in previous chapters.

5.2   Aim

The aim of this investigation was to determine the suitability of the ACL Instrument for measuring oxidative stability and peroxides levels in polysorbates. The following set of experiments were undertaken to assess the capability of the ACL Instrument:

1) Two grades of polysorbate 80, (high purity polysorbate 80 (HP-PS80) and Tween 80 were tested using the ACL Instrument, to determine whether a difference in the CL curves could be detected

2) Polysorbates 20, 60 and 80 were tested to compare the shapes of the CL curves

3) Two batches of Polysorbate 80 Eu Pharm and three batches of Tween 80 were tested to investigate the possibility of using the CL technique as a fingerprinting method for determining the quality of the polysorbate

4) A comparison of the ACL Instrument and Rancimat for measurement of oxidative stability of polysorbates was carried out

5) The ACL Instrument, Rancimat and iodometric titration were compared for the detection of batch-to-batch variation in polysorbate 80 and Tween 80

5.3 Experimental

5.3.1 *Materials*

Materials used for testing are detailed in Table 5-1. High purity polysorbate 80 (460414) (HP-PS80) and Tween 80 (426262) were obtained from Croda. Polysorbate 20 Ph Eur (CAS 9005-64-5), polysorbat 60 Ph Eur (9005-67-8), and polysorbate 80 Ph Eur (9005-65-6), were obtained from Sigma Aldrich. Two batches of polysorbate 80 Ph Eur (BCBJ7603V and BCBH5882V) and three batches of Tween 80 Ph Eur (BCBG4950V, BCBJ4213V and BCBJ8859V), were purchased from Sigma Aldrich. 22mm borosilicate glass slides were supplied by ACL Instruments. 150mm clear glass reaction vessels were purchased from Metrohm. Glacial acetic acid, 2,2,4-trimethylpentane, potassium iodide, potassium dichromate, sodium thiosulfate, sodium dodecyl sulfate, hydrochloric acid and starch were purchased from Fisher Scientific.

Material	Batch Number	Supplier
High Purity Polysorbate 80	460414	Croda
Tween 80	426262	Croda
Polysorbate 20 Ph Eur	BCBF8583V	Sigma Aldrich
Polysorbat 60 Ph Eur	BCBD9369V	Sigma Aldrich
Polysorbate 80 Ph Eur	BCBF4913V	Sigma Aldrich
Polysorbate 80 Ph Eur	BCBJ7603V	Sigma Aldrich
Polysorbate 80 Ph Eur	BCBH5882V	Sigma Aldrich
Tween 80 Ph Eur	BCBG4950V	Sigma Aldrich
Tween 80 Ph Eur	BCBJ4213V	Sigma Aldrich
Tween 80 Ph Eur	BCBJ8859V	Sigma Aldrich

Table 5-1 - Batches of polysorbate and Tween 80 under investigation

5.4   Methods

5.4.1   *Measurement of oxidative stability using isothermal CL*

The measurement of CL was carried out using the ACL Instrument. Operating parameters of the ACL Instrument were the same as those given in Chapter 3, section 3.4.3. Samples, weighing between 6.8-16.5mg, were subjected to a conditioning stage for 10 minutes at ambient temperature in nitrogen, before a temperature ramp after which an isothermal temperature profiles at, 100, 110 or 120°C was held. Between runs the polysorbate samples were stored in the dark, under nitrogen in amber bottles, at ambient temperature. Samples were tested in duplicate.

5.4.2   *Measurement of accumulated hydroperoxides*

Measurement of accumulated peroxides was carried out according to the method described in Chapter 4, section 4.4.2. Samples weighing from 9.4-16.8mg were tested in triplicate.

5.4.3   *Determination of oxidation onset temperature (OOT)*

A dynamic temperature profile was used with synthetic air as the reaction gas, to understand how the substances behaved across a temperature profile. The sample was heated from 30-200°C at a rate of 2.98°C/min. The ACL Instrument was operated using bottled synthetic air at a flow rate of 30mL/min. Samples were weighed onto 22mm borosilicate glass slides and placed in the furnace cell, they were then subjected to conditioning for 10 minutes at 30°C prior to the temperature ramp. The oxidation onset temperature (OOT) was then calculated manually with tangents placed on the curve to provide an indicator of stability.

5.4.4   *Determination of peroxide value*

Peroxide value (PV) was measured according to the method detailed in Chapter 4, section 4.4.3.

5.4.5   *Measurement of oxidative stability using the Rancimat*

This was carried out according to the method in Chapter 3, section 3.4.2. Samples were tested in triplicate at 50, 60, 70, 80, 90, 100, 110 and 120°C. Both oxidation induction time and stability time (defined in section 3.1.4) were evaluated.

5.4.6 *Data processing*

Oxidation induction time (OIT) and oxidation onset temperature (OOT) for the polysorbate oxidation were calculated from the CL curves, smoothed with a 10 point Savitzky Golay filter, as described in Chapter 3, section 3.4.6.

5.5   Results and Discussion

5.5.1 *Effect of heating rates on polysorbate tested under nitrogen*

Polysorbates 20, 60 and 80 were tested using dynamic runs in nitrogen with two different heating rates: 2.98°C/min and 1°C/min, to determine the effect of heating on CL curve shape and the total luminescence intensity (TLI) (cts/g). The slower heating resulted in a more repeatable shape when visually comparing the curves. An example of this is shown for polysorbate 80, Figure 5.2.
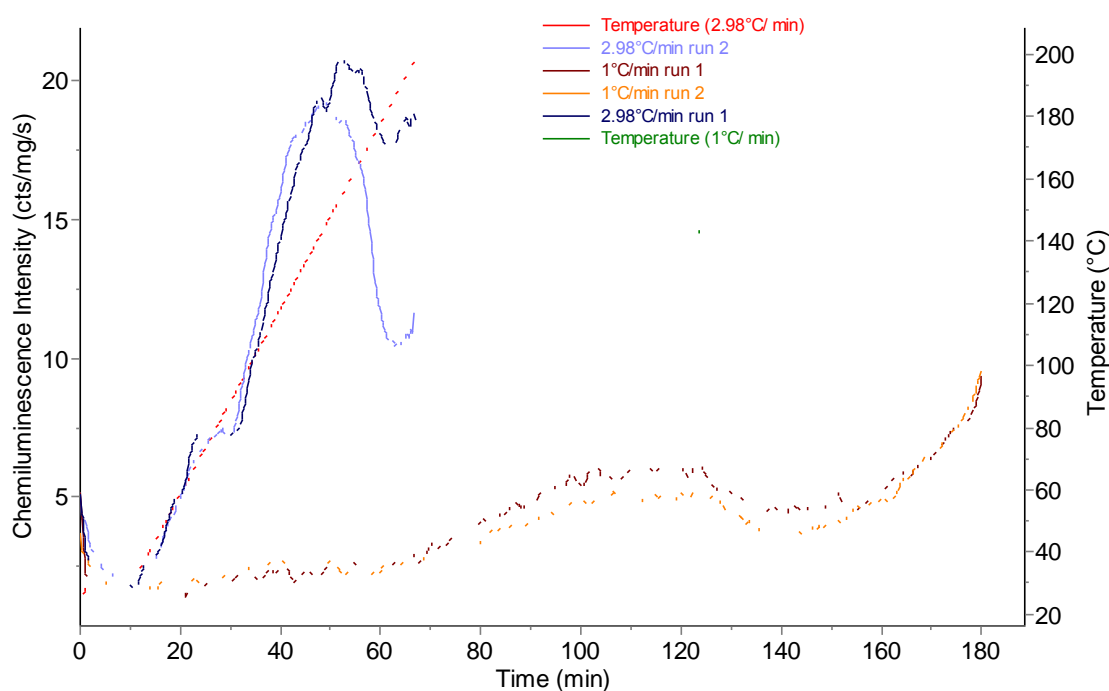
Figure 5.2 - CL curves of PS80 subjected to fast (2.98°C/min) and slow (1°C/min) heating rates
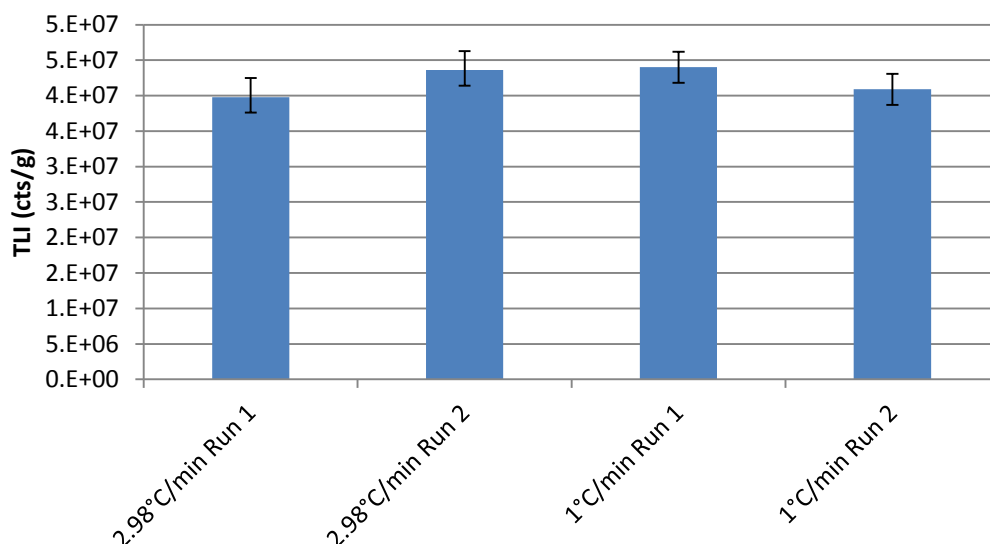
Figure 5.3 - TLI values for PS80 subjected to fast and slow heating rates

The TLI (cts/g) values obtained for the two heating rates in PS80 were similar, Figure 5.3 and these were considered formally using a t-test. The resulting P values were PS80 (p= 0.811), PS60 (p=0.188) and PS20 (p=0.604) indicating that the difference between the TLI (cts/g) obtained for the two heating rates, across all the samples was not statistically significant. The faster heating rate was therefore chosen for efficiency, as it was possible to carry out shorter runs and additionally, when testing under nitrogen, the TLI, is used as a quantitative comparator between samples, with the curve shape being less important for comparison between samples in this type of testing.

5.5.2 *Comparison of HP-PS80 and Tween 80*

The testing of HP-PS80 (460414) and Tween 80 (426262) under a dynamic temperature profile in nitrogen, Figure 5.4, showed that HP-PS80 had a slightly higher residual level of hydroperoxides than Tween 80 indicated by the higher CLI reached during the three runs and also the mean value for the TLI, Table 5-2. Tween 80 had lower mean TLI (cts/g) (2.22×10^7) than HP PS80 (4.84×10^7), Table 5-2, and when compared with a 2-sample t-test the difference was not statistically significant (p=0.056).
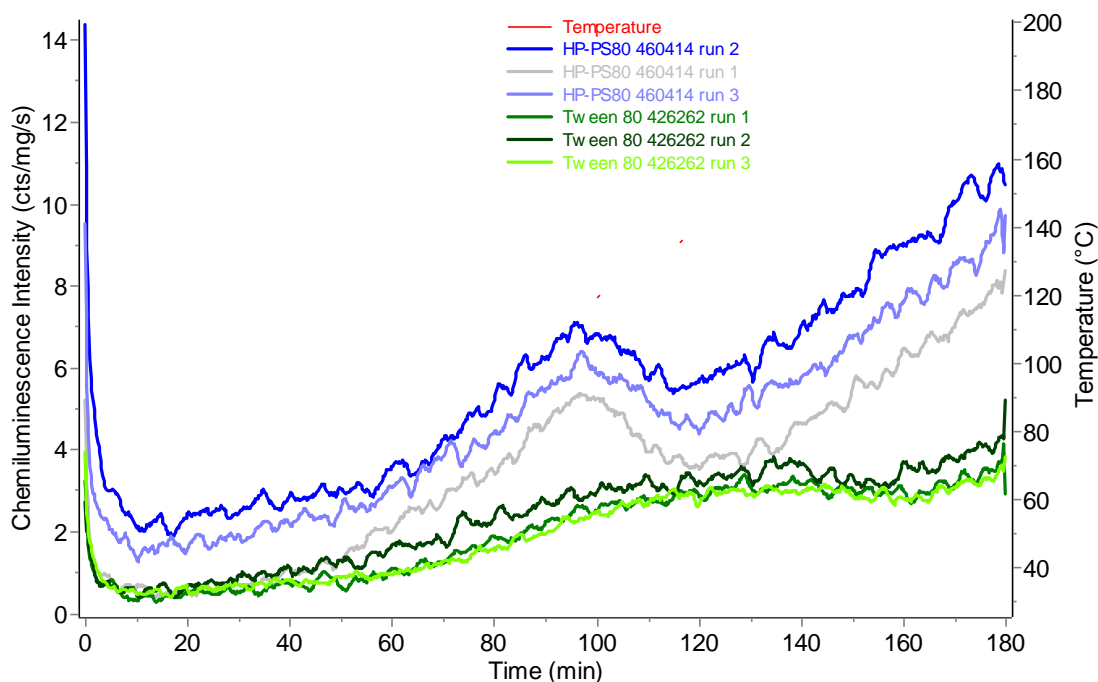
Figure 5.4 - CL curves of HP-PS80 and Tween 80 in nitrogen

	TLI (cts x 10^7/g)					
	Run 1	**Run 2**	**Run 3**	**Mean**	**SD**	**%RSD**
HP PS80 (460414)	3.71	5.88	4.92	4.84	1.09	22.48
Tween 80 (426262)	2.09	2.52	2.05	2.22	2.61	11.74

Table 5-2 - Total luminescence intensity (cts/g) for PS80 tested under nitrogen

It was not possible to quantify the level of hydroperoxides in these batches, as the integrated values were not absolute and could not be converted into a concentration of hydroperoxides, as previously discussed in Chapter 4, section 4.7. Until a standard method is developed for the ACL Instrument, that gives a definitive measure of peroxides, it will remain possible only to compare two or more substances to understand their differences. It is not currently possible to consider one substance and its measurements of CL in isolation to indicate peroxide levels.

It was expected that peroxide levels in Tween 80 would be higher than in HP-PS80 as HP-PS80 undergoes a chromatographic refining process to reduce the levels of peroxide, however, these results indicate the opposite. These results therefore raise questions about the purity of the HP-PS80 as it should contain lower levels of peroxides compared to unrefined varieties. These results could also indicate that tests used to quantify peroxides e.g. peroxide value used as standard tests by

manufacturers of polysorbate, may not be as sensitive as the ACL Instrument for detecting low levels of peroxides.
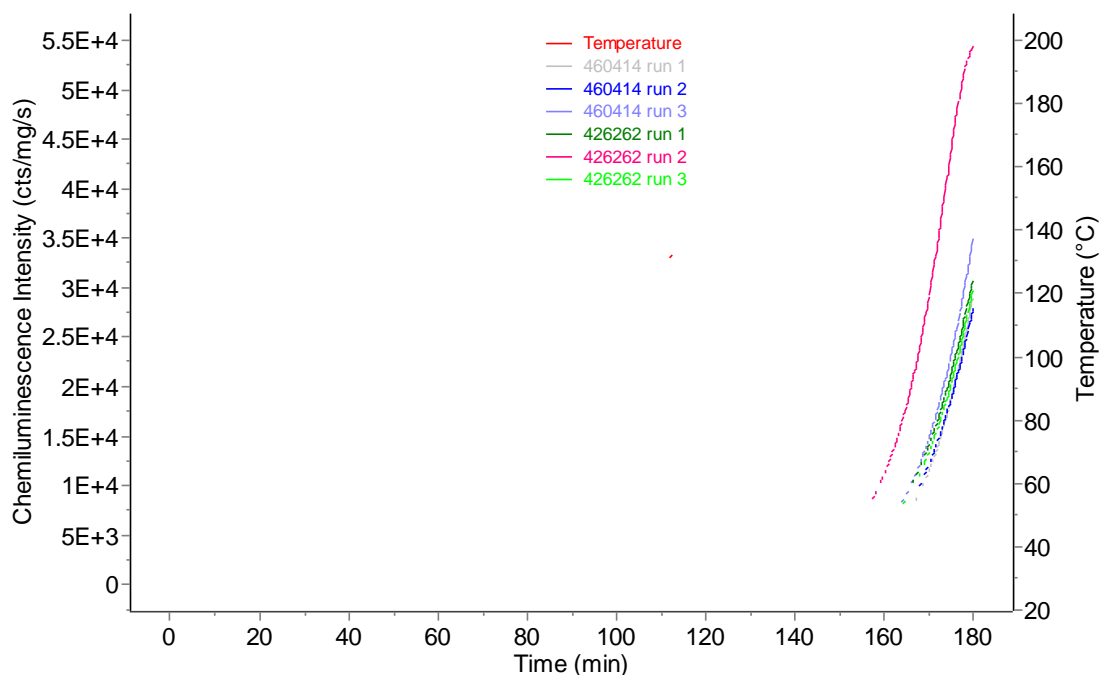
Figure 5.5 - CL curves of HP-PS80 and Tween 80 in synthetic air (dynamic temperature profile)

	OOT (°C)					
	Run 1	**Run 2**	**Run 3**	**Mean**	**SD**	**%RSD**
HP PS80 (460414)	183.88	181.81	182.96	182.88	1.04	0.57
Tween 80 (426262)	182.63	178.45	180.28	180.45	2.10	1.16

Table 5-3 - OOTs for HP-PS80 and Tween 80

The testing of polysorbates using a dynamic temperature profile under synthetic air allowed the determination of the OOT from the curves in Figure 5.5 and summarised in Table 5-3. This measure was used to compare the oxidative stability of HP-PS80 and Tween 80. It can be concluded that the mean OOTs are very similar indicating that both polysorbates have similar stability, with Tween 80 having a slightly lower OOT (180.45h) than HP-PS80 (182.88h). The OOTs were compared with a 2-sample t-test and the difference was not statistically significant (p=0.214). The standard deviations are small, indicating good repeatability. More specifically, the standard deviation for Tween 80 is slightly higher than HP-PS80 as run 2 of Tween 80 had a slightly lower onset temperature, with its curve appearing further to the left than the curves for other all other runs.

Further testing was undertaken to investigate whether the batches could be differentiated through testing under isothermal conditions in synthetic air at three temperatures, 100, 110 and 120°C. These temperatures were chosen to enable an appropriate run time as lower temperatures would have resulted in run times of greater than 100 hours which would be unfeasible. For routine testing of a number of samples, a run length of 100 hours would mean that throughput of the machine was low, as only one sample can be tested at once and this would not be feasible in the pharmaceutical testing scenario, but for the purposes of this research, these temperatures gave a compromise between run length and the production of a CL curve which could be analysed. Higher temperatures may not have given rise to CL curves that contained distinguishing features such as those seen in the CL curves of HP-PS80, Figure 5.6. These temperatures, 100, 110 and 120°C have allowed the visualisation of different oxidation events on the CL curves.
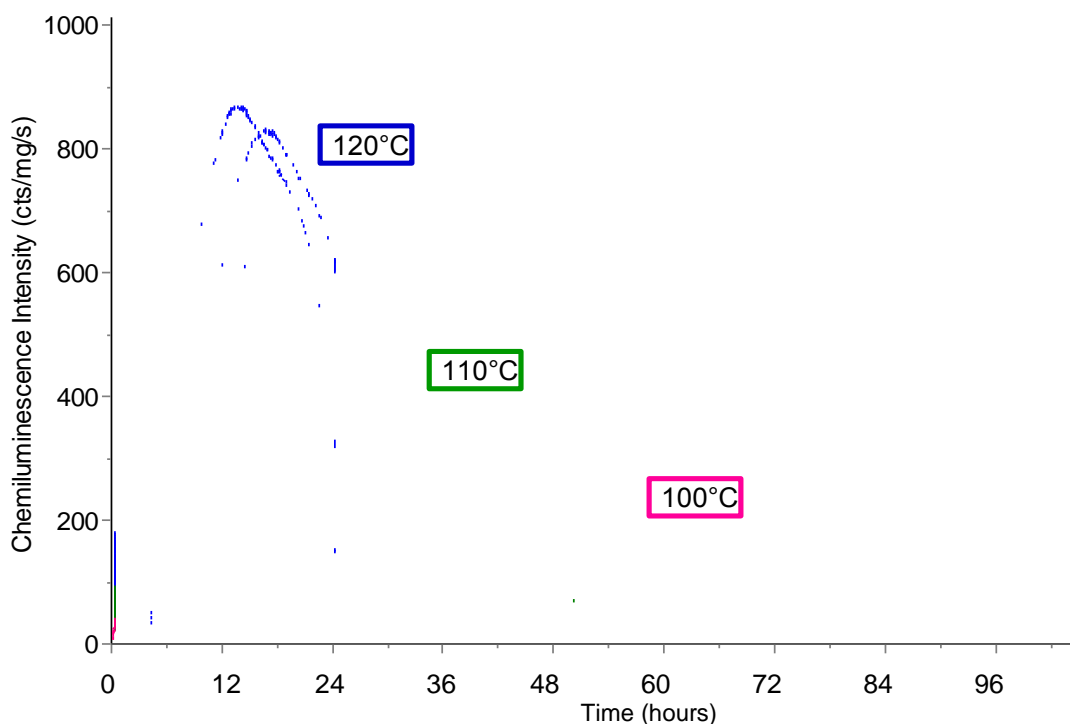
Figure 5.6 - CL curves of HP-PS80 at 100, 110 and 120°C

When considering Figure 5.6, the samples run at all of the three temperatures show an initial sharp rise in CL, followed by a fall. After this point the CL continued to increase to a minor peak, before a broader major peak occurred around CLI$_{max}$ which displayed a shoulder on its right hand side. The lower temperature runs, carried out at 100°C

gave better resolution in terms of the initial part of the CL curve i.e. up to 24 hours, however a run length of 4 days would not be practical for the routine usage of this machine. The time to reach CLI_{max} at 100°C was in the order of 40 hours which would result in very low throughput of samples and hence would not be appropriate for routine testing. If in future work, information from the initial part of the curve could be correlated to another measure of oxidative stability. It may be possible to stop the run at a certain point and use this data for measurement, however this would require calibration to a standard, and it is useful to track the whole oxidation process for the extra information it provides.

The repeats at each temperature showed some evidence of variation. For the samples run at 120°C, the main sources of variation were in the intensity of CLI_{max} and also during the initial peak. In the sample run at 100°C, good repeatability was evident around the major curve for two runs, with the greatest variability occurring during the initial stages of the run i.e. in the period up to 24 hours. The three runs carried out at 110°C appeared to have the best repeatability. The clear differences in the early stage of the CL curves prior to the main peak, for all temperatures, could be due to sample heterogeneity, as polysorbates are known to contain diverse mixtures of degradation products, or it may be a result of an unstable species undergoing oxidation at these high temperatures. The features of the curve will be discussed later in this chapter, with a direct comparison of HS-PS80 and Tween 80 CL curves shown in Figure 5.13.

Figure 5.7 shows the CL curves of Tween 80 at 100, 110 and 120°C, it is clear that the repeatability is better than for the CL curves shown in Figure 5.6. For HP-PS80 the main difference is the repeatability of the first oxidation event in the CL curve. For Tween 80 this appears as one event with all runs at each temperature exhibiting similar curves whilst for HP-PS80 there is less consistency in behaviour, Figure 5.6. The CL curve shape around the CLI_{max} in Tween 80 again appears to exhibit better repeatability at 120°C compared to HP-PS80, Figure 5.7. The CLI_{max} in Tween 80 at 110°C was repeatable in terms of the intensity for all runs, but for time to CLI_{max}, one sample reached CLI_{max} 0.5 day later than the other two runs. Three runs were performed at the lower temperature of 100°C and showed good repeatability, with the CL curves superimposed. It was not possible to calculate an OIT from the CL curves as there was no baseline, and it appeared that oxidation occurred from the start of the run.
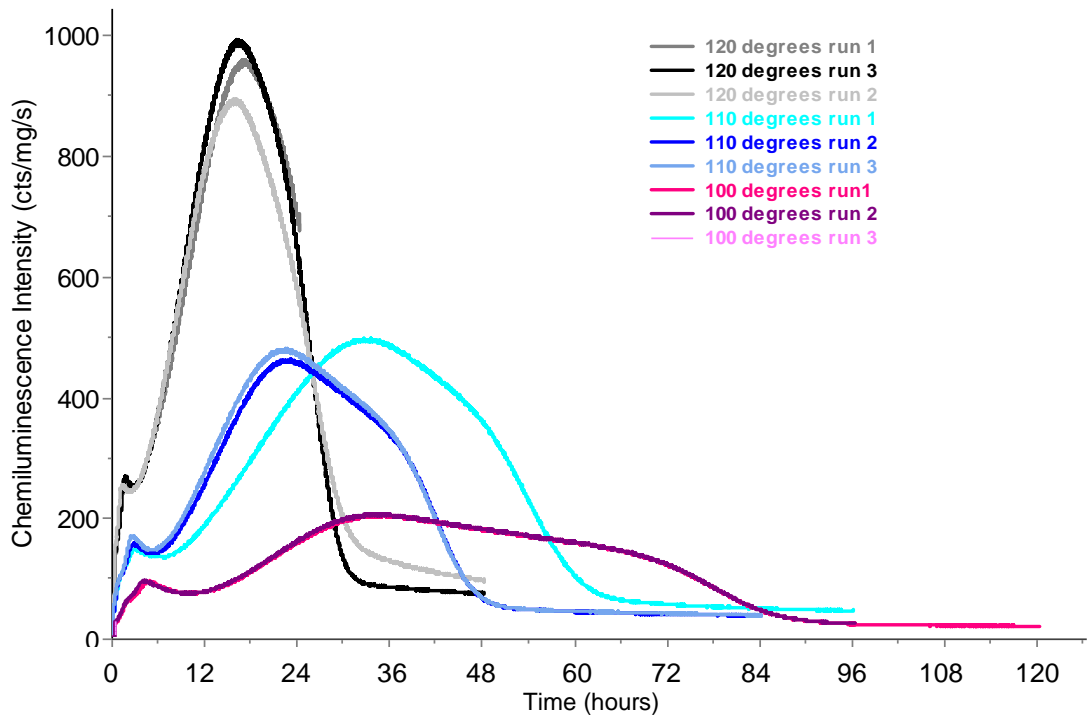
Figure 5.7 - CL curves of Tween 80 at 100, 110 and 120°C
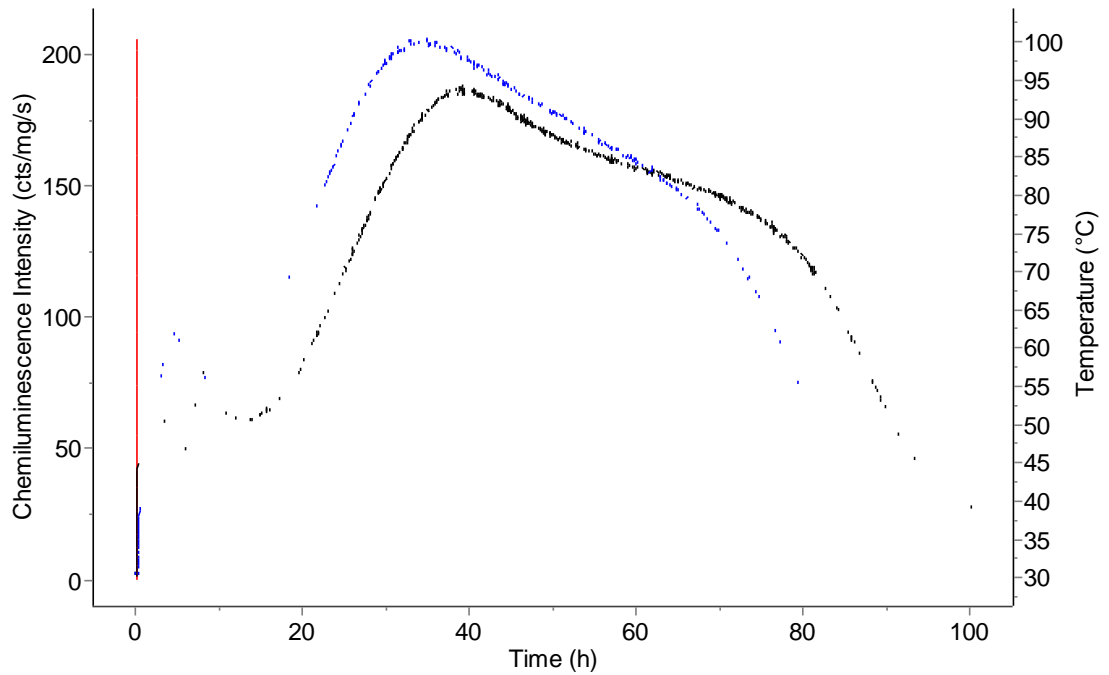
Figure 5.8 - CL curves of HP-PS80 (—) and Tween 80 (—) at 100°C (Temperature —)

Figure 5.8 highlights the differences in CL curves between HP-PS80 and Tween 80 at 100°C. There is a clear difference in shape between the two materials in the early part of the CL curve i.e. up to 17 hours, where HP-PS80 displays three distinct peaks, whilst

Tween 80 shows one broad peak with a slight shoulder on the left hand side. The triple peaks in HP-PS80 show that three distinct oxidation events are taking place. The broad peak in Tween 80 could represent one oxidation event, or it could represent several oxidation events that overlap and therefore form one large broad peak. Another explanation for the differences in curve shape is that the refining process could have removed impurities from the HP-PS80 that would have also oxidised in this region, so the CL curve shows resolved peaks in this area in contrast to Tween 80 CL curve where these peaks are not resolved because the impurities have not been removed and are also oxidising.

The refining process is designed to result in a higher purity for PS80 however due to the chemicals used in the process there is the possibility that residual levels that are not sufficiently high enough for the product to fail quality checks, could still have an adverse effect on the stability of the substance over time. The technology used by Croda to refine polysorbates aims to remove or reduce polar and oxidative impurities, including: moisture, residual catalyst, peroxides and aldehydes, impurities detected by Kishore *et al* in their work on the degradation of polysorbates 20 and 80 [141]. The chromatographic process utilised for refining does not alter the chemical structure of the polysorbates [131]. It is therefore unlikely that the three peaks in HP-PS80 could be caused by chemicals that are present after the refining process, but this possibility remains. Croda state that the rational for refining is that it removes polar impurities and hence helps to reduce API interaction, maintaining both the stability of the drug and the finished formulation [131].

The small differences in peaks in the CL profiles of different polysorbates, such as those in Figure 5.8, could be useful indicators of quality if identification of the chemical species giving rise to the peaks in the CL curve was carried out and this is discussed in the future work, section 5.7.

5.5.3 *Comparison of the oxidative stability of HP-PS80 and Tween 80 using the Rancimat*

The comparison between the ACL Instrument and the Rancimat for measuring the oxidative stability of HP-PS80 and Tween 80 was challenging. This was because the temperatures used for testing with the ACL Instrument, to achieve a realistic run time,

were high at 100, 110 and 120°C. Despite the run time being in the order of ~5 days at 100°C, there was no clear induction time and this meant that the determination of OIT was not possible, as there was no baseline from which to draw the tangents. A lower temperature may have enabled the quantification of an OIT but it was not possible to test the polysorbates at temperatures lower than 100°C on the ACL Instrument as the run times of over 5 days were unfeasible.

Samples of HP-PS80 and Tween 80 were tested on the Rancimat to facilitate comparison of the two machines. The OITs determined by the Rancimat at the temperatures used to run the ACL Instrument (100, 110 and 120°C) were very short, Table 5-4. This reflected the nature of the CL curves, with oxidation starting at the beginning of the run. The Rancimat therefore gave a very low OIT as the conductivity level in the measuring vessel had risen sufficiently for the automatic calculation to occur. Testing was extended to lower temperatures in order to determine an OIT.

Temp (°C)	HP PS80 - 460414		Tween 80 - 426262	
	Rancimat mean OIT (h)	ACL peak 1 (h)	Rancimat mean OIT (h)	ACL peak 1 (h)
50	38.85		110.13	
60	30.76		9.96	
70	10.80		0.05	
80	2.65		0.05	
90	0.70		0.04	
100	0.71	33.55	0.05	42.58
110	0.64	25.70	0.04	22.83
120	0.61	16.12	1.38	14.32

Table 5-4 - OITs of HP PS80 and Tween 80 measured using Rancimat and time to peak 1 determined by the ACL Instrument

Figure 5.9 shows the OITs calculated from the Rancimat and the time to CLI_{max} from the ACL analysis. It is clear from observing Figure 5.9 that at the temperatures chosen, the Rancimat was not a suitable way to measure oxidative stability of polysorbate.
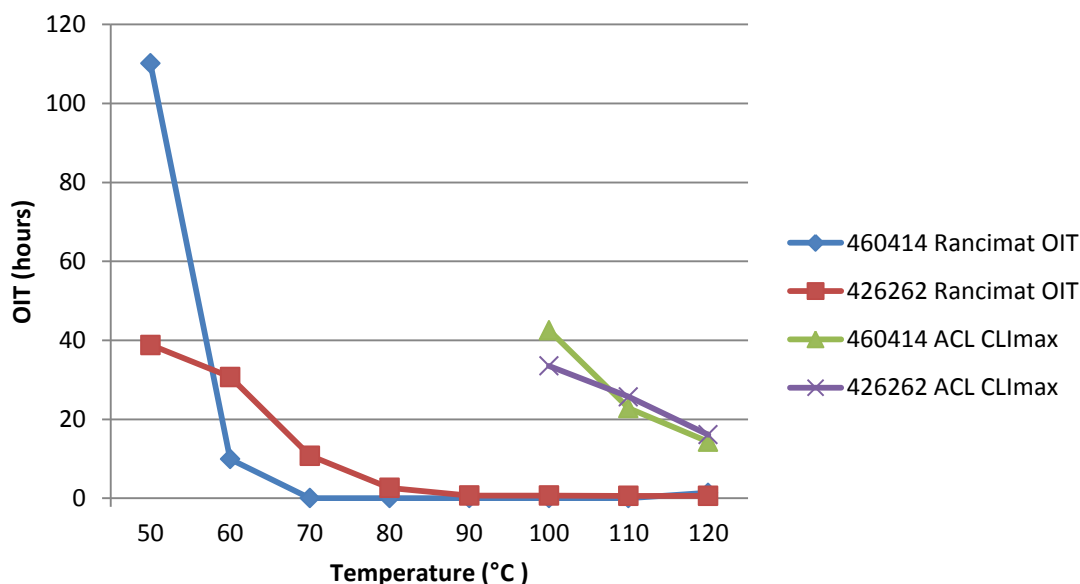
Figure 5.9 – OITs of HP-PS80 and Tween 80 determined by the Rancimat shown in comparison to ACL CLI$_{max}$

One possible way of overcoming this difficulty in Rancimat measurement with the early onset of oxidation in polysorbates would be to adjust the evaluation time on the machine settings. In the case of polysorbates the conductivity rise in the Rancimat measuring vessel associated with the initial peak in oxidation before 20 hours as observed on the CL curves in Figure 5.8, causes the evaluation of OIT to occur. If the evaluation was suppressed until after the larger peak at around 40 hours, this would allow for the calculation of OIT.

5.5.4 *Comparison of polysorbates 20, 60 and 80*

The CL curves of polysorbates 20, 60 and 80 are shown in Figure 5.10. The repeatability of the two runs for PS80 and PS60 was good with both curves showing similar features with relatively close overlap. It was difficult to determine an OIT for these samples, as there was no clear baseline, with the onset of oxidation occurring as soon as the run was started. When considering the time to CLI$_{max}$, it is clear that PS80 displayed the shortest time to reach CLI$_{max}$ (~8 hours) indicating that it is the least stable of the three polysorbates, which is in agreement with the literature as explained in section 5.1.3. In contrast, PS20 had a slightly longer time to CLI$_{max}$ (~13 hours), but a higher CLI at CLI$_{max.}$ Data was unavailable for the second run of PS20 due to an error in data transfer.
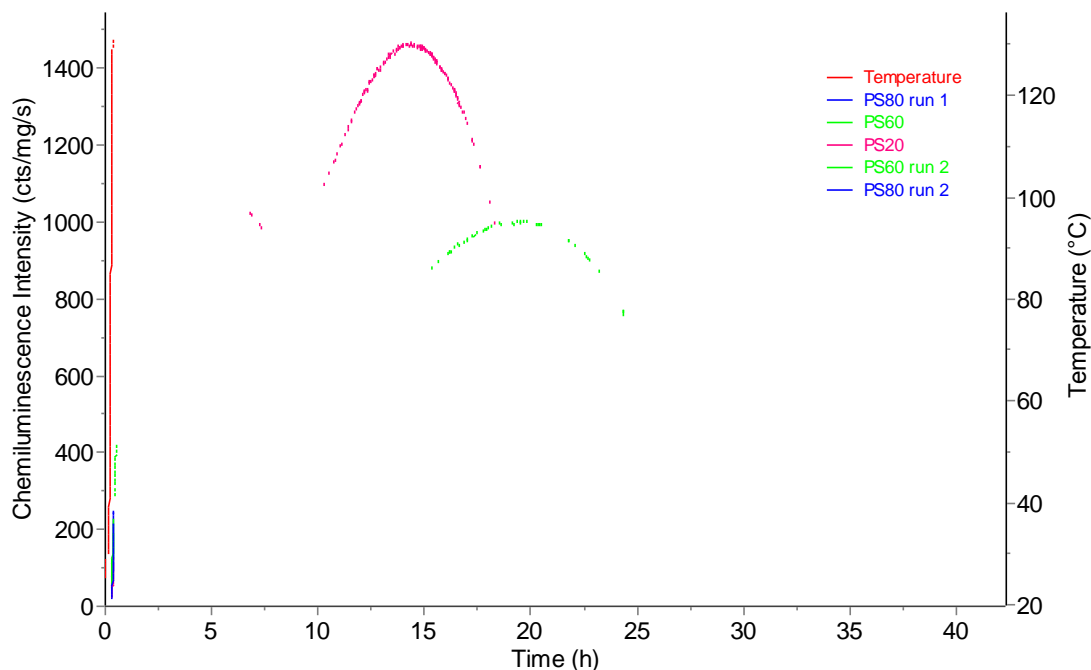
Figure 5.10 – CL curves of polysorbate 20, 60 and 80 at 130°C

PS60 displayed the longest time to CLI_{max} and had a similar CLI at the CLI_{max} to PS80. When considering the TLI, PS80 displayed the lowest TLI (2.19×10^{10} cts/g), with PS20 (4.52×10^{10} cts/g) and PS60 (4.05×10^{10} cts/g) being similar. It was not possible to associate these differences in TLI to polysorbate structure in this case, as other methods would be required and these are discussed in the future work, section 5.7.

5.5.5 *Measurement of batch-to-batch variation in polysorbates using the ACL Instrument, iodometric titration and the Rancimat*

Three batches of Tween® 80 and two batches of polysorbate 80 Eur Ph from Sigma Aldrich were used to investigate whether CL could be used to detect batch-to-batch variability and this was compared to OITs and stability times determined through testing on the Rancimat and PV measurements determined using iodometric titration.

Material	Batch
Tween® 80	BCBG4950V
Tween® 80	BCBJ4213V
Tween® 80	BCBJ8859V
Polysorbate 80 Eur Ph	BCBH5882V
Polysorbate 80 Eur Ph	BCBJ7603V

Table 5-5 - Batch numbers of Tween 80 and Polysorbate 80 Ph Eur

Samples were tested under isothermal conditions in duplicate on the ACL Instrument at 110°C and the CL curves of Tween 80 are shown in Figure 5.11. Variability was

observed between the three batches of Tween 80 i.e. BCBG4950V and BCBJ8859V displayed similar shaped curves, whereas the curve of BCBJ4213V shows distinct differences after the $CLI_{max.}$ After 70 hours and 100 hours when each of the runs for BCB4213V were terminated, the CLI was still falling and had not reached the baseline, indicating that oxidation was still occurring. In contrast, it appears that batches BCBG4950V and BCBJ8859V had undergone oxidation as the CLI had returned to the baseline.
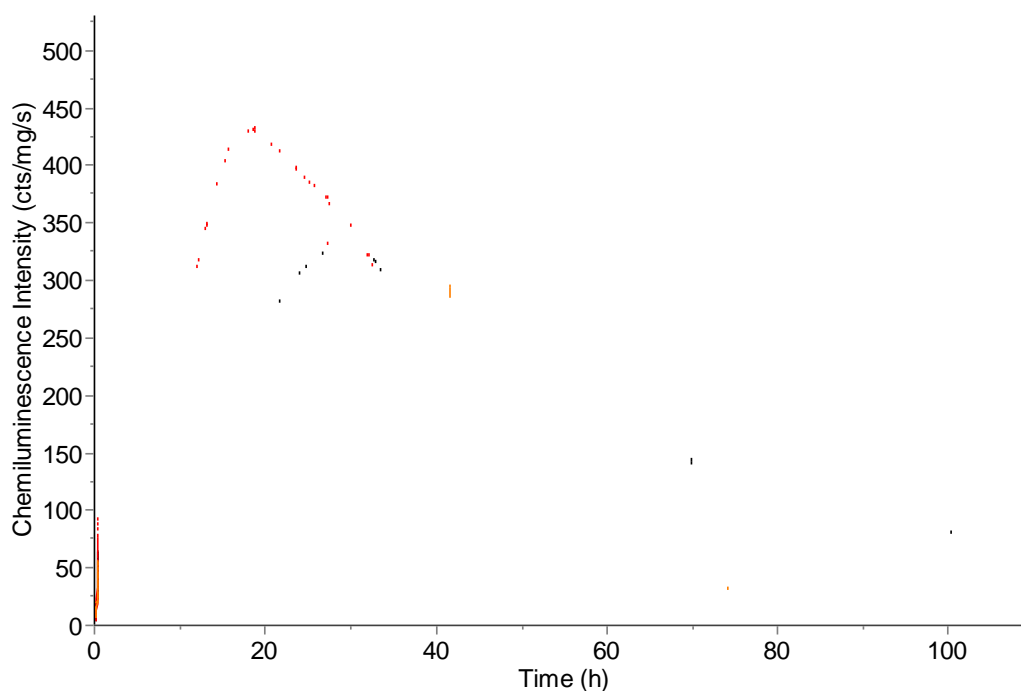
Figure 5.11 - CL curves of three different batches of Tween 80 at 110°C
BCBJ4213V (—), BCBG4950V (—), BCBJ8859V (—)

As well as the inter-batch variability, there was also some intra-batch variability, and this could make fingerprinting of batches more challenging. The CL curves within batches had slightly different times to, and intensity of, $CLI_{max.}$ Across all batches of Tween 80, the CL curves showed an initial small peak followed by a large main peak. This can be contrasted to the CL curves of two batches of PS80 Eur Ph shown in Figure 5.12, which display three peaks. Both batches of PS80 Eur Ph show an initial sharp peak with an intensity of around 150 cts/mg/s which then rises to another slightly broader peak around 17 hours with an intensity of 275 cts/mg/s, followed by a very broad peak of similar intensity 325 cts/mg/s which spans from 30 hours onwards. Using the ACL Instrument alone it is not possible to elucidate the particular chemical

species giving rise to the CL. It was hypothesised that the three different peaks are caused by different chemical species undergoing oxidation, with more reactive, less stable species oxidising before 10 hours and a much larger number of species going on to oxidise after 10 hours.
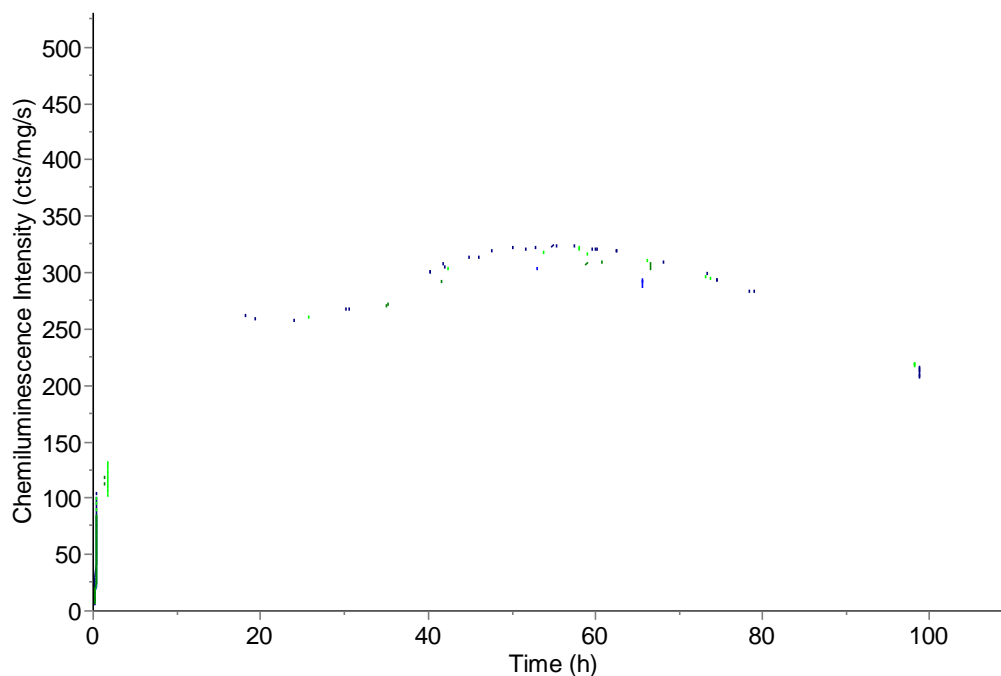
Figure 5.12 - CL curves of two batches of polysorbate Eur Ph at 110°C
(— BCBJ7603V run 1, — BCBJ7603V run 2, — BCBH5882V run 1, — BCBH5882V run 1)

Figure 5.13 shows all results from the batch testing and the distinctly different shaped curves of PS80 Eur Ph batches compared to Tween 80 batches can be observed. Tween 80 oxidation reactions in batches BCBG4950V and BCBJ8859V, shown in Figure 5.13 appear to finish over the time period, whereas polysorbate 80 reactions continue, suggesting that the oxidation reactions in polysorbate continues for more than the 100 hours run time. The repeatability of the PS80 Eur Ph appears to be better with CL curves being more similar, this is better than the repeatability seen in Tween 80 and indicates that there is potentially lower sample heterogeneity in PS80 Eur Ph than in Tween 80.

The lack of a clear baseline before oxidation started meant that it was not possible to calculate OITs for these samples, and had they have been calculated they would have been a misrepresentation of OIT. Calculating TLI to the CLI_{max} and comparing this between batches was considered however this was not possible as the PS80 batches

saw the CLI_{max} occurring on the third peak in the CL curve whereas the Tween 80 samples saw the CLI_{max} occurring on the second peak of the CL curve and comparing the TLI to this point may not have been a suitable choice of comparison. This is in contrast to analysis in section 5.5.3 where it was possible to compare the time to CLI_{max} as the CL curves all had the same shape and number of peaks, so it was clear to distinguish a common CLI_{max}. If runs were continued beyond 100 hours and the CL returned to a baseline, it would then be possible to compare TLI of the CL curve across the batches, however running the machine for over 100 hours is unfeasible in terms of throughput as it would allow 4 samples to be tested per 4 week period and long run times also increase the probability of complications during the run when the machine is left unattended e.g. gas supply running out during the run, chiller unit requiring the water to be topped up or the data drive becoming full.
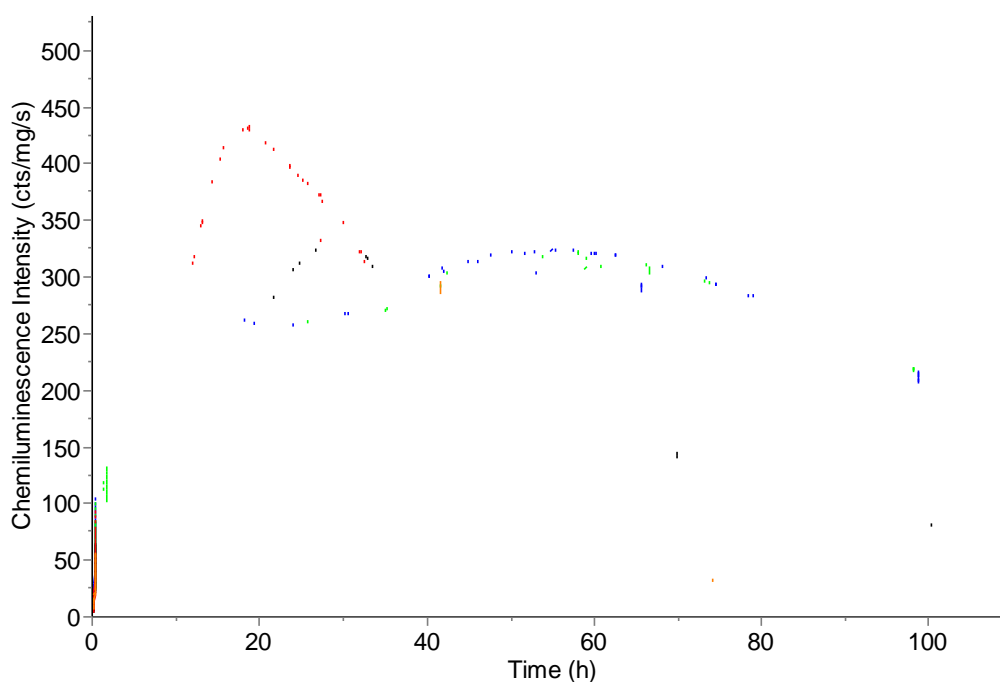
Figure 5.13 - CL curves of PS80 Eur Ph and Tween 80 batches
BCBJ4213V (━), BCBG4950V (━), BCBJ8859V (━), BCBJ7603V (━), BCBJH5882V (━)

As well as considering the oxidative stability of polysorbates it is also possible to compare batches in terms of their peroxide content. The batches of Tween 80 and polysorbate 80 Eur Ph were tested for peroxide levels using CL with a dynamic temperature profile under nitrogen and peroxide value titrations. The repeatability of the CL method was also considered, to investigate sample homogeneity.

Figure 5.14 through to Figure 5.18 show the CL curves for the batches tested under nitrogen. From observation of the curves shown in Figure 5.14 through to Figure 5.18 the two batches of Tween 80 BCB4950V and BCBJ4213V reached the highest CLI during the testing at ~18cts/mg/s and ~14cts/mg/s respectively, with the CLI at the peak for batches of PS80 (BCBJ8859V, BCBH5882V, BCBJ7603V) all being below ~12 cts/mg/s.
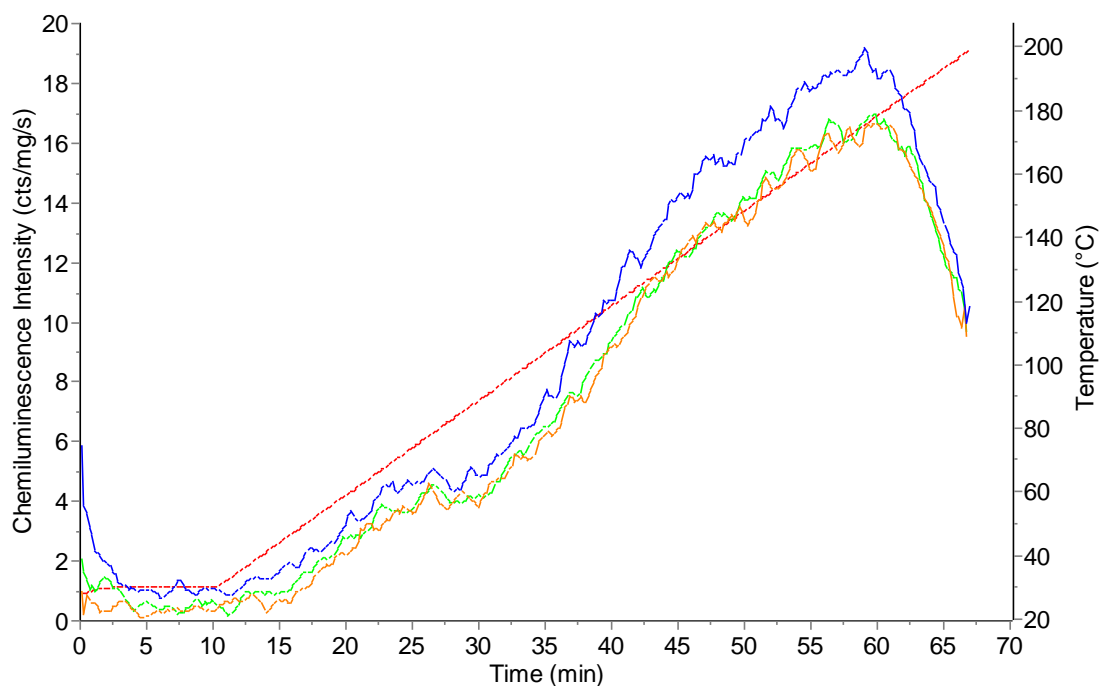
Figure 5.14 – Tween 80 BCB4950V dynamic runs in nitrogen

(—— temperature, —— run 1, —— run 2, —— run 3)
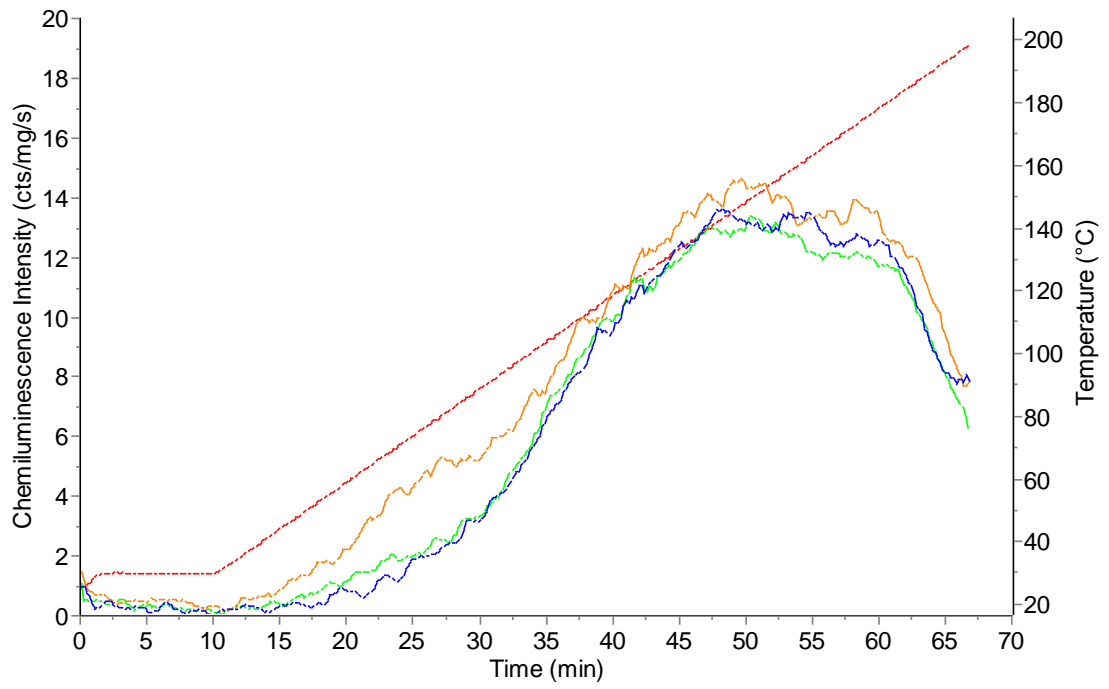
Figure 5.15 – Tween 80 BCBJ4213V dynamic runs in nitrogen

(— temperature, — run 1, — run 2, — run 3)
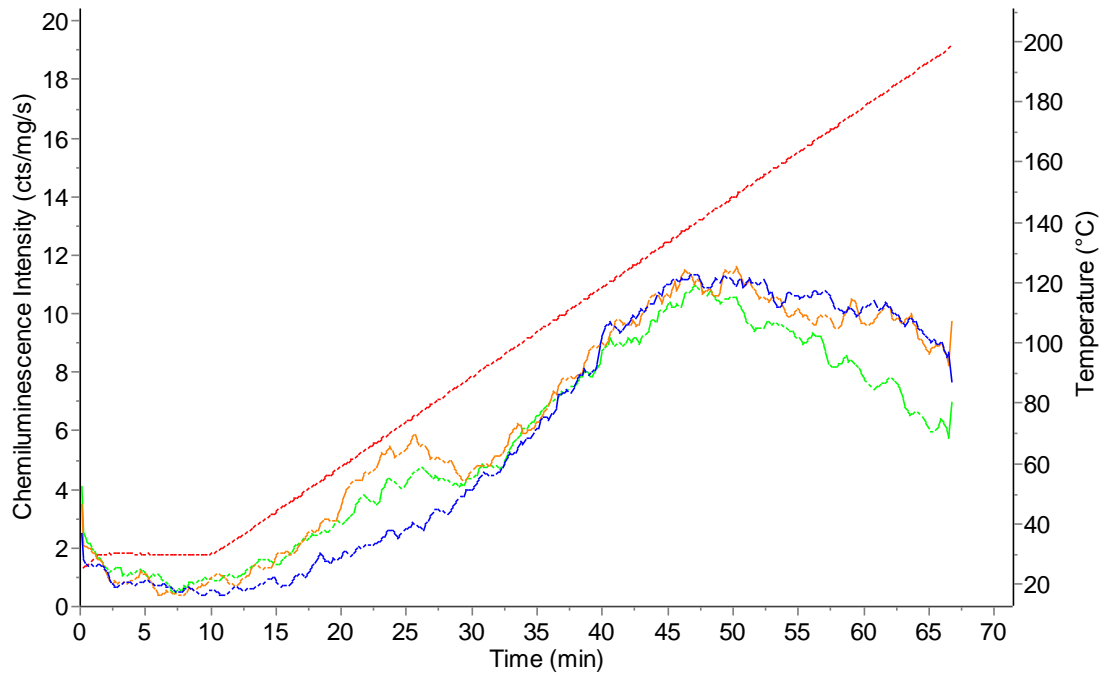
Figure 5.16 – Tween 80 BCBJ8859V dynamic runs in nitrogen

(— temperature, — run 1, — run 2, — run 3)
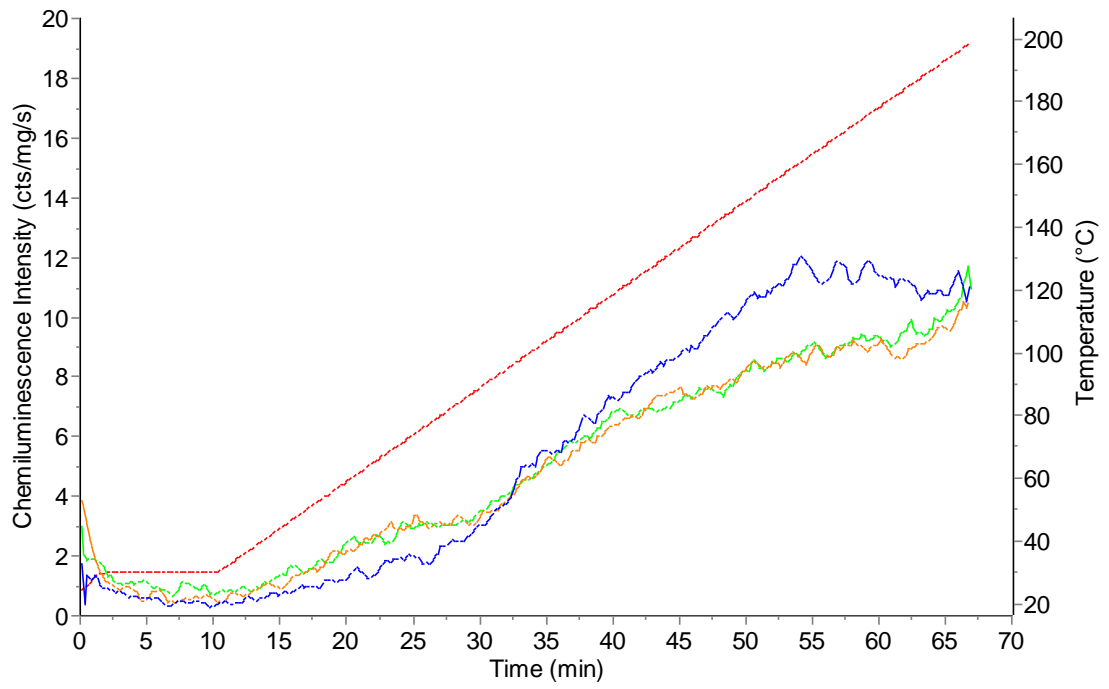
Figure 5.17 – PS80 BCBH5882V dynamic runs in nitrogen

(— temperature, — run 1, — run 2, — run 3)
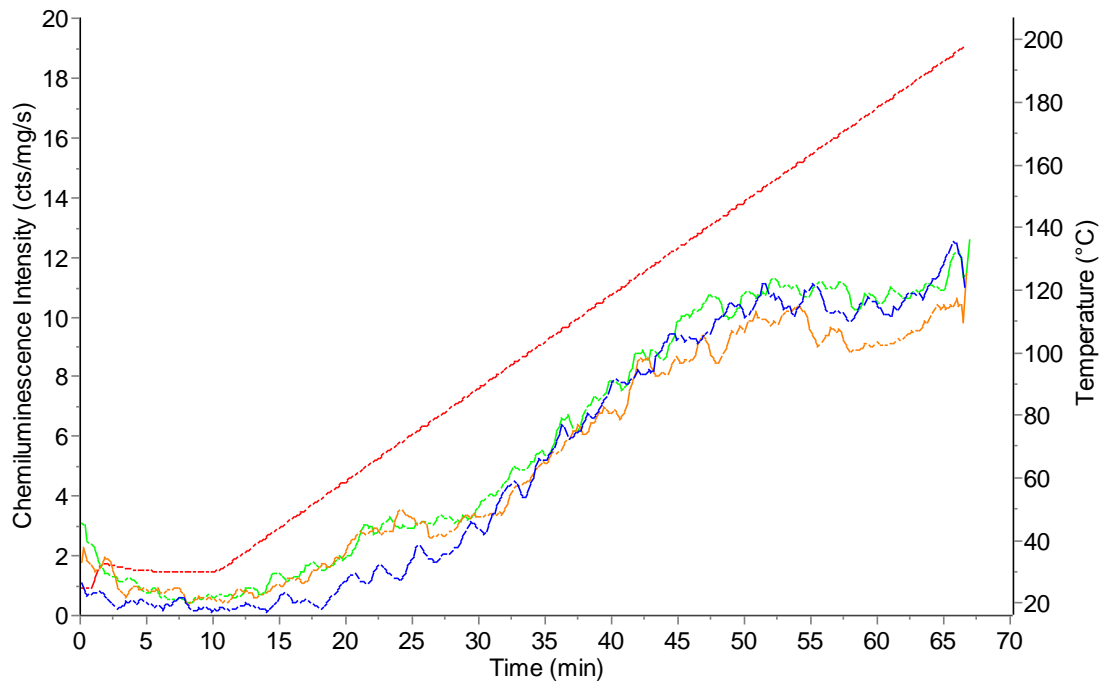
Figure 5.18 – PS80 BCBJ7603V dynamic runs in nitrogen

(— temperature, — run 1, — run 2, — run 3)
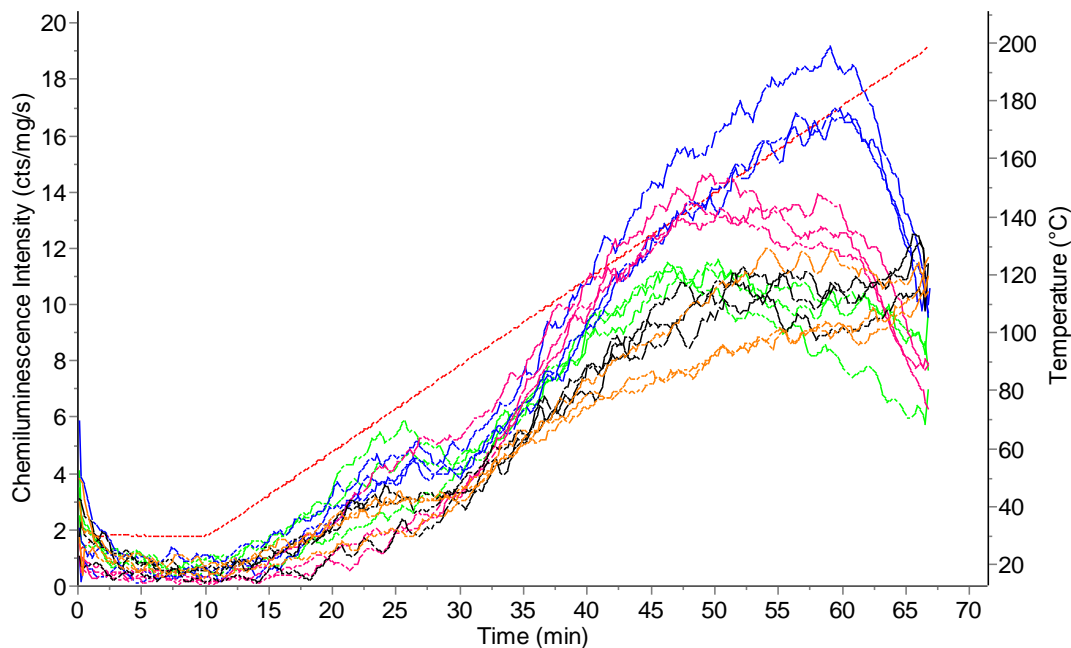
Figure 5.19 - CL curves of three batches of Tween 80
(—— BCBJ4213V, —— BCBJ8859V, —— BCBG4950V) and two batches of PS80 Eur Ph (—— BCBJ7603V, ——
BCBH5882V), run under dynamic temperature profile in nitrogen

Figure 5.19 shows the superimposed CL curves in nitrogen for the batches of PS80 and Tween 80. The PS80 batches reach slightly lower intensities during the course of the temperature ramp, compared to the Tween 80 batches however this difference is small, being around 4cts/mg/s. This result demonstrates the sensitivity of the technique in highlighting subtle differences between batches and potentially an advantage over other methods such as PV, which is discussed further in this section.

The difference between batches was further analysed through the total luminescence intensity (TLI) values attainted from integrating the CL curves. In addition to this the batches were tested using the Rancimat to determine oxidative stability and iodometric titration to determine their PV. The TLI values, Rancimat OIT and stability time (t$\triangle$k) and PVs along with the %RSDs were compared, Table 5-6.

Batch	TLI (cts x 10^7/g)		PV (meq peroxide/kg)		Rancimat OIT		Rancimat t$\triangle$k	
	Mean	%RSD	Mean	%RSD	Mean (h)	%RSD	Mean (h)	%RSD
PS80_BCBH5882V	2.04	5.86	1.46	25.40	0.97	4.28	1.61	7.45
PS80_BCBJ7603V	2.17	6.53	1.78	2.12	1.00	2.65	1.59	0.36
T80_BCBG4950V	3.09	9.54	5.27	30.75	0.55	1.06	1.13	5.39
T80_BCBJ4213V	2.57	9.65	8.31	0.79	0.51	1.96	0.98	4.14
T80_BCBJ8859V	2.33	5.71	5.19	28.40	0.60	5.00	1.16	5.28

Table 5-6 – TLI, PV and Rancimat results for PS80 and Tween 80 batches

The %RSD associated with PVs for two batches is very low, at 0.79% and 2.12%, however for the other three batches, it is much higher, above 25%. In contrast, the results for CLI have %RSDs ranging from 5.71-9.65%, showing that they are generally low and exhibit greater consistency. The measurements of OIT and tΔk from the Rancimat showed good repeatability with low %RSDs of 1.06-5.00% for OIT and 0.36-7.45% for tΔk, this is in contrast to research carried out by Hulse and Forbes, where the Rancimat was used to test the oxidative stability of polysorbates and the conclusion drawn was that it lacked sensitivity and repeatability [150]. The repeatability of the four measures within batches is compared graphically in Figure 5.20. The TLI measurements (cts x 10^7/g) and PVs show similar patterns across the batches in Figure 5.20, but it may not be appropriate to draw firm conclusions from this data as the iodometic titration volumes that were used were very low (0.2-2.4ml), which meant that the measured PVs (1.04-8.38 meq peroxide/kg) values were at the lower limit of the assay which was stated as 0.5meq peroxide/kg by Frankel [59]. Another factor which may have contributed towards the high %RSD of the PV results is that the determination of end point was difficult due to the colour of the polysorbates being similar to the titration reagents. In addition to this, it has been reported [151] [152] that error in the results can be caused by the reactivity of peroxides present, which may be a reason for the difference in patterns between the PV measurement and CL measurement. Shulin [152] reported that hydroperoxides with low reactivity were formed in non-ionic surfactants such as polysorbate which limited the use of the iodometric determination of PV and additionally non-ionic surfactants were also found to interfere with the liberated iodine making endpoint determination difficult.
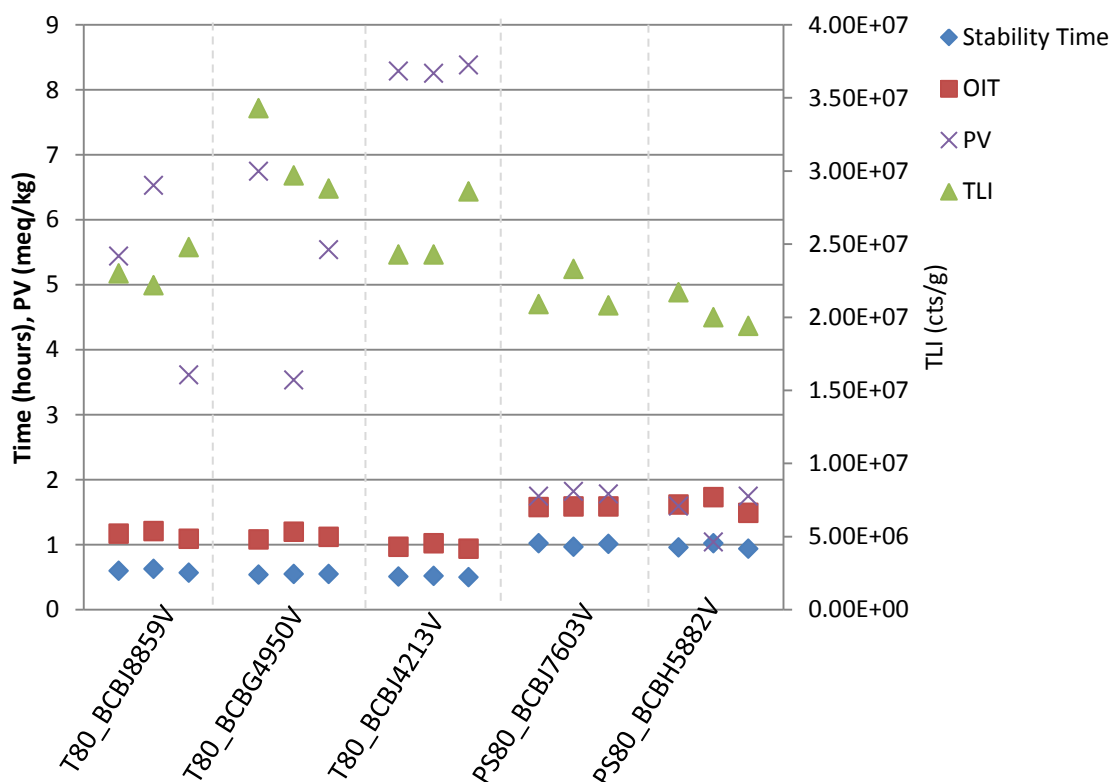
Figure 5.20 – Rancimat OIT and stability times at 110°C, PV and TLI of PS80 and Tween 80 batches (3 repeats shown for each batch, batches separated by vertical dashed lines)

In PV, if peroxides are not reactive with iodine at room temperature in the minutes that it takes to perform the titration, then this is not captured in the PV measurement. In contrast, with CL measurements, the sample is heated and forced to degrade hence peroxide decomposition is measured and not all of these peroxides present that gave rise to CL emission would be captured in the titration based PV method. OITs, stability times and TLIs displayed in Figure 5.20 show that the Rancimat gives repeatable results for both OIT and stability time measurements and the results show a difference in oxidative stability between the batches of PS80 Eur Ph and the batches of Tween 80. A difference between the PS80 Eur Ph and Tween 80 was also seen in the PV and TLI results with the trend the opposite way round. The batches that have a lower OIT and stability time have a higher PV and TLI (T80_BCBJ8859V, T80_BCBG4950V, T80_BCBJ4213V), which suggests they are less stable than the batches with high OIT and stability time, and lower PV and TLI (PS80_BCBJ7603V, PS80_BCBH5882V).

5.6 Conclusions

This chapter has explored the potential of the ACL Instrument and CL for application to the testing of selected polysorbates. It was hypothesised that CL would provide a more sensitive test for oxidative stability than the Rancimat and that the CL measurement of peroxide levels would provide more information and be more sensitive than iodometric based titrations. Results have shown that CL is a potentially useful technique for measuring the oxidative stability of polysorbates, however at the high temperatures investigated in this study, chosen to keep run times feasible, oxidation began very quickly and therefore determination of a baseline from which to calculate OIT was difficult. Performing runs at lower temperatures would increase the run time, but may slow the onset and initial rate of oxidation and would potentially generate CL curves from which baseline determination may be possible. Results from the Rancimat also indicated that at high temperatures, polysorbates oxidise quickly, however the results were in agreement with the ACL Instrument in terms of being able to discriminate between batches of PS80 and Tween 80.

This study has shown that the CL testing of polysorbates under oxidative conditions results in subtly different CL curves for different type, grades and batches of polysorbate. It was not possible to ascertain what the differences in the CL curves are attributable to solely based on CL data, however the results show the potential of CL to be used as a fingerprinting technique, which may provide more information than existing methods such as peroxide value which, in this case also highlighted the batch-to-batch differences captured by the CL method.

Using CL it was possible to distinguish between Tween 80 and HP-PS80, with clear differences evident in curve shape over a range of temperatures under oxidative conditions and under nitrogen. It was also possible to identify differences in the CL curve between different polysorbates, 20, 60 and 80. It was not possible to clearly observe batch-to-batch variation between the three batches of PS80 Eur Ph because of a high level of intra-batch variability up to the CLI_{max}. The variation seen in the polysorbates CL curves backs up the suggestions of Kishore *et al* [141], that to ensure the integrity of protein based pharmaceuticals, excipient stability should be studied

further and should be included into quality control strategies to ensure they are fit for purpose in terms of oxidative stability and peroxide level.

Using CL as a fingerprinting tool for polysorbates at these temperatures warrants further investigation and consideration of the latter part of the curve, where differences were seen between PS80 and Tween 80 (Figure 5.13), or the earlier part of the curve (Figure 5.8), could give additional options for fingerprinting. This study only considered measures from the CL curve up to the CLI_{max} however it would be possible to consider the whole curve if run times were long enough to allow for the termination stage of oxidation to come to an end and the CLI to drop back down to values close to the starting values.

When considering the %RSD values from the CL and PV methods, due to inconsistencies in the repeatability of the peroxide value, this chapter concluded that CL offered a more repeatable testing method to measuring peroxide content in polysorbates due to the forced degradation of accumulated peroxides within a sample and the elimination of operator error that potentially impacts on the results of PV from iodometric titrations. It was concluded that CL could potentially be developed as a fingerprinting tool, which would warrant further work in characterising polysorbates of satisfactory and unsatisfactory quality using CL and other indicators to aid the analysis and development of a library against which to test polysorbates of unknown quality. This research showed that the Rancimat can be used to provide repeatable results, but its sensitivity should be investigated by extending testing to lower temperatures and investigating the evaluation mode, discussed in the future work, section 4.8.

As with any accelerated stability testing method, there are implications as to how these results obtained at elevated temperatures are extrapolated to give a picture of polysorbate stability at room temperature and if this method was to be utilised in shelf life prediction, this would need to be addressed. However, in the case of peroxide quantification, this is not an issue, as what is trying to be achieved is a static measurement of current peroxide level, in contrast to oxidative stability testing where results may be extrapolated to predict stability over time.

5.7   Future work

To establish a more detailed understanding of the information captured by the CL measurement of polysorbates, it may be necessary to use additional techniques alongside CL, such as differential scanning calorimetry, which has previously been used to study polysorbates [153] and edible oils [154]. Chadha and Bandari [132] highlighted the importance of using several thermal and spectroscopic techniques to investigate physical and chemical drug-excipient interactions.

In this research, polysorbates were considered in isolation as neat samples, however a useful approach would be to consider how the CL technique works when testing polysorbates that have been formulated with drug substance or polysorbates in solution as these may better represent behaviour in formulations. Ha *et al* [4] found that in 20% aqueous solutions of polysorbate 80, peroxide formation was faster and reached a level 10 times higher than in un-diluted polysorbate 80.

Another approach to further characterise the chemistry behind the CL signals could involve using electron spin resonance spectroscopy to understand the radical reactions giving rise to the CL signal. This however, is a very complex technique and considering there are so many breakdown products of polysorbates as highlighted by Kishore *et al* [141] it may be difficult to link and particular type of peroxide to an excipient-drug incompatibility.

The appearance and differences between CL curves could be linked to the stability of the polysorbate and this may impact on the quality of the formulation in the longer term. By analysing polysorbates before they are added to a formulation, it may be possible to investigate how the initial stability and degradation state could potentially impact on the longer-term quality of the formulation. This would involve characterising polysorbates before formulation, during formulation and at points during the shelf life of the formulation, so would take a considerable amount of time to gather results. This may further the understanding of whether artefacts from CL analysis relate to stability parameters in the final formulation, as currently there appears to be a lack of information regarding this issue. By adding CL analysis into the set of testing techniques, this would allow the CL data to be correlated to other measures of stability, enriching the value of the CL information. It would be important to track the

peroxides in the formulation over time, as polysorbates can also degrade by autoxidation forming peroxides which were not initially contained in the bulk. It would also be useful to characterise polysorbates before and after refining to understand the effect on the CL curve and what species may give rise to particular peaks that differ between HP-PS80 and Tween 80.

As previously mentioned, techniques like CL may offer increased sensitivity over existing stability methods, such as PV, which could help to further the understanding of how these substances behave. Another investigation that could provide useful information for formulators would be to utilise CL testing alongside other methods to test polysorbates before and after the refining process to understand the effects of refining on stability.

As detailed in Chapter 3 and Chapter 4, in addition to the basic instrument configuration which allows the user to heat samples in an oxygen-rich environment or an inert gas, the ACL Instrument has additional hardware modules which can be utilised for measuring the oxidation profile and peroxide levels under controlled humidity and exposure to UV and white light [145]. It therefore provides a platform for scientists involved in early drug development to investigate the effect of excipients on stability, whilst tracking CL emissions, under different combinations of conditions as may be specified in stability testing regulation. An additional module is available which can be used to split CL emissions [84] into their individual wavelengths, which then may make it possible to understand the chemistry behind the peroxide reactions.

One technique that could be utilised alongside CL is MALDI-TOF MS which has been identified as a suitable method by which the heterogeneity of polysorbates can be determined [155]. This may be a useful tool for understanding the degradation state via the presence of degradation products. This could be utilised in understanding the effect of the refining process on polysorbate stability. In addition, if testing the final formulation over time, mass spectral differences could be analysed to look for correlation to quality parameters, but this is something that could only be measured with access to a final formulation. Recommendations for industry regarding the use of the ACL Instrument for measuring oxidative stability of polysorbates are summarised in Chapter 8 section 8.4.

Rancimat testing of polysorbates could be investigated further to understand how lower temperature testing could be used or another potential route for investigation is the alteration of measurement parameters such as evaluation suppression. This function of the Rancimat can be used for substances that undergo oxidation in steps [71]. This would allow for the conductivity rise associated with the initial oxidation event or events to be discounted and the measurement of OIT commence after these, at a conductivity specified by the operator. This would involve some initial testing in order to determine the evaluation suppression level.

Chapter 6. Method development for ozone detection in pharmaceutical containers subject to container integrity testing via high voltage leak detection (HVLD)

6.1 Introduction

6.1.1 *The importance of container integrity testing*

Containers are designed to house the final pharmaceutical formulation and the purpose of the container is to keep the pharmaceutical product in, protect it from oxidative degradation, ensure sterility and keep out other contaminants, such as particulates and chemicals whilst facilitating the administration of the pharmaceutical product.

The design of one type of container (which this research focusses on), a flip off cap pharmaceutical vial, can be seen in Figure 6.1.
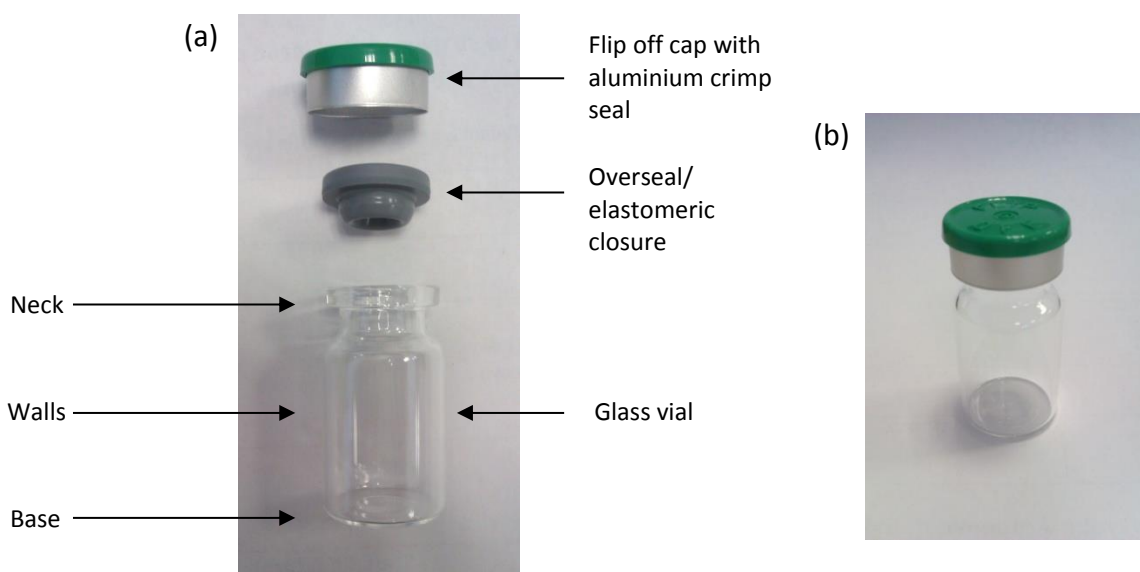
Figure 6.1 - Flip off cap pharmaceutical vial (a) before assembly (b) after assembly, prior to crimping

As the container plays a crucial role in the protection of the final formulation its integrity is paramount and hence breaches in container integrity leading to product loss, or contamination of product though microbial ingress or entry of chemicals or particulates can have severe implications for product quality and patient safety and from an economic perspective due to loss of batches, investigations and damaged reputations. Containers can be damaged prior to departure from the supplier, in

transit, or during the process of handling, filling or sealing at the pharmaceutical facility. Consequently handling procedures and systems that move containers throughout the plant and along filling lines are designed to minimise damage, however, some damage may occur and hence all containers must be checked.

Some examples of Food and Drug Administration (FDA) recalls related to container integrity failures are listed in Table 6-1. Typically these recalls have been due to cracks in the vial neck and stopper and over seal defects.

Date	Product	Issue	Company
17/12/2010	FLUVIRIN (Influenza Virus Vaccine) 2010-2011. Formula Multidose Vials	Lot # 111812P1 recalled due to cracks in the vial necks carry the potential risk of compromised product sterility.	Novartis Vaccines and Diagnostics, Inc. Cambridge, MA
13/4/2010	RabAvert Rabies Vaccine Kits (Rabies Vaccine for Human Use)	Single batch recalled as the stopper and metal crimp dislodge from the vial completely when removing the protective cap.	Novartis Vaccines and Diagnostics Marburg, Germany
11/10/2005	Recall of Plasma Protein Fraction (Human) 5% USP	Lot 26N39N1 was processed during a period of time when the equipment used to secure an over seal on the bottle was noted to have fallen out of proper adjustment.	Talecris Biotherapeutics Clayton, North Carolina
29/08/2005 26/08/2005	Recall of Albumin (Human) 25 %, Albuminar 100 mL (Updated)	One bottle of Albuminar in Japan was found with a stopper defect that may allow product leakage. The same stopper batch as that used in Japan was also used on these lots.	ZLB Behring L.L.C. King of Prussia, PA
29/08/2005	Recall of Albumin (Human) 25 %, Albuminar 100 mL	One bottle of Albuminar in Japan has been found with a stopper defect that may allow product leakage. The same stopper batch as that used in Japan was also used on these two lots.	ZLB Behring L.L.C. King of Prussia, PA

Table 6-1 - FDA recalls due to failures in container integrity

6.1.2 *Container integrity testing methods*

Container integrity testing is intrinsic to product development and quality assurance. Due to the nature and variety of packaging types available, a number of container integrity testing methods exist and typically several methods are used in combination. As well as testing for leaks, some of these methods also consider the fill level of the container, its cosmetic appearance, whether particulates are present in the liquid formulation and for defects in the over seal. Some methods utilised for container integrity testing include: dye migration, vacuum decay, manual and automated visual inspection methods and high voltage leak detection (HVLD).

Dye migration testing involves the container being submersed in a liquid containing a dye. If the dye is found inside any of the containers, this indicates the presence of leaks.

Vacuum decay testing involves enclosing the container in a chamber where a vacuum is then drawn. After a period of equalization time, the absolute pressure change is recorded and a change in the pressure indicates a leak. This method can be used off-line, semi-automatically and on-line [156]. Vacuum decay can be used to test a number of different container types from tablet blister packs and pouches to vials and ampoules.

Manual visual inspection is a straight forward and inexpensive method for the detection of significant leaks and the presence of particulates in containers. This is a subjective approach and is dependent on the skill and concentration of the operator so is not used as a stand-alone method, but is useful as some leaks will be detected. Studies have been carried out into the performance of operators and these have found that more experienced operators could perform inspections more quickly than inexperienced operators and rejected more containers than those who were less experienced, showing the strong influence of the operator on results [157]. Automated visual inspection methods, such as the Brevetti ATM32/18 in Figure 6.4, attempt to capture what the human eye sees, by using cameras, hence speeding up the process of manual visual inspection and removing operator subjectivity.

High voltage leak detection (HVLD) is used to test for cracks in glass vials and ampoules and is increasingly used for testing plastic containers such as syringes and plastic vials. Due to the nature of the technique, only liquid filled containers can be tested as the method relies on the contact of liquids with the inside of the container surface and additionally flammable liquid cannot be passed though the machine due to the risk of fire and explosion.

The principle by which HVLD machines operate is through the application of a low-frequency, high voltage (maximum 30kV) to a container with liquid inside. The liquid must have a minimum conductivity of 1.5–2.5 µs/cm. As containers are passed along rollers, Figure 6.3, a high voltage is applied across them. If the container is sealed properly and has no cracks, there will be no change in current detected. In the case of

unsealed or cracked containers, the liquid within the container bridges the crack or gap between the seal and this allows current to flow. Impedance in the high voltage field differs to that for an acceptable container and it is this difference in current that is measured and gives rise to the rejection of the container [158].

Figure 6.2 - Vial undergoing HVLD [159]
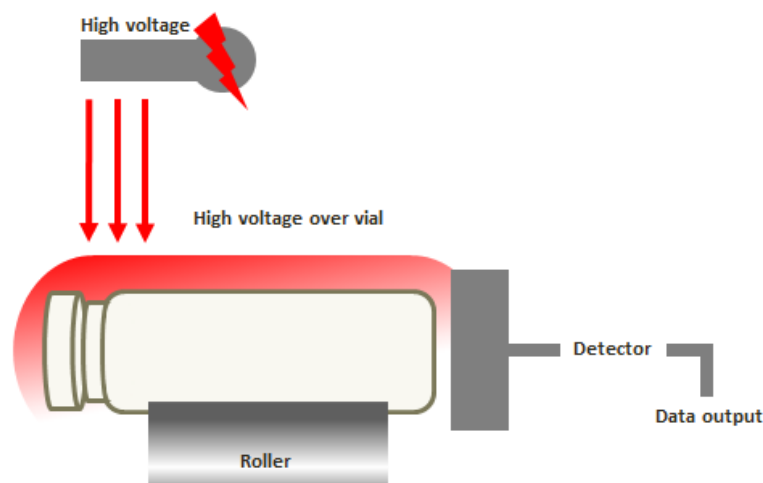
Figure 6.3 - HVLD measurement schematic

6.1.3 *Container integrity testing methods implemented within the sterile vial filling industry*

Selecting a container integrity testing method depends on a number of factors including regulatory requirements, type of container, the product and product performance criteria. For some types of packaging, certain container integrity tests are not suitable. Each method has advantages and limitations and consequently a number of methods are used in combination. For example, in the case of testing crimped sealed vials, automated visual inspection methods, such as the Brevetti systems discussed in this section, cannot test for cracks in glass occurring around the neck of the vial, visible in Figure 6.1 (a), as the neck is covered by the crimped seal, shown in Figure 6.1 (b), so cameras cannot see behind this. To test for these defects, HVLD is

more appropriate as the HVLD machine allows for the detection of leaks in parts of the vial that are not visible to cameras.

The Brevetti ATM 32/18 inspection system, Figure 6.4, is a visual system for the inspection of pharmaceutical products. It operates at high speed (up to 400 containers per minute) with high resolution inspection enabling the testing of a number of quality parameters including: presence of particles, gross fill, aluminium-seal integrity and flip-cap inspection (missing flip off, missing over seal, missing stopper and uncrimped seal), glass defects and cake (solid lumps) inspection. The system can be used to inspect a variety of container types including vials, ampoules, pre-filled syringes and cartridges [160]. The Brevetti ATM 32/18 has two inspection modules that inspect for the same set of defects. Each vial is inspected by 6 cameras. Cameras 1 and 3 detect particulates, camera 2 identifies cracks below the meniscus and gross under fill, cameras 2B and 4B detect particles from the bottom view and camera 5 identifies missing flip off cap, missing over seal, missing stopper and uncrimped seals.

Figure 6.4 -Brevetti ATM32/18 Automated Inspection System

Prior to testing on the Brevetti ATM 32/18, vials are tested using the Wilcomat®, an automated inspection system that tests for leaks in containers. Containers are passed into a sealed testing area and a vacuum is drawn. Leaks are detected when there is a loss of vacuum. The sensitivity of the machine is greater than the standard vacuum decay method by 16-18 times [161].

The Brevetti K6 large volume parenteral inspection unit, Figure 6.5, comprises of several cameras. Camera 1 detects flip off colour and cameras 2, 3, 4 and 5 inspect for fill levels and cosmetic defects. Cameras 6 and 7 detect reflecting particles and cameras 8 and 9 detect non-reflecting particles. Cameras 10 and 11 inspect for aluminium seal defects and the presence of a stopper and cameras 12 and 13 inspect for reflecting particles. 'Good' vials, i.e. those that satisfy all tests carried out, could then potentially be transported to the Bosch KLD 2042 HVLD machine for crack detection.

Figure 6.5 - Brevetti K6 large volume parenteral inspection machine

Vials can be tested using the Eisai 588, automated visual inspection machine. Vials are fed into a star wheel which then passes them onto a turret where there are two inspection stations, each one consisting of two lenses. The first station detects for the presence of particulates and the second station identifies particulates and gross high or low fills and hence each vial is inspected twice for particulates. The Eisai 588 has the capacity to process 12,000 containers per hour. After being inspected on the Eisai, vials could then potentially be tested for cracks on a Bosch KLD 1042 HVLD, Figure 6.6.

Figure 6.6 - Bosch KLD 1042 High Voltage Leak Detection machine

The Eisai 288 has the capacity to process 18,000 containers per hour. This machine works in a similar way to the Eisai 588, with the main difference between the two machines being the size of container that can be tested. With the Eisai 288 the maximum diameter of container is 18mm and the range of vial heights is 45-70mm, whereas with the Eisai 588 larger containers can be tested, with a maximum diameter of 28mm and a height range of 95-120mm.

The Bosch KLD 2042 HVLD and the Bosch KLD 1042 test for leaks, hairline fissures, empty containers and faulty closures, in containers filled with electrically conducting material. When a high voltage is passed over the vial, cracked vials are detected as they have a higher conductivity. These vials are rejected automatically. There are four channels (electrode blocks) which test for cracks on several parts of the vial surface. Channel 1 tests the base and lower body, channel 2 the centre and the lower body, channel 3 the upper and centre body and channel 4 the shoulder and neck. These areas of the vial are shown in Figure 6.1.

For the Bosch KLD 1042 HVLD, the maximum container diameter is 10-32mm with a maximum height of 130mm. Depending on the diameter of the vials, the machine can check 24,000 vials per hour (13mm diameter, 3ml ampoule) or 18,000 per hour (18mm diameter, 5ml ampoule). For the Bosch KLD 2042 HVLD, the maximum container

diameter is 30-55mm with maximum container height 130mm. Depending on the diameter of the vials, the machine can check 10,000 vials per hour (46mm diameter, 50ml vial) or 6,000 per hour (55mm diameter, 100ml vial) [158].

6.1.4 *Issues with high voltage leak detection and evidence for detrimental effects on drug substance*

It is claimed that HVLD systems are a non-destructive testing methods [162]. It is therefore crucial that the method does not cause any detriment to the product inside. The generation of ozone through the action of high voltage on air is theoretically solid. In the 1800s, the ability to produce ozone via a high voltage was recognised and as Rubin [163] describes, the production of ozone using high voltages was investigated by Siemens [164] who used high voltage and a 'silent discharge' method (now referred to as dielectric-barrier discharge) to produce ozone from oxygen or air. The high voltage passing through air provides the energy to break the bond in the O_2 molecule and allow the formation of ozone (O_3). This principle is used in commercially available ozone generators today.

The manufacturer of the machine under investigation in this research, Bosch, recognises that ozone is produced in the atmosphere around the machine and an exhaust fan and catalytic unit are integrated into the machine. However, Bosch has not conducted tests to determine whether ozone is produced within vials passed though the HVLD system. The hypothesis remains that there may be a possibility that ozone could be produced in vials containing a headspace composed of air however limited research has been carried out into the testing of this claim.

Data from McGinley *et al* from Hospira Inc [165] suggested that HVLD can degrade pharmaceuticals and this has created a loss of confidence in using this inspection method for biopharmaceuticals in particular, as these are typically expensive products that are protein based, with complex structures that are prone to oxidation and degradation. A concern exists at GSK that minor changes to the protein structure that may not be detected by traditional analytical techniques may affect the function of the protein, which in turn may alter the desired pharmaceutical effect and for this reason, no vials containing protein-based pharmaceuticals are leak tested on the HVLD.

The study by McGinley *et al* that provides evidence for ozone generation inside a vial was carried out at the global pharmaceutical company Hospira Inc [166]. They studied product degradation resulting from the use of a HVLD instrument [166]. Two degradation products, that were later found to be oxidised forms of the drug product, were observed following HVLD. Testing for these degradation products at several stages of the production and finishing process revealed that the degradation products only appeared after the vial had been passed though the HVLD machine. It was thus hypothesised that the cause of the product degradation may be due to the production of ozone inside the vial when the high voltage was passed across it.

This hypothesis was investigated by McGinley *at al* [166] who varied the composition of the vial headspace using air, oxygen and nitrogen. They reported that having an oxygen headspace resulted in higher degradation product levels than an air headspace and when nitrogen was used no degradation product was observed. This would be in accordance with the production of ozone being higher in a 100% oxygen environment compared with that of air, which contains 21% oxygen. The lack of degradation product in the presence of a nitrogen headspace was a further indication that the degradant was related to oxygen.

Further testing of this hypothesis was undertaken using a chemical probe, 2,3-dimethyl-2-propene, which on contact with ozone converted to acetone. The conversion of the probe to acetone was measured using headspace gas chromatography after passing the vial through the HVLD machine. Acetone was detected therefore indicating the presence of ozone.

Substantiation of the evidence gathered regarding the effect of headspace composition and the conversion of the probe to acetone after HVLD was then undertaken by treating the drug product with ozone, to see if the same degradation products were observed following the passage of the vial through HVLD. The same degradation products were observed confirming that the formation could be attributed to attack from ozone.

McGinley *et al* [166] stated that care should be taken when using a HVLD machine to test containers with the following characteristics: low concentrations of active ingredient, no antioxidants and an air headspace. Also in this study, a low fill volume

(1mL in 3mL vial) was used, with a highly oxidatively sensitive product. The issue with the degradation of the drug product was addressed when the fill volume was increased possibly due to the fact that less oxygen was available for conversion to ozone. After this investigation, Hospira took the decision to fill the vial headspaces with nitrogen and the HVLD is no longer used in the testing protocol for this particular product. No degradation has been observed in subsequent batches.

Although ozone was identified as being responsible for the degradation of the drug product, the presence of ozone in the vial was not directly measured. The evidence presented was produced by an indirect indicator of the presence of ozone i.e. through the conversion of a chemical probe, but no direct measurement was made. The issue is that the probe may be susceptible to conversion to acetone by another substance and hence the results of this study could be questioned. Ideally indirect methods such as the one presented here using 2,3-dimethyl-2-propene should be correlated to a direct measurement of the substance under investigation, in this case ozone.

Following the publication of results by Hospira [165], GSK suspended testing of protein containing drug products on the HVLD machine to remove any possibility of drug product breakdown. Protein products/vaccines are of significantly higher value than any of GSK's products currently inspected with HVLD. Protein products/vaccines are now only tested using other container integrity testing methods to minimise risk of product damage.

6.1.5 *Effect of ozone on proteins*

Biopharmaceuticals unlike small molecular weight chemically synthesised drugs, have large protein molecular structures which are complex and consequently their manufacture is more challenging and expensive. Small changes to the molecular structure that occur during manufacturing can have a significant impact on the activity of the drug and these may be difficult to detect since such complex molecular structures are difficult to characterise [167]. It is therefore crucial that the manufacturing process is designed to minimise the likelihood of any changes in the molecular structure and this extends to ensuring that container integrity testing does not cause product degradation. As discussed in 6.1.4, concern exists around the use of HVLD for biopharmaceuticals due to the possible degradation resulting from the

oxidative effect of ozone attack on proteins. As well as the detrimental effects of ozone, Peleg [168] states that *'the dissociation products of ozone in water may be more powerful oxidization agents than ozone itself'*, which is of great concern.

A number of studies have been carried out to determine the effect of ozone on proteins and biological molecules. Cataldo [169] found that the attack of ozone is generally directed towards aromatic rings within proteins, tryptophan and tyrosine being reactive, and phenylalanine being less reactive. The amide bonds of the main protein chain are not degraded by ozone, so no significant chain scission occurs and the primary structure of the protein remains intact. Ozone was however found to cause changes in the secondary and tertiary structure of proteins, due to partial oxidation of aromatic monomeric units and/or cysteine units. The reaction of thiol groups in cysteine into disulphide cross links, caused denaturation and changes in solubility that could lead to precipitation [169] which could pose issues if this occurred in a pharmaceutical product that was going to be administered parenterally.

Sharma and Graham reported that hydrocarbon based amino acids (glutamic acid) and amides (asparagines, arginine, and glutamine) have side chains that react slowly with ozone. Serine and threonine also react slowly with ozone. Histidine displays a higher reactivity to ozone, due to the presence of an imidazole ring, which is in agreement with the Hospira study [165], where oxidation of the imidazole ring in the drug product occurred. Sharma and Graham [170] reported that cysteine has high reactivity with ozone attributable to its SH group, which further confirms the findings of Cataldo [169]. Sharma and Graham [170] state that aromatic amino acids, tryptophan and phenylalanine, have a high reactivity with ozone as the aromatic ring and benzyllic hydrogens enhance reactivity. Rates of reaction are controlled by reactions of ozone on un-protonated amino acids, so reaction rates are therefore low below pH 7.

These findings confirm that ozone can cause changes to the protein structure which could have serious implications in terms of the activity of a drug substance. It is therefore essential to determine whether ozone is formed during HVLD so that steps can be taken to prevent its formation and hence eliminate or reduce the possible effects on protein degradation.

6.1.6 *Ozone and methods for measurement of ozone*

Ozone was first documented by Dutch chemist Martinus Van Marum in the late 1700s, but it was not classified until 1840 when German Chemist Christian Friedrich Schönbein gave it the name ozone, meaning "bad smell". Its molecular formula, O_3, was proved by Jacques-Louis Soret in 1865 by indirect measurement of its density [171] and confirmed by Schönbein in 1867 [163]. Ozone is a strong oxidising agent, with a distinct odour and has a number of applications including the disinfection of waste water and removal of organic and inorganic contamination e.g. pharmaceuticals from wastewaters [172].

Before describing a number of methods for ozone analysis, it is important to note that there are several species that are known to interfere with ozone analysis including: nitrogen dioxide, hydrogen peroxide and chlorine [173, 174]. The extent to which these substances affect the analysis depends largely on the method that is being used. Interfering species will be discussed specifically for each of the methods mentioned in this review.

Schönbein developed a method to detect ozone in the atmosphere based on a simple reaction between ozone, potassium iodide and corn starch [175]. Potassium iodide reacts with water and ozone to form potassium hydroxide, oxygen and elemental iodine (Equation 6.1). In aqueous solution or in a moist environment, the potassium iodide salt will break into its ions I^- and K^+ (Equation 6.2), and the iodide then goes onto react with elemental iodine forming a triiodide ion (Equation 6.3) which combines with the amylose contained in the starch to form a complex with a red-blue colour (Equation 6.4) [176].

$$2KI + H_2O + O_3 \rightarrow 2KOH + O_2 + I_2 \qquad \textbf{Equation 6.1}$$

$$KI + H_2O \rightarrow K^+(aq) + I^-(aq) \qquad \textbf{Equation 6.2}$$

$$I^- + I_2 \rightarrow I_3^- \qquad \textbf{Equation 6.3}$$

$$I_3^- + amylose \rightarrow I_3^-/amylose\ complex \qquad \textbf{Equation 6.4}$$

For the capture of interfering species such as oxides of nitrogen, when bubbling gas through a potassium iodide bottle, Thorp [177] recommended placing an absorption tube containing chromic acid and a tube containing potassium permanganate before the potassium iodide bottle, to ensure that only pure ozone was reacting with the potassium iodide. A downside of traps is that that they can also capture some of the ozone, making subsequent measurements of ozone concentration inaccurate [178].

Schönbein investigated other chemicals for their ability to react with ozone and these included: manganous salts and thallium oxide, two substances that turn brown on reaction with ozone with the latter having the advantage that it does not react with nitrites, known to interfere in ozone analysis. In addition to these chemicals, he also looked at substances that decolourise upon exposure to ozone, including Indigo and litmus [163]. Following Schönbein's early investigations, further work has been carried out into the determination of ozone with potassium iodide and Indigo and these are discussed in further detail in section 6.1.7, 6.1.8 and 6.1.9. More specifically the methods for ozone measurement considered include: the determination of ozone using iodine and colorimetric methods based on potassium indigo trisulfonate, bis(terpyridine)iron(II) and sodium diphenylaminesulfonate as well as commercial methods.

6.1.7 *Determination of ozone using UV spectroscopy*

Ozone concentration in the gaseous and aqueous phases can be determined directly via UV spectroscopy where ozone gives rise to a broad peak with a maximum at 260nm however some reports state the maximum as 258nm. There are a number of different reports of the actual value of the molar absorption coefficient of ozone and these are summarised in Table 6-2.

Reported molar absorption coefficient/$M^{-1}cm^{-1}$	Reference
3600	[179]
2930 ± 70	[180]
2000	[181]
2900	[182]
3314 ± 70	[183]
2950	[174]
3292 ± 70	[184]
3150	[185]

Table 6-2 - Reported molar absorption coefficients for ozone 255-260nm in aqueous solutions

Gaseous concentrations of ozone can be measured using a UV flow through cell. UV absorbance at 245nm is utilised in some commercially available ozone monitors [186] and also in small lightweight personal ozone monitors. The rapid decay rate of ozone in aqueous solutions and the variation in the reported molar absorption coefficients mean that monitoring of ozone via UV spectroscopy in aqueous solutions is difficult. Methods detailed in the following sections can be used to determine ozone in the aqueous phase.

6.1.8 *Determination of ozone using iodine*

Byers and Saltzman [187] reported that uncertain stoichiometry and a lack of specificity with many existing methods was still an issue in the 1950s, but that iodide chemical methods were some of the more promising methods for the determination of ozone.

For the determination of the concentration of ozone in air, air is passed through a neutral solution of potassium iodide. After acidification of this solution, it is then titrated with standardised sodium thiosulfate. Acidification just before titration is important to decompose iodates as these can be formed when ozone is bubbled through water at high ozone concentrations. Thorp [177] reported a sensitivity of detection of 0.0013mg ozone per cubic centimetre of 2M potassium iodide solution. In this method sufficient quantities of air must be passed though the iodine solution for the ozone to react. At a concentration of 0.1 ppm, 9.9 litres of air must be passed through each cubic centimetre before ozone can be detected [177]. These methods would be suitable for continuous air monitoring, but would not be suitable for monitoring smaller samples of air, as the volumes for testing would be too low.

One issue reported in the literature around iodine methods is that a number of studies have been carried that report different values for the ozone:iodine stoichiometry ranging from 0.65 - 1.5 [188]. Boyd *et al* [189] reported that the stoichiometry of the ozone:iodine reaction was pH dependant and that in neutral unbuffered solutions, one molecule of ozone liberated more than one molecule of iodine, an I_2/O_3 ratio of 1.5. Ingols *et al* [190] reported that at pH 9.0 one molecule of ozone liberated one molecule of iodine.

Hodgeson [191] found the stoichiometry of the ozone and iodine reaction to be 1:1 at concentrations greater than 1.6ppm. Through investigations using the Nederbragt ozone detector, a linear function of ozone concentration was observed, as determined by neutral KI, from 0.05 to at least 30 ppm implying that below 1.6ppm this stoichiometry will also apply. The findings of Kopczynski and Bufalini [192] agree with that of Hodgeson [191], showing that the reaction between ozone and iodide proceeds as follows:

$$O_3 + 2H^+ + 2I^- = O_2 + H_2O + I_2$$
<div align="right">**Equation 6.5**</div>

Kopczynski and Bufalini [192] disagreed with the findings of Boyd [189] in that their investigations showed that 1:1 stoichiometry is valid with experimental error above a concentration of 2ppm.

As the stoichiometry of this reaction is highly dependent on factors such as pH and concentration, and there appears to be a lack of a general consensus on appropriate reaction conditions, other methods must also be considered.

6.1.9 *Determination of ozone using colorimetric methods*

There are a number of colourimetric methods for the determination of ozone, one of which is the Indigo method. This method enables the determination of aqueous concentrations of ozone using potassium indigo trisulfonate (PIT) [193]. Aqueous PIT shows a peak in absorbance at 600nm. Upon reaction with ozone, ozonolysis of the carbon-carbon double bond in PIT results in the formation of sulfonated isatin, Figure 6.7, which eliminates the absorbance at 600nm (as sulfonated isatin does not absorb at 600nm) and forms the basis of the measurement principle. The pattern that is seen

when PIT is exposed to increasing ozone is that there is a linear decrease in the absorbance at 600nm.

Indigo trisulfonic acid
ε_{600nm} 20,000M^{-1} cm^{-1}

Isatin sulfonic acid
ε_{600nm} 0.0M^{-1} cm^{-1}
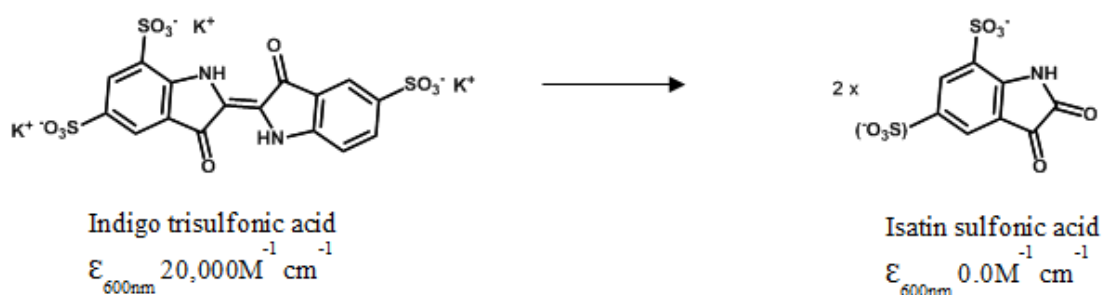
Figure 6.7 – Conversion of Indigo trisulfonate to sulfonated isatin by the action of ozone [30]

The direct and selective reaction of the double bond of PIT with ozone is what makes this method so straightforward. PIT reacts with 1:1 stoichiometry with ozone. When there is a high rate of mixing, the one carbon-carbon double bond present in PIT reacts with ozone with a very high reaction rate constant. Amino groups on the PIT molecule are protonated at low pH so they are unreactive [193].

Bader and Hoigné [182] recommended PIT for use when the measurement of ozone directly at 258nm is not appropriate, for example when the concentration of ozone is lower than 0.1mg/L or when the background absorption is quite high. Following the proposal of this method by Bader and Hoigné [182], PIT has been used widely as an indicator for ozone detection.

Subsequent to the development of the Indigo method by Bader and Hoigné [193], a standard was published by Bader and Hoigné [182]. The precision, speed, specificity and ease of reagent handling in this method have resulted in modifications to the method being published to suit specific requirements. An adaption of Bader and Hoigné's [182] Indigo method is the standard method published by the American Public Health Association (APHA) for the determination of residual ozone in drinking water following treatment by ozone to destroy organic compounds.

A consideration with the Indigo method when using this for the determination of ozone in drinking water is around interferences from other compounds and ways of overcoming these are listed in the standard. For example, hydrogen peroxide can react

slowly with ozone and organic peroxides react rapidly so ozone measurement must be carried out within 6 hours of adding reagents so that these reactions do not have time to take place. Bromine formed through the oxidation of Br⁻ ions and the presence of 1 mole of HOBr is equivalent to 0.4 moles of ozone, and this must be taken into account when analysing the results. Interference by chlorine, which may be present in drinking water, can be masked with malonic acid. Oxidised forms of Mn(II) decolorize PIT, so measurement should be made relative to a blank where the ozone has been selectively destroyed. If it is not possible to carry out a blank determination, the standard states that 0.1mg/L ozonated manganese gives a response of 0.08mg/L apparent ozone [174].

Collins *et al* [194] presented an alternative approach to gas phase ozone determination based on extracting gaseous samples with a glass syringe and injecting these samples into bottles containing PIT solution. Small volumes of gas (10mL) were sampled and immediately reacted with PIT solution. The effect of shaking time was also evaluated. It was found that higher liquid ozone concentrations were achieved with longer shaking times and 20 seconds was the optimum for allowing the gaseous ozone to react with the PIT solution.

A further adaptation of the method of Collins *et al* [194] was described by Chiou *et al* [195]. Chiou *et al's* [195] modified Indigo method, to facilitate the determination of both gaseous and aqueous ozone concentrations, was an adaptation of Bader and Hoigne's [193] method and also the work by Collins *et al* [194] and Hart *et al* [184].

In Chiou *et al's* method, ozone concentrations were calculated using Equation 6.6 and Equation 6.7 for gas samples and Equation 6.6 and Equation 6.8 for aqueous samples.

$$C = 48,000 \ \frac{\Delta A_{600}}{M_{In}} \qquad \text{Equation 6.6}$$

$$\Delta A_{600} + \frac{V_i \ (R_i - R_m)}{V_0} \qquad \text{Equation 6.7}$$

$$\Delta A_{600} + \frac{V_i \ R_i - (V_i + V_0) R_m}{V_0} \qquad \text{Equation 6.8}$$

Where: C = Ozone concentration (mg/L), M_{ln} = PIT molar absorptivity at 600nm assuming a 1:1 stoichiometric ratio for the reaction between PIT and ozone ($M^{-1}cm^{-1}$), ΔA_{600} = Normalized absorbance drop of PIT reagent at 600nm (cm^{-1}), R_i = Initial absorbance of PIT reagent at 600nm (cm^{-1}), R_m = Absorbance of mixed reagent and sample mixture at 600 nm (cm^{-1}), V_1 = PIT reagent volume (mL), V_0 = Ozone sample volume (mL).

Chiou *et al* [195] trialled the use of a gas tight syringe for sampling and also for reacting ozone samples with PIT to see if improvements in the precision of the method could be achieved. Hart [184] reported that the reproducibility of chemical methods could be improved through the use of syringes as they reduce ozone loss through minimising the contact of ozone with air. The syringes used in the study by Chiou *et al* [195] had an accuracy of at least ± 1% of their full scale, as this was deemed to be a crucial part of the method. The precision (standard deviation) of the method was estimated to be around ± 5% and both the accuracy and precision of the results could be improved by increasing the fraction of reagent decolourisation. In order to ensure that PIT reagent decolourisation was at least 10%, suitable initial absorbance of PIT reagent R_i and volumes V_i and V_0 (Equation 6.7 and Equation 6.8) were chosen. Chiou *et al* [195] stated that most of the error observed would be due to volume inaccuracies.

Chiou *et al* [195] made a number of assumptions in the experimental method with respect to the molar absorptivity of gaseous ozone at 258nm being 3,000 $M^{-1} cm^{-1}$ and the stoichiometric ratio being 1:1 and when the results of direct absorbance at 258nm were correlated with absorbance of PIT at 600nm, the molar absorptivity of PIT was calculated as 23,150 $M^{-1} cm^{-1}$ ± 80 $M^{-1} cm^{-1}$.

A challenge in the research carried out in this thesis, was that only small volumes of gas were available for sampling. It was therefore difficult to measure the ozone concentration directly in the headspace gas, as removal of this with a gas tight syringe and insertion into a quartz cuvette would have resulted in a dilution of concentration and possibly sample losses upon injection into the quartz cuvette. However, by using the modified Indigo method [195] and extracting the headspace gas into a gastight syringe containing PIT reagent, then reacting this and measuring the absorbance of PIT

reagent at 600nm, this would enable the determine of the ozone concentration and this is something that is explored later in this chapter.

Bis(terpyridine)iron(II)

Tomiyasu and Gordon [188] investigated the measurement of ozone via the decrease in UV absorbance at 552nm of bis(terpyridine)Iron(II), ($Fe(terpy)_2^{2+}$), in dilute hydrochloric acid. They observed a quantitative relationship between the volume of ozone added and the concentration of $Fe(terpy)_2^{2+}$ that reacts with the ozone [188]. The relationship between the decrease in absorbance at 552nm and the increase in residual ozone concentration was observed to be linear. They compared this method to direct UV absorbance of ozone at 260nm and found there to be a good correlation suggesting percentage accuracy for the comparison of 2.2%. The $Fe(terpy)_2^{2+}$ method was also compared to the Indigo method from Bader and Hoigné [182] and a percentage accuracy for this comparison was 2.1%. Direct determination of the stoichiometry of the ozone and $Fe(terpy)_2^{2+}$ reaction was undertaken by measuring the change in ozone concentration at 260nm (molar absorptivity 3300 $M^{-1} cm^{-1}$) and the change in $Fe(terpy)_2^{2+}$ concentration at 552nm. The ratio of [$Fe(terpy)_2^{2+}$ consumed]/[ozone consumed] was found to be 1.99 ± 0.03. Equation 6.9 was the proposed equation for the reaction based on this determination.

$$2Fe(terpy)_2^{2+} + O_3 + 2H^+ \rightarrow 2Fe(terpy)_2^{3+} + O_2 + H_2O$$ **Equation 6.9**
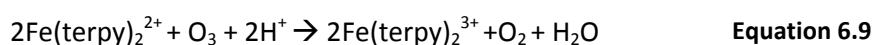
Tomiyasu and Gordon [188] reported the detection limit of the $Fe(terpy)_2^{2+}$ method to be 4µg/L ozone, whereas with Indigo it was 1µg/L ozone [193]. An advantage of the $Fe(terpy)_2^{2+}$ method is that the reaction with ozone happens very quickly, i.e. in one second. An advantage over the iodide method is that chlorine does not interfere as much with $Fe(terpy)_2^{2+}$, and can be masked with malonic acid. In addition, hydrogen peroxide does not interfere with $Fe(terpy)_2^{2+}$ which can be the case with the iodide method.

Sodium diphenylaminesulfonate

Sodium diphenylaminesulfonate (NaDS) reacts with ozone forming a turquoise blue product with an absorption maximum at 593nm. The applicability of this method for ozone determination was investigated by Bovee and Robinson [178]. The reagent is less susceptible to interference than iodide and interferences that do occur produce a

different colour to that produced by reaction with ozone, noticeable by an experienced operator. Optimum results are obtained at pH 3 and at low temperatures to avoid the instability of the NaDS. The stability of NaDS is of the order of days at 0°C but is lower at room temperature. An issue that is highlighted with this method is that it was calibrated against the iodide method and not against a direct measurement of ozone and hence no firm conclusion on its accuracy can be determined.

6.1.10 *Commercial solutions for ozone detection*

In terms of commercially available kits for ozone detection, Ozone Solutions provide a kit for the colorimetric visual detection of ozone, Figure 6.8. It includes an activator solution, measuring cup (25mL sample) and ampoules containing a reagent substance. The top of the ampoule, containing the reagent substance, is cracked and inserted into the cup containing the sample to be measured. The ampoule draws up the sample and the two liquids react and a colour change can be observed. The ampoule is then compared to a set of ampoules representing 0.6-3 ppm ozone, Figure 6.8.

Other commercially available solutions for measuring ozone require large sample sizes, for example, gaseous ozone analysers draw a large volume of gas past a detector or aqueous ozone analysers. Another limitation of these commercially available solutions is that they are not as customisable to the specific requirements as wet chemical methods. In addition, commercially available solutions can be expensive, with prices starting from $395, [196] and in the case of this research project, it was not feasible to purchase a detector.
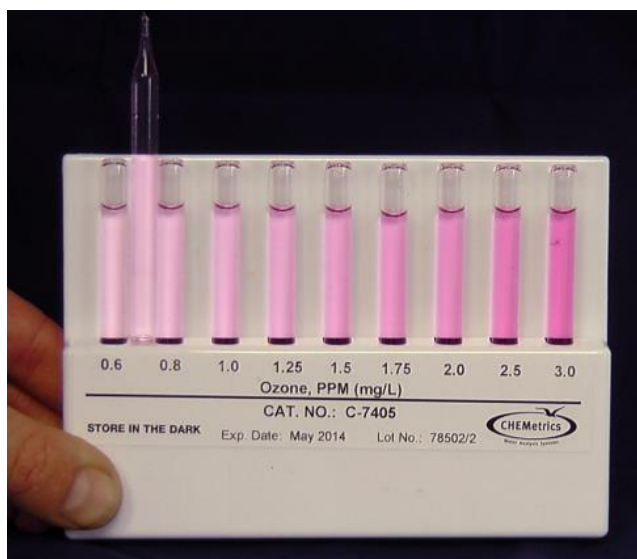
Figure 6.8 - K7402 colorimetric ozone detection kit from Ozone Solutions [197]

6.1.11 *Choice of method in this research*

The vial packaging system which is under investigation in this research comprises three components: the glass vial, elastomeric closure and aluminium crimp seal, Figure 6.1. In the case of pharmaceutical vials, typically the vial volumes are less than 100mL and hence the volume of the gaseous headspace and fluid inside the vial in which to measure ozone are low. Consequently the ozone concentration may be extremely low as the theoretical concentration of ozone that can be produced from the oxygen contained in this air headspace is low. It is difficult to calculate the theoretical concentration of ozone that may be produced in the vial headspace due to the unknown factor of percentage conversion of oxygen to ozone in the headspace when the vial is subjected to HVLD, however, estimations have been calculated using the ideal gas equation and these are shown in Table 6-3 .

$3O_2 \rightarrow 2O_3$ conversion (%)	g/mL	g/L	mg/L
100	9.20×10^{-3}	9.1965	9196.46
1	9.20×10^{-5}	0.0920	91.96
3	2.76×10^{-4}	0.2759	275.89
5	4.60×10^{-4}	0.4598	459.82

Table 6-3 - Theoretical gaseous concentrations of ozone achievable for different % conversion rates of oxygen to ozone in a 50mL headspace (calculated using the ideal gas equation)

If ozone is formed in the gas phase it may also transfer into the aqueous phase so method development therefore needs to consider approaches to measuring ozone in the aqueous and gaseous phases. Measuring ozone in the closed system of a container

under investigation would be ideal, however removal of a sample could be considered, as well as other indirect methods such as those that use probes or indicators, if it is not possible to measure ozone directly. These should where possible be correlated to a direct method of ozone measurement to ensure their validity.

Researchers investigating measurement methods for ozone identify a number of factors that can give rise to error in the ozone measurement. These include experimental parameters such as reactions with glassware, trace contaminants or other reagents. Other issues that arise in the measurement of ozone are due to its instability, volatilization from solution and rapid decomposition in water [188]. It is important that these factors are considered and where possible steps taken to minimise the error. For example, ensuring that clean glassware was used at all times and that equipment with good ozone resistance was used to avoid its degradation thereby resulting in reduced ozone concentrations and contamination. The rapid decomposition of ozone in water was considered, as this is a crucial parameter for a method that will be transferred to the pharmaceutical facility because there may be delays between sampling and measurement.

It was also important to investigate the effect of handling, as this is a contributory factor towards ozone decomposition. Handling refers to how the samples under investigation (aqueous samples in vials) are moved around the laboratory and moved when samples are being removed for UV measurement. For example – if one sample was shaken and this was not applied to all samples, this would give rise to misleading results. Handling gas or aqueous mixtures containing ozone must be carried out with accuracy and with high repeatability as ozone can be short lived and its dissociation back to oxygen can be increased by the handling and the transferring of mixtures. The use of a gas tight syringe would reduce the effects of handling however, some handling must occur, so it was important where possible to limit potential losses.

The Indigo method was identified as the most appropriate test for ozone due to its simplicity compared to tests which were considered, but discounted, for reasons that are summarised in Table 6-4. The indigo method was identified as having fewer potential interferences and was also the most applicable method to the testing scenario in this case. More specifically it was predicted that ozone concentrations

encountered inside the vials would be low, consequently this method provided a suitable limit of detection. A modification was made to the APHA 4500-O_3 standard method [174], rather than reacting aqueous ozone samples with an aqueous solution of PIT, the aqueous solution of PIT would be placed inside the vial with the intention that any ozone generated inside the vial could immediately react. This would avoid passing vials of water through the HVLD machine and then reacting this with PIT, which would introduce a time delay and may allow time for the ozone to decompose.

Method	Reason against application in this scenario
Iodine/Ozone reaction	Uncertainties around stoichiometry [187-189], large volumes of air required to pass through test solution [177]
Gas tight syringe and potassium indigo trisulfonate [194, 195]	Only small volumes of gas were available for testing, larger volumes were needed. Method was found to be time consuming. Time delays between HVLD and measurement meant that headspace gas sampling or liquid sampling (water in the vial) was not appropriate as ozone may have broken down in the 6 hour window.
Bis(terpyridine)iron(II) absorbance [188]	Limit of detection was not as low as the indigo method.
Sodium diphenylaminesulfonate absorbance [178]	Optimum results could be obtained at pH 3 and low temperature, but in this scenario it was not possible to control pH or temperature. The method is also calibrated against the iodine method which was discounted due to differing reports on stoichiometry.
Commercially available ozone detection kits [197]	Large samples size (25mL) required. Time delays between HVLD and measurement meant that liquid sampling of water in the vial was not appropriate as ozone may have broken down in the 6 hour window. Not customisable for this application.

Table 6-4 - Methods considered for ozone detection and reasons against utilisation in this research

6.2   Aim

The aim of this study was to identify and adapt, or develop a method to detect ozone that may be generated in the headspace of containers (in this case flip-off cap glass vials) undergoing high voltage leak detection (HVLD) and develop a protocol for testing the vials subject to HVLD. More specifically, the aim was to: 1) develop a method that could identify the presence or absence of ozone and 2) if possible quantify the concentration of ozone. When developing the method it was crucial to investigate and eliminate features of the proposed protocol for testing that could potentially give rise to error i.e. time delays between running vials through HVLD and measurement of ozone and exposure of vials to light.

Ozone, if generated in the headspace of the container would be present in the gas phase and may also transfer into the aqueous phase. Development of a method for detecting ozone in vials, therefore considered the aqueous and gaseous phases. A

preferable technique for measurement of ozone inside the vial would be from the exterior, without opening the vial, as the state of the vial contents would be preserved and not interfered with, so it could be expected that results would be reliable. These are important factors that were considered in this study and this chapter details research into the following areas:

1) testing of an ozone generation system to determine ozone output for use in further experimental work

2) development of a method for the detection of ozone in vials, preferably a direct method which would consider both the gaseous and aqueous phases

3) testing of a method for ozone detection

4) adaptation of the method for use on HVLD machine

5) proposal of a protocol for testing for ozone in vials that had been passed through the HVLD machine

Several methods were considered for point 2) and these are discussed later in section, 6.5. Chapter 7 presents the results from implementation of the protocol developed in this chapter.

6.3 Methods

As this chapter is detailing method development, the details of methods used are included under each heading in the discussion. Throughout this chapter, an adaptation of the APHA 4500-O3: Standard Methods for Examination of Water and Wastewater [174], was utilised for ozone measurement.

The APHA method is based on the UV measurement of potassium indigo trisulfonate (PIT) ($C_{16}H_7N_2O_{11}S_3K_3$), and the difference in absorbance between a sample and a blank. Equation 6.10 is the APHA equation that is used to calculate ozone concentration in the APHA method:

$$\text{mg } O_3/L = \frac{100 \times \Delta A}{f \times b \, x \, V}$$

Equation 6.10

where ΔA is the difference in absorbance between the sample and a blank, b is the path length of the cell (cm) V is the volume of the sample (mL) (normally 90 mL) and f

is a sensitivity factor of 0.42. The blank was made up of PIT and deionised water and the sample comprised PIT and ozonated water. The standard method was adapted, because it was not possible to use it for this particular application for a number of reasons.

1) The volumes investigated in this research were low, i.e. vials containing only 6mL of liquid (the APHA standard used a 90 mL sample added to 10mL IR)

2) The potential theoretical concentration of ozone formed in the headspace was low and due to the short lived nature of ozone it may not have transferred into the liquid phase before decomposition.

3) When taking into consideration the lag time between putting the vials through the HVLD and measuring the absorbance (up to 6 hours) the likelihood of the ozone moving into solution and remaining in solution without decomposition for long enough to subsequently measure with PIT was questionable.

Due to these reasons it was desirable to place the PIT inside the vial to react with any potential gaseous ozone that was generated instantaneously as it formed inside the headspace. PIT is a suitable material for this purpose as it reacts rapidly with ozone $\kappa = 9.4 \times 10^7 \, M^{-1} s^{-1}$ [198].

Equation 6.10 was adapted to calculate the ozone concentration for this experimental scenario. 6mL of IR1 was present in the vial for HVLD exposure and no additional liquid was added to the vial, so only gaseous ozone was present to react with the IR1. It was therefore deemed suitable to remove the two volume terms (100 and V) from the original equation as in this case the values were both 6mL and hence would cancel each other out. The modified equation took the form of Equation 6.11.

$$\text{mg } O_3/L = \frac{\Delta A}{f \times b}$$
Equation 6.11

6.4 Materials

Potassium indigo trisulphonate, phosphoric acid and sodium dihydrogen phosphate were purchased from Sigma Aldrich. Borosilicate glass vials were supplied by Amilco. Quartz cuvettes with septum lids were purchased from NSG Precision Cells, Inc. BD

Microlance™ needles and BD disposable 5mL syringes were purchased from Fisher Scientific.

6.4.1 *Ozone generation system*

An ozone generator was made in-house at Newcastle University to provide flexibility in ozone generation capability. Figure 6.9 is a photograph of the ozone generator which is based on the dielectric-barrier discharge principle and has a variable voltage, thereby allowing the rate of ozone generation to be controlled. A low current (~9mA), high voltage (~3kV) is applied across a gap containing air. The ionization of molecular oxygen occurs allowing the recombination of oxygen ions with molecular oxygen to form ozone. Commercially available ozone generators are expensive than and also are not as flexible in terms of their operation as required for the purpose of this research [199].
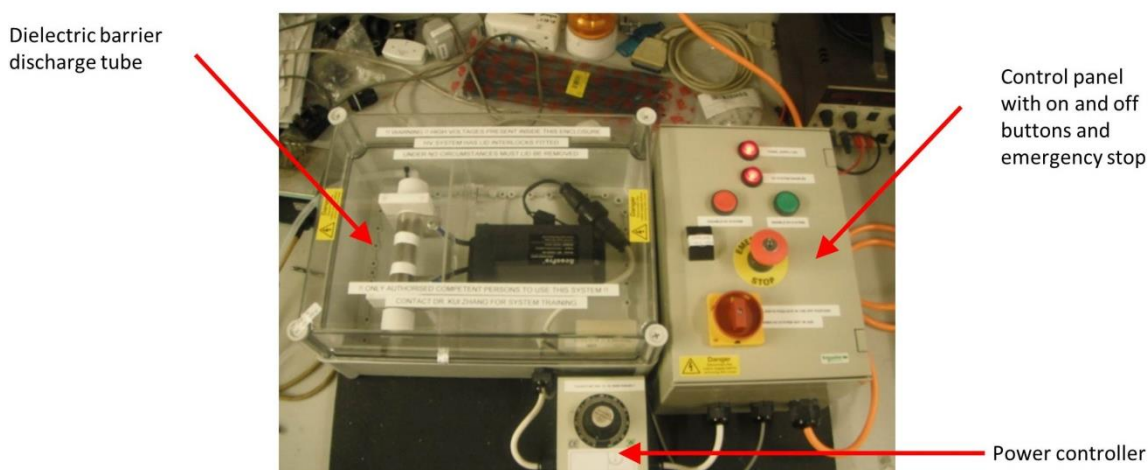
Figure 6.9 - Ozone generator

Figure 6.10 shows a schematic of the experimental setup used to generate ozone. The ozone generator was fed with bottled compressed air from a cylinder connected to it through a polycarbonate flow meter (0.4-5 L per minute) with a precision adjusting valve for accurate leak free flow control (Cole Parmer). Maintaining a sufficient flow rate through the discharge tube is critical for maintaining ozone generation, as with low flow rates, the air inside the tube is heated which causes less ozone to be formed and more ozone to be broken down. Heat removal is increased with increased flow through the tube and molecules of ozone formed are swept out of the tube and are

not destroyed [200]. An optimum flow rate was decided and is discussed in 6.5.3. Silicone tubing was used to connect the ozone meter with the ozone bubbler.
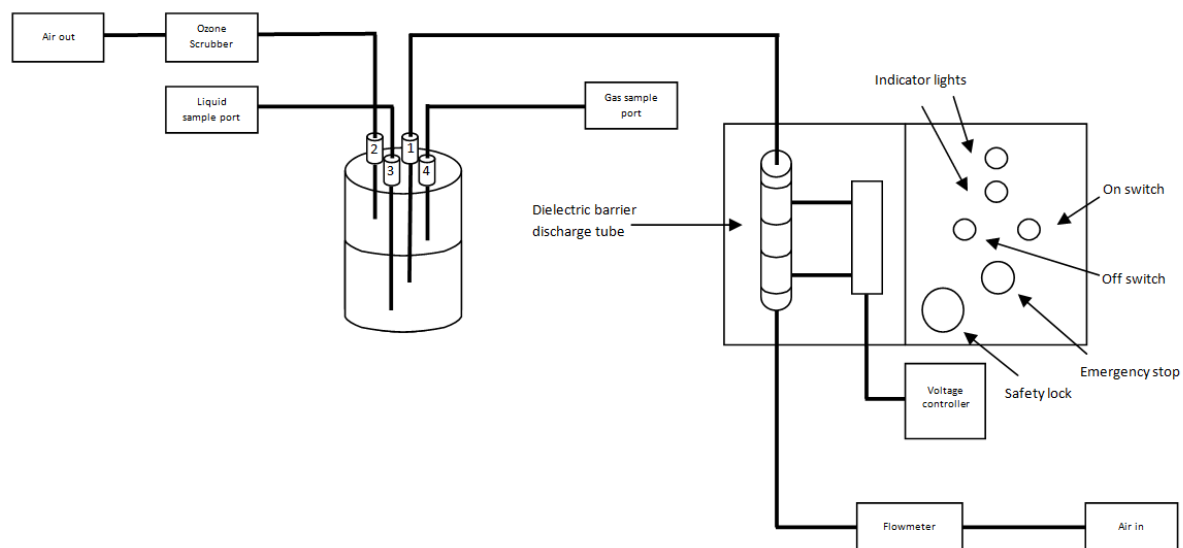
Figure 6.10 - Schematic of ozone generator and bubbler

A dielectric-barrier discharge tube, Figure 6.11, was made from a borosilicate glass tube 160mm in length, with an inner diameter of 26mm and an outer diameter of 28mm. Electrodes, made from 30mm wide, 0.05mm stainless steel shim were placed around the glass tube, with a gap of 40mm between electrodes. The electrodes were sealed onto the glass tube using polytetrafluoroethylene (PTFE) tape, to prevent ozone formation between the electrodes and glass tube, which would lead to corrosion of the electrodes. A piece of mesh, 105mm in length containing holes 0.5mm in diameter was positioned inside the glass tube within the area covered by the electrodes. The glass tube was sealed at each end with PFTE end caps containing PTFE O-rings. Barbed male elbows ¼ npt thread were used for the air inlet and air outlet. The glass tube was mounted on two PTFE supports, with a 40mm gap between the tube and the polyvinylidene fluoride housing.
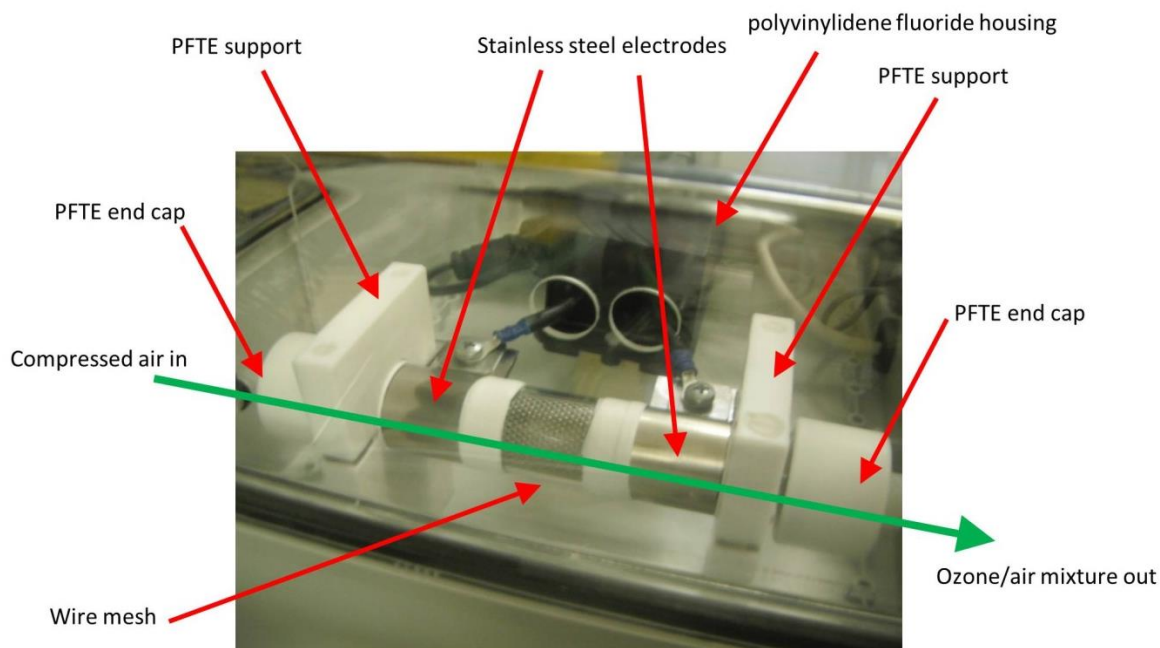
Figure 6.11 - Dielectric-barrier discharge tube

A high voltage is applied from the electrodes, which moves across the tube. The wire mesh inside the tube enables a higher conversion of oxygen to ozone to be achieved. Compressed air enters the glass tube from one end and passes through the tube. When the oxygen inside the tube passes though the high voltage area, ozone is produced and the air/ozone mixture passes out of the opposite end of the tube. The air/ozone mixture then enters the ozone bubbler through a tube that is positioned below the water level. The ozone bubbler was made from a 500ml Schott Duran glass bottle with a 4-port screw cap (polypropylene) with screw connections (black, M8 thread) and silicone seals on each port. The 4 ports were designated as: port 1 - ozonized air in, port 2 - ozonized air out, port 3 - liquid sample port and port 4 - gas sample port, Figure 6.10.

The air/ozone mixture bubbles though the water at a constant flow rate and leaves the ozone bubbler through a vent. It is not appropriate due to health and safety to vent off ozone into the environment, so an ozone destruction device is required. For ozone destruction, an activated carbon filter can be used as a catalyst, which reacts with and removes ozone from the air. This air then passes into the fume hood. The whole unit operates in a fume hood to ensure no ozone is released into the laboratory atmosphere. The high voltage element of the ozone generator is locked inside insulated housing, to ensure that these parts cannot be reached by the operator.

Switches to turn the machine on are only operable using a lock, the key to which is held only by trained operators.

6.5 Results and Discussion

6.5.1 *Calibration of borosilicate glass vials and quartz cuvettes for the measurement of the UV absorbance using potassium indigo trisulfonate*

Method

A stock solution of PIT was prepared by dissolving 0.6gL^{-1} (1mM) PIT in 20mM phosphoric acid [193]. The absorbance of stock solution was above 3 which was too high to measure on the spectrophotometer so it was diluted to 10µM in order to achieve an absorbance of below 1, and this was used as a calibration standard. 10 borosilicate glass vials (3mL size) were filled with 3ml 10µM PIT solution, and 2 quartz cuvettes were filled 10 times and the UV absorbance was measured using a scanning mode over wavelengths 400-700nm to allow visualisation of the PIT peak at 600nm.

Results and discussion

For the direct measurement of ozone at 258nm, quartz or fused silica is required as both materials are transparent below the wavelength of 350nm. It is therefore not possible to directly measure ozone through pharmaceutical vials, as these are made of borosilicate glass which is only transparent between the wavelengths 350 and 2000nm. The method that was therefore selected was based on the absorbance of PIT solution at 600nm, providing the possibility of measuring absorbance though the borosilicate glass vials. A complication is that the vials used in the investigation exhibit slight irregularities in wall thickness and curvature and these affect the path length and give rise to variation in the absorbance and hence concentration that is determined from UV spectroscopy. This variation was accounted for by testing to identify the level of variation inherent within a batch of vials.

Additionally it was necessary to determine whether it was possible to carry out repeatable measurements through borosilicate glass vials and hence the results were compared to measuring the absorbance of PIT solution in quartz cuvettes. The 3mL vial size was chosen because this was the size of vial that could fit within the sample holder of the UV spectrophotometer.

Poor repeatability was observed in the measurements taken through the borosilicate glass vials, whereas for the quartz cuvettes repeatability was much better. This can be observed in the individual value plot of the absorbance, in Figure 6.12. The mean and the standard deviation of the absorbance measured through the glass vials was higher than that of the quartz cuvettes, Table 6-5, indicating the poorer repeatability of the data.
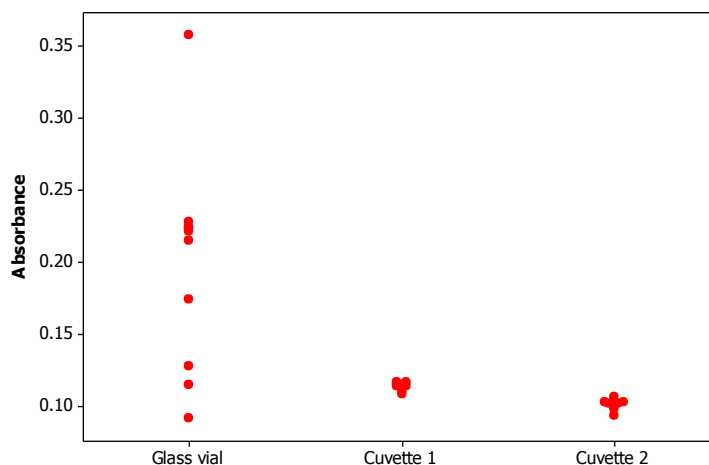
Figure 6.12 - Individual value plot for absorbance of PIT solution measured through borosilicate glass vials and quartz cuvettes

Sample holder	Mean Absorbance	Standard Deviation
Glass vial	0.198	0.076
Cuvette 1 (quartz)	0.114	0.003
Cuvette 2 (quartz)	0.101	0.004

Table 6-5- Mean and standard deviations of the UV absorbance of PIT solution measured through borosilicate glass vials and quartz cuvettes

One reason for the greater variability observed in the results from glass vials is a consequence of the forming process used in vial manufacture which results in differences in wall and base thickness and base shape. If the walls of the vials vary slightly in thickness and curvature, this affects the scatter of the light path that is transmitted through the glass, thus affecting the light reaching the detector.

Another issue arose from the placement of the vials in the UV spectrophotometer. The housing is designed to hold square cuvettes with a footprint of 1cm x 1cm but 3mL glass vials have a larger footprint of 1.5cm x 1.5cm. Consequently housing within the UV spectrophotometer was slightly adapted but the positioning of each glass vial

within the machine may have been slightly different, hence also affecting the scattering of light.

The testing of UV absorbance through glass vials was therefore ruled out for the following reasons:

1) The vial size was too large to fit into the UV housing to ensure repeatable measurements.

2) Differences in vial wall thickness and curvature interfered with the measurement method.

3) A vial size of 3mL would provide insufficient volume of PIT solution to perform repeat measurements as part of the final testing protocol, also insufficient headspace to allow ozone to be formed and larger vials would not fit into the UV spectrophotometer housing.

4) The spectrophotometer that was used to house the 3mL glass vials had no data recording capacity to be able to store data from scanning wavelengths, meaning that only single wavelength absorbance readings were possible, which would limit the available information.

An alternative UV/Vis spectrophotometer, the Jenway 6705, was unable to house the vials tested in this initial study, so it was decided that the samples should be removed from the vials and tested using quartz cuvettes. This approach would ensure repeatability of the measurement. This would require samples to be removed from the vials and therefore a method using gas tight syringes was investigated, as proposed by a number of researchers [184, 194, 195] and discussed in section 6.1.9. This approach is discussed in section 6.5.7.

6.5.2 *Testing the ozone generator output using an ozone bubbler*

Method

The output of the ozone generator was tested by bubbling ozone/air mixture air from the generator through 300ml distilled water at room temperature. To begin the experiment, the compressed air supply of 1L/minute was used and the timer was started when the ozone generator and ozone bubbler were switched on.

3ml samples of water were removed at 5 minutes intervals, via port 3, Figure 6.10, using a 5ml Plastipak® syringe (barrel and plunger polypropylene, plunger stopper synthetic rubber (latex free), lubricant silicone oil) and after transferring the sample to a quartz cuvette the UV absorbance at 258nm was measured. The reference blank sample was distilled water at room temperature. Sampling continued until 305 minutes to observe whether ozone decomposition occurred after the ozone supply had been switched off after 140 minutes.

A second experiment was carried out with a reduced sampling frequency, of every 30 minutes, over a period of 120 minutes to investigate whether results from the first experiment were repeatable at a lower sampling rate.

Results and discussion

The ozone generator was initially tested to check for ozone output. The air/ozone mixture leaving the ozone generator was bubbled though deionised water, to enable the aqueous concentration of ozone to be determined. Furthermore it was also necessary to establish the ozone concentration that could be achieved in deionised water to inform future experimental plans.

Initial testing of the ozone generator output was carried out using direct measurement of the UV absorbance of ozone in distilled water at 258nm. Using the Beer Lambert Law, Equation 6.12, it was possible to calculate the concentration of ozone in the distilled water.

$$A = \varepsilon b c$$ **Equation 6.12**

Where: concentration of sample (c) is expressed in moles per litre (M, path length (b) is expressed in centimetres and the molar absorptivity (ε) $M^{-1}cm^{-1}$. The absorbance (A) has no units.

Figure 6.13 shows that with increased bubbling time (run1), ozone was being produced by the generator and was dissolving in the deionised water within the bubbler. The ozone concentration was 1.26mg/L at 140 minutes when the ozone bubbler was turned off. It was interesting to note that the ozone concentration continued to rise after the ozone supply had been turned off until 305 minutes when the measurements were stopped, indicating that ozone present in the bubbler continued to dissolve in

the deionised water. The ozone concentration reached 1.59 mg/L after 305 minutes, with the exception of an outlier at 300 minutes where the ozone concentration appeared to be 2.73 mg/L.

Figure 6.13 shows that, despite concerns raised in the literature about rapid decomposition of ozone in aqueous solution, in this case, ozone remained in solution for 160 minutes after the ozone bubbler has been switched off. This was seen to be a useful initial indicator of the time window that may exist for carrying out the measurement of ozone. However, this test was repeated, Figure 6.13 (run 2), with less frequent sampling, but it was not possible to replicate the level of ozone concentration achieved in the first experimental run shown in Figure 6.13. This could have been due to the volume depletion from more frequent removal of samples causing concentration of the ozone, whereas with less frequent sampling, volume was retained for longer and ozone was therefore less concentrated. In addition to this, the temperature of the water and room may affect the transfer of oxygen and decomposition into the water and these factors are not possible to control in the testing scenario for which methods were being investigated.
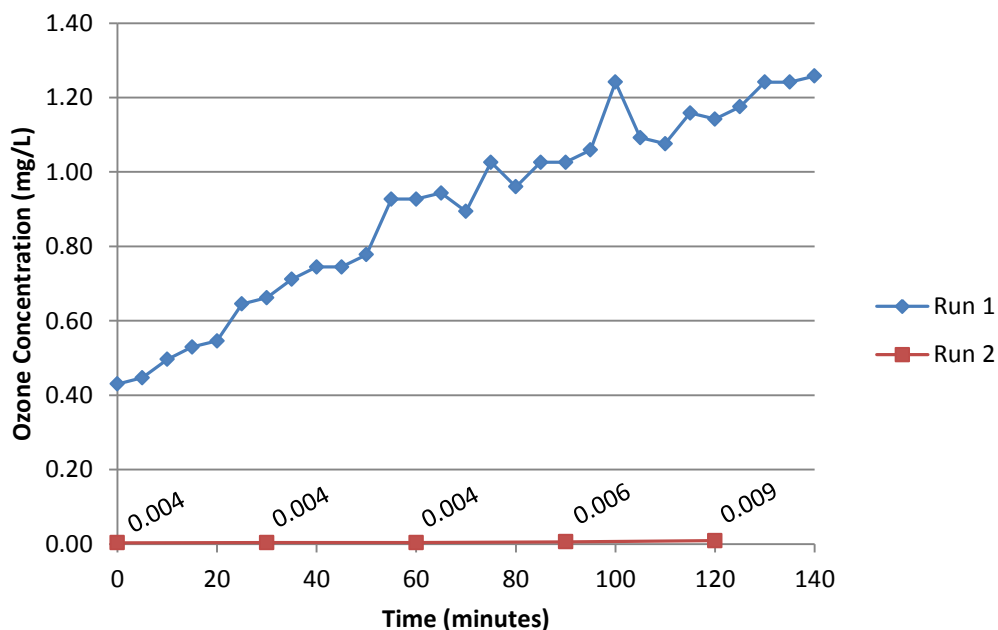
Figure 6.13 - Change in ozone concentration of distilled water at 258nm, with ozone bubbling time

Due to the difficulty in replicating the results from run 1 and the difficulty ensuring replicable water and room temperatures, it was decided that the gaseous output of

the ozone generator would be investigated using a UV flow through cell. This is discussed in the following section. Additionally, due to the difficulty in achieving aqueous ozone solutions, the investigation then looked at exploring measurements of the gas phase and using indirect methods such as the Indigo method to capture gaseous ozone into the liquid phase containing PIT.

6.5.3 *Design of experiments study to test ozone generator output*

Method

A multilevel factorial design was implemented to investigate the effect of two factors: gas flow rate through the generator (L/h) and electrical power supplied to the generator (Watts), as these were the factors that are important for ozone concentration and were controllable. Three levels were considered for each factor, Table 6-6. The gas supply for the ozone generator was ambient air and an air pump was used to achieve the required flow rates and they were measured using a flow meter (Cole Parmar).

Factor	Low	Medium	High
Gas Flow (L/h)	1	2	3
Electrical Power (Watts)	10	15	20

Table 6-6 - Factors and levels investigated in the DOE to test ozone generator output

The response variable was UV absorbance and it was measured using a flow through cell linked to a spectrophotometer. This UV absorbance value was then converted to a concentration for ozone, using the Beer Lambert Law, section 6.5.2. The runs were carried out in a randomised order. After adjusting the flow rate and electrical power, the system was allowed to run for 30 seconds before the UV absorbance measurement was taken, to allow for the system to settle. Three replicates were performed for each combination of factors, giving a total of 27 runs.

Results and discussion

Utilising a UV flow through cell it was possible to determine the optimum settings to achieve the highest ozone concentration from the ozone generator. In dielectric barrier discharge methods, as used in this study, high electrical power and low flow rate, can lead to heat generation inside the tube which can cause the degradation of ozone. This was taken into account in the set-up of the DOE with 30 seconds given for

the system to settle between setting the parameters and taking the absorbance measurement. This was deemed to be appropriate to prevent the heating of the glass tube when the electrical power was high and the flow rate low.

The interaction plot in Figure 6.14 shows that when the flow rate is increased from 1 to 2 L/hr, ozone concentration decreases and when the electrical power is high (20W) the ozone concentration is low. The ozone concentration is highest at medium electrical (15W) power with low flow rate (1 L/hr).
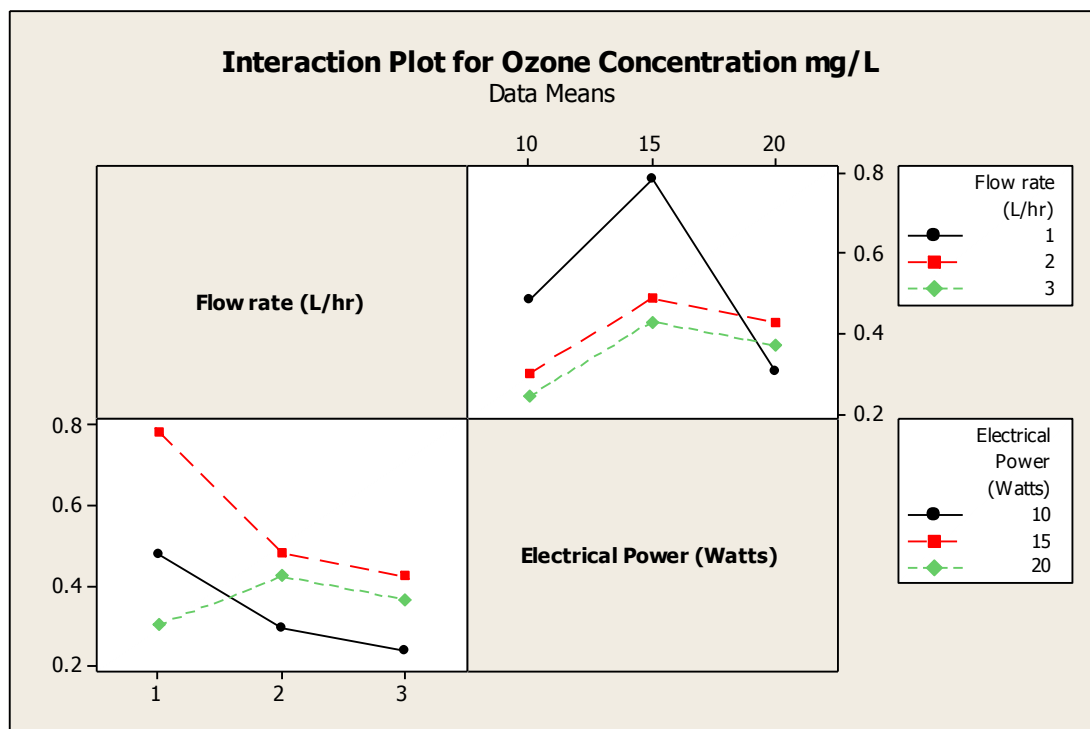
Figure 6.14 - Interaction plot of ozone concentration, electrical power and flow rate

The contour plot of ozone concentration, flow rate and electrical power, Figure 6.15, shows the combination of flow rate and electrical power that gives rise to the highest concentration of ozone. The combination of a low flow rate and medium electrical power produced the highest ozone concentration. This was further confirmed by the interaction plot, Figure 6.14, which shows an overlap of lines between low flow rate and high electrical power. The reasoning behind this is that when air/ozone mixture is being passed through the dielectric barrier discharge tube at low flow rates, when the electrical power is high, this can cause a rise in temperature within the tube, which can cause the ozone that is produced to decompose quickly. At higher flow rates, there is not such a strong effect from temperature as the flow is sufficiently fast to remove the ozone/air mixture before decomposition can occur. The lowest ozone concentration is

seen at high gas flow rate and low electrical power, as the ozone generation capacity is much lower with lower electrical power and coupled with high flow rate means that the air is moving too quickly through the tube and hence only limited amount of ozone can be produced as the residence time in the tube is not long enough.
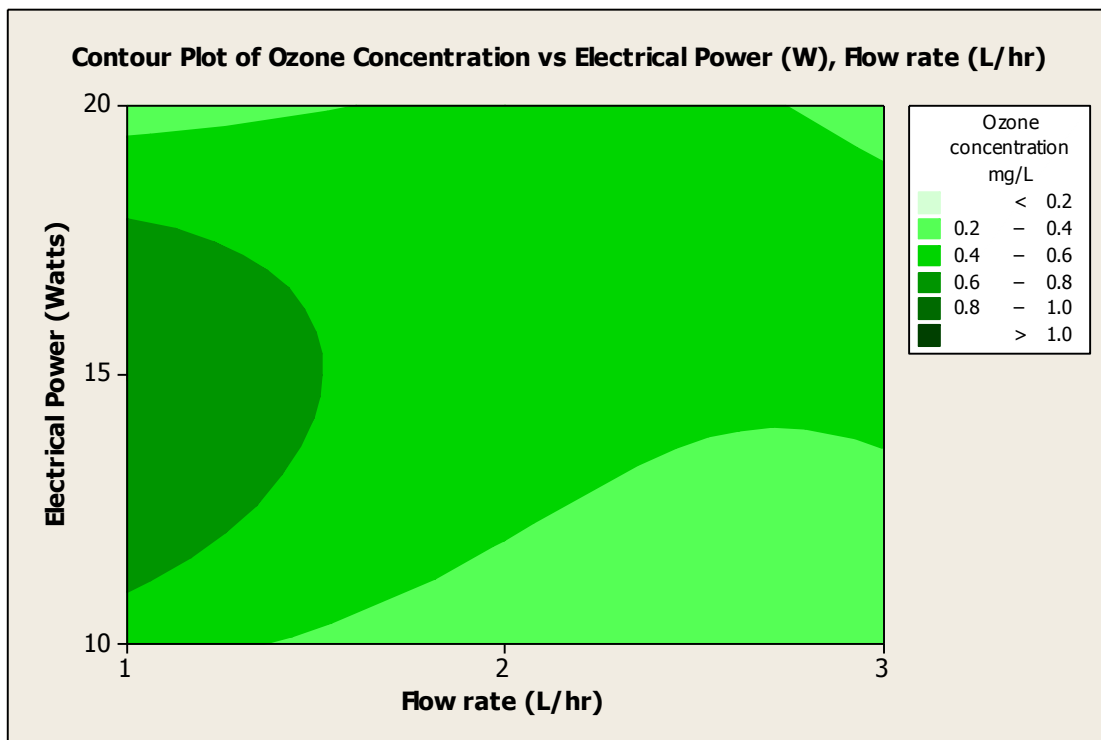
Figure 6.15 - Contour plot of showing the interaction of ozone concentration, electrical power and flow rate

When considering the interaction plot for flow rate and electrical power, Figure 6.14, it can be observed that the combination of these factors that produces the highest absorbance (ozone concentration) is when the system is run using 15 W electrical power and a low flow rate, 1L/hr. The resulting concentration was 0.784mg/L (average over three readings, standard deviation 0.111).

The system was run at this setting throughout the subsequent experiments to ensure that the optimum concentration of ozone was being generated and to avoid problems of ozone decomposition at high temperatures cause by the higher power settings. The output was taken as an approximation as it has been reported that ozone generators do not necessarily give consistent ozone concentration outputs [194].

6.5.4 *UV detection of hydrogen peroxide*

Method

Aqueous solutions of hydrogen peroxide (8mM and 16mM) were tested on the Jenway 6705 UV Spectrophotometer against a baseline of deionised water. A hydrogen peroxide standard curve was constructed using a range of hydrogen peroxide concentrations from 0 – 10mM. The absorbance measurements were taken using a scanning mode across wavelengths 190-700nm.

Results and discussion

During the initial testing of the ozone generator, when attempting to achieve aqueous solutions of ozone using the ozone bubbler, a peak was observed at around 222nm. This was tested on two different bench top UV spectrophotometers as well as with a UV probe. All machines were in agreement that the peak at 258nm was not present, but that a peak at 200nm, 217nm and 222nm was observed depending on the machine used. After consulting the literature about the decomposition products of ozone, it was hypothesised that this peak indicated the presence of hydrogen peroxide (H_2O_2), a decomposition product of ozone. This was investigated further by considering the absorbance of solutions of hydrogen peroxide attained by scanning across the wavelengths 190-300nm to see if the peaks corresponded to that observed in the ozonized water. Figure 6.16 shows the absorbance of the ozonized water sample along with two different concentrations of aqueous hydrogen peroxide. The peaks occur at the same wavelength and it was therefore concluded that hydrogen peroxide was being formed from the decomposition of ozone in water.

The formation of hydrogen peroxide as a decay product has implications for the stability of pharmaceuticals. Hydrogen peroxide like ozone is an oxidising agent that could react with, and cause changes to the structures of the API. Hydrogen peroxide has a high oxidation potential of 1.78V, which is only slightly lower than that of ozone, 2.07V [201].
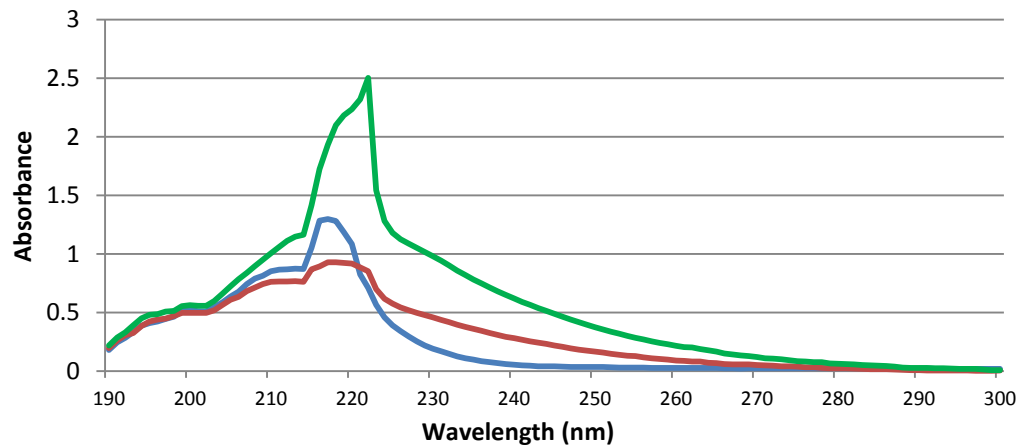
Figure 6.16 - UV spectrum of hydrogen peroxide

(— ozonated water sample, — 8mM H_2O_2, — 16mM H_2O_2)

The observation that hydrogen peroxide formed through ozone decomposition gives a distinct peak at 217nm provides another potential method for indirect ozone detection. The detection of hydrogen peroxide in vials containing only deionised water was therefore proposed as a method for indirect ozone detection, as the presence of hydrogen peroxide in sealed vials could only come from the decomposition of ozone.

A standard curve for hydrogen peroxide was created and the relationship between hydrogen peroxide concentration and UV absorbance at 217nm was found to be linear in the concentration range 0 – 10mM, which is shown in the standard curve in Figure 6.17. This data was then available to determine hydrogen peroxide concentrations from unknown samples, should hydrogen peroxide be detected.

$$y = 0.1613x - 0.0336$$
$$R^2 = 0.9937$$
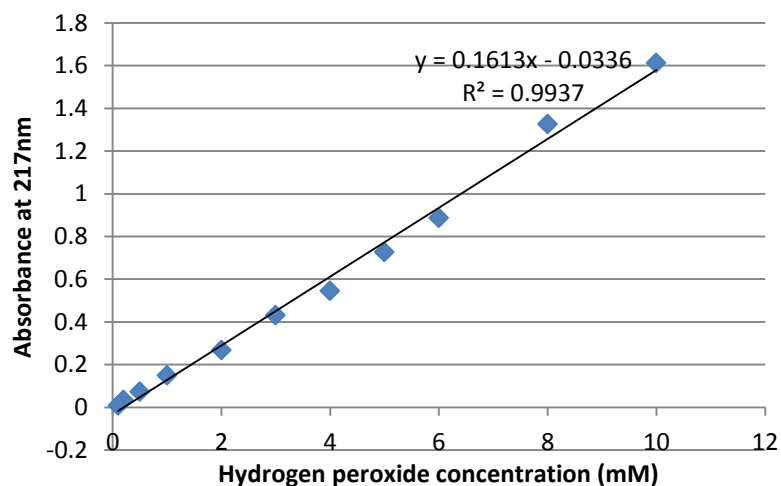
Figure 6.17 - Hydrogen peroxide standard curve

6.5.5   *Indigo method and hydrogen peroxide*

Method

IR1 was made up with distilled water as recommended in the APHA method [174]. To test the effect of hydrogen peroxide on IR1, a stock of IR1 was also made up with 10mM hydrogen peroxide instead of distilled water.

Discussion and results

The APHA method for the measurement of ozone states that hydrogen peroxide and organic peroxides decolourise the indigo reagent slowly, so as long as measurements are taken within 6 hours the measurement should not be affected. However the method also states that organic peroxides may react more rapidly [174]. By replacing the distilled water in IR1 with hydrogen peroxide, this was investigated. The absorbance of IR1, IR1 with hydrogen peroxide and 10mM hydrogen peroxide were scanned across wavelengths 190-700nm and the results are shown in Figure 6.18. IR1 showed an absorbance at 600nm of around 0.04 and IR1 + 10mM H_2O_2 also gave an absorbance of 0.04 at 600nm, showing that no decolourisation of indigo took place at that concentration of hydrogen peroxide. H_2O_2 (green) shows no peak at 600nm that could interfere with measurement of IR1 at 600nm. The peak at around 219nm, Figure 6.19, indicates the presence of hydrogen peroxide in the sample (red) and this corresponds to the peak seen in 10mM hydrogen peroxide (green) in the absence of IR1. The blank sample (blue), IR1 made up with distilled water shows no peak at 219. This confirms that hydrogen peroxide does not cause decolourisation of indigo reagent at these concentrations and that it could be detected at ~219nm in the presence of IR1.
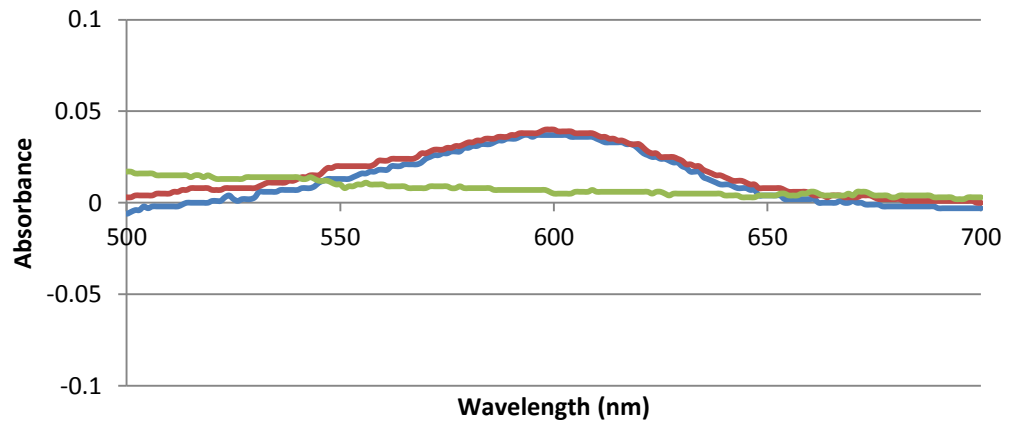
Figure 6.18 - Effect of hydrogen peroxide on Indigo trisulfonate between wavelengths 500-700nm

(— IR1, — IR1 + H_2O_2, — 10mM H_2O_2)
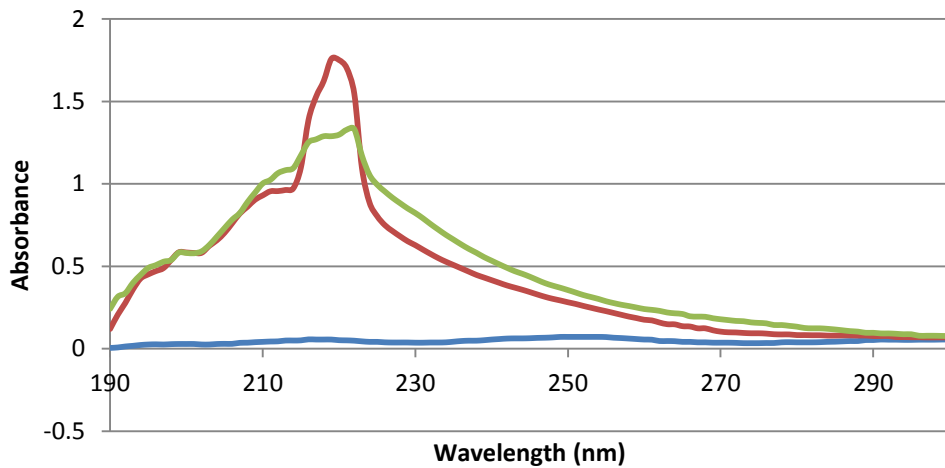
Figure 6.19 - Effect of hydrogen peroxide on Indigo trisulfonate between wavelengths 190-290nm

(— IR1, — IR1 + H_2O_2, — 10mM H_2O_2)

It was proposed to measure any hydrogen peroxide formed in deionised water that had been through the HVLD system. The UV absorbance of the water in the vials could be measured before and after integrity testing on the HVLD. Any increase in hydrogen peroxide would indicate that ozone had been formed in the vial and had decomposed and this could then be correlated to any change in the observed IR1 concentration.

6.5.6 *Difficulties associated with the measurement of ozone - decomposition of ozone - testing the effect of acetic acid on aqueous ozone stabilization*

Method

Ozone was bubbled though 50mL of 1mM acetic acid, 5mM acetic acid and water for 180 seconds with the ozone generator set at 1L/min gas flow and 15 Watts power input. Ozone concentration was determined by the APHA method using Indigo reagent 2 (IR2) and smaller volumes were used compared to the standard method. Instead of total volume of 100mL and sample volume of 90mL, volumes were scaled down to a total volume of 10mL and sample volume of 9mL which are more representative of the volumes that may be encountered in pharmaceutical vials later in this research.

Results and discussion

A report by Sehested *et al* [202] showed that the decomposition of ozone in water could be stabilised using acetic acid. He found that 0.1mM acetic acid significantly reduced the decay rate of ozone in aqueous solutions and 5mM almost completely quenched the chain destruction. The initial decomposition rate for a 100-200 μM ozone solution was 10-15 times lower than the initial rate without acetic acid. This was tested experimentally in this research but the same results were not replicable. Figure 6.20 shows the decomposition of ozone in water, 1mM and 5mM acetic acid and it appears that the decomposition of ozone was greater in the acetic acid solutions than in the water itself.
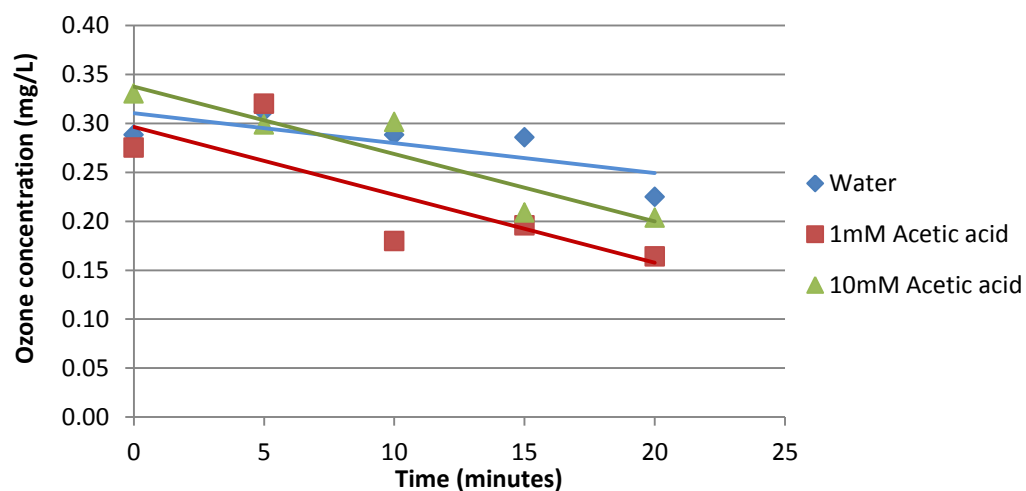
Figure 6.20 - Ozone decomposition in water, 1mM and 10mM acetic acid

Due high variability seen in the results shown in Figure 6.20 and when considering the previous difficulties in measuring ozone in water directly at 258nm, it was decided that measurement of ozone in water and investigating the stabilisation of ozone was not an appropriate method to take forward and that an indirect method, that utilising PIT, which more quickly captured ozone before it decayed would be more appropriate. The PIT method was then further investigated to understand its limitations.

6.5.7   *Applicability of the method proposed by Chiou et al [195]*

The method for measuring ozone concentration proposed by Chiou *et al* [195] was investigated to assess its applicability for testing. The method proposes initially drawing Indigo solution into the gas tight syringe and then drawing up the gas or liquid sample, allowing this to react and then measuring the UV absorbance at 600nm of the sample.

This method was found to be unsuitable for the intended application due to the fact that drawing up liquids or gas from the headspace into the gas tight syringe was time consuming and therefore the measurements were slow to perform. This would make it difficult to be able to perform testing on a high number of samples in quick succession. In addition to this, with regard to the proposed protocol, measurements could not be performed on site at GSK due to material handling restrictions and safety concerns. Consequently the samples needed to be tested as soon as possible on return to Newcastle University to reduce error and the breakdown of ozone that may have occurred before measurement. If vials containing water were passed through the high voltage leak detection (HVLD) instrument and then transported back to the laboratory at Newcastle to be tested via the gas tight syringe approach, the time delay between HVLD and testing would be too long and any ozone generated inside the vial would decompose before testing.

In addition to this, a problem was also identified in the equation reported by Chiou *et al* [195]. An error in the equation resulted in the calculation of concentrations that were negative, and therefore it was not possible to use this equation to calculate the results. This method was therefore discounted.

6.5.8 *Development of an ozone assay based on potassium indigo trisulfonate*

It was established that quartz cuvettes must be used for all UV measurements (section 6.5.1) and that it was not possible to take measurements through the glass vials. It was therefore decided to investigate the American Public Health (APHA) standard method 4500-O3 [174] for the detection of ozone in waste water, an ozone detection method based on the PIT method presented by Bader and Hoigné [182] that uses quartz cuvettes in the measurement of absorbance. The benefit of using PIT solution over measuring the UV absorbance of ozone at 258nm is that the reaction of ozone with PIT occurs very rapidly and hence captures the concentration of ozone at a certain point in time. If ozone was measured directly at 258nm, the ozone concentration may fall between sampling and measurement as it has been reported that ozone is unstable in solution [190] and this has also been found in this study, with the presence of hydrogen peroxide (produced from the breakdown of ozone) being detected.

60 mL vials were filled with a low volume, as this provided a large headspace thereby maximising the potential oxygen available for conversion to ozone under high voltage. It was decided that into each 60mL vial, 12mL of indigo reagent 1 (IR1) (named in APHA method) [174] would be added to provide enough volume of IR1 for triplicate samples to be taken for the measurement of UV absorbance, before and after putting it through the HVLD machine, whilst also leaving a large headspace in which ozone could potentially be produced during the process. There was some uncertainty surrounding the potential success of the method, as the possible conversion rate (if any) of oxygen to ozone in the vial headspace was unknown, and expected to be low when considering Table 6-3.

The initial experiment sought to investigate whether ozone purged into the headspace of the vial would transfer into the liquid phase and react with the IR1 and cause a change in absorbance.

Method for testing the effect of headspace purging time with ozone on the absorbance of Indigo reagent

A 60mL vial was filled with 12mL Indigo reagent 1 (IR1) and the headspace was purged with ozone/air mixture for 60, 120, 180, 240 seconds. The vials were then capped and crimped. UV absorbance was then measured in triplicate at 600nm.

Results and discussion

Preliminary experiments in the laboratory setting confirmed that purging of the headspace above the IR1 with ozone/air mixture allowed ozone to transfer into the liquid phase and react with IR1, causing the absorbance to decrease when compared to a blank sample of unreacted IR, shown in Figure 6.21. The absorbance of IR1 before purging was 0.400 and this fell to 0.333 after a 60 second purge with air/ozone mixture, 0.328 after 120 seconds, 0.290 after 180 seconds and 0.291 after 240 seconds.
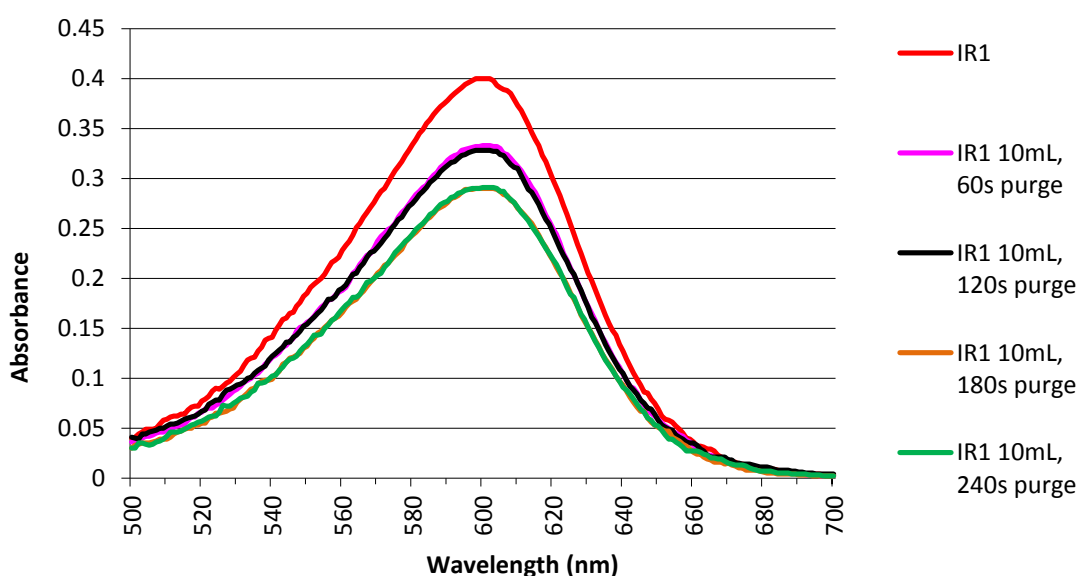
Figure 6.21 - Change in absorbance of Indigo with ozone headspace purging time

6.5.9 *Proposed protocol for testing vials undergoing HVLD*

Before testing vials containing IR1 on the HVLD, it was first necessary to investigate the potential influence of a number of parameters of the proposed testing protocol on the results. The proposed protocol involved filling vials with IR1 at Newcastle University, transporting these to the site (approximately 60 minutes), running them through the HVLD and transporting the vials back to Newcastle University for testing, Figure 6.22. Testing was therefore carried out to investigate the effect of two parts of the proposed protocol: the effect of time on the absorbance of IR1 in sealed vials (protocol parameter 1), the effect of time on the absorbance of IR once reacted with ozone (protocol parameter 2). Other experimental factors were also considered such as instrument error and repeatability of measurements.
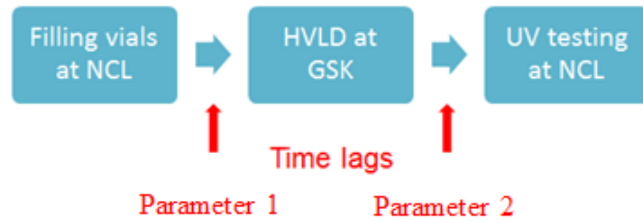
Figure 6.22 - Schematic of testing protocol

The development of a robust method that was able to provide reliable results despite the lag times in measurement before and after HVLD would not only be useful in this particular testing but also if testing were to be carried out on site. If testing were to be carried out on site in the quality control laboratory it is high unlikely that vials would be prepare minutes before they were put through the HVLD, and also unlikely that testing would be carried out as soon as vials came off the HVLD, so it was critical to carry out this investigation into the effects of time lags on measurement reliability.

6.5.10 *Testing of protocol parameter 1 – Effect of time on the absorbance of IR1 in a sealed vial*

Method a) Testing the effect of time (protocol parameter 1) on absorbance of IR1

60 mL vials were rinsed out with distilled water to remove any debris and ensure they were clean. The vials were then rinsed out with IR1 and subsequently filled with 12mL of indigo reagent (IR1). They were capped and crimped and after 2 minutes, the UV absorbance was measured in triplicate. A Jenway 6705 UV spectrophotometer was used in scanning mode, scanning between wavelengths 400-800nm. Samples were removed from the vials via the septum using a 5mL Plastipak syringe with BD Microlance™ needle. The vial was then left for a period of time, after which the absorbance of the IR1 was measured again in triplicate. Time points used were 1, 2, 3, 4, 5 and 6 hours after filling as 6 hours represents the maximum time that would pass between vials being filled and being put through the HVLD. The vials were not protected from light.

Results and discussion

This set of experiments was designed to investigate protocol parameter 1 - the effect of time on the absorbance of IR1 in a sealed vial. The expected ozone concentration

that may be present in the vial headspace after HVLD is very low, with estimates made using the ideal gas equation and theoretical conversion rates, shown in Table 6-3, section 6.1.11. IR1 was the reagent of choice, as it can be used to detect ozone in the lowest concentration range (0.01 – 0.1 mg O_3/L). If this reagent was decolourised in initial tests on the HVLD, the tests could then be repeated using Indigo reagent 2 (IR2), which can be used to test for higher concentration ranges 0.05-0.5 mg O_3/L. Although the theoretical concentrations of ozone appear to be much higher than the concentration range measurable by IR1, the theoretical concentrations are for gaseous calculations, so the ozone gas then must pass into solution and react with IR1. Also, some ozone may decompose quickly and hence not be available to react.

The hypothesis for this scenario i.e. the effect of time on IR1 absorbance in sealed vials, was that there would be no decrease in absorbance of IR1 over time, however the results suggested otherwise. In this case, the absorbance appeared to drop to 86.63% after 3 hours, which is a large drop in a short space of time. The APHA standard method from which this method has been adapted, states that the stock solution should be discarded when its absorbance falls to 80% the original value, which is typically after one week [174]. As this measurement acts as the baseline before HVLD a drop of absorbance of this magnitude between filling the vials and running them through the HVLD would give misleading results i.e. if there was no ozone produced during HVLD, this measurement would lead to a false positive test for ozone, leading to the conclusion that ozone was produced in the headspace. Whereas what was actually the case was that IR1 absorbance dropped before the vials were loaded onto the HVLD machine.
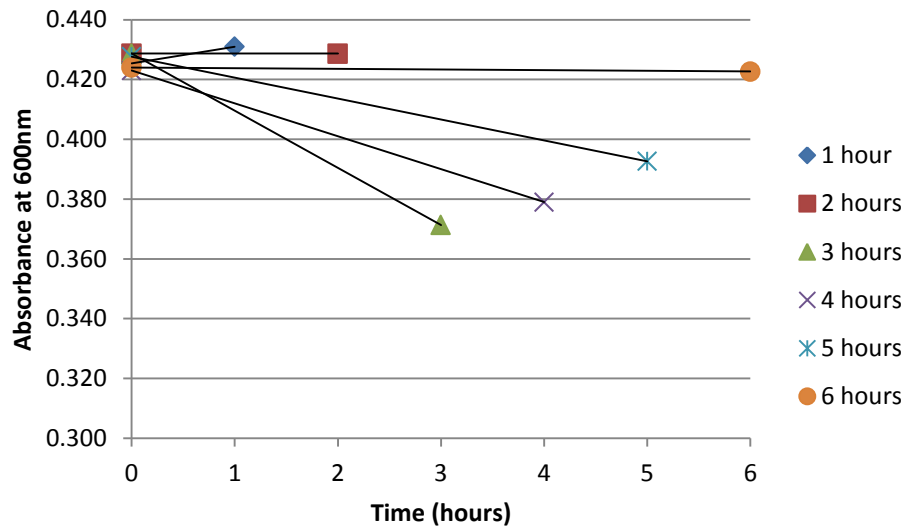
Figure 6.23 - Change in IR1 absorbance at 600nm over time with exposure to light

To obtain the results presented in Figure 6.23, 6 vials were filled with IR1 and were exposed to light. Absorbance was measured at the time of filling and after 1-6 hours. Figure 6.23 shows the change in the absorbance of IR1 at 600nm over residence time in the vial, it is clear that the absorbance dropped after 3, 4 and 5 hours, but appeared to remain similar to the initial absorbance after 6 hours, for which there was no clear explanation. After 1 hour in the vial, the mean absorbance at 600nm had risen slightly, and after 2 hours it had remained the same. It was necessary to have a window of at least 3 hours between filling the vial with IR1 and subjecting the vials to HVLD, to enable the transportation to the site. These results were therefore not satisfactory and this experiment was repeated to further investigate the reason behind the drop in absorbance.
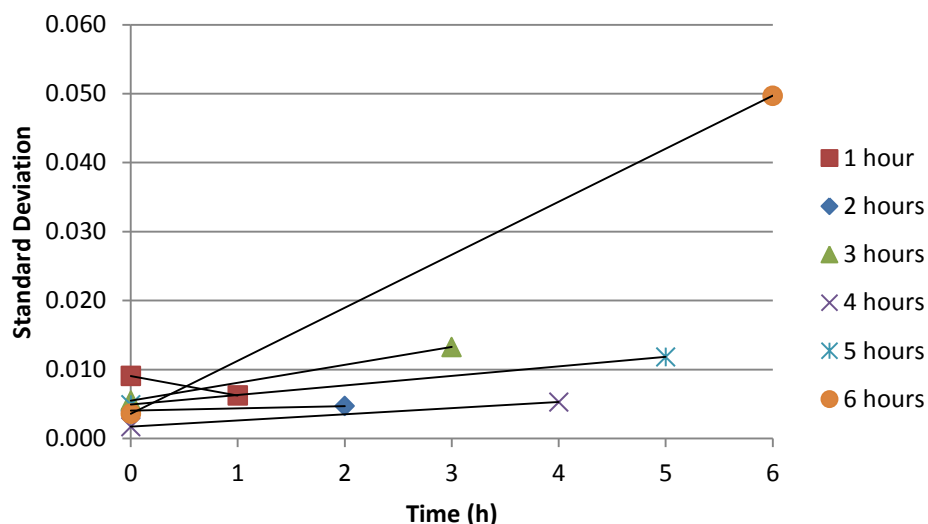
Figure 6.24 - Change in standard deviation over time with exposure to light

When considering Figure 6.24 which shows the standard deviation of the triplicate measurements at each time point, it is clear that the standard deviation increases after 3, 4, 5 and 6 hours. With a marked difference between the standard deviation at 6 hours compared to the other results. This was due to one of the readings at 6 hours being an outlier.

The reagent that was used, IR1, should be replaced when its absorbance drops to 80% of its initial absorbance. Considering the percentage drop in absorbance between the initial reading for each sample and the readings after the relative times had elapsed, shows the impact of time on IR1 absorbance. Figure 6.25 shows the percentage drop in absorbance between the initial absorbance of the sample at time 0 hours and the respective time for each sample. After 1 hour there was an increase in absorbance of 1.4%, after 2 hours there had been no drop in absorbance, however after 3 hours, the drop in absorbance was 13.37%, which appeared to be high considering that over 1 week it could be expected that the stock solution would decrease by 20%. After 4, 5 and 6 hours, the percentage drop was 10.4%, 8.18%, 0.31% respectively.

A drop in absorbance of this magnitude after the vials have been filled and before they have been passed through the HVLD to test for ozone, would mean that the final results could be misleading and that a drop in absorbance which may be attributed to ozone formation, could in fact be a decrease in absorbance of the IR1 itself. These issues could be addressed by transporting the stock solution to site and filling the vials

on site, to minimise the delay between filling vials and taking absorbance readings, however this poses more problems in terms of material transfer. Bringing sealed vials onto the site is safe, whereas filling vials on site would require significant risk assessment and also access to a laboratory on site which was not possible.
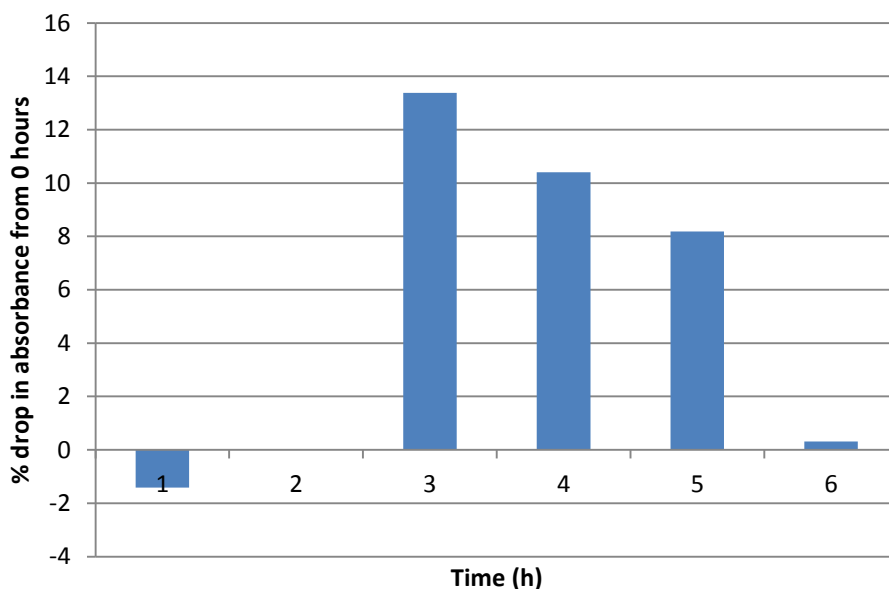
Figure 6.25 - % drop in absorbance between time 0 and time x with exposure to light

This test was repeated to investigate the effect of excluding light and whether this would mitigate the decrease in absorbance. It was hypothesised that the exclusion of light may help stabilise the IR1, despite the literature stating that IR is stable to UV light. In this case, a low volume of IR1 was used and this may have made it more susceptible to UV degradation.

Method b) Testing the effect of time on the absorbance of IR1 in a sealed vial with the exclusion of light (protocol parameter 1)

This method was the same as that in the previous experiment (method a), with the exception that light was excluded by covering the vials in aluminium foil.

Results and discussion

The results of this investigation showed that even by excluding the effect of light, a drop in absorbance still occurred after 4, 5 and 6 hours, Figure 6.26, however, the results from 1, 2 and 3 hours are questionable, as they show an increase in

absorbance. It is not technically possible for an increase in absorbance to occur in the IR1, and this could therefore be attributable to instrument error, unclear cuvettes, or the effect of bubbles on the measurement.
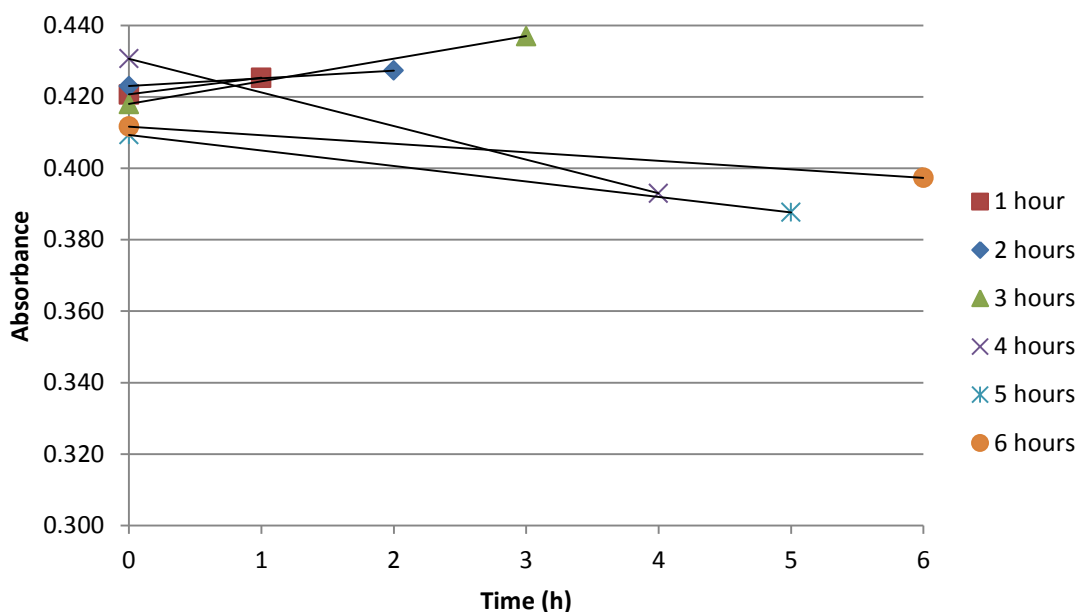
Figure 6.26 - Change in absorbance of IR1 with time with exclusion of light

The boxplot in Figure 6.27 shows the mean and range of absorbance measurements of the baseline (0 hours) compared to after 1-6 hours. The results were combined from all of the time points from 1-6 hours to see the overall effect of introducing a time delay before testing. Results for those vials exposed to light are shown alongside those non-exposed vials.

It can be concluded that the range of absorbance values measured at time 0 hours was much narrower than the absorbance values after a time lag of between 1-6 hours when samples were exposed to light. The mean absorbance value dropped after exposure to light. When light was excluded, the absorbance values measured after 1-6 hours had a narrower range when compared to the range of the exposed measurements. The mean absorbance at the baseline (0.426) compared to the results after 1-6 hours (0.404) for exposed samples showed a drop in absorbance.

The mean absorbance at the baseline (0.419) compared to the results after 1-6 hours (0.411) for non-exposed samples showed a smaller drop in absorbance than in the

exposed samples which suggests that the exclusion of light was a positive measure in terms of reducing the impact of the IR1 absorbance differences over time.
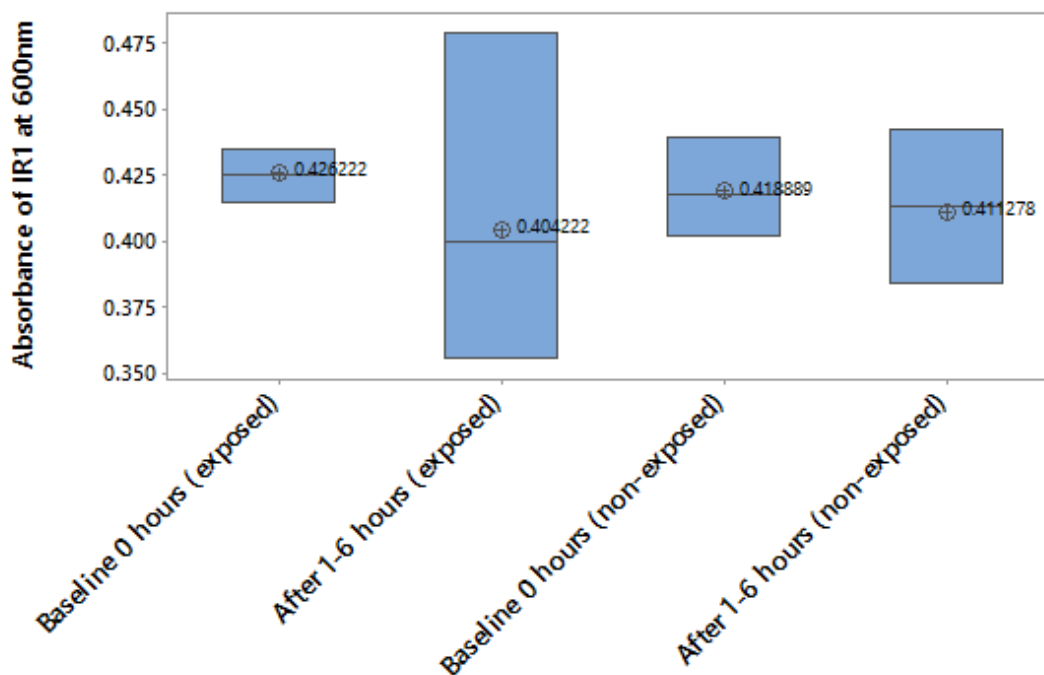
Figure 6.27 – Boxplot showing the means and range of absorbance of IR1 before and after lag-time for exposed and non-exposed samples

What was important was that the range of the data from the experiments not exposed to light, from the time points after filling, is similar to that at time 0 hours and the means are almost identical. The range of absorbance of IR1 measured as a baseline and across the time points is summarised in Table 6-7.

	Absorbance range at time zero	Absorbance range across time points 1-6 hours	Absorbance range across all measurements
Light	0.006	0.060	0.060
Dark	0.021	0.021	0.021

Table 6-7 - Range of absorbance in exposed and non-exposed samples

The replicates for both the samples exposed to light and those protected from light from time point 0 hours and the collated time points were tested for significance with a 95% confidence interval, 2 sample t-test. The samples exposed to light showed a significant difference in absorbance between the 0 hours and the collated time points (p=0.008), whereas the samples stored in the dark did not exhibit a significant difference between the two sets of data (p=0.161). These results show that the effect of light on the absorbance of IR1 was statistically significant and that it appeared to

have a detrimental effect on the absorbance of IR1. When testing the data from each time point for significant differences in absorbance between time 0 and a specific time point, significant differences were found between the results at 0-3, 0-4 and 0-5 hours for both exposed and non-exposed samples, the p values for these tests are summarised in Table 6-8.

Time lag (hours)	P value (exposed)	P value (non-exposed)
0-1	0.439	0.50
0-2	1.00	0.307
0-3	0.020*	0.016*
0-4	0.005*	0.012*
0-5	0.042*	0.007*
0-6	0.967	0.161

Table 6-8 - Statistical difference in absorbance of exposed and non-exposed samples after time lag *indicated statistically significant differences

The effect of light exposure has been considered throughout the analysis of the results of these experiments, however, when considering the method that was followed and the expectation that IR should not drop to below 80% of its initial absorbance within one week, it was expected that the effect of light over this timeframe of 6 hours would not have such a significant effect. The other possibility for the observed changes in absorbance was baseline drift of the UV spectrophotometer over time, which was subsequently investigated.

A set of experiments was performed to test the repeatability between vials at the same time point (inter-vial) and the repeatability of samples from one vial (intra-vial) at each time point, with the objective of investigating whether the changes in absorbance in the previous experimental procedure were a result of baseline drift.

Method c) Testing inter- and intra- vial repeatability and the effect of UV spectrometer baseline drift (protocol parameter 1)

60mL vials were filled according to the method described in method a), section 6.5.10. Three measurements of IR1 stock solution were made, to determine the repeatability of the stock solution. Three vials for each time point were then investigated and the absorbance was measured after 2 minutes in triplicate and after the final time point. The UV machine was base lined with water before each set of three measurements on each vial.

Results and Discussion

The results of this experiment gave 9 absorbance measurements across 3 vials, i.e. 3 replicates for each time point. As the initial absorbance of IR1 in each vial may have differed, the initial absorbance was subtracted from the absorbance from each time point to see the real change in absorbance. Figure 6.28 shows the results from this experiment. Theoretically the absorbance change in each vial would be zero however there may be instrumental error and the aim of this experiment was to uncover this. There appears to be one outlying result in the data from 3 hours, however, despite this result, the data lies around the zero line, with a narrow range.
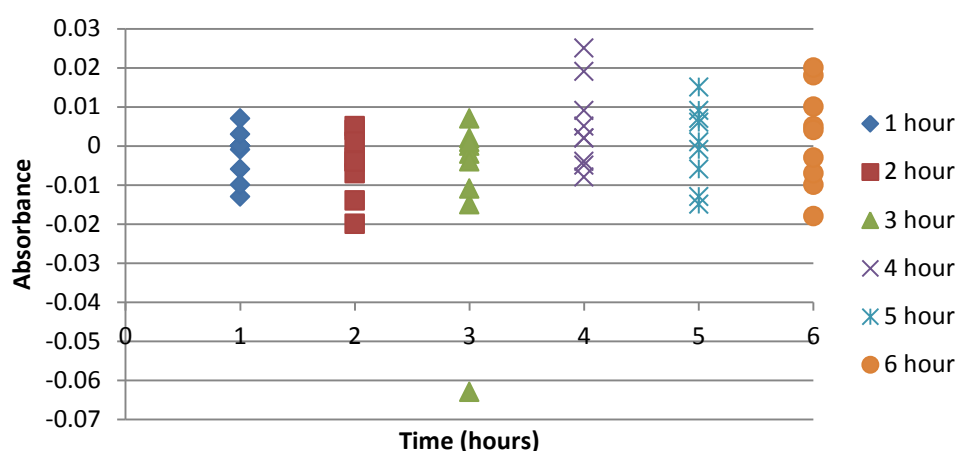
Figure 6.28 - Change in absorbance between time zero and measurement time for all vials

When considering the change in mean absorbance as shown in Figure 6.29, a negative change in absorbance is observed over the first three hours, after 4, 5 and 6 hours, the absorbance change is positive. It is theoretically not possible for the absorbance to increase, as the concentration of IR1 cannot increase, so this positive change in absorbance was attributed to instrument error. The overall trend in absorbance is increasing over time, which again is not possible, so the error seen in the data was attributable to instrumental error.
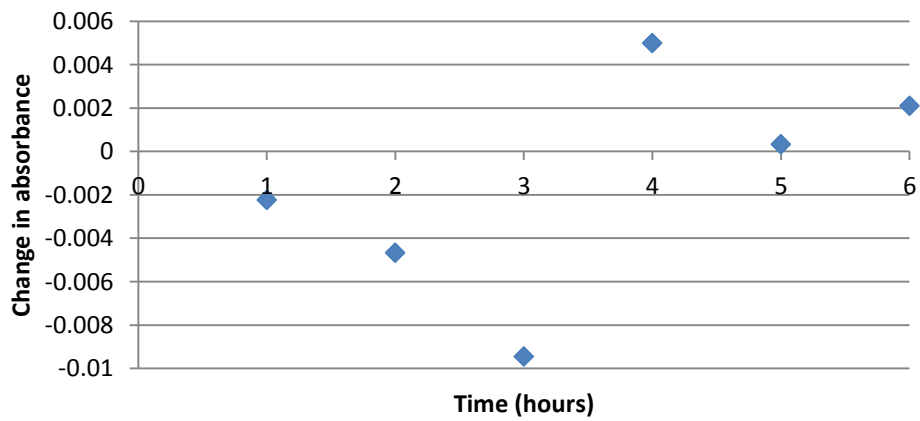
Figure 6.29 - Change in mean absorbance between time zero and 1-6 hours

The range of absorbance values across all vials at point zero and across all vials at other time points is summarised in Table 6-9. The range for measurements after time, was less than for the measurements at time point zero, and the range across all measurements was approximately the same as the range at time zero, suggesting that there was no significant effect of time on absorbance.

Sample	Range
Time zero all vials	0.074
Time x all vials	0.034
All time points (zero and x)	0.075

Table 6-9 - Range of absorbance measurements across all vials at point zero and at other time points

The results from absorbance measurements after filling vials were compared and no statistically significant differences were found, which can be observed through the p values in Table 6-10.

Vials	P value
1 hr 2 min, 2 hr 2 min	0.977
1 hr 2 min, 3hr 2 min	0.395
1 hr 2 min, 4 hr 2 min	0.853
1 hr 2 min, 5 hr 2 min	0.959
1 hr 2 min, 6 hr 2 mi	0.975
2 hr 2 min, 3hr 2 min	0.403
2 hr 2 min, 4 hr 2 min	0.873
2 hr 2 min, 5 hr 2 min	0.980
2 hr 2 min, 6 hr 2 min	1.000
3hr 2 min, 4 hr 2 min	0.479
3hr 2 min, 5 hr 2 min	0.423
3hr 2 min, 6 hr 2 min	0.399
4 hr 2 min, 5 hr 2 min	0.899
4 hr 2 min, 6 hr 2 min	0.868
5 hr 2 min, 6 hr 2 min	0.979

Table 6-10 - p values from 2-sample t-test of UV absorbance at 600nm of IR1 in vials at time zero

Statistical testing of the absorbance of PIT in each vial at time point zero and the individual time points was tested using a 2-sample t-test to determine if the

differences were statistically significant between the absorbance before and after the time lag. The p-values for each vial are summarised in Table 6-11. Only one vial out of the 18 vials tested showed a statistically significant drop in absorbance (p value = 0.024), the other two vials tested at the same time point did not show a statistically significant drop in absorbance (p-values = 0.0553 and 0.260), so this did not cause concern. This significant drop could however have been caused by more vigorous shaking, so this highlighted that a very thorough process was required to ensure certain vials were not shaken more than others. In the real testing scenario presented in Chapter 7, each vial was shaken whilst rolling through the machine, but there was an element of transfer back to the in-feed of the machine, where shaking could only be controlled by a certain amount, through careful handling.

Vials	P value
Vial 1 time zero vs 1 hours	0.384
Vial 2 time zero vs 1 hr	0.304
Vial 3 time zero vs 1 hr	1.000
Vial 1 time zero vs 2 hr	0.024
Vial 2 time zero vs 2 hr	0.553
Vial 3 time zero vs 2 hr	0.260
Vial 1 time zero vs 3 hr	0.541
Vial 2 time zero vs 3 hr	0.923
Vial 3 time zero vs 3 hr	0.372
Vial 1 time zero vs 4 hr	0.412
Vial 2 time zero vs 4 hr	0.509
Vial 3 time zero vs 4 hr	0.066
Vial 1 time zero vs 5 hr	0.789
Vial 2 time zero vs 5 hr	0.512
Vial 3 time zero vs 5 hr	0.085
Vial 1 time zero vs 6 hr	0.124
Vial 2 time zero vs 6 hr	0.516
Vial 3 time zero vs 6 hr	0.235

Table 6-11 - P values from 2-sample t-test of UV absorbance at 600nm of IR1 at time 0 vs absorbance at time X

6.5.11 *Testing of protocol parameter 2 – the effect of time on the stability of IR1 in a sealed vial after exposure to ozone*

A set of experiments were performed to understand the effect of protocol parameter 2 – the effect of time on absorbance of IR1 after exposure to ozone. The APHA method [174] states that hydrogen peroxide and other organic peroxide do not interfere with

the method if ozone is measured less than 6 hours after the addition of reagents. Additionally the APHA standard method [174] recommends that solutions that have been in contact with ozone are measured within 4 hours of being reacted, however this is problematic for this particular scenario due to the experimental requirements of transporting samples from the site. A measurement window of 6 hours was investigated, as this was the maximum time that would be required for transport and testing of the vials after they had been subject to HVLD.

Method a) - testing the effect of lag time on measurement repeatability for IR1 after exposure to ozone (protocol parameter 2)

The absorbance of a stock solution of IR1 was measured and vials were then filled with 12mL IR1 and purged with ozone/air mixture. Based on the design of experiments results for the ozone generator output, the settings that were chosen were low flow rate 1L/min and medium wattage, 15W. This gave an approximate ozone concentration in the ozone/air mixture of 0.785mg/L. The vial headspaces were purged for 10 seconds, to allow for three times the headspace volume to pass through the vial, thereby replacing the air headspace with the air/ozone headspace. The vial was then crimped and capped, covered in aluminium foil and inverted 3 times to mix the IR1 and headspace (this occurs on the HVLD machine as the vials are rolled along the rollers when leaving the machine).

The absorbance of IR1 was measured 2 minutes after purging to determine whether an initial decolourisation of IR1 had occurred and it was determined again after each specific time point (1, 2, 3, 4, 5, and 6 hours) to determine the window for measurement. Measurements were taken in triplicate at each time point and a mean absorbance calculated.

Results and discussion

The headspace of vials containing indigo reagent were purged and after 2 minutes the IR1 absorbance was measured and had not dropped significantly however, after covering the vial with aluminium foil and waiting until the final time point (2, 3, 4, 5 or 6 hours), the IR1 had been almost completely decolourised in all vials, Figure 6.30.
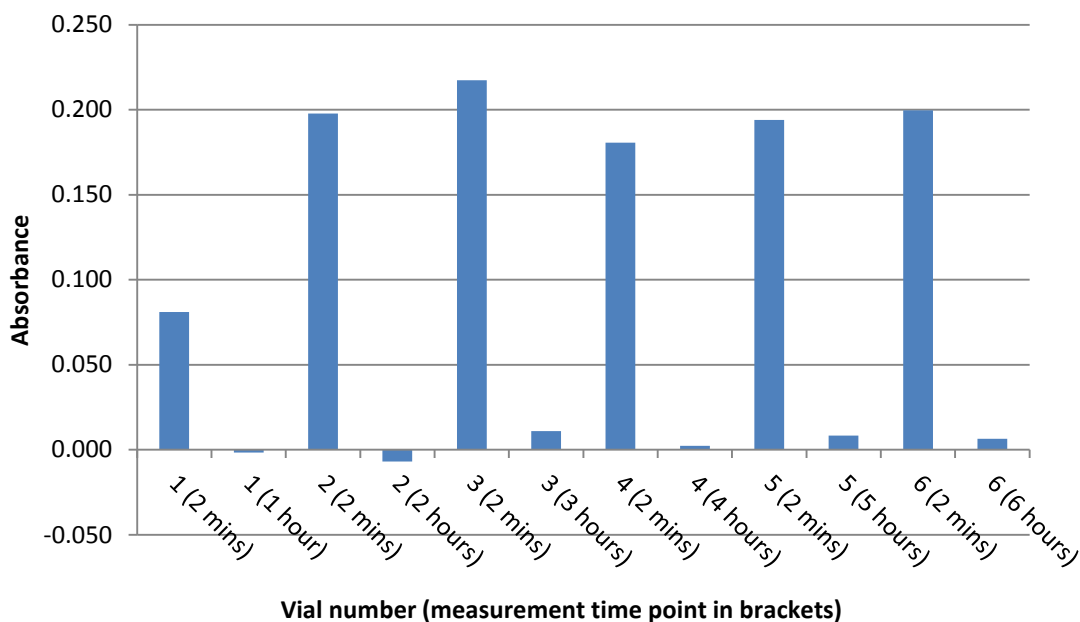
Figure 6.30 - Drop in IR1 absorbance over time (after 10 second ozone purge)

This suggested that the initial ozone dose produced by the purge was too high, as the aim was not to totally decolourise the IR1, therefore the experiment was repeated with a reduced ozone loading dose, in order to decolourise the IR1 only partially to investigate the stability of the reacted IR1 over time. To be able to test the stability of IR1 once it has been reacted with ozone, it was necessary to subject the IR1 to an amount of ozone that did not totally decolourise it. The ozone loading dose was reduced by shortening the purge time to lower the concentration of ozone in the headspace of the vial.

Method b) - determining a suitable purge time and fill volume to investigate the effect of lag time on measurement repeatability for IR1 after exposure to ozone (protocol parameter 2)

In order to determine the volume of ozone required to retain some absorbance of IR1, a series of vials were filled with increasing volumes of IR1 and the headspaces were subjected to a 1 second purge with ozone/air mixture. Although this method appears crude, it was sufficient for the testing required.

Vials were filled with 12, 16, 20, 24, 28, 32, 36, 40, 44, 48mL IR1, with 12mL representing the minimum volume required for testing and 48mL representing the maximum fill volume above which there would be insufficient headspace. An ozone/air mixture was introduced into the vials for 1 second, at a flow rate of 1L/min and an

electrical power of 15W. After the ozone/air introduction, the vials were capped and crimped, and then vigorously shaken 3 times over a period of 1 minute and after 2 minutes the absorbance was measured. Vials were shaken to ensure that the ozone/air mixture was able to thoroughly react with the IR1 thus causing the maximum change in absorbance.

Results and discussion

Figure 6.31 shows that fill volumes between 12mL and 28mL saw a drop in IR1 absorbance to near zero. When the fill volume was increased to 32mL, a low level of IR1 absorbance was retained after the reaction with the ozone/air mixture and this increased as the fill volume increased to 48mL, Figure 6.31. At a fill volume of 48mL and with a 1 second purge of air/ozone mixture, the absorbance remained at 61% of the absorbance of the blank, so this fill volume was chosen to be used in the next set of experiments to investigate whether the absorbance changed over time after reacting IR with the air/ozone mixture and capping and crimping the vial. This was carried out to establish whether there would be any detrimental effect on the absorbance measurements taken after transporting the vials back to Newcastle University (protocol parameter 2, Figure 6.22).
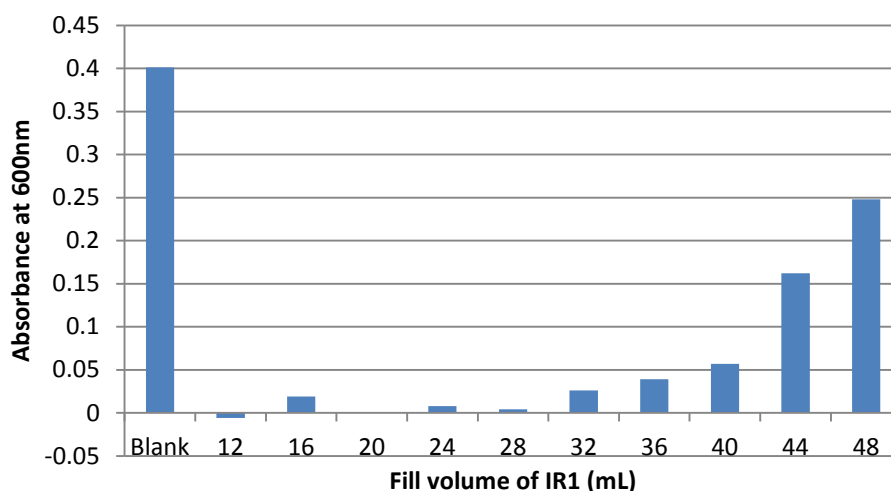
Figure 6.31 - Effect of fill volume on IR1 absorbance after treatment with ozone/air

Method c) - testing the effect of lag time on measurement repeatability for IR1 after exposure to ozone (protocol parameter 2) – revised method

6 vials were filled with 48mL of IR1. Each vial was purged for 1 second with air/ozone mixture, crimped and capped and subsequently shaken 3 times over a period of 1 minute. Absorbance was measured after 2 minutes and again after time points: 1, 2, 3, 4, 5 and 6 hours.

Results and discussion

The bar chart, Figure 6.32, shows the effect of time on the absorbance of IR1 after ozonizing vials containing 48mL of IR1. The absorbance was measured 2 minutes after the reaction with ozone and then again after the specified time point. The bar chart also shows the mean of the initial three repeat measurements of the IR1 stock solution.
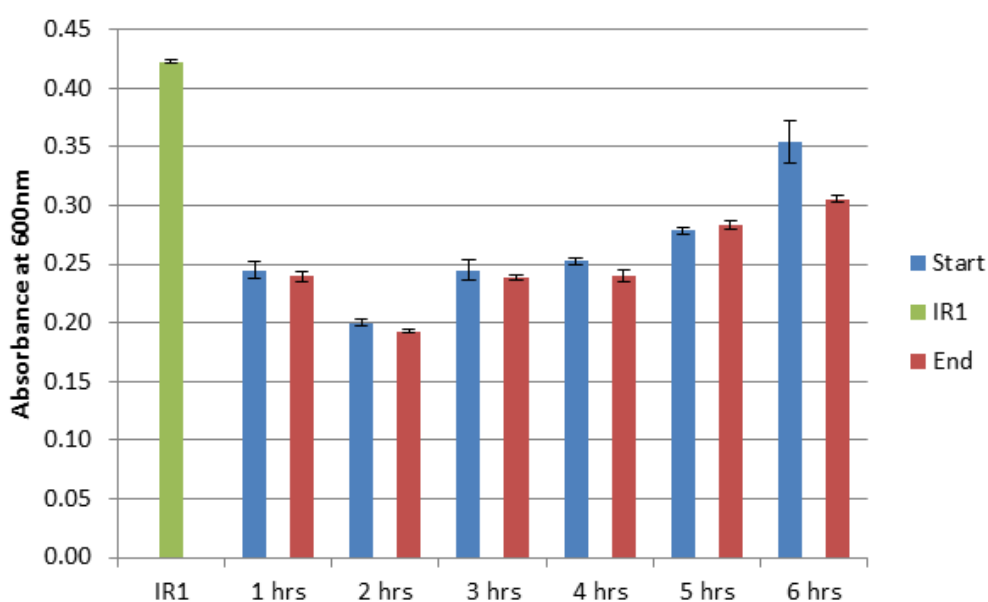
Figure 6.32 - Change in absorbance of IR1 over time (after ozonation)
Error bars represent standard error of the mean

It is evident that there was very little difference between the start and end absorbance values for the IR1 across all time points, with the exception of the sample that was measured after 6 hrs where the difference was more pronounced. There appeared to be a greater change in absorbance in this sample, however when considering the error bar of the absorbance measured after 2 minutes, shown in Figure 6.32, then it is possible to appreciate why there appears to be a marked difference between the start and end readings after 6 hours. This may require further investigation, however if the

time between vials being run through the HVLD and UV testing is kept to below 5hrs then this should not pose a problem.

Also, if the experiment were to be repeated, then it might be possible to change the initial measurement time point to 5 minutes, to give the ozone/indigo time to react fully. Another factor in this experiment that may have given rise to the results at 6 hours was that the vials were shaken after the introduction of ozone, and it maybe have been the case that the shaking effect was not uniform across the 6 vials and hence the vial at 6 hours may have received less shaking which meant that its initial reading was higher than it may have been with more shaking. This would result in ozone reacting with indigo over the time period and causing the absorbance to drop further after the initial measurement. In addition to this, measurement of the absorbance of the IR1 in each vial before ozonation, would give a more accurate result in the actual testing on the HVLD, as this would give a more accurate starting point to compare the results from after passing through the HVLD.

6.6   Conclusions and recommended testing protocol

The Indigo method was the method of choice after considering several methods presented in the literature. After analysing the results from the exposed and non-exposed experiments and contrasting these to the experiment performed with 3 vials at each time point, it was concluded that UV spectrometer baseline drift played a role in the decrease in absorbance in the previous experiments in section 6.5.10. The practice of taking a baseline with water, and washing the cuvette out with IR1 before each set of three repeat measurements gave more accurate results than those attained by taking a baseline and using this for the whole set of UV measurements, as this made the measurements prone to baseline drift. The exclusion of light did appear to make a difference to the results obtained in the first two experiments however, the effect of light could have been masked by baseline drift. However as this measure is easily practicable through individual wrapping of vials in foil or storage in a sealed box, this was employed to mitigate against potential error.

There was no significant difference in the absorbance readings across the 18 vials at time zero as shown by the results in Table 6-10, so rather than fill each vial separately and take a reading before passing through the HVLD machine, it would be sufficient to

measure the absorbance of the stock solution in triplicate and then fill the vials and transport them to the site to proceed with passing these through the HVLD rather than testing the starting point of each vial individually. However if each vial was measured separately then the error could be accounted for, for each vial. Piercing the septum to remove samples before HVLD, should not pose a problem for container integrity, as the septum of the vial ensures that after removal of a needle, an airtight seal is maintained. However, it was decided that three repeat UV measurements could be taken of the IR1 after the vial had been filled, but before it had been sealed, in order to avoid piercing the septum.

The literature review and experimental work in this chapter has helped to define a testing protocol for investigating whether ozone is produced in vials undergoing HVLD. The recommended protocol for ozone detection using the modification of the APHA Indigo method [174] is summarised in section 6.6.1 and the testing protocol for ozone detection via the detection of hydrogen peroxide is detailed in 6.6.2.

6.6.1 *Method for detection of ozone in vials subjected to HVLD through measurement of the UV absorbance of PIT*

1) Vials filled with 12mL freshly prepared IR1 at Newcastle University. The UV machine base-lined before each measurement with water and the cuvette was rinsed with IR before measurements taken. Three samples (2mL per sample) removed from the vial with a Plastipak syringe and BD Microfine needle and three UV measurements carried out, to provide a baseline measurement for each vial prior to vial capping and crimping. (2 hours)
2) Vials (containing 6mL IR1) transported to the site in the dark (1 hour)
3) Vials passed through HVLD (2 hours)
4) Vials transported back to Newcastle University (1 hour)
5) UV machine base lined before each measurement with water, cuvette then rinsed with IR before measurements taken. Three UV measurements taken from each vial (2 hours)

   *Steps 1) – 3), should be carried out within a 6 hour timeframe.

   *Steps 3) – 5) should be carried out within a 6 hour timeframe.

6.6.2 *Method for detection of hydrogen peroxide (formed from the decomposition of ozone) in vials subjected to HVLD through the measurement of UV absorbance*

1) Vials filled with 6mL of water, capped and crimped at Newcastle University. Three UV measurements of deionised water taken as a baseline for all vials (base line of air) (1 hour)

2) Vials transported to the site in the dark (1 hour)

3) Vials passed through HVLD (2 hours)

4) Vials transported back to Newcastle University (1 hour)

5) Three UV measurements taken from each vial (UV machine base lined before each measurement with air) (2 hours)

6.7 Future work

Future work involved implementing the methods in section 6.6.1 and 6.6.2 to test whether ozone is produced in vials that are subjected to HVLD, analysing the error of measurement and investigating whether the method was applicable for this testing. This is discussed in Chapter 7.

It would be very useful to make a model high voltage leak detection instrument that could be utilised in the research laboratory setting. This would involve designing a platform which could subject a vial to 20kV, which would then allow the headspaces and liquid contained within the vials to be tested straight after exposure to the HVLD. This would then facilitate the direct detection ozone via UV absorbance as there would be minimal time delay between passing through the model HVLD and being able to carry out UV absorbance measurements in the research and development laboratory. Creating a model HVLD system would also allow pharmaceutical formulations to be tested and then undergo characterisation to detect any degradation products if ozone was produced.

Chapter 7. Testing for ozone production in vials subjected to high voltage leak detection

7.1   Introduction

In the previous chapter the potential of the Indigo method, utilising potassium indigo trisulphonate (PIT), was investigated and a modified approach to the American Public Health Association (APHA) method was tested and identified as being appropriate for use within the constraints of the proposed testing protocol. This chapter utilises the PIT method developed and applies it to the testing of vials that have been passed through the high voltage leak detection (HVLD) machine to determine whether ozone was produced.

7.2   Materials and Methods

Potassium indigo trisulphonate, phosphoric acid and sodium dihydrogen phosphate were purchased from Sigma Aldrich. Borosilicate glass vials were supplied by Amilco. Quartz cuvettes were purchased from NSG Precision Cells, Inc. BD Microlance™ needles and BD disposable 5mL syringes were purchased from Fisher Scientific.

7.2.1   *Method for detection of ozone in vials subjected to HVLD through measurement of the UV absorbance of PIT*

The protocol proposed in 6.6.1 was taken forward to use in the testing:

1) Vials were filled with 12mL freshly prepared IR1 at Newcastle University. The UV machine was base-lined before each measurement with water and the cuvette was rinsed with IR before measurements taken. Three samples (2mL per sample) were removed from the vial with a Plastipak syringe and BD Microfine needle and three UV measurements were carried out, to provide a baseline measurement for each vial prior to vial capping and crimping. (2 hours)

2) Vials (containing 6mL IR1) were transported to the site in the dark (1 hour)

3) Vials passed were through HVLD (2 hours)

4) Vials were transported back to Newcastle University (1 hour)

5) The UV machine was base lined before each measurement with water, cuvette then rinsed with IR before measurements taken. Three UV measurements taken from each vial (2 hours)

*Steps 1) – 3), should be carried out within a 6 hour timeframe.

*Steps 3) – 5) should be carried out within a 6 hour timeframe.

60mL vials were rinsed with distilled water to remove possible debris, dried in an oven and allowed to cool. They were rinsed and filled with 12mL of Indigo reagent 1 (IR1), made according to the APHA method [174]. 6mL was removed for the purpose of performing three replicate UV absorbance measurements (each requiring 2mL) which gave a baseline measurement for each vial and vials were then subsequently capped and crimped by hand using Wheaton E-Z™ 20mm hand operated crimpers. Vials were labelled on the outside wall with a marker pen.

Vials were then transported to the site in the absence of light and passed through the HVLD machine. The numbered vials were passed through the machine in a random order to reduce the time delay in re-ordering the vials for the next pass. This ensured that vials were passed through the HVLD as quickly as possible. Vials were then transported back to Newcastle University and triplicate measurements of absorbance across wavelengths from 400-800nm were performed on each vial containing IR1.

Five test sets of vials were used and each test set was passed through the HVLD a specific number of times, summarised in Table 7-1. The size of the initial test set (test set 1) was chosen to be 20 vials however it was subsequently reduced to 10 vials for test sets 2-5 due to the difficulty of performing all of the required testing within the timeframe of 6 hours as detailed in Chapter 6. Additionally, after the initial testing (test 1 - Table 7-1) time on site was limited so this required the test sets sizes to be reduced.

Test set	Number of Vials (Indigo)	Number of Vials (Water)	Number of passes through HVLD
1	20	20	20
2	10	10	15
3	10	10	10
4	10	10	5
5	10	10	1

Table 7-1 - Testing setup

7.2.2 *Method for detection of hydrogen peroxide (formed from the decomposition of ozone) in vials subjected to HVLD through the measurement of UV absorbance*

The protocol proposed in 6.6.2 was taken to use in the testing:

1) Vials were filled with 6mL of water, capped and crimped at Newcastle University. Three UV measurements of deionised water acted as a baseline for all vials (base line of air) (1 hour)

2) Vials transported to the site in the dark (1 hour)

3) Vials passed through HVLD (2 hours)

4) Vials transported back to Newcastle University (1 hour)

5) Three UV measurements taken from each vial (UV machine base lined before each measurement with air) (2 hours)

60mL vials were rinsed with distilled water to remove possible debris, dried in an oven and allowed to cool. They were rinsed and filled with 6mL of deionised water and vials were then subsequently capped and crimped by hand using Wheaton E-Z™ 20mm hand operated crimpers. Vials were labelled on the outside wall with a marker pen.

As with the vials containing PIT, these vials were transported to the site in the absence of light and passed through the HVLD machine, in a randomised order. The size of the test sets and the number of passes of each vial through the HVLD machine are shown in Table 7-1. After returning to Newcastle University, triplicate measurements of water samples from each vial were taken, across wavelengths 190-300nm.

7.2.3 *Statistical analysis of data*

Paired t-tests were carried out using Minitab 16 Statistical Software to analyse whether any differences existed in the UV measurements before-and-after HVLD. The null hypothesis (H_0) was that there was no difference between the means before and after HVLD. The null hypothesis was rejected at a p-value of <0.05 indicating a 5% significance level.

7.3 Aim

The aims of this research were to test vials undergoing HVLD to ascertain if ozone was produced during this process and at what concentration ozone was produced in the

vial. Further to this goal was to identify and propose any potential improvements to the methodology, identify any potential consequences of the findings and consider steps for mitigation of ozone formation.

7.4 Results and Discussion

7.4.1 *Testing for the presence of ozone in vials using the PIT detection method*

The effect of 20 passes through the HVLD machine on the absorbance of IR1 is shown in Figure 7.1. Error bars representing standard error of the mean show that there was a clear difference between the before and after results. Statistical testing of these results is discussed later in this section.
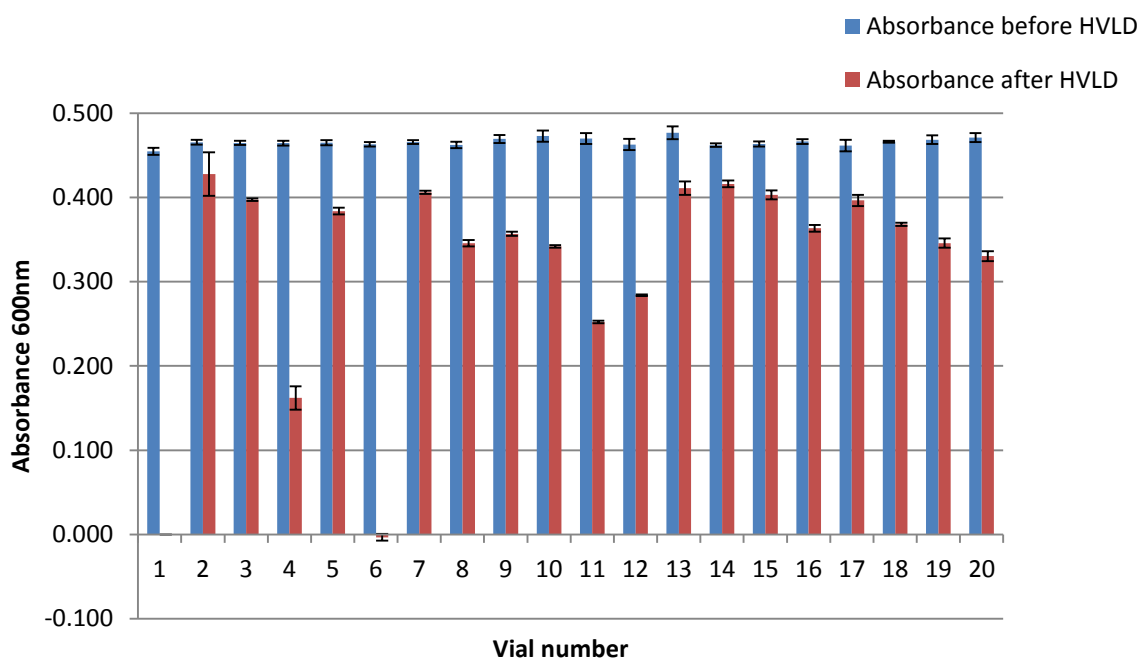
Figure 7.1 - Effect of HVLD on UV absorbance of IR1 at 600nm (worst case scenario)

The absorbance readings taken after HVLD for vial 1 were unavailable due to a data transfer problem. All vials from 2-20 showed a decrease in absorbance of IR1 after HVLD compared to the initial baseline. This indicates that ozone was produced in the vial headspace for this particular fill volume when vials were subjected to 20 passes through the HVLD. The variation in results before HVLD was narrow, which was expected from initial testing in the previous chapter, where it was shown that there were no statistical differences between vials filled from the same solution of IR1. The variation in absorbance after the vials have been put through HVLD was much wider,

however the error bars are very similar to the before HVLD measurements. This suggests that drop in absorbance was caused by the HVLD and not the UV measurement error. There could be a number of reasons for the variation: the HVLD machine affects vials in different ways, however this is unlikely as the voltage applied to the vial is the same for each vial; that the handling between the end of each HVLD pass and the beginning of the next varied between vials and therefore affected the reaction of ozone and PIT through varying degrees of shaking during transit; or the crimping of the vials varied and allowed ozone to penetrate through the stopper and crimp seal, which is unlikely. It was clear to see that immediately after the vials were removed from the HVLD machine that vial 6 was totally decolourised, Figure 7.2, which indicated that the level of ozone produced was higher than the limit of the assay which was 1.0 mg.

Figure 7.2 - Vial 6 (decolourised) and vial 7 (not decolourised)

Whilst carrying out the testing on site at GSK the machine became jammed and the line stopped a number of times. This was due to difficulties with the manual feed of a low number of vials which was unavoidable. The total testing time on site at GSK was predicted to be in the order of 20 minutes however it took approximately 1.5 hours. The time window of 6 hours between filling and passing through the HVLD was therefore exceeded, with the HVLD exposure completed ~9 hours after the start of the initial filling of vials and the time between beginning the HVLD and finishing the measurements of the UV absorbance after HVLD was a maximum of ~7 hours. Therefore a change to the protocol was made to keep within the testing timeframe. The number of vials in each test set was reduced to 10, as this was a parameter that could be controlled and reduced the preparation and testing time for the UV

absorbance measurements, which thus provided some flexibility should any delays in testing on the HVLD occur due to machine jams.

The next step was to investigate the effect of the lower number of passes through the HVLD machine on ozone formation in the vial headspace. Test sets 2-5 were passed through the HVLD and subjected to different numbers of passes, according to Table 7-1. The results are presented in the form of bar graphs to compare the absorbance before and after HVLD for each specific number of passes.

Figure 7.3, Figure 7.4, Figure 7.5 and Figure 7.6 show the results for the different number of passes of vials through the HVLD machine on the absorbance of PIT.

Figure 7.3 highlights clear differences between before and after measurements after 15 passes through the HVLD and in a similar way to the results from 20 passes, more variation is seen in the absorbance of PIT after HVLD, however the error remains similar.
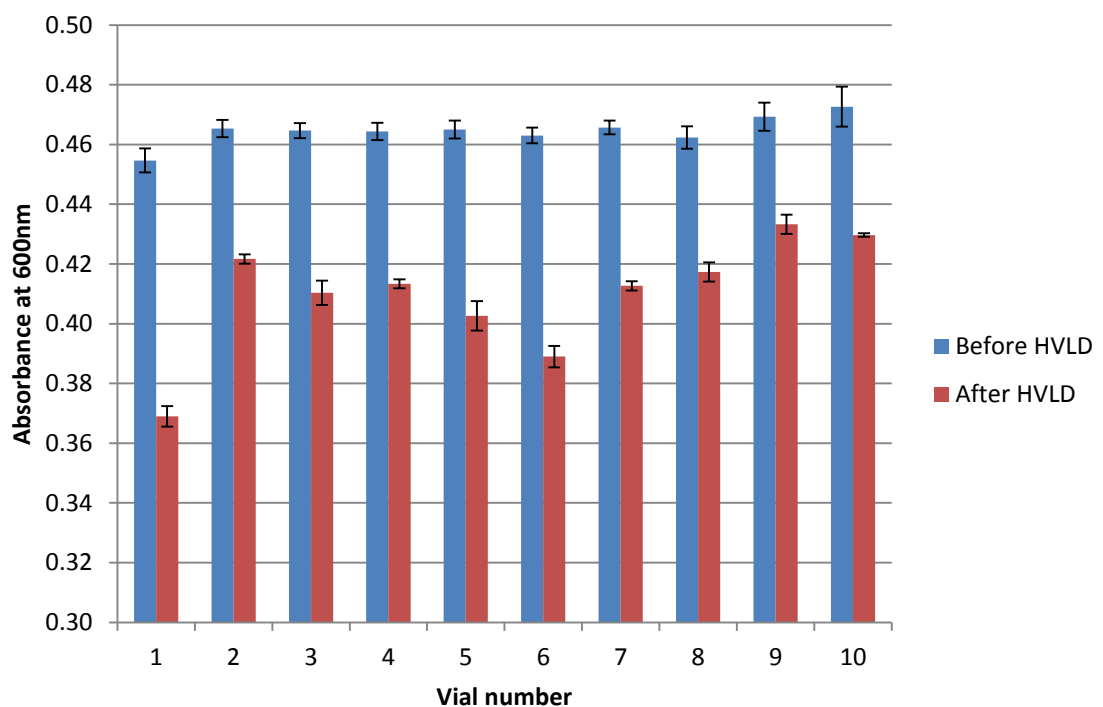
Figure 7.3 - Effect of 15 passes through HVLD on UV absorbance of IR1 at 600nm

Error bars represent standard error of the mean
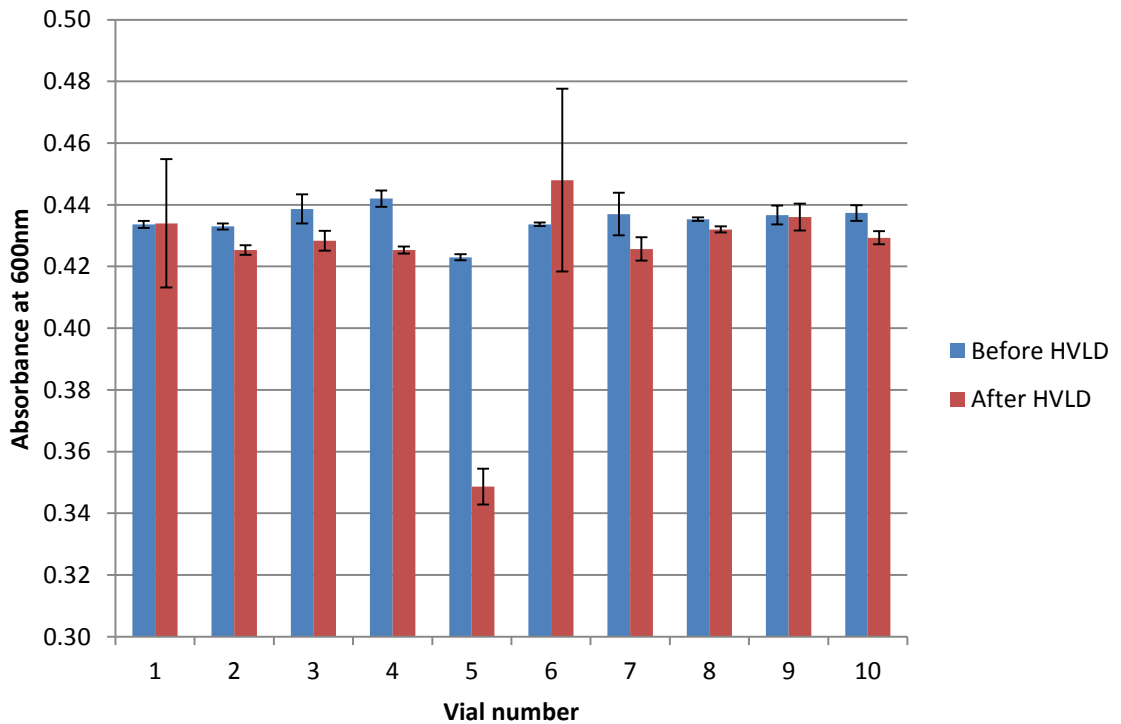
Figure 7.4 - Effect of 10 passes through HVLD on UV absorbance of IR1 at 600nm
Error bars represent standard error of the mean

The results from the vials passed through the HVLD 10 times, Figure 7.4, show that there were some larger errors in the measurement in two of the vials after HVLD, which show a mean absorbance that is higher than before HVLD. In vial 5, there was a clear drop in absorbance after HVLD and in other vials this was less pronounced. This may suggest that 10 passes do not generate as much ozone as 15 and 20 passes. This is discussed further in this section, when statistical analysis was carried out on the results.

The results from vials passed through the HVLD 5 times, Figure 7.5, show low error in measurement across all vials with the exception of vial 9 which has larger error bars for both before and after measurements. It is clear to see a marked drop in absorbance after HVLD in vials 1, 4, 6, 7 and 10.

Across the 10 vials passed through the HVLD 1 time, Figure 7.6, there appears to be in general, a smaller decrease in absorbance across these vials, whereas vials 6, 7 and 9 appear to showed a marked drop in absorbance.
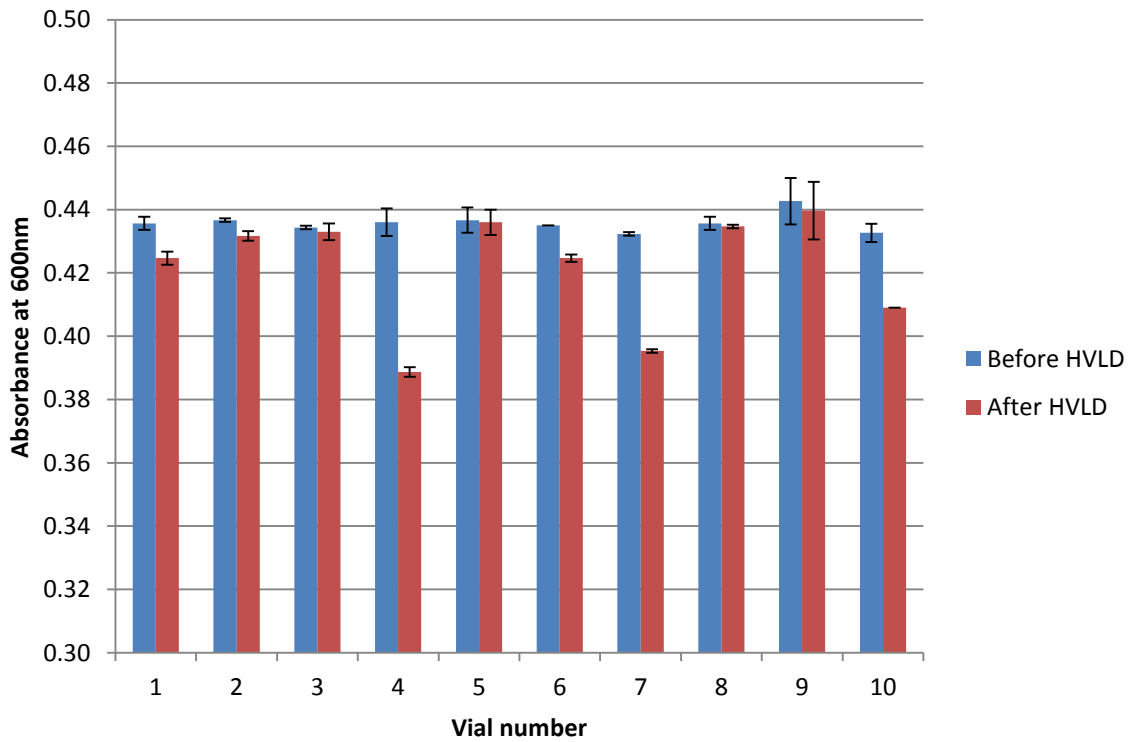
Figure 7.5 - Effect of 5 passes through HVLD on UV absorbance of IR1 at 600nm
Error bars represent standard error of the mean
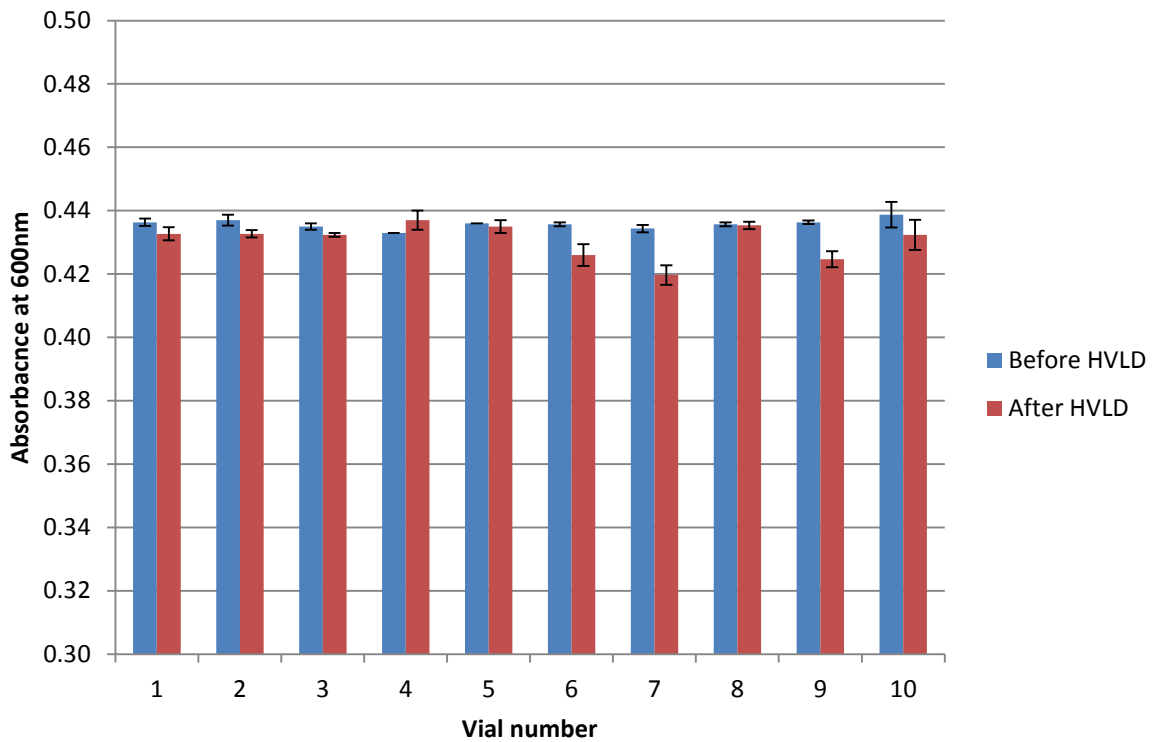
Figure 7.6 - Effect of 1 pass through HVLD on UV absorbance of IR1 at 600nm
Error bars represent standard error of the mean

The statistical difference between the mean absorbance for the three measurements from each vial, before and after HVLD, was investigated using a paired t-test. Table 7-2 shows the p-values for the test carried out for each vial. All vials subjected to 20 or 15 passes through the HVLD showed a significant drop in absorbance after HVLD exposure. Three out of the 10 vials that underwent 10 passes showed a significant drop in absorbance whilst 6 out of 10 vials that were subject to 5 passes showed a significant drop. The results from the vials that were subjected to only 1 pass through the HVLD showed that 4 out of 10 vials displayed a significant drop in absorbance.

Passes	Vial number									
	1	2	3	4	5	6	7	8	9	10
1	0.053	0.096	0.015	0.147	0.478	0.035	0.014	0.742	0.022	0.321
5	0.024	0.013	0.529	0.003	0.837	0.004	0.000	0.478	0.748	0.005
10	0.981	0.029	0.099	0.003	0.002	0.487	0.163	0.063	0.890	0.094
15	0.001	0.003	0.004	0.001	0.001	0.002	0.002	0.003	0.004	0.008
20	0.000	0.000	0.015	0.002	0.001	0.001	0.006	0.000	0.002	0.001

Table 7-2 - p values from paired t-tests of before and after HVLD measurements for each vial (p value <0.05 shows significant difference in absorbance at 600nm after HVLD). Shaded cells indicate vials undergoing significant changes in absorbance

When applying Equation 6.11 to calculate the ozone concentration in all vials subjected to HVLD, the range of ozone concentrations was between -0.34 – 1.11mg O_3/L, and this is shown in Figure 7.7.

There is a clear pattern evidenced with an increase in ozone concentration as the number of HVLD passes is increase from 1 pass which is the standard number of passes for HVLD testing, to 20 passes (worst case scenario testing). The highest concentration in Figure 7.7 represents the sample that was totally decolourised and it is hypothesised that the concentration of ozone produced may have exceeded the limit of the chosen method.
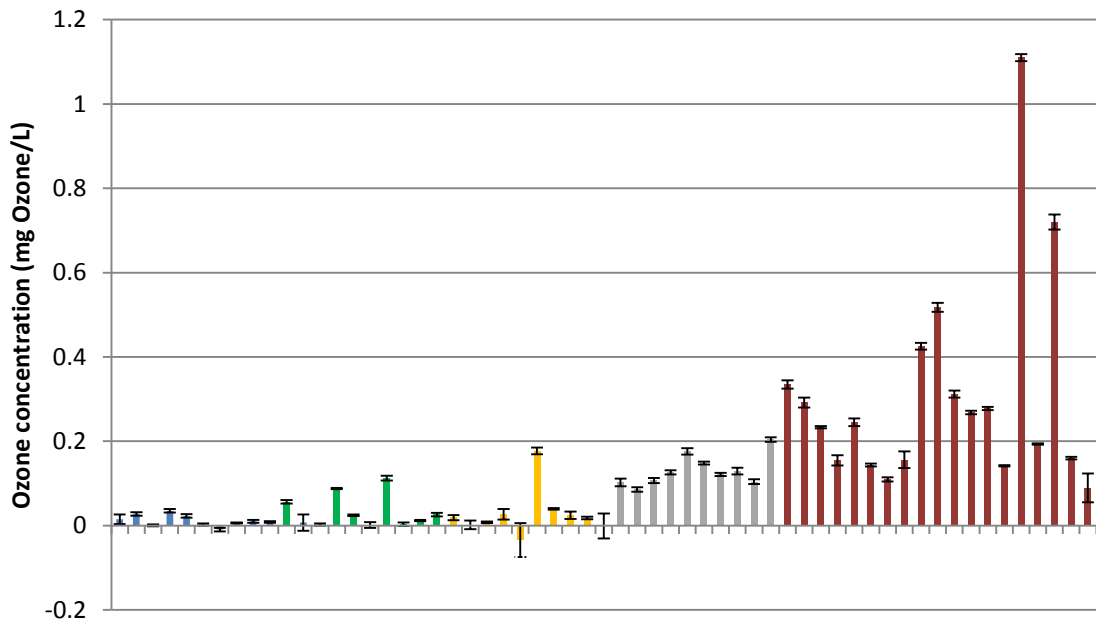
Figure 7.7 - Ozone concentrations detected in vials using the Indigo method

(1 pass ■, 5 passes ■, 10 passes ■, 15 passes ■, 20 passes ■, error bars represent standard error of the mean)

A number of inconsistencies were observed in the results, including the wide concentration range of ozone detected in vials undergoing 20 passes (0.1-1.1mg) which could be a consequence of a number of aspects pertaining to the experiment:

1) The vials were hand crimped on site at Newcastle University and this could have resulted in different seal integrities that may have allowed for the passage of ozone through the gap between the seal and the glass. This is not highly likely as all were crimped in the same fashion. However in the manufacturing environment vials would have been crimped by a machine and hence this process would be uniform and should not introduce any error.

2) The fill volumes of the vials were controlled, using Plastipak syringes to measure volumes however minor inconsistencies may have materialised due to small differences in the volume in the vials due to errors associated with the minimum graduation on the syringes. In addition to this, transfer of IR1 using these syringes and fine needles resulted in bubbles within the cuvette, which with tapping, attempts were made to minimise this, however, bubbles are known to interfere with UV absorbance measurements.

3) The pass order of vials in each test set was randomised to minimise time delays associated with the reordering the vials as discussed previously. This could have resulted in some vials being subject to passes through the HVLD in quick succession, which may have resulted in more ozone being formed in the vial and reacting with the PIT in a short period of time, before decomposition occurred compared with a vial that was passed through a longer time after its previous pass. If pass order was controlled this would have incurred a delay between passes, whereas it was decided that it was better to pass all the vials through in quick succession. In reality during HVLD testing, vials would only pass through the machine once, so this would not be something that could affect vials in practice.

4) Due to the technical disruptions that were encountered when using the HVLD machine, i.e. the machine stopped several times during the process of running vials through hence the movement of vials was halted and this could therefore have affected the mixing action of the headspace gas and PIT solution, which may have affected how much ozone reacted with the PIT solution. In the real case, with an automatic feed, vials should move smoothly through the machine, ensuring that each vial is subject to the same passage conditions. However breakdowns would inevitably occur at some points during testing.

It is not possible to determine which of the previously presented five reasons is the most likely cause for the variation in results, however all could have played some part in the variation seen.

7.4.2 *Assumptions of the PIT ozone detection method*

In reality in the manufacturing context, the vial contains a liquid and a gas phase, and ozone that is formed in the gas phase may transfer into the liquid phase. The original APHA method was designed to measure ozone in water and the water to be tested was added to PIT solution to react. The PIT method adapted in this study, although measuring the ozone present in the liquid phase, is fundamentally capturing the ozone that has been formed in the gas contained in the vial headspace that is transferred to the liquid. As the vial moves along the rollers in the HVLD machine, this causes the PIT

solution and headspace gas to interact and allows the PIT to react with ozone formed in the headspace. This method does not accurately represent the amount of ozone that would transfer into the liquid if for instance this liquid was a different substance, as PIT was chosen because it reacts quickly with the ozone present in the liquid phase and also with ozone present in the gas phase [193]. Filling vials with a different liquid, for example water, may not cause ozone to transfer to the liquid phase to as great an extent. What the method provides is an indication of how much ozone has been formed in the headspace however any ozone remaining in the headspace that did not react with PIT was not accounted for as the headspace was not tested.

An alternative option was the removal and testing of the headspace and this was considered in Chapter 6 section 6.5.7, however the off-site testing requirements meant that this was not possible as the time delay between passing through the HVLD and removal of headspace samples using a gas tight syringe was too long the ozone would have time to decompose, resulting in unreliable test results. In future, if testing was carried out onsite and within a short period of time after HVLD, then the testing of the headspace may be an option.

7.4.3 *Testing for the presence of ozone in water vials undergoing HVLD using direct UV absorbance*

Vials containing deionised water were also passed through the HVLD machine, Table 7-1. Absorbance was measured across the wavelengths 190-300nm to detect the potential presence of hydrogen peroxide, a decomposition product of ozone, and also for the direct detection of ozone.

Prior to testing, the absorbance of a sample of fresh deionised water was measured across UV wavelengths 190-300nm to act as a baseline. This baseline was subtracted from the spectra of all samples measured. A set of control vials were first filled with deionised water and their UV absorbance measured after 15 hours to observe any changes in spectra. The objective was to determine whether or not filling the vials on the previous day could affect the results. The control spectra with the baseline subtracted are given in Figure 7.8.
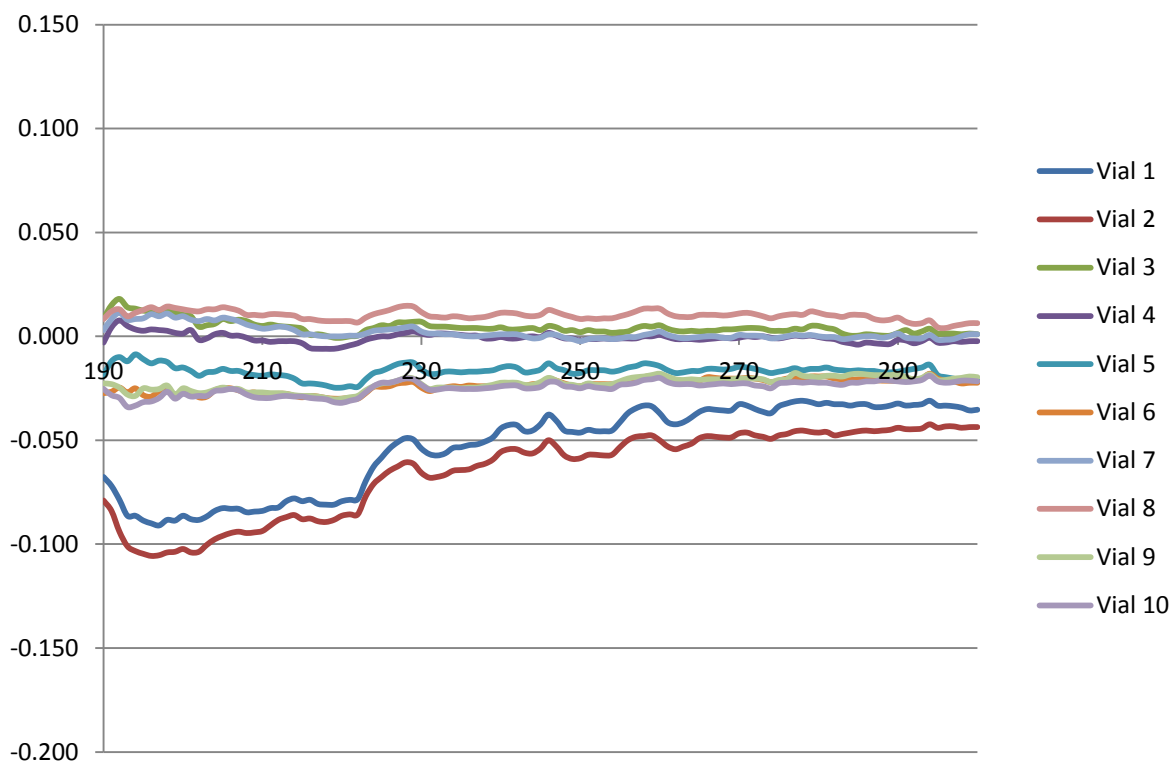
Figure 7.8 - UV spectra of water from control vials, filled and left for 15 hours

The 10 spectra in the water control shown in Figure 7.8 show some peaks around 227, 240, 245 and 258nm. These have very low absorbance intensities and in some cases show negative absorbance. Vial 1 and 2 show negative absorbance and this could be due to an error on the UV machine. When comparing the water control in Figure 7.8 to the water vials that underwent 20 passes through the HVLD in Figure 7.9 there are clear differences. In Figure 7.9 there are several prominent peaks in each spectrum depicting a higher absorbance than in the water control. There is one broad peak around 227nm, which was initially thought to be attributable to hydrogen peroxide (210-230nm [203]) and another broad peak around 258nm, which was assigned to ozone.

The UV spectrum of 0.001M H_2O_2 was also plotted in Figure 7.9 but there was little similarity in the spectra of water passed through the HVLD and 0.001M H_2O_2. The spectrum of 0.001M H_2O_2 does not show any peak at 227nm, so this shows that the peak at 227nm may correspond to another species. It was not possible to attribute this to another species.
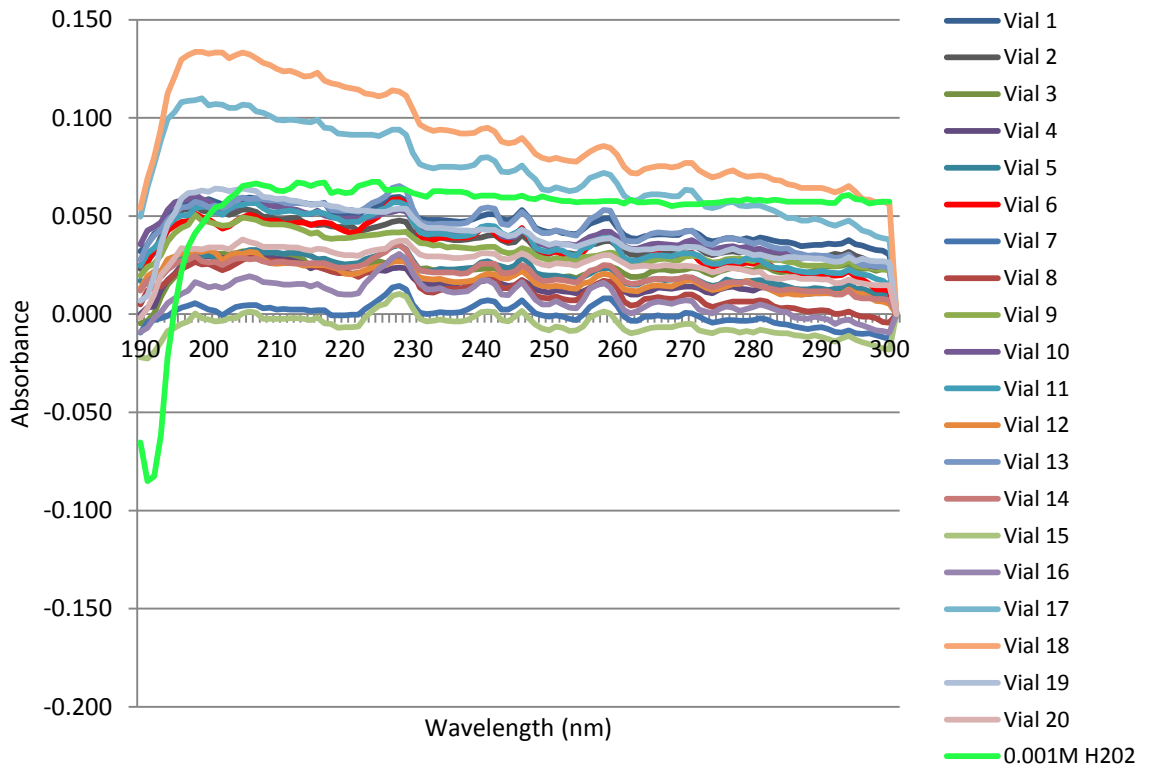
Figure 7.9 – UV spectra of deionised water after 20 passes through HVLD
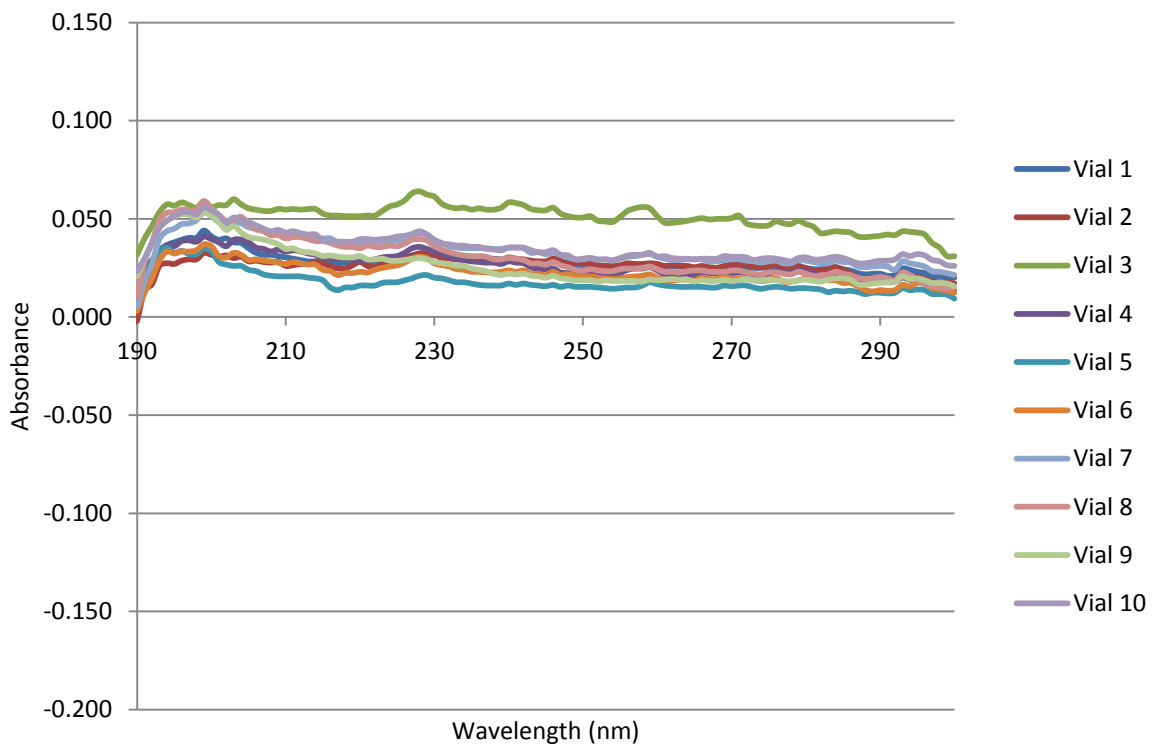
Figure 7.10 – UV spectra of deionised water after 15 passes through HVLD

When considering the results from the vials that underwent 15 passes through the HVLD, Figure 7.10, the intensity of absorbance at the prominent peaks is reduced, with the exception of one spectrum which stands out with higher absorbance around the peaks. Vials undergoing 10 passes through the HVLD, Figure 7.11, showed similar spectra to those that underwent 15 passes. Those vials that underwent 5 passes through the HVLD, Figure 7.12, and 1 pass, Figure 7.13, displayed more prominent peaks than the vials undergoing 15 and 10 passes, however the intensity of the absorbance was not as high as the peaks in vials undergoing 20 passes.
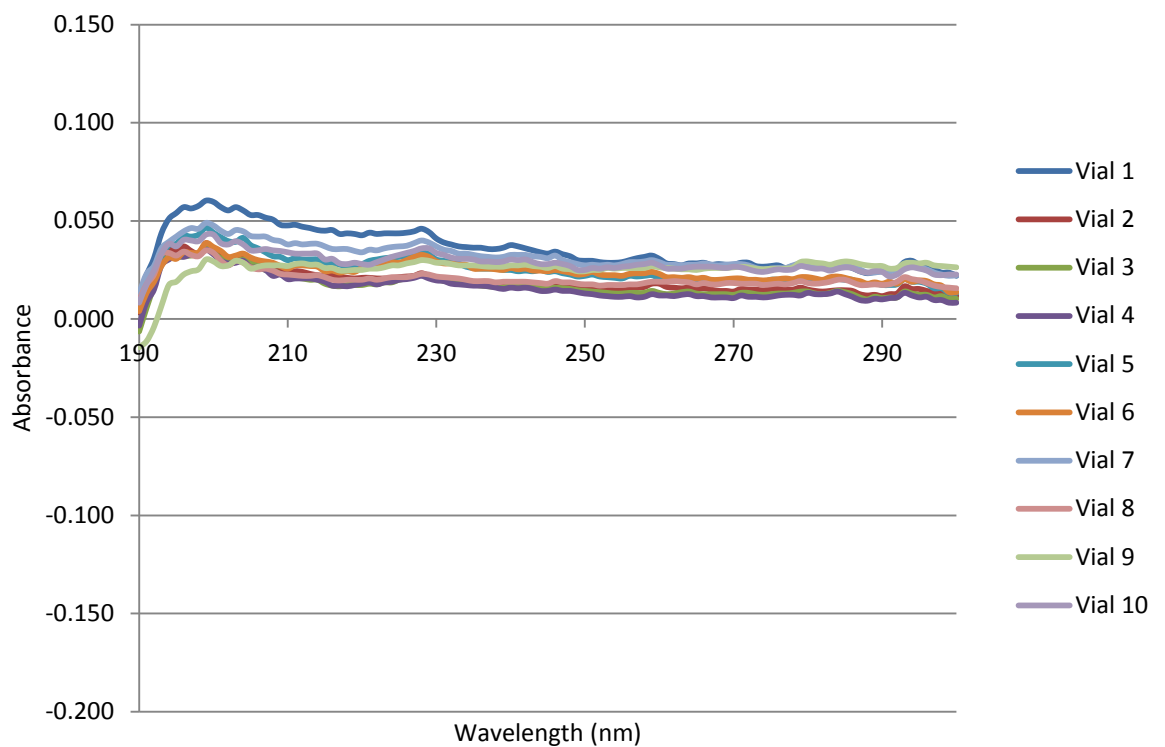
Figure 7.11 – UV spectra of deionised water after 10 passes through HVLD
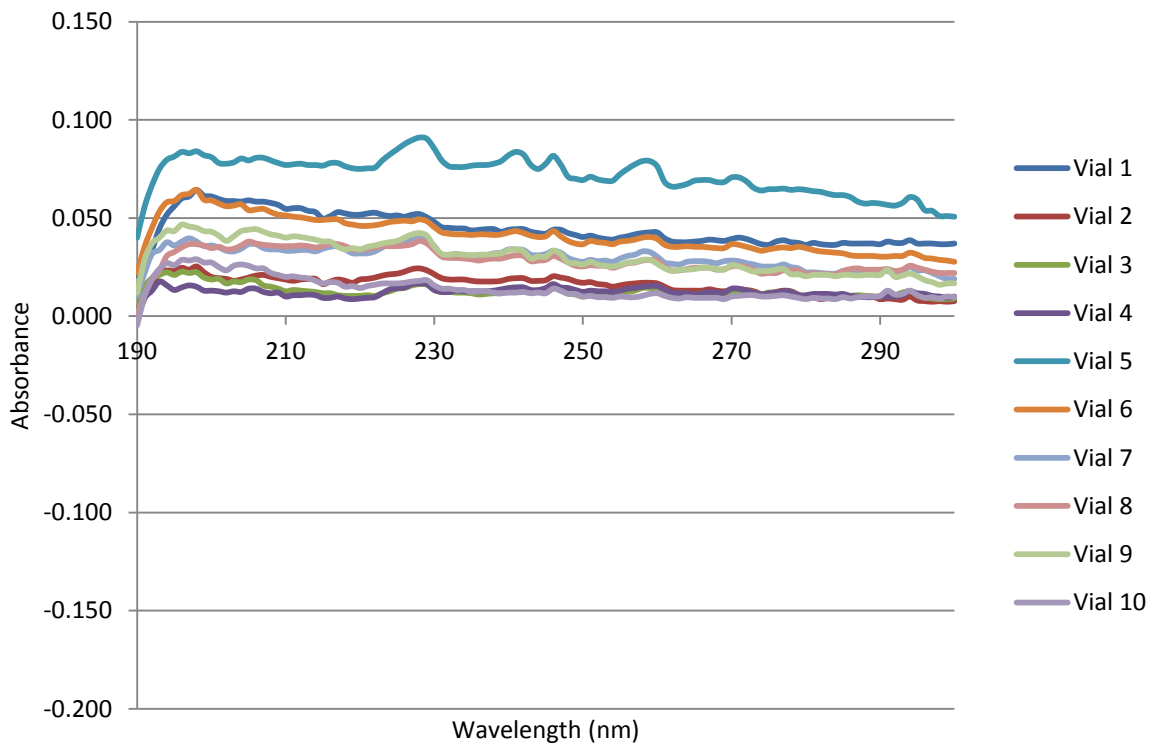
Figure 7.12 – UV spectra of deionised water after 5 passes through HVLD
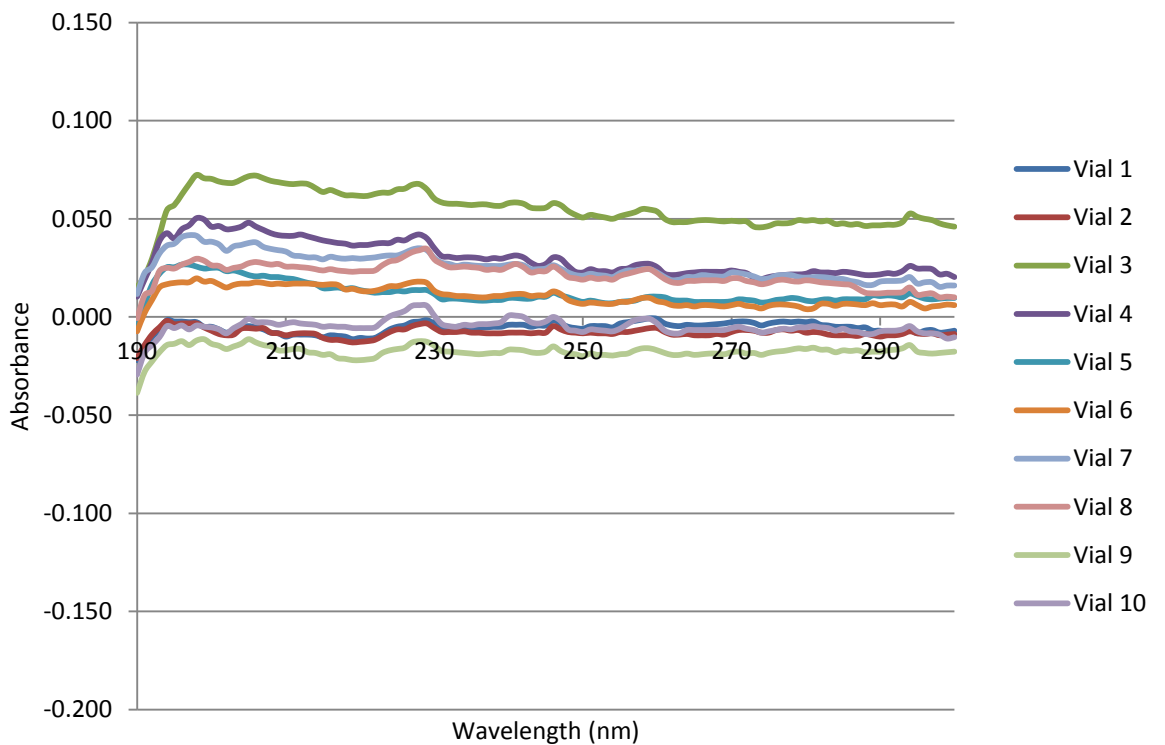
Figure 7.13 – UV spectra of deionised water after 1 pass through HVLD

As it was not possible to detect hydrogen peroxide which could then infer that ozone was present in the vial, so the absorbance values obtained for water at 258nm, across

all vials, were used to calculate the ozone concentration. Figure 7.14 shows the mean concentrations of ozone for each set of vials passed through the HVLD and although there appears to be a slight trend of increasing ozone concentration with increasing number of passes, the overlap of the error bars highlights that there is no clear link between number of passes and hence it can be concluded that there is no real difference across the means and the slight upward trend cannot be attributed to an increase in ozone concentration. The direct UV method utilised combined with this experimental protocol therefore appears to be insufficiently sensitive to accurately detect ozone at this concentration (0.203-0.543 mg/L). Absorbance measurements giving rise to these results were taken up to 6 hours after vials were passed through the HVLD, therefore it may be possible that the initial ozone concentration after HVLD was higher, however as ozone is known to degrade quickly, this experimental protocol and method has not enabled the accurate determination of the ozone concentration. The peaks at 227nm and 258nm in the UV spectra that were initially attributed to hydrogen peroxide are potentially noise from the instrument as they are present in the water control, when water was left overnight and re-tested, with the spectra shown in Figure 7.8.
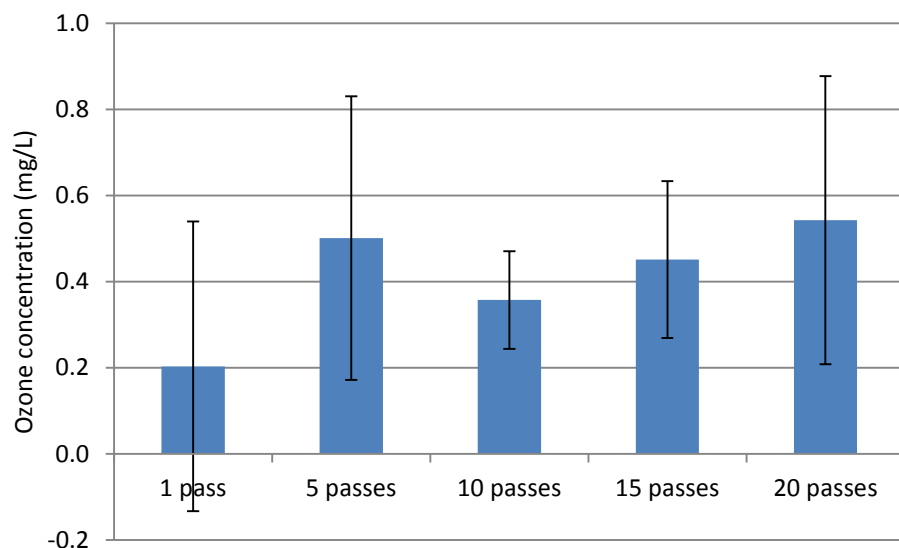
Figure 7.14 – Mean concentrations of ozone in vials (n=10) passed through HVLD as determined by direct UV absorbance at 258nm

7.5   Conclusions

7.5.1   *Ozone formation in vials undergoing HVLD as determined by PIT method*

These results have shown the effect of the number of passes through the HVLD on ozone formation in 60mL vials, filled with 6mL of IR1. It can be concluded that there is a significant difference in absorbance, and therefore a significant increase in ozone concentration, after the vials have undergone 20 passes through the HVLD and in several vials undergoing a lower number of passes. This provides evidence that ozone is formed in the vial headspace after only 1 pass, although the concentration of ozone produced is low. Passing vials through the HVLD 20, 15, 10 or 5 times is unrealistic in a normal testing environment but was chosen to challenge the system. In addition to this, the vials that were challenged in this testing had a low fill volume to allow a large headspace in which ozone could be produced but such low fill volumes would not be used in practice.

The Hospira study which was a catalyst for this work did not mention fill volume as a parameter, it only addressed the composition of headspace whilst the vial contained a low concentration of active ingredient and no antioxidant [165]. It is expected that if fill volume was increased and the headspace decreased, towards a realistic fill volume, then the concentration of ozone formed would be so low that it would be difficult to measure in the liquid phase. Furthermore, the level may be so low that it would not affect the drug product. This will be discussed in the subsequent section on future work.

7.5.2   *Ozone formation in water vials undergoing HVLD as determined by direct UV measurement*

With regards to the testing of vials containing deionised water, the spectra obtained indicated changes in the water after passing through the HVLD. These were initially attributed to hydrogen peroxide and ozone. After using the Beer Lambert Law to quantify the levels of ozone, it was concluded that the method was not sufficiently sensitive to be able determine the concentration of ozone as the error was large. Although it was not possible to accurately quantify the amounts of ozone, with a different experimental protocol that facilitated the measurement of UV absorbance at

258nm in a shorter timeframe after HVLD, it may be a feasible methodology if degradation can be minimised.

7.5.3 *Potential implications of results for pharmaceutical products*

With the low theoretical concentration of ozone that would be produced in the headspace of a vial, shown in Chapter 6 section 6.1.11, and the low concentrations produced in this study, the concerns for GSK are minimal due to the low number of passes that a vial is subjected to in the manufacturing environment. This coupled with a much higher fill volume, would minimise the potential for ozone formation inside the vial headspace. If vials were tested with a higher fill volume and ozone was found to be present, the effects could be mitigated by filling the headspace with nitrogen as suggested in the Hospira study [165].

7.6   Future work

The IR1 used in these tests did not undergo a 1 in 10 dilution as set out in the standard APHA method, so rather than being used to detect ozone between the concentrations ranges 0.01-0.1mgO$_3$/L, it was possible to detect 10 times this concentration. In the standard method, the IR1 undergoes a 1 in 10 dilution when a sample is added, as the method is used to measure liquid samples. It may therefore be possible to use a 1 in 10 dilution of IR1 to increase the sensitivity of the method to investigate the best case scenario of a filled vial, which would give rise to lower concentrations of ozone.

This testing explored the worst case scenario of low fill volume vials and has confirmed the findings in the Hospira study that ozone was produced in low fill volume vials. For the further investigation of ozone formation in vials subjected to HVLD, it would be necessary to use a fill volume that is more representative of a standard fill such as 50mL in a 60mL vial. Vials could be passed through the HVLD for a different number of passes and the absorbance of the PIT measured. Achievement of this would necessitate the dilution of the IR1 to 1 in 10 to represent the concentration that would be used when sampling liquids with the APHA method. Less ozone would be produced in the smaller headspace so the concentrated PIT solution used in the initial testing would not provide sufficient sensitivity.

To add to this body of evidence, the future work would include passing totally filled vials through the HVLD to investigate whether ozone is produced from dissolved oxygen, or whether it passes from the headspace into the liquid. Passing an empty vial through the HVLD would allow the gaseous sampling of the vial however this would have to be carried out on site for the measurement to be performed in a short timeframe after HVLD to avoid ozone decomposition.

The implementation of a design of experiments (DOE) study to investigate specific machine/process/product parameters would allow GSK to understand more about the machine/process/product parameters or characteristics that are critical for ozone production in containers. The DOE study could be carried out to investigate the effects of machine parameters and vial/fill parameters on ozone generation. This would include investigating the effects of voltage, the number of passes through HVLD that the vials are subjected to, the fill volume/vial volume ratio and the pH of the vial contents, on ozone concentration. The relationship between number of passes, fill volume, fill concentration and ozone concentration could be ascertained in more detail and could provide a more efficient way of gathering data than by varying one factor at a time. Once a better understanding is developed surrounding how the HVLD affects ozone formation in vials then steps can be taken to mitigate ozone formation, by for example, filling vial headspaces with nitrogen, or by only testing these containers using other integrity testing methods if this is required.

Other potential areas for investigation, beyond this include looking into the effect of HVLD on drug products by passing product through the machine and testing this for impurities. The investigation could also consider minimum levels of ozone that could cause damage to drug products by exposing drug products to ozone and measuring their impurity profiles using standard methods such as high performance liquid chromatography. Any impurities that were detected could be compared to the impurity profiles of drug products that had been passed through the HVLD. In order to facilitate this, a reliable ozone generation system with online measurement of ozone concentration would be required. Should ozone found to be causing impurities in drug products then investigation could be carried out into mitigation of ozone formation in vials. Recommendations for industry regarding ozone formation in vials undergoing HVLD are summarised in Chapter 8 section 0.

Chapter 8.   Conclusions and recommendations for industry

This study has encompassed three areas of analytical testing in pharmaceutical manufacture: rapid microbiology, oxidative stability and container integrity testing. The diversity in the areas of research is a reflection of the amount of development and consideration of new methods being undertaken at GlaxoSmithKline and the nature of collaborative research with changing priorities. The research has shown the potential of the role of rapid microbiology methods; the potential for new approaches in measuring oxidative stability to contribute towards future testing of pharmaceutical products to improve efficiency, maintain quality and provide more in-depth information than current methods; and has highlighted previously unseen results on ozone formation arising from HVLD testing.

8.1   Rapid microbial methods

Initial research into rapid microbiology methods (RMMs) reviewed the work being undertaken in the pharmaceutical industry into validation of new methods to improve microbial testing, highlighted the potential advantages that RMMs can offer to pharmaceutical manufacturers and discussed the barriers to their implementation. It was concluded that the case-by-case consideration of the adoption of RMMs should investigate all factors to ensure that barriers to implementation can be overcome and appropriate approaches are adopted. Despite the increasing availability of RMMs and recognition from regulators as to the importance of RMMs, the need for more harmonised regulation and guidance from the key regulatory authorities was identified as a key barrier to the adoption of RMMs. Several methods utilised and under validation were discussed and the potential of MALDI-TOF MS could be explored in the future with a suitable team of experts from the instrument manufacturers and key personnel in the microbial quality control teams of pharmaceutical companies. It was not possible in this research to investigate this topic due to financial constraints and changes of overall project direction. A thorough cost benefit analysis should be considered for the implementation of MALDI-TOF MS to the microbial testing situation. From this study a set of recommendations from industry is made around the use of TMMs and RMMs in pharmaceutical development and manufacturing and these can be found in Table 8-1.

Area	Recommended action to be taken
Suitability of RMMs in new product development and manufacturing	As new pharmaceutical products are being developed, the suitability of the inclusion of RMMs in the microbiological testing of products should be considered and validation of these methods built into the product development process where appropriate to gain cost savings and efficiency.
Continued use of TMMs in routine manufacturing	TMMs should continue to be used where appropriate in routine manufacturing, as validation of RMMs could be costly and may offer little benefit in very established production processes.
Sharing of best practice	The industry should share best practice around the validation of RMMs in order to make the validation process more efficient for others in the future.

Table 8-1 - Recommendations for industry around microbial methods

8.2 Comparison of the Rancimat and ACL Instrument for measuring the oxidative stability of corn and Menhaden oil

This research highlighted the potential for the Rancimat and ACL Instrument to be used interchangeably, through the strong correlation between the OITs determined for corn oil and Menhaden oil. It showed the potential of the ACL Instrument as a method for measuring oxidative stability and one which compares favourably to the Rancimat when considering OIT measurements. It was concluded that the ACL Instrument was able to provide more information about the oxidative behaviour of a substance than the Rancimat due to the visibility of multiple oxidation events on the CL curve in contrast to the integrated signal generated by the Rancimat.

Comparison of results from Menhaden and corn oil showed that the total luminescence intensity (TLI) showed an oil dependence in terms of its correlation with the Rancimat OIT. The lower OITs and the lower activation energy (E_a) displayed by Menhaden oil indicated that it was less stable that corn oil at the same testing temperatures which was expected due to the higher concentration of PUFA which made the oil more susceptible to oxidation.

The research highlighted that aluminium pans caused a catalytic effect on the oxidation of corn oil and that borosilicate glass slides gave more repeatable results. For the purpose of measuring the oxidative stability of oils such as corn oil, it was therefore recommended that glass slides are used as they are inert and devoid of the catalytic activity associated with aluminium pans.

The six month storage study showed that subtle changes in oxidative stability may be detectable with the ACL Instrument however it was inconclusive as to whether, over a

period of 6 months, the oxidation state of the corn oil changed significantly. A longer time period of storage would be required to investigate this further.

Limitations of the work were the length of the runs and the low number of repeats possible considering the length of the runs and operating only one ACL Instrument, which broke down on two occasions. From these conclusions and the conclusions in the following sections 8.3 and 8.4, a set of recommendations for industry is made around the future use of the ACL Instrument in pharmaceutical development and manufacturing and these can be found in Table 8-2, section 8.4.

8.3 Comparison of the ACL Instrument and iodometric titration for the measurement of peroxides

The results from this research were in support of the hypothesis that the ACL Instrument could not provide an absolute value for peroxide levels, which would be correlated to the PV when testing across different oils and across oils aged at different temperatures. The CL method was found to be comparable to PV in terms of precision and some results showed a strong correlation between the TLI and PV for corn oil and Menhaden oil at a number of temperatures, but this was not seen across all results from aged samples. It was concluded that this could have been due to the different fatty acid compositions for the two oils, giving rise to different types of peroxide, which were detected to differing extents by the methods investigated. This suggested that compared to CDV and PV, which are used as a comparative indicators across a number of oils, CL measurement of peroxides cannot yet be used in this way. From this research it was not possible to conclude which method gave the most reliable measure of peroxides however it is expected than the CL method may capture many different types of peroxide in contrast to the PV method which only captures peroxides that are reduced by the iodide ion.

The ACL Instrument is less labour intensive, easier and quicker to set up, produces a lot less chemical waste and does not require a fume hood as with the PV method. However one major disadvantage of the ACL Instrument is the throughput of samples which is much lower than the titration method. The ACL Instrument provides more information about the substance e.g. in this research the visualization of the bell

shaped curve vs. lack of bell shaped curve could be considered when measuring peroxides as well as values calculated from the CL curve.

It was concluded that for the ACL Instrument to be utilised for the quantification of peroxide levels, a calibration model would need to be developed using oils of acceptable quality. This would then form the basis of a CL standard for particular oils to which samples of unknown quality could then be compared to.

8.4 The ACL Instrument as a fingerprinting tool for determining polysorbate stability

This research explored two hypotheses: 1) CL would provide a more sensitive test for oxidative stability of polysorbates than the Rancimat; 2) the CL measurement of peroxide levels would provide more information and be more sensitive than iodometric based titrations.

It was concluded that CL is a potentially useful technique for measuring the oxidative stability of polysorbates however at the high temperatures investigated in this study, chosen to keep run times feasible, oxidation began very quickly and therefore determination of a baseline from which to calculate OIT was difficult. Results from the Rancimat were in agreement with the ACL Instrument in terms of being able to discriminate between batches of PS80 and Tween 80. The Rancimat provided repeatable results, however its sensitivity needed to be investigated further by testing at lower temperatures and investigating the evaluation suppression mode to prevent low OITS caused by early oxidation events.

The CL testing of polysorbates under oxidative conditions resulted in subtly different CL curves for different types (polysorbate 20, 60 and 80), grades and batches of polysorbate. It was possible to distinguish between Tween 80 and HP-PS80, with clear differences evident in CL curve shape over a range of temperatures under oxidative conditions and under nitrogen. Using CL as a fingerprinting tool for polysorbates at these testing temperatures warrants further investigation and consideration of the latter part of the curve beyond the CLI_{max} (not investigated in this study) which could give additional options for fingerprinting.

CL offered a more repeatable testing method than PV for measuring peroxide content in polysorbates when considering the %RSD values from both methods. This was due to the forced degradation of accumulated peroxides in CL testing and the elimination of operator error that potentially impacted on the PVs from iodometric titrations.

It was not possible to ascertain which species the differences in the CL curves were attributable to solely based on CL data, however the results showed the potential of CL to be used as a fingerprinting technique, which may provide more information than existing methods such as the Rancimat or peroxide value which, in this case also highlighted the batch-to-batch differences captured by the CL method.

Area	Recommended action to be taken
1) Measurement of oxidative stability	The ACL Instrument has potential to be used in oxidative stability testing on raw materials, using the OIT as a measure of stability. Further characterisation of the CL curves of 'acceptable quality' excipients is required to confirm the spectral fingerprint of these excipients.
2) Quantification of peroxides	To be able to utilise the ACL Instrument in the routine testing of peroxide levels, a calibration model would need to be developed using oils of acceptable quality. This is explained further in point 5) in this table.
3) Operational considerations – sample holder	When carrying out any testing using the ACL Instrument it is recommended that borosilicate glass slides are used as sample holders, as aluminium pans can exert a catalytic effect on the oxidation of the substance being measured.
4) Long term stability	The ACL Instrument and an additional humidity hardware module should be investigated as a method of tracking oxidation with CL. This could be applied to final formulations under long term stability conditions, as would be used in routine pharmaceutical stability testing.
5) Routine testing of excipients using the ACL Instrument (e.g. polysorbates)	The testing of raw materials using the ACL Instrument should be incorporated into routine raw material testing. For each incoming raw material that is formulated with a pharmaceutical, the raw material should be tested on the ACL Instrument to obtain CL curves in synthetic air to calculate OIT (h) and obtain a CL curve in nitrogen to calculate TLI (cts/g). This would allow the development of a library of CL spectra which could then be analysed alongside data on product performance obtained from finished product stability testing.
6) Stability testing of protein based final formulations	The ACL Instrument is not suitable for the testing of protein-based final formulations at the high temperatures utilised in this study, as these would destroy the protein. There is potential to run the ACL Instrument at lower temperatures but this would require further research into the suitability of this testing.
7) Understanding the effect of refining	To understand the effect of refining on the CL curve of the polysorbate and investigate further the peaks appearing in HP-PS80 (Figure 5.8, Chapter 5) it would be important to test polysorbate 80 before and after refining and investigate the shape of the CL curve.

Table 8-2 - Recommendations for industry around the use of the ACL Instrument in pharmaceutical research and manufacturing

8.5 Development and implementation of a method for ozone detection in pharmaceutical containers subject to container integrity testing via high voltage leak detection

This research, through a literature review, considered many methods detailed for measuring ozone. Experimental work helped to define a testing protocol for investigating whether ozone is produced in vials undergoing high voltage leak detection (HVLD). The recommended protocol for ozone detection was based on a modification of the APHA Indigo method [174] and an additional testing protocol for ozone detection via the detection of hydrogen peroxide was also recommended. These methods were taken forward and used in testing of vials that were subject to HVLD.

The vials in this research had a low fill volume to allow a large headspace in which ozone could be produced but such low fill volumes would not be used in practice. Vials were passed through the HVLD 20, 15, 10 and 5 times which was unrealistic for a normal testing environment but were chosen to challenge the system. Vials were also passed through 1 time, to represent the real testing scenario. There was a significant difference in absorbance, and therefore a significant increase in ozone concentration, after the vials had undergone 20 passes through the HVLD and in several vials undergoing a lower number of passes. This testing also provided evidence that ozone was formed in the vial headspace after only 1 pass, although the concentration of ozone produced was low.

It was expected that if fill volume was increased and the headspace decreased, towards a realistic fill volume then the concentration of ozone formed would be so low that it would be difficult to measure in the liquid phase. Furthermore, the level may be so low that it would not affect the drug product. It was not possible to carry out this testing so this was detailed in the future work.

With regards to the testing of vials containing deionised water, the spectra obtained indicated changes in the water after passing through the HVLD which were initially attributed to hydrogen peroxide and ozone. However, after quantifying the levels of ozone, it was concluded that the method was not sufficiently sensitive to be able to determine the concentration of ozone as the error was large. It was concluded that if a different experimental protocol was implemented that facilitated the measurement of

UV absorbance at 258nm in a shorter timeframe after HVLD, this may still be a feasible methodology to measure the presence of ozone.

With the low theoretical concentration of ozone that would be produced in the headspace of a vial, shown in Chapter 6 section 6.1.11 and the low concentrations detected in this study, the concerns for pharmaceutical companies are minimal due to the low number of passes that a vial is subjected to in the manufacturing environment. This coupled with a much higher fill volume would minimise the potential for ozone formation inside the vial headspace. If vials were tested with a higher fill volume and ozone was found to be present, the effects could be mitigated by filling the headspace with nitrogen as suggested in the Hospira study [165].

From this study into ozone formation in vials undergoing HVLD a set of recommendations for industry is made around future work and these can be found in Table 8-3.

Area	Recommended action to be taken
1) Testing of best case scenario (standard fill volume)	The testing of vials with a standard fill volume and 1 pass through HVLD (standard conditions) should be carried out to understand if ozone is produced. The concentration of indigo may need to be reduced to a 1 in 10 dilution of IR1 in order to improve the sensitivity of the technique when a small headspace is present.
2) Ozone challenge of drugs tested on HVLD	Drugs that are routinely passed through the HVLD should be exposed to low concentrations of ozone and tested for degradation products, in order to fully understand the implications of low level ozone that may be produced in the headspace.
3) Mitigation of risk	If during the best case scenario testing in point 1) ozone was produced, mitigation strategies would need to be considered, such as filling headspaces with inert gas.

Table 8-3 - Recommendations for industry around the HVLD testing of vials

References

1.	Evens, R.P. and K.I. Kaitin, *The Biotechnology Innovation Machine: A Source of Intelligent Biopharmaceuticals for the Pharma Industry Mapping Biotechnology's Success.* Clinical Pharmacology and Therapeutics, 2014. **95**(5): p. 528-532.

2.	Frokjaer, S. and D.E. Otzen, *Protein drug stability: a formulation challenge.* Nature Reviews Drug Discovery, 2005. **4**(4): p. 298-306.

3.	Ramasamy, S.V., N.J. Titchener-Hooker, and P. Lettieri, *Life cycle assessment as a tool to support decision making in the biopharmaceutical industry: Considerations and challenges.* Food and Bioproducts Processing, 2014 In Press.

4.	Ha, E., W. Wang, and Y.J. Wang, *Peroxide Formation in Polysorbate 80 and Protein Stability.* Journal of Pharmaceutical Sciences, 2002. **91**(10).

5.	AOCS, *Official Method Cd 8b-90 Peroxide Value Acetic Acid-Isooctane Method*, 2009.

6.	Rao, G., A. Moreira, and K. Brorson, *Disposable Bioprocessing: The Future Has Arrived.* Biotechnology and Bioengineering, 2009. **102**(2): p. 348-356.

7.	Read, E.K., R.B. Shah, B.S. Riley, J.T. Park, K.A. Brorson, and A.S. Rathore, *Process Analytical Technology (PAT) for Biopharmaceutical Products: Part II. Concepts and Applications.* Biotechnology and Bioengineering, 2010. **105**(2): p. 285-295.

8.	Newby, P., *Implementation, validation and registration of rapid microbiological methods*, in *European Pharmaceutical Review* 2008. p. 67-73.

9.	Food and Drug Administration, *21CFR610.12*, 2013, Food and Drug Administration.

10.	U.S. Food and Drug Administration, *Code of Federal Regulations, Title 21*, 2012.

11.	ICH, *Q5C Quality of Biotechnological Products: Stability Testing of Biotechnological/Biological Products*, 1995, International Conference on Harmonisation of Technical Requirements for Registration of Pharmaceuticals for Human Use: Geneva.

12.	Balboni, M.L. *Process Analytical Technology Concepts and Principles*. Pharmaceutical Technology October 2003 [cited 2014 28/09]; Available from: http://www.webcitation.org/6SvirrTnP.

13. U.S. Food and Drug Administration, *Pharmaceutical cGMPs for the 21st Century - A Risk-Based Approach*, 2004: Rockville, MD.

14. U.S. Food and Drug Administration, *Guidance for Industry. PAT - A Framework for Innovative Pharmaceutical Development, Manufacturing and Quality Assurance* 2004: Rockville, MD.

15. Kalavati Suvarna, A.L., Patricia Hughes, Richard L Friedman. *Case Studies of Microbial Contamination in Biologic Product Manufacturing*. American Pharmaceutical Review January/February 2011; Available from: http://www.webcitation.org/6Svj3P3xv.

16. U.S. Department of Health and Human Services. Food and Drug Administration. Center for Biologics Evaluation and Research, *Guidance for Industry: Validation of Growth-Based Rapid Microbiological Methods for Sterility Testing of Cellular and Gene Therapy Products. DRAFT GUIDANCE*, 2008.

17. *British Pharmacopoeia: SC IV L. Alternative Methods for Control of Microbiological Quality*, 2012.

18. Riley, B.S., *A regulators view of rapid microbiology methods.* European Pharmaceutical Review, 2011. **16**(5).

19. European Directorate for the Quality of Medicines & HeathCare, *European Pharmacopeia 7.0* in *5.1.6 Alternative methods for control of microbiological quality* 2011: Strasbourg.

20. Gray, J.C., A. Stärk, M. Berchtold, M. Mercier, G. Neuhaus, and A. Wirth. *Introduction of a Rapid Microbiological Method as an Alternative to the Pharmacopoeial Method for the Sterility Test*. American Pharmaceutical Review September/October 2010 [cited 2014 28/09]; Available from: http://www.webcitation.org/6SvjWNsOA.

21. Miller, M.J., ed. *Encyclopedia of Rapid Microbiological Methods, Volume II* PDA and Davis Healthcare International Publishing.

22. bioMérieux SA. *ScanRDI® - Automated real-time microbial detection and enumeration method*. 2014 [cited 2014 16/02]; Available from: http://www.webcitation.org/query?id=1392572894236566.

23. GSK, *ChemScanRDI System: Principles of the Technology and Analytical Procedure (in-house presentation)* 2008.

24. Azbil BioVigilant, Inc,. *IMD-A 300 Series Instantaneous Microbial Detection Systems*. 2012 [cited 2014 16/02]; Available from: http://www.webcitation.org/query?id=1392573005133585.

25. Azbil BioVigilant, I., *IMD-A® Series Rapid Biologic Detection System for Air - Product Specification*, 2013.

26. Pharmacopeia, U.S., *<1223> 35th Revision. Validation of alternative microbiological methods*, United States Pharmacopeial Convention, Maryland,USA.

27. Food and Drug Administration, *21CFR11 Electronic Records; Electronic Signatures*, 2013.

28. Azbil BioVigilant, I. *Azbil BioVigilant IMD - Pharmaceutical Applications*. 2014; Available from: http://www.webcitation.org/query?url=http%3A%2F%2Fwww.biovigilant.com%2Fapplications%2Fpharmaceutical-applications%2F&date=2014-05-04.

29. Hata, D.J., L. Hall, A.W. Fothergill, D.H. Larone, and N.L. Wengenack, *Multicenter Evaluation of the New VITEK 2 Advanced Colorimetric Yeast Identification Card.* Journal of Clinical Microbiology, 2007. **45**(4): p. 1087-1092.

30. Wallet, F., C. Loiez, E. Renaux, N. Lemaitre, and R.J. Courcol, *Performances of VITEK 2 colorimetric cards for identification of gram-positive and gram-negative bacteria.* Journal of Clinical Microbiology, 2005. **43**(9): p. 4402-4406.

31. *Vitek 2 TM The Fully Automated Solution*, 2008, bioMérieux.

32. Chen, H., G. Marino, A.M. Cundell, and M.M. Siegel. *Rapid Identification of USP Objectionable Microorganisms in Pharmaceutical Ingredients by MALDI-TOF Mass Spectrometry*. in *American Society for Mass Spectrometry*. 2000.

33. Williams, T.L., D. Andrzejewski, J.O. Lay, and S.M. Musser, *Experimental factors affecting the quality and reproducibility of MALDI TOF mass spectra obtained from whole bacteria cells.* Journal of the American Society for Mass Spectrometry, 2003. **14**(4): p. 342-351.

34. Fenselau, C. and P.A. Demirev, *Characterization of intact microorganisms by MALDI mass spectrometry.* Mass Spectrometry Reviews, 2001. **20**(4): p. 157-171.

35. Demirev, P.A. and C. Fenselau, *Mass Spectrometry for Rapid Characterization of Microorganisms.* Annual Review of Analytical Chemistry, 2008. **1**: p. 71-93.

36. *Expert Opinion. Bruker Daltonics at the 18th European Congress of Clinical Microbiology and Infectious Diseases (ECCMID) Brochure LS-39*, 2008, Bruker Daltonics.

37. Bruker Corporation. *MALDI Biotyper*. 2014 [cited 2014 23/08]; Available from: http://www.webcitation.org/6S32ofBSD.

38. Hartmeyer, G.N., A.K. Jensen, S. Bocher, M.D. Bartels, M. Pedersen, M.E. Clausen, R. Abdul-Redha, R. Dargis, P. Schouenborg, N. Hojlyng, M. Kemp, and J.J.E. Christensen, *Mass spectrometry: Pneumococcal meningitis verified and Brucella species identified in less than half an hour.* Scandinavian Journal of Infectious Diseases, 2010. **42**(9): p. 716-718.

39. U.S. Food and Drug Administration. *FDA News Release: New test system identifies 193 different yeasts and bacteria known to cause illness*. 2013 [cited 2014 16/02]; Available from: http://www.webcitation.org/query?id=1392573298334029.

40. PDA, *Evaluation, Validation and Implementation of New Microbiological Testing Methods. Technical Report No. 33*, May/June 2000.

41. Microbiology Consultants, LLC. *http://rapidmicromethods.com/*. 2014 [cited 2014 16/02]; Available from: http://www.webcitation.org/query?id=1392573717519406.

42. Duguid, J., E. Balkovic, and G.C.d. Moulin, *Rapid Microbiological Methods: Where Are They Now?* American Pharmaceutical Review, 2011. **14**(7).

43. Newby, P., G. Dalmaso, S. Lonardi, B. Riley, P. Cooney, and K. Tyndall, *The Introduction of Qualitative Rapid Microbiological Methods for Drug Product Testing.* Pharmaceutical Technology, 2004.

44. Moldenhauer, J., *Validation of Rapid Microbiology Systems Based upon PDA Technical Report No. 33*, 2002.

45. Sandle, T. *Automated Microbial Identification: A Comparison of USP and EP Approaches*. American Pharmaceutical Review 2013 [cited 2014 28/09]; Available from: http://www.webcitation.org/6SvjnbDe9.

46. Microbiology Consultants, LLC,. *RMMs and the regulatory environment*. 2014 [cited 2014 16/02]; Available from: http://www.webcitation.org/query?id=1392573803321613.

47. Jensen, S., H. Oestdal, M.R. Clausen, M.L. Andersen, and L.H. Skibsted, *Oxidative Stability of Whole Wheat Bread During Storage.* LWT - Food Sci Technol, 2011. **44**(3): p. 637-642.

48. Shim, S.D. and S.J. Lee, *Shelf-life Prediction of Perilla Oil by Considering the Induction Period of Lipid Oxidation.* European Journal of Lipid Science and Technology, 2011. **113**(7): p. 904-909.

49. Dantas, M.B., A.R. Albuquerque, A.K. Barros, M.G. Rodrigues Filho, N.R. Antoniosi Filho, F.S.M. Sinfrônio, R. Rosenhaim, L.E.B. Soledade, I.M.G. Santos, and A.G. Souza, *Evaluation of the Oxidative Stability of Corn Biodiesel.* Fuel, 2011. **90**(2): p. 773-778.

50. Karavalakis, G., S. Stournas, and D. Karonis, *Evaluation of the Oxidation Stability of Diesel/Biodiesel Blends.* Fuel, 2010. **89**: p. 2483-2489.

51. Bannister, C.D., C.J. Chuck, M. Bounds, and J.G. Hawley, *Oxidative Stability of Biodiesel Fuel.* Proceedings of the Institution of Mechanical Engineers, Part D: Journal of Automobile Engineering, 2009. **225**(1): p. 99-114.

52. Fearon, P., S. Bigger, and N. Billingham, *DSC Combined with Chemiluminescence for Studying Polymer Oxidation.* Journal of Thermal Analysis and Calorimetry, 2004. **76**(1): p. 75-83.

53. Celina, M., A.B. Trujillo, K.T. Gillen, and L.M. Minier, *Chemiluminescence as a Condition Monitoring Method for Thermal Aging and Lifetime Prediction of an HTPB Elastomer.* Polymer Degradation and Stability, 2006. **91**(10): p. 2365-2374.

54. Woo, L., A. Khare, C. Sandford, M. Ling, and S. Ding, *Relevance of High Temperature Oxidative Stability Testing to Long Term Polymer Durability.* Journal of Thermal Analysis and Calorimetry, 2001. **64**(2): p. 539-548.

55. *International Conference on Harmonisation of Technical Requirements for Registration of Pharmaceuticals for Human Use (2003) Q1A(R2) Stability testing of new drug substances and products.*

56. Zhu, D., G.G.Z. Zhang, K.L.S.T. George, and D. Zhou, *A Novel Accelerated Oxidative Stability Screening Method for Pharmaceutical Solids.* Journal of Pharmaceutical Sciences, 2011. **100**(8): p. 3529-3538.

57. FDA. *Advisory to Drug and Dietary Supplement Manufacturers, Compounding Pharmacies and Distributors of Excipients and Dietary Ingredients – FDA Detects*

High Levels of Peroxide in Crospovidone. 2010 [cited 2014 16/02]; Available from: http://www.webcitation.org/query?id=1392574459716140.

58.   FDA. *Recall -- Firm Press Release: Abbott Announces Voluntary Worldwide Recall of Two Lots of Calcilo XD Low-Calcium/Vitamin D-Free Infant Formula with Iron Powder in 14.1-Ounce (400g) Cans*. 2008 [cited 2014 16/02]; Available from: http://www.webcitation.org/query?id=1392574231359175.

59.   Frankel, E.N., *Lipid Oxidation*. 2nd ed2005: PJ Barnes & Associates

60.   Betts, J., *The Kinetics of Hydrocarbon Autoxidation in the Liquid Phase.* Quarterly Reviews, Chemical Society, 1971. **25**(2): p. 265-288.

61.   Kanner, J. and I. Rosenthal, *An assessment of lipid oxidation in foods.* Pure and Applied Chemistry, 1992. **64**(12): p. 1959-1964.

62.   Wasylaschuk, W.R., P.A. Harmon, G. Wagner, A.B. Harman, A.C. Templeton, H. Xu, and R.A. Reed. *Evaluation of Hydroperoxides in Common Pharmaceutical Excipients*. Journal of Pharmaceutical Sciences 2007 [cited 96 1]; 106-116].

63.   Klein, R.A., *The detection of oxidation in liposome preparations.* Biochimica et Biophysica Acta-Lipids and Lipid Metabolism 1970. **210**(3): p. 486-489.

64.   Carlsson, D.J. and J. Lacoste, *A Critical Comparison of Methods for Hydroperoxide Measurement in Oxidised Polyolefins.* Polymer Degradation and Stability, 1991. **32**: p. 377-386.

65.   Antolovich, M., P.D. Prenzler, E. Patsalides, S. McDonald, and K. Robards, *Methods for testing antioxidant activity.* The Analyst, 2002. **127**: p. 183-198.

66.   Devasagayam, T.P.A., K.K. Boloor, and T. Ramasarma, *Methods for estimating lipid peroxidation: An analysis of merits and demerits.* Indian Journal of Biochemistry & Biophysics, 2003. **40**(October): p. 300-308.

67.   Abuja, P.M. and R. Albertini, *Methods for monitoring oxidative stress, lipid peroxidation and oxidation resistance of lipoproteins.* Clinica Chimica Acta, 2001. **306**: p. 1-17.

68.   Akoh, C.C. and D.B. Min, eds. *Food Lipids: Chemistry, Nutrition & Biotechnology*. 3rd ed. 2008, CRC Press.

69.   DeRouchey, J.M., J.D. Hancock, R.H. Hines, C.A. Maloney, D.J. Lee, H. Cao, D.W. Dean, and J.S. Park, *Effects of rancidity and free fatty acids in choice white grease on growth performance and nutrient digestibility in weanling pigs.* Journal of Animal Science, 2004. **82**(10): p. 2937-2944.

70. Sigma-Aldrich. *Peroxide test sticks Quantofix*®. 2014 [cited 2014 16/02]; Available from: http://www.webcitation.org/query?id=1392576485510823.

71. Metrohm, *873 Biodiesel Rancimat Manual 8.873.1003 05.2007 ars/jb*, Metrohm Ion Analysis.

72. Méndez, E., J. Sanhueza, H. Speisky, and A. Valenzuela, *Comparison of rancimat evaluation modes to assess oxidative stability of fish oils.* Journal of the American Oil Chemists' Society, 1997. **74**(3): p. 331-332.

73. Matthäus, B., *Determination of the Oxidative Stability of Vegetable Oils by Rancimat and Conductivity and Chemiluminescence Measurements.* Journal of the American Oil Chemists' Society, 1996. **73**(8): p. 1039-1043.

74. ACL Instruments. *Chemiluminescence Instrument Hardware Basic Configuration Leaflet 1.1 General*. [cited 2014 16/02]; Available from: http://www.webcitation.org/query?id=1392576775977373.

75. *Instrument Version 5.0: User Installation & Operation Manual*, in *ACL Instruments AG*2010.

76. Luna, F.M.T., B.S. Rocha, E.M. Rola Jr, M.C.G. Albuquerque, D.C.S. Azevedo, and C.L. Cavalcante Jr, *Assessment of biodegradability and oxidation stability of mineral, vegetable and synthetic oil samples.* Industrial Crops and Products. **33**(3): p. 579-583.

77. Farhoosh, R., *The Effect of Operational Parameters of the Rancimat Method on the Determination of the Oxidative Stability Measures and Shelf-Life Prediction of Soybean Oil.* Journal of the American Oil Chemists' Society, 2007. **84**(3): p. 205-209.

78. Mateos, R., M. Uceda, M. Aguilera, M. Escuderos, and G. Beltrán Maza, *Relationship of Rancimat Method Values at Varying Temperatures for Virgin Olive Oils.* European Food Research and Technology, 2006. **223**(2): p. 246-252.

79. *British Standards Institution. BS EN 14112:2003 Fat and Oil Derivatives - Fatty Acid Methyl Esters (FAME). Determination of Oxidation Stability (Accelerated Oxidation Test)* London: BSI, 2003.

80. *British Standards Institution. BS EN ISO 6886:2008. Animal and Vegetable Fats and Oils. Determination of Oxidative Stability (Accelerated Oxidation Test)* London: BSI, 2008.

81. Garcia-Campana, A.M. and W.R.G. Baeyens, *Principles and Recent Analytical Applications of Chemiluminescence.* Analusis, 2000. **28**(8): p. 686-698.

82. Russell, G.A., *Deuterium-isotope Effects in the Autoxidation of Aralkyl Hydrocarbons. Mechanism of the Interaction of Peroxy Radicals.* Journal of the American Chemical Society, 1957. **79**(14): p. 3871-3877.

83. Lacey, D.J. and V. Dudler, *Chemiluminescence from polypropylene. Part 1: Imaging thermal oxidation of unstabilised film.* Polymer Degradation and Stability, 1996. **51**(2): p. 101-108.

84. ACL Instruments. *Basic Configuration*. 2014; Available from: http://www.webcitation.org/6PXKZv8kT.

85. Burkow, I.C., P. Moen, and K. Overbo, *Chemiluminescence as a Method for Oxidative Rancidity Assessment in Autoxidised Marine Oils.* Journal of the American Oil Chemists' Society, 1992. **69**(11): p. 1108-1111.

86. Burkow, I.C., L. Vikersveen, and K. Saarem, *Evaluation of Antioxidants for Cod Liver Oil by Chemiluminescence and the Rancimat Method.* Journal of the American Oil Chemists' Society, 1995. **72**(5): p. 553-557.

87. Käser, F. and M. Bohn, *Decomposition in HTPB Bonded HMX Followed by Heat Generation Rate and Chemiluminescence.* Journal of Thermal Analysis and Calorimetry, 2009. **96**(3): p. 687-695.

88. Käser, F. and B. Roduit, *Prediction of the Ageing of Rubber using the Chemiluminescence Approach and Isoconversional Kinetics* Journal of Thermal Analysis and Calorimetry, 2008. **93**(1): p. 231-237.

89. DIN, *51835-1*, in *Petroleum Products - Part 1: Determination of the Oxidation Stability of Oils by Measuring the Chemiluminescence* 2013.

90. DIN, *51835-2*, in *Petroleum Products - Part 2: Determination of the Oxidation Stability of Lubricating Greases by Measuring the Chemiluminescence* 2013.

91. Stepanyan, V., A. Arnous, C. Petrakis, P. Kefalas, and A. Calokerinos, *Chemiluminescent Evaluation of Peroxide Value in Olive Oil.* Talanta, 2005. **65**(4): p. 1056-1058.

92. Szterk, A. and P. Lewicki, *A New Chemiluminescence Method for Detecting Lipid Peroxides in Vegetable Oils.* Journal of the American Oil Chemists' Society, 2010. **87**(4): p. 361-367.

93.   Rolewski, P., A. Siger, M. Nogala-Kalucka, and K. Polewski, *Chemiluminescent Assay of Lipid Hydroperoxides Quantification in Emulsions of Fatty Acids and Oils.* Food Research International, 2009. **42**(1): p. 165-170.

94.   Pardauil, J.J.R., L.K.C. Souza, F.A. Molfetta, J.R. Zamian, G.N. Rocha Filho, and C.E.F. da Costa, *Determination of the oxidative stability by DSC of vegetable oils from the Amazonian area.* Bioresource Technology. **102**(10): p. 5873-5877.

95.   Knothe, G. and R.O. Dunn, *Dependance of Oil Stability Index of Fatty Acid Compounds on Their Structure and Concentration and Presence of Metals.* Journal of the American Oil Chemists Society, 2003. **80**(10): p. 1021-1026.

96.   Hasenhuettl, G. and P. Wan, *Temperature Effects on the Determination of Oxidative Stability with the Metrohm Rancimat.* Journal of the American Oil Chemists' Society, 1992. **69**(6): p. 525-527.

97.   Farhoosh, R., R. Niazmand, M. Rezaei, and M. Sarabi, *Kinetic Parameter Determination of Vegetable Oil Oxidation Under Rancimat Test Conditions.* European Journal of Lipid Science and Technology, 2008. **110**(6): p. 587-592.

98.   Zlatkevich, L. and A. Kamal-Eldin, *Chemiluminescence in Studying Lipid Oxidation*, in *Analysis of Lipid Oxidation*, A. Kamal-Eldin and J. Pokorny, Editors. 2005, AOCS Press.

99.   Jacobson, K., B. Stenberg, B. Terselius, and T. Reitberger, *Oxidation of stressed injection moulded polyolefins and polyamide 6 as measured by chemiluminescence.* Polymer Degradation and Stability, 2000. **68**(1): p. 53-60.

100.   Paz, I. and M. Molero, *Catalytic Effect of Solid Metals on Thermal Stability of Olive Oils.* Journal of the American Oil Chemists' Society, 2000. **77**(2): p. 127-130.

101.   Alexa, R.I., J.S. Mounsey, B.T. O'Kennedy, and J.C. Jacquier, *Oxidative Stability of Water/Oil Mixtures as Influenced by the Addition of Free Cu2+ or Cu-Alginate Gel Beads.* Food Chemistry, 2011. **129**(2): p. 253-258.

102.   Gijsman, P., M. Kroon, and M. van Oorschot, *The Role of Peroxides in the Thermooxidative Degradation of Polypropylene.* Polymer Degradation and Stability, 1996. **51**(1): p. 3-13.

103.   Jacobson, K., *Oxidation of Ultra High Molecular Weight Polyethylene (UHMWPE) Part 3: Decomposition of Hydroperoxides with SO2 and its Effect on*

the *Chemiluminescence Signal.* Polymer Degradation and Stability, 2006. **91**(10): p. 2292-2299.

104. Kim, H., T. Hahm, and D. Min, *Hydroperoxide as a Prooxidant in the Oxidative Stability of Soybean Oil.* Journal of the American Oil Chemists' Society, 2007. **84**(4): p. 349-355.

105. Reynhout, G., *The Effect of Temperature on the Induction Time of a Stabilized Oil.* Journal of the American Oil Chemists' Society, 1991. **68**(12): p. 983-984.

106. Frankel, E.N., *In search of better methods to evaluate natural antioxidants and oxidative stability in food lipids.* Trends in Food Science & Technology, 1993. **4**: p. 220-224.

107. Pignitter, M. and V. Somoza, *Are Vegetable Oils always a reliable source of vitamin A?* Sight and Life, 2012. **26**(1): p. 18-27.

108. Anderson, J., *Control for Profit.* Transactions of the Institute of Measurement and Control 1996. **18**(1): p. 3.

109. van de Voort, F., A. Ismail, J. Sedman, J. Dubois, and T. Nicodemo, *The determination of peroxide value by fourier transform infrared spectroscopy.* Journal of the American Oil Chemists' Society, 1994. **71**(9): p. 921-926.

110. Ruiz, A., M.J.A. Canada, and B. Lendl, *A rapid method for peroxide value determination in edible oils based on flow analysis with Fourier transform infrared spectroscopic detection.* Analyst, 2001. **126**(2): p. 242-246.

111. Klaypradit, W., S. Kerdpiboon, and R. Singh, *Application of Artificial Neural Networks to Predict the Oxidation of Menhaden Fish Oil Obtained from Fourier Transform Infrared Spectroscopy Method.* Food and Bioprocess Technology. **4**(3): p. 475-480.

112. Yamamoto, Y., E. Niki, R. Tanimura, and Y. Kamiya, *Study of Oxidation by Chemiluminescence. IV. Detection of Low Levels of Lipid Hydroperoxides by Chemiluminescence.* Journal of the American Oil Chemists' Society, 1985. **62**(8): p. 1248-1250.

113. Gupta, B.L., *Microdetermination techniques for H2O2 in irradiated solutions.* Microchemical Journal, 1973. **18**(4): p. 363-374.

114. Bou, R., R. Codony, A. Tres, E.A. Decker, and F. Guardiola, *Determination of hydroperoxides in foods and biological samples by the ferrous oxidation–xylenol*

orange method: A review of the factors that influence the method's performance. Analytical Biochemistry, 2008. **377**(1): p. 1-15.

115.   Yildiz, G., R. Wehling, and S. Cuppett, *Comparison of four analytical methods for the determination of peroxide value in oxidized soybean oils.* Journal of the American Oil Chemists' Society, 2003. **80**(2): p. 103-107.

116.   Billingham, N.C., E.T.H. Then, and P.J. Gijsman, *Chemiluminescence from peroxides in polypropylene. Part I: Relation of luminescence to peroxide content.* Polymer Degradation and Stability, 1991. **34**(1-3): p. 263-277.

117.   Navas, M. and A. Jiménez, *Chemiluminescent Methods in Olive Oil Analysis.* Journal of the American Oil Chemists' Society, 2007. **84**(5): p. 405-411.

118.   Nielsen, N.S., M. Timm-Heinrich, and C. Jacobsen, *Comparison of wet-chemical methods for determination of lipid hydroperoxides* 2003, Blackwell Publishing Ltd. p. 35-50.

119.   Moh, M.H., Y.B. Che Man, F.R. van de Voort, and W.J.W. Abdullah, *Determination of peroxide value in thermally oxidized crude palm oil by near infrared spectroscopy.* Journal of the American Oil Chemists' Society, 1999. **76**(1): p. 19-23.

120.   Pegg, R.B., *Measurement of Primary Lipid Oxidation Products*, in *Current Protocols in Food Analytical Chemistry* 2001, John Wiley & Sons, Inc.

121.   ACL Instruments, *Leaflet 1.1 Applications: Stability and Quality of Biodiesel*.

122.   International Fragrance Association, *Analytical Method: Determination of the Peroxide Value (October 17th, 2011)*, 2011.

123.   Abd El-Moneim Mahmoud, E., J. Dostalova, D. Lukesova, and M. Dolezal, *Oxidative Changes of Lipids during Microwave Heating of Minced Fish Flesh in Catering.* Czech Journal of Food Sciences, 2009. **27**: p. S17-S19.

124.   Farhoosh, R. and S.M.R. Moosavi, *Evaluating the Performance of Peroxide and Conjugated Diene Values in Monitoring Quality of Used Frying Oils.* Journal of Agricultural Science and Techonology, 2009. **11**(2): p. 173-179.

125.   Marmesat, S., A. Morales, J. Velasco, M.V. Ruiz-Méndez, and M.C. Dobarganes, *Relationship between changes in peroxide value and conjugated dienes during oxidation of sunflower oils with different degree of unsaturation.* Grasas y Aceites, 2009. **60**(2): p. 155-160.

126. Crowe, T. and P. White, *Adaptation of the AOCS official method for measuring hydroperoxides from small-scale oil samples.* Journal of the American Oil Chemists' Society, 2001. **78**(12): p. 1267-1269.

127. Shahidi, F., ed. *Bailey's Industrial Oil and Fat Products*. Sixth Edition ed. 2005, John Wiley & Sons, Inc.

128. Osawa, C.C., L.A.G. Gonçalves, and S. Ragazzi, *Determination of hydroperoxides in oils and fats using kits.* Journal of the Science of Food and Agriculture, 2007. **87**(9): p. 1659-1666.

129. Käser, F., B. Roduit, and S. Wuelfert. *Oxidative stability assessment of organic materials - chemiluminescence as a useful tool* 2014 [cited 2014 10/09]; Available from: http://www.webcitation.org/6SaREPoix.

130. Crowe, T.D. and P.J. White, *Adaptation of the AOCS official method for measuring hydroperoxides from small-scale oil samples.* Journal of the American Oil Chemists' Society, 2001. **78**(12): p. 1267-1269.

131. Croda International Plc. *Super Refined™ Excipients*. 2014 [cited 2014 28/08]; Available from: http://www.webcitation.org/6SAmIWVvv.

132. Chadha, R. and S. Bhandari, *Drug–excipient compatibility screening—Role of thermoanalytical and spectroscopic techniques.* Journal of Pharmaceutical and Biomedical Analysis, 2014. **87**(0): p. 82-97.

133. Bharate, S.S., S.B. Bharate, and A.N. Bajaj, *Incompatibilities of Pharmaceutical Excipients with Active Pharmaceutical Ingredients: A Comprehensive Review.* Journal of Excipients and Food Chemicals, 2010. **1**(3): p. 3-26.

134. ICH, *Q1A(R2) Stability testing of new drug substances and products.*, 2003, International Conference on Harmonisation of Technical Requirements for Registration of Pharmaceuticals for Human Use: Geneva.

135. ICH, *Q3B(R2) Impurities in New Drug Products*, 2006: Geneva.

136. ICH, *Q3A(R2) Impurities in New Drug Substances* 2006, International Conference on Harmonisation of Technical Requirements for Registration of Pharmaceuticals for Human Use: Geneva.

137. International Pharmaceutical Excipients Council. *Qualification of Excipients for Use in Pharmaceuticals*. 2008 [cited 2014 18/08]; Available from: http://www.webcitation.org/6Rv7SpMpA.

138.   Singh, S., J. Zhang, C. O'Dell, M.-C. Hsieh, J. Goldstein, J. Liu, and A. Srivastava, *Effect of Polysorbate 80 Quality on Photostability of a Monoclonal Antibody.* AAPS PharmSciTech, 2012. **13**(2): p. 422-430.

139.   Maggio, E.T., *Polysorbates, Peroxides, Protein Aggregation, and Immunogenicity A growing Concern.* Journal of Excipients and Food Chemicals, 2012. **3**(2).

140.   Paul A. Harmon, K.K., Eric Nelson, Mark Mowery, Robert A. Reed,, *A novel peroxy radical based oxidative stressing system for ranking the oxidizability of drug substances.* Journal of Pharmaceutical Sciences, 2006. **95**(9): p. 2014-2028.

141.   Kishore, R., S. Kiese, S. Fischer, A. Pappenberger, U. Grauschopf, and H.-C. Mahler, *The Degradation of Polysorbates 20 and 80 and its Potential Impact on the Stability of Biotherapeutics.* Pharmaceutical Research, 2011. **28**(5): p. 1194-1210.

142.   Jenkins, N., *Modifications of therapeutic proteins: challenges and prospects.* Cytotechnology, 2007. **53**(1): p. 121-125.

143.   Yao, J., D.K. Dokuru, M. Noestheden, S.S. Park, B.A. Kerwin, J. Jona, D. Ostovic, and D.L. Reid, *A Quantitative Kinetic Study of Polysorbate Autoxidation: The Role of Unsaturated Fatty Acid Ester Substituents.* Pharmaceutical Research, 2009. **26**(10): p. 2303-2313.

144.   Coates, L.V., M.M. Pashley, and K. Tattersall, *The stability of antibacterials in polyethylene glycol mixtures.* Journal of Pharmacy and Pharmacology, 1961. **13**(1): p. 620-624.

145.   Cory, W.C., C. Harris, and S. Martinez, *Accelerated degradation of ibuprofen in tablets.* Pharmaceutical Development and Technology, 2010. **15**(6): p. 636-643.

146.   James, K.C. and R.H. Leach, *A stability study of chloramphenicol in topical formulations.* Journal of Pharmacy and Pharmacology, 1970. **22**(8): p. 607-611.

147.   Lam, X., W. Lai, E. Chan, V. Ling, and C. Hsu, *Site-Specific Tryptophan Oxidation Induced by Autocatalytic Reaction of Polysorbate 20 in Protein Formulation.* Pharmaceutical Research, 2011. **28**(10): p. 2543-2555.

148.   Narang, A., D. Desai, and S. Badawy, *Impact of Excipient Interactions on Solid Dosage Form Stability.* Pharmaceutical Research. **29**(10): p. 2660-2683.

149. Narang, A.S., V.M. Rao, and D.S. Desai, *Effect of antioxidants and silicates on peroxides in povidone.* Journal of Pharmaceutical Sciences, 2012. **101**(1): p. 127-139.

150. Hulse, W. and R. Forbes, *DRAFT Determination of oxidative degradation potential and assessment of peroxide levels using Rancimat and chemiluminescence analysis of sorbitan monooleate, PEG 400 and white soft paraffin (unpublished work)*, 2010, Institute of Pharmaceutical Innovation, University of Bradford.

151. Gray, J., *Measurement of lipid oxidation: A review.* Journal of the American Oil Chemists' Society, 1978. **55**(6): p. 539-546.

152. Shulin, D., *Quantitation of hydroperoxides in the aqueous solutions of non-ionic surfactants using polysorbate 80 as the model surfactant.* Journal of Pharmaceutical and Biomedical Analysis, 1993. **11**(2): p. 95-101.

153. Kishore, R.S.K., A. Pappenberger, I.B. Dauphin, A. Ross, B. Buergi, A. Staempfli, and H.-C. Mahler, *Degradation of polysorbates 20 and 80: Studies on thermal autoxidation and hydrolysis.* Journal of Pharmaceutical Sciences, 2011. **100**(2): p. 721-731.

154. Kowalski, B., K. Ratusz, D. Kowalska, and W. Bekas, *Determination of the oxidative stability of vegetable oils by Differential Scanning Calorimetry and Rancimat measurements.* European Journal of Lipid Science and Technology, 2004. **106**(3): p. 165-169.

155. Frison-Norrie, S. and P. Sporns, *Investigating the Molecular Heterogeneity of Polysorbate Emulsifiers by MALDI-TOF MS.* Journal of Agricultural and Food Chemistry, 2001. **49**(7): p. 3335-3340.

156. Guazzo, D.M., *Current Approaches in Leak Testing Pharmaceutical Packages.* PDA Journal of Pharmaceutical Science and Technology, 1996. **50**(6): p. 378-385.

157. Akers, M.K., D. Larrimore, and D. Guazzo, *Parenteral Quality Control: Sterility, Pyrogen, Particulate, and Package Integrity Testing*, 2003, Marcel Dekker Inc.

158. Bosch, *Leak detection machine KLD 1042*, 2010, Robert Bosch GmbH.

159. Pharmaceutical Online. *Solutions For Container Closure Integrity Testing At Interphex High Voltage Leak Detection – Offline And 100% Online Solutions*.

2012 [cited 2014 24/08]; Available from:
http://www.webcitation.org/6S4dMOHoy.

160. Brevetti CEA. *Inspection Systems: Opera2* 2014 [cited 2014 16/02]; Available from: http://www.webcitation.org/query?id=1392577092640140.

161. WILCO AG. 2014 [cited 2014 16/02]; Available from:
http://www.webcitation.org/query?id=1392577233094981.

162. pti Inspection Systems, *Inspection Solutions for the Pharmaceutical Industry: Micro Leak Testing of Liquid Filled Packaging E Scan 625*, in *Packaging Technologies and Inspection* 2011.

163. Rubin, M.B., *The History of Ozone. The Schönbein Period, 1839-1868.* Bulletin for the History of Chemistry, 2001. **26**(1): p. 40-56.

164. Siemens, W., *Ueber die elektrostatische Induction und die Verzögerung des Stroms in Flaschendräten.* Phys. Chem, 1857. **102**(120): p. 66

165. McGinley, C.M., A. Thiel, K. Olson, Ø. Loe, D. Loffredo, and J. Joseph, *Poster: Degradation of Drug Product Caused by a Leak Detection Instrument: Mechanistic Studies of Degradation*, Hospira, Inc., Lake Forest, IL 60045.

166. McGinley, C.M., P. Bigwarfe, A. Thiel, K. Olson, D. Loffredo, and J. Joseph, *Degradation of Drug Product Caused by a Leak Detection Instrument*, in *AAPS Annual Meeting & Exposition* 2007: San Diego.

167. Schellekens, H., *Manufacture and quality control of biopharmaceuticals.* Economia de la Salud, 2007. **6**(6): p. 34-344.

168. Peleg, M., *The chemistry of ozone in the treatment of water.* Water Research, 1976. **10**(5): p. 361-365.

169. Cataldo, F., *On the action of ozone on proteins.* Polymer Degradation and Stability, 2003. **82**(1): p. 105-114.

170. Sharma, V.K. and N.J.D. Graham, *Oxidation of Amino Acids, Peptides and Proteins by Ozone: A Review.* Ozone: Science & Engineering, 2010. **32**(2): p. 81-90.

171. Platten, J.K. and P. Costesèque, *Charles Soret. A short biography - on the occasion of the hundredth anniversary of his death.* The European Physical Journal E: Soft Matter and Biological Physics, 2004. **15**(3): p. 235-239.

172. Ershov, B. and P. Morozov, *The kinetics of ozone decomposition in water, the influence of pH and temperature.* Russian Journal of Physical Chemistry A, Focus on Chemistry, 2009. **83**(8): p. 1295-1299.

173. Cohen, I.C., A.F. Smith, and R. Wood, *A field method for the determination of ozone in the presence of nitrogen dioxide.* Analyst, 1968. **93**(1109): p. 507-517.

174. American Public Health Association, *Method 4500-O3: Standard Methods for the Examination of Water and Wastewater* 1992, APHA: Washington, DC.

175. Burns, D.T., *Early problems in the analysis and the determination of ozone.* Fresenius' Journal of Analytical Chemistry, 1997. **357**(2): p. 178-183.

176. Costello, K. *Ozone: The Good, the Bad, and the Useful* 2011.

177. Thorp, C.E., *Starch-Iodide Method of Ozone Analysis.* Industrial & Engineering Chemistry Analytical Edition, 1940. **12**(4): p. 209-209.

178. Bovee, H.H. and R.J. Robinson, *Sodium Diphenylaminesulfonate as an Analytical Reagent for Ozone.* Analytical Chemistry, 1961. **33**(8): p. 1115-1118.

179. Taube, H., *Photochemical reactions of ozone in solution.* Transactions of the Faraday Society, 1957. **53**(0): p. 656-665.

180. Kilpatrick, M.L., C.C. Herrick, and M. Kilpatrick, *The Decomposition of Ozone in Aqueous Solution1,2.* Journal of the American Chemical Society, 1956. **78**(9): p. 1784-1789.

181. Boyd, A.W., C. Willis, and R. Cyr, *New determination of stoichiometry of iodometric method for ozone analysis at pH 7.0.* Analytical Chemistry, 1970. **42**(6): p. 670-672.

182. Bader, H. and J. Hoigné, *Determination of Ozone In Water By The Indigo Method: A Submitted Standard Method.* Ozone: Science & Engineering, 1982. **4**: p. 169-176.

183. Forni, L., D. Bahnemann, and E.J. Hart, *Mechanism of the hydroxide ion-initiated decomposition of ozone in aqueous solution.* The Journal of Physical Chemistry, 1982. **86**(2): p. 255-259.

184. Hart, E.J., K. Sehested, and J. Holoman, *Molar absorptivities of ultraviolet and visible bands of ozone in aqueous solutions.* Analytical Chemistry, 1983. **55**(1): p. 46-49.

185. Hoigne, J., *Chemistry of aqueous ozone and transformation of pollutants by ozonation and advanced oxidation processes.* The handbook of environmental chemistry, 1998. **5**: p. 83-142.

186. Teledyne Technologies Incorporated. *Model 454 Process Ozone Monitor*. 2014 [cited 2014 16/02]; Available from: http://www.webcitation.org/query?id=1392577367273808.

187. Byers D, H. and E. Saltzman B, *Determination of Ozone in Air by Neutral and Alkaline Iodide Procedures*, in *Ozone chemistry and technology* 1959, American Chemical Society. p. 93-101.

188. Tomiyasu, H. and G. Gordon, *Colorimetric determination of ozone in water based on reaction with bis(terpyridine)iron(II).* Analytical Chemistry, 1984. **56**(4): p. 752-754.

189. Boyd, A.W., C. Willis, and R. Cyr, *Determination of stoichiometry of the iodometric method for ozone analysis at pH 7.0.* Analytical Chemistry, 1970. **42**(6): p. 670-672.

190. Ingols, R.S., R.H. Fetner, and W.H. Eberhardt, *Determining Ozone in Solution*, in *Ozone Chemistry and Technology*1959, American Chemical Society p. 102-107.

191. Hodgeson, J.A., R.E. Baumgardner, B.E. Martin, and K.A. Rehme, *Stoichiometry in the neutral iodometric procedure for ozone by gas-phase titration with nitric oxide.* Analytical Chemistry, 1971. **43**(8): p. 1123-1126.

192. Kopczynski, S. and J. Bufalini, *Some Observations on Stoichiometry of Iodometric Analyses of Ozone at pH 7.0.* Analytical Chemistry, 1971. **43**(8): p. 1126-1127.

193. Bader, H. and J. Hoigné, *Determination of ozone in water by the indigo method.* Water Research, 1981. **15**(4): p. 449-456.

194. Collins, A.G., M.R. Farvardin, and Z. Shen, *An Alternative Approach to Gas Phase Ozone Determination.* Ozone: Science & Engineering, 1989. **11**(1): p. 115-125.

195. Chiou, C.-F., B.J. Mariñas, and J.Q. Adams, *Modified Indigo Method For Gaseous And Aqueous Ozone Analyses.* Ozone: Science & Engineering, 1995. **17**: p. 329-344.

196. Ozone Solutions Inc. *Ozone Solutions: Products: Dissolved Ozone* 2014 [cited 2014 16/02]; Available from: http://www.webcitation.org/query?id=1392577686774328.

197.   Ozone Solutions Inc. *K-7404: Dissolved Ozone Vacuvial Kit*. 2014 [cited 2014 14/09]; Available from: http://www.webcitation.org/6SagZm9t0.

198.   Munoz, F. and C. von Sonntag, *Determination of fast ozone reactions in aqueous solution by competition kinetics.* Journal of the Chemical Society, Perkin Transactions 2, 2000(4): p. 661-664.

199.   Diaz, R., D. Menendez, and F. Tabares, *High Frequency Ozone Generation System*, in *Ozone: Science & Engineering*2001, Taylor & Francis. p. 171-176.

200.   Yehia, A., A. Mizuno, and M.A.M. El-Osealy, *Calculation of ozone generation in AC corona discharge reactor.* Japanese Journal of Applied Physics Part 1-Regular Papers Short Notes & Review Papers, 2004. **43**(8A): p. 5558-5561.

201.   Lenntech. *Ozone reaction mechanisms*. 2013 [cited 2014 16/02]; Available from: http://www.webcitation.org/query?id=1392579443333471.

202.   Sehested, K., H. Corfitzen, J. Holcman, and E.J. Hart, *Decomposition of ozone in aqueous acetic acid solutions (pH 0-4).* The Journal of Physical Chemistry, 1992. **96**(2): p. 1005-1009.

203.   Chu, W., Y.R. Wang, and H.F. Leung, *Synergy of sulfate and hydroxyl radicals in UV/S2O82−/H2O2 oxidation of iodinated X-ray contrast medium iopromide.* Chemical Engineering Journal, 2011. **178**(0): p. 154-160.